Midbrain dopaminergic neuron fate specification of pluripotent stem cells

Ines Jaeger

Thesis submitted for the degree of Doctor of Philosophy

MRC Clinical Sciences Centre, Imperial College London 2012

I declare that the work described in this Thesis is my own unless otherwise stated.

Ines Jaeger

Acknowledgements

It is a pleasure to thank the many people who made this PhD a reality. First and foremost, my deepest sense of gratitude goes to my supervisor Dr. Meng Li. This work would not have been possible without her continuous support, guidance and patience. I expand my thanks to the entire lab, past and present, especially, Emily, Xinsheng and Charlie, who have made this entire process not only bearable, but entertaining and enjoyable. I am thankful to my office mate, colleague, collaborator and friend Jess who had always time when I needed help. I also would like to thank our collaborators Mark Ungless, Steve Dunnett, Sophie Precious, and Andreas Heuer. Thanks go also to Dirk Dorrman, Lein Snipes, Ki Heng, and James Elliot for their help on the fluorescence activated cell sorters and microscopes.

I am especially grateful to my beloved friends, Aida, Bibi, Carina, Claire, Hegias, Hendrik, Isi, Joseba, Kerstin, Korinna, Michel-Raphael, Sarah, Silke and Sybille for their support and love during the journey in obtaining my PhD.

And most importantly, I would like to thank my parents, Doris and Olaf Jaeger. They were there to commiserate with me when I was discouraged and celebrate with me when I had successes. Their love and encouragement have been a constant source for me since I was little; therefore, I dedicate this thesis to them.

Abstract

Disorders of dopaminergic neurons in the midbrain are associated with various brain diseases such as Parkinson's disease (PD), for which there are no effective treatments. Pluripotent stem cells (PSCs) offer a remarkable potential for finding new therapeutic strategies because they are self-renewable and capable to differentiate into all cell types. However, biomedical applications of PSCs require knowledge of the molecular mechanisms directing PSCs into midbrain dopaminergic (mDA) cell fate.

During development the generation of mDA neurons is induced by the extrinsic molecules SHH, FGF8 and WNT1 in the caudal region of the *Otx2* positive domain, which marks the presumptive fore- and midbrain, and rostrally to the future hindbrain expressing *Gbx2*.

In this study I have further investigated the role of FGF signalling in the generation of mDA neurons. Here, I have used mouse epiblast stem cells (EpiSCs). Based on their developmentally primed pluripotent state, we assumed that they represent a more suitable system when compared with mouse embryonic stem cells. I validated neural differentiation of EpiSCs as an alternative model to study neural development *in vitro*. I found that inhibition of the FGF/ERK activity at the onset of EpiSC differentiation initiated expression of *Wnt* and *Shh* and further induced ventral midbrain progenitor markers, accompanied by suppressing caudalisation as well as forebrain induction. To maintain ventral midbrain progenitor fate, cells required a period of endogeneous FGF/ERK signalling. Subsequent treatment of FGF8 and SHH, which restricts progenitors from adopting alternative fates, led to highly efficient production of authentic mDA neurons. These neurons exhibited functional, neuron-like properties and when implanted into the striatum of mouse PD model strongly restored parkinsonian features without any signs of overgrowth.

In conclusion, a temporally controlled modulation of FGF/ERK activity during neural differentiation from PSCs is crucial for reliable and highly efficient generation of functional authentic mDA neurons.

Table of Contents

List of Figures

List of Tables

List of Abbreviation

1 Introduction 1

1.1 Pluripotent stem cells 1

1.1.1 Stem Cells 1

1.1.2 Characteristics of pluripotency 2

1.1.3 Pluripotent stem cell lines 2

1.1.4 Pluripotent stem cells as model to study neural development 5

1.2 Midbrain dopaminergic development 5

1.2.1 Neural induction 5

1.2.2 Neural patterning – regionalisation and specification of midbrain dopaminergic neurons 8

1.2.3 Isthmus assiociated factors 10

1.2.4 Floorplate associated factors 17

1.2.5 Genes regulating midbrain dopaminergic development 19

1.3 Strategies for neural differentiation *in vitro* of pluripotent stem cells 21

1.3.1 Embryoid body differentiation 21

1.3.2 Stromal co-culture system 21

1.3.3 Monolayer differentiation 22

1.4 FGF pathway 22

1.4.1 FGF ligands 22

1.4.2 FGF receptors 23
1.4.3 FGF signalling 23
1.4.4 FGF modulation 25
1.4.5 Multiple roles of the FGF pathway during neural development 26
1.5 Hypthesis and aims 28
2 Materials and Methods 33
2.1 Cell Culture 33
2.1.1 Routine ESC and iPSC culture 33
2.1.2 Derivation of EpiSC from ESC 33
2.1.3 Routine EpiSC culture 34
2.1.4 Freezing ESCs, iPSCs and EpiSCs 34
2.1.5 Thawing ESCs, iPSCs and EpiSCs 34
2.2 Neural differentiation 34
2.3 Flow cytometry 36
2.4 Electophysiological studies 36
2.5 Animal work 37
2.5.1 Animals 37
2.5.2 Lesion surgery 37
2.5.3 Graft surgery 38
2.5.4 Drug-induced rotations 38
2.6 Molecular biology methods 39
2.6.1 Quantitative PCR 39
2.6.2 Protein extraction and quantification 39

2.6.3 Western Blot analysis 40

2.6.4 Immunofluorescence staining 40

2.6.5 Quantitative analysis of immunocytochemistry 41

3 Epiblast stem cells as an alternative model to study neural differentiation *in vitro*.. 45

3.1 Comparison of neural induction in ESCs cell and EpiSCs 46

3.2 Discussion 51

4 Temporally controlled modulation of FGF/ERK signalling directs a midbrain dopaminergic fate 53

4.1 Blockade of FGF/ERK signalling upon exit of epiblast pluripotent state accelerates neural fate commitment 54

4.2 Inhibition of FGF/ERK activity at the onset of EpiSC differentiation promotes mDA progenitor characteristics 59

4.3 FGF/ERK inhibition affects anterior-posteriorisation and the maintenance of OTX2 in nascent neural progenitors 65

4.4 Highly reliable and efficient production of mDA neurons by ERK inhibitor-primed neural progenitors 70

4.5 Dopaminergic neuron differentiation of mouse iPSCs in response to ERK inhibition 73

4.6 Differential activity of SHH and FGF8 in mDA fate specification and differentiation 75

4.7 WNT alone or in combination with SHH cannot replace ERK inhibitor in inducing midbrain progenitor cell fate 80

4.7.1 The effects of early SHH activation on mDA induction 80

4.7.2 The effects of GSK3ß inhibition on mDA induction 81

4.7.3 The effects of combined treatment of SHH and CHIR99021 on mDA induction 83

4.8 Discussion 95

5 Functional analysis of *in vitro* derived midbrain dopaminergic neurons 100

5.1 *In vitro* generated mDA neurons exhibit functional neuronal characteristics 100

5.2 Transplantation of *in vitro* generated mDA progenitors in a mouse model of Parkinson's disease 104

5.2.1 Modification of differentiation protocol 104

5.2.2 Transplantation of EpiSC-derived mDA progenitors; pilot study 109

5.2.3 Head to head comparison of EpiSC-derived mDA grafts with ventral midbrain tissue in 6-OHDA-lesioned mouse models of PD 114

5.3 Discussion 119

6 Concluding remarks and future directions 121

7 Bibliography 127

8 Appendix 156

List of Figures

Figure 1.1 Schematic illustration of the signalling centres which establish the antero-posterior axis. 29

Figure 1.2 Drawing of midbrain DA neural development 30

Figure 1.3 Schematic illustration of the pathways implicated in the generation of mDA neurons. 31

Figure 3.1 Accelerated neural differentiation potential of EpiSCs. 49

Figure 3.2 Synchronised neuroectodermal differentiation from EpiSCs. 50

Figure 4.1 Inhibition of FGF/ERK activity accelerates the exit of EpiSCs from a pluripotent stage. 56

Figure 4.2 Inhibition of FGF/ERK activity accelerates neural fate conversion of EpiSCs. 58

Figure 4.3 Inhibition of FGF/ERK on the exit of the epiblast pluripotent stage promotes the generation of mDA progenitor cells. 63

Figure 4.4 Blockade of FGF/PI3K signalling does not induce expression of mDA regulatory genes. 64

Figure 4.5 Early blockade of FGF/ERK activity modulates anterior –posterior characteristics of neural progenitor cells. 68

Figure 4.6 Early blockade of FGF/PI3K activity does not promote the generation of neural progenitors with anterior characteristics. 69

Figure 4.7 Temporally controlled FGF/ERK activity promotes the production of functional, authentic mDA neurons. 72

Figure 4.8 Efficient generation of mDA neurons from mouse iPSCs. 74

Figure 4.9 Temporally controlled FGF/ERK activity in combination with SHH and FGF8 promotes the production of DA neurons. 77

Figure 4.10 Activation of SHH signalling promotes the production of DA neurons by repressing the transcript level of genes for a GABAergic neuronal fate. 78

Figure 4.11 Effect of SHH and/or FGF8 in EpiSC MD. 79
Figure 4.12 Activation of SHH pathway is not sufficient for complete mDA induction. 85
Figure 4.13 Early inhibition of FGF/ERK acts partly via the SHH pathway. 86
Figure 4.14 SHH treatment cannot induce midbrain neural progenitor fate. 88
Figure 4.15 Activation of SHH alone cannot replace early blockade of FGF/ERK pathway in the generation of DA neurons. 89
Figure 4.16 Activation of the WNT pathway does not mirror the effects of early ERK inhibition in neural differentiation. 91
Figure 4.17 SHH and CHIR99021 treatment partly mimics early ERK inhibition. 93
Figure 4.18 Early stimulation of SHH and WNT pathway cannot substitute ERK inhibition in the generation of DA neurons. 94
Figure 5.1 Pitx3-GFP positive cells exhibit functional neuron-like electrophysiological properties. (kindly provided by Dr. Jessica Risner-Janiczek). 103
Figure 5.2 Early blockade of FGF signalling and postliminary enhancement of SHH signalling support generation of ventral midbrain progenitor cells. 107
Figure 5.3 ERK inhibition followed by stimulation of the SHH signalling promotes the generation of DA neurons. 108
Figure 5.4 EpiSC-derived cells display robust induction of ventral midbrain progenitor fate at the day of transplantation. 111
Figure 5.5 Bar graph of amphetamine-induced rotational behaviour 8 weeks after transplantation of lesioned, d5 and d7 MD cultures mice (kindly provided by Dr. Sophie Precious and Andreas Heuer). 112
Figure 5.6 Substantial graft-derived reinnervation of the lesioned striatum 8 weeks after transplantation of d5 and d7 MD cultures (kindly provided by Dr. Sophie Precious and Andreas Heuer) 113
Figure 5.7 Behavioural analysis in E12.5 VM- versus d7 MD-grafted mice (kindly provided by Dr. Sophie Precious and Andreas Heuer). 116

Figure 5.8 Characterisation of neurons in 6-OHDA lesioned mouse models of PD grafted with either d7 MD or VM cells (kindly provided by Dr. Sophie Precious and Andreas Heuer). 118
Figure 6.1 Proposed model of FGF signalling in mDA neural differentiation. 126

List of Tables

Table 1.1 The 23 members of the FGF family can be divided into 7 groups according their evolutionary relationship and and gene-location analysis. 32

Table 2.1 Pluripotent stem cell lines used for the investigations of this thesis. 42

Table 2.2 List of factors used for neural differentiation. 42

Table 2.3 List of gene specific primers for qPCR. 43

Table 2.4 List of primary antibodies for immunocytochemistry. 44

List of Abbreviation

AP	Anterior-posterior
ANOVA	Analysis of Variance
ANR	Anterior neural ridge
AVE	Anterior visceral endoderm
cDNA	Complementary DNA
d	day
DA	Dopaminergic
DNA	Deoxyribonucleic acid
E	Embryonic day
EB	Embryoid bodies
EpiSC	Epiblast stem cell
ESC	Embryonic stem cell
GFP	Green fluorescence protein
hESC	human ESC
ICM	Inner cell mass
iPSC	Induced pluripotent stem cell
IsO	Isthmic Organiser
LIF	Leukemia inhibitory factor
MD	Monolayer differentiation
mDA	Midbrain dopaminergic
MHB	Midbrain hindbrain border
mRNA	Messenger RNA
NPC	Neural progenitor cell
NSC	Neural stem cell
PCR	Polymerase chain reaction

PD	Parkinson’s disease
PD0325901	potent FGF/ERK inhibitor
PSC	Pluripotent stem cell
RNA	Ribonucleic acid
SN	Substantia Nigra
VTA	Ventral tegmental area
ZLI	Zona limitans intrathalamica

1 Introduction

In the nervous system dopaminergic (DA) neurons exist in different regions including the olfactory bulb, retina, hypothalamus and the ventral midbrain. DA neurons are usually identified by their expression of tyrosine hydroxylase (TH), the rate-limiting enzyme in the synthesis of dopamine. The ventral midbrain contains two cores of DA neurons, the substantia nigra (SN) and the ventral tegmental area (VTA). The SN is a part of the nigrostrial system and regulates motor function whilst the VTA belongs to the mesolimbic system and is involved in emotional behaviour. Disorders involving neurons of the VTA are linked to Schizophrenia and depression whereas the preferential degeneration of DA neurons in the SN is believed to be the primary cause of Parkinson's disease (PD) (Hirsch, Graybiel et al. 1988; Sesack and Carr 2002; Dailly, Chenu et al. 2004).

Stem cell-based transplantation is a promising approach for the treatment of PD. The generation of patient-specific induced pluripotent stem cells offers further, perhaps more realistic in shorter term, biomedical applications of stem cells in disease modelling and drug development. However, realising the potential of stem cells requires in depth understanding of the mechanisms that control the generation of mDA neurons during development.

1.1 Pluripotent stem cells

1.1.1 Stem Cells

Stem cells have the potential to self-renew for indefinite periods in culture and to give rise to one or more specialised cell types along the developmental path. There are many kinds of stem cells that can be distinguished by their capacity to differentiate.

The zygote and the first blastomeres, derived from the first division of the zygote, are totipotent stem cells (Tarkowski 1959; Gardner 1998). They are capable of forming the entire embryo including the extra-embryonic tissue. As the blastomeres continue to cleave and divide, they form the trophoblast and the inner cell mass (ICM). The ICM further develops into the hypoblast and epiblast. Cells from the epiblast are pluripotent as they contribute to all cell lineages and can form a chimera when transplanted into another blastocyst (Gardner, 1998). Through the subsequent process of gastrulation, cells of the epiblast give rise to the three germ layers: mesoderm, ectoderm, and endoderm. Cells of the mesoderm, ectoderm, and endoderm are considered to be multipotent as they are the progenitor cells of only one germ layer and terminally differentiate into a somatic cell type specific to that germlayer.

1.1.2 Characteristics of pluripotency

Pluripotency is defined as the ability of a single cell to generate all cell lineages of an organism. Stable pluripotent stem cell (PSC) lines can be derived from the epiblast and teratomas under specific culture conditions or generated from somatic cells by introduction of specific transcription factors.

The functional pluripotency of a cell can be determined by three independent experiments: 1) the spontaneous differentiation of PSCs in culture, 2) the formation of teratomas and teratocarcinomas by injection of PSCs into an immune compromised adult animal, and 3) chimera incorporation and germline transmission when PSCs are injected into a pre-implantation blastocyst.

1.1.3 Pluripotent stem cell lines

Embryonic stem cells

Embryonic stem cells (ESCs) are pluripotent cells derived from the epiblast of the pre-implantation embryo (Kaufman et al., 1983). These cells are defined by their expression of the key pluripotency markers *Nanog, Oct4, Sox2, Klf4, Rex1*, and *Stella* (Avilion et al., 2003; Guo et al., 2009; Mitsui et al., 2003; Okamoto et al., 1990; Payer et al., 2003; Ramalho-

Santos et al., 2002; Rogers et al., 1991). Furthermore female ESCs exist in a pre-X-inactivation state maintaining two active X-chromosomes (Nichols and Smith, 2009).

Initially, mouse ESCs were maintained on mitotically inactivated mouse embryonic fibroblast cells in the presence of fetal bovine serum (Evans and Kaufman, 1981). Later studies identified the leukemia inhibitory factor (LIF) as an important component to maintain pluripotency by activating the transcription factor STAT3 (Matsuda et al., 1999; Niwa et al., 1998; Stewart et al., 1992). LIF in combination with the bone morphogenetic protein (BMP) were able to suppress differentiation and allowed the propagation of ESCs in a feeder layer free condition (Ying et al., 2003a). However, ESCs expanded in fully defined medium containing LIF and the two small molecules that inhibit mitogen-activated protein kinase (MAPK) signalling and glycogen synthase kinase-3 ß (GSK3ß) showed an upregulation of *Nanog* and *Oct4* positive cells representing the so called ground state of pluripotency (Nichols and Smith, 2009; Silva et al., 2008a).

Epiblast stem cells

The generation of a stable PSC line from the epiblast of a postimplantation embryo has been first reported 2007 (Brons et al., 2007; Tesar et al., 2007). These cells are consequently called epiblast stem cells (EpiSCs). The maintenance of their pluripotent state requires Activin A and fibroblast growth factor 2 (FGF2) (Tesar et al., 2007). Using the same condition, EpiSCs can also be produced from ESCs (Guo et al., 2009). Though EpiSCs express the core pluripotent markers *Nanog, Oct4*, and *Sox2*, they are distinct from ESCs (Chenoweth and Tesar, 2010; Eggan, 2007). Unlike ESCs, EpiSCs display a high expression level of genes that mark the postimplantation epiblast such as *Fgf5*, *Brachyury*, *Gata6*, *Nodal*, *Foxa2*, and *Otx2* (Brons et al., 2007; Tesar et al., 2007). In addition, these cells grow as flat compact colonies and need cell-cell interaction to survive (Brons et al., 2007). Studies on EpiSCs further observed that one copy of the X chromosome is epigenetically silenced in female cells (Guo et al., 2009). Although EpiSCs can form teratomas, they have very limited capacity to contribute to blastocyst chimeras (Brons et al.,

2007; Rossant, 2008; Tesar et al., 2007). EpiSCs are therefore thought to be more advanced in their development when compared to ESCs and thus they are also called primed PSCs (Nichols and Smith, 2009).

Induced pluripotent stem cells

Reprogramming of somatic cells to become induced pluripotent stem cells (iPSCs) by overexpressing the key transcription factors for pluripotency, *Oct4, Sox2, Klf4* and *c-Myc*, was first reported in 2006 by Takahashi and Yamanaka (Takahashi and Yamanaka, 2006). Since then it has been demonstrated that iPSCs can also be derived from a variety of mouse tissues (Aoi et al., 2008; Eminli et al., 2008; Kim et al., 2008; Stadtfeld et al., 2008). These cells functionally resemble ESCs as they differentiate *in vitro* into the cell types of all three germ layers, form teratomas and contribute to chimeras and germline transmission (Maherali and Hochedlinger 2008, Okita et al 2007, Wernig et al 2007). Genome-wide microarray analyses further revealed that the global expression pattern of iPSCs is more similar to ESCs than the somatic cells from which they were derived, and that a majority of genes specific for ESCs are reactivated in iPSCs (Okita et al., 2007; Wernig et al., 2007). Additionally, during reprogramming of female somatic cells the silenced X-chromosome is again activated (Maherali et al., 2007) as it is the case for ESCs.

After successful reprogramming of mouse somatic cells, scientists demonstrated reprogramming of various human somatic cells (Aasen et al., 2008; Giorgetti et al., 2009; Park et al., 2008; Takahashi et al., 2007; Yu et al., 2007) as well as the generation of disease-specific iPSC lines (Carvajal-Vergara et al., 2010; Ebert et al., 2009; Lee et al., 2009; Marchetto et al., 2010; Park et al., 2008; Raya et al., 2009; Soldner et al., 2009). These disease-specific iPSCs provide a powerful tool for disease modelling *in vitro* and drug development. Once technical limitations are eliminated, iPSCs represent an alternative source for cellular replacement therapies because patient–specific iPSCs for cell or tissue grafts will not lead to immunological rejection.

Human embryonic stem cells

In 1998, human ESCs were derived from pre-implantation stage embryos that were donated for research after being targeted for disposal either because they were surplus embryos or because they were of poor quality. These cells are considered to be pluripotent because they express the core genes of pluripotency *Nanog*, *Oct4* and *Sox2* (Adachi et al., 2010; Hay et al., 2004; Matin et al., 2004; Xu et al., 2009; Xu et al., 2008; Zaehres et al., 2005), differentiate into cells of all three germ layers (Hoffman and Carpenter, 2005), and form teratomas after injection into an immune-deficient animal (Thomson et al., 1998). Human ESCs share several features with mouse EpiSCs forming cell colonies with a flat morphology, reduced tolerance to passaging as single cells, dependence on FGF2 and Activin signalling (Xu et al., 2008), and the tendency towards X chromosome inactivation in female cell lines (Silva et al., 2008b). Consequently, they display more a primed pluripotent state than the ground state of mouse ESCs.

1.1.4 Pluripotent stem cells as model to study neural development

PSCs can be stimulated to differentiate into many different neuronal subtypes by use of *in vitro* models mimicking underlying molecular and cellular mechanisms of *in vivo* developmental processes (Lee et al., 2000b; Li et al., 2005; Perrier et al., 2004; Watanabe et al., 2005; Wichterle et al., 2002; Ying et al., 2003b). Conversely, insights into the mechanisms that direct stem cells into a specific neural fate may provide an improved understanding of the mechanism of neural differentiation *in vivo*, particularly for early human development. Therefore, the approach of hESC and disease-specific hiPSC allows us to dissect the complex mechanism of normal and pathological neurodevelopment.

1.2 Midbrain dopaminergic development

1.2.1 Neural induction

The first insights into the understanding of how cells of the ectoderm become neural tissue came from the pioneering work of Spemann and Mangold nearly 100 years ago (Spemann and Mangold, 1923). Using differently pigmented species of amphibians to distinguish the cells of donor and host, they transplanted a small piece of the dorsal blastopore lip of the gastrulating embryo, now known as Spemann's ''organizer'', into the ventral side of another embryo at gastrula stage. They found that the cells of host tissue formed a secondary axis composed of a neural tube, notochord and paraxial muscles demonstrating the capability of the organiser to induce neural fate in vertebrate embryos. Equivalent organizing regions were found in zebrafish (shield), chick (Henson's node), and mouse (node) embryos (Beddington, 1994; Boettger et al., 2001; Shih and Fraser, 1996). Each of these organisers induces a neural plate not only within the same species but also when transplants are carried out across classes (Blum et al., 1992; Hatta and Takahashi, 1996; Kintner and Dodd, 1991), suggesting an evolutional conserved strategy for neural induction.

Experiments showed that explants from the frog ectoderm, a region fated to become epidermis and neural tissue, gave rise to epidermal cells when cultured without the addition of growth factors. In contrast, when the ectodermal explants were dissociated into single cells, the cells became neural (Godsave and Slack, 1989; Grunz and Tacke, 1989). A number of BMP antagonists secreted by the organizer have been identified as essential molecules in neural induction such as Noggin (Furthauer et al., 1999; Lamb et al., 1993; Smith and Harland, 1992; Smith et al., 1993; Zimmerman et al., 1996), Chordin (Piccolo et al., 1996; Sasai et al., 1995; Sasai et al., 1994), Follistatin (Fainsod et al., 1997; Hemmati-Brivanlou et al., 1994), Cerberus (Bouwmeester et al., 1996; Piccolo et al., 1999), XNr3 (Hansen et al., 1997; Smith et al., 1995), Gremlin/Drm and Dan (Dionne et al., 2001; Eimon and Harland, 2001; Hsu et al., 1998; Khokha et al., 2003; Pearce et al., 1999). Based on the findings in amphibians, the phenomenon of neural induction was explained by the 'default model' which proposes that ectodermal cells convert into neural plate in the absence of

extrinsic signals, while BMP activity directs them to become epidermis (Munoz-Sanjuan and Brivanlou, 2002).

Recent observations in chick and mice indicate that the process of neural induction is more complex than can be explained by the default model alone. In chick, mis-expression of BMP antagonists in the extra-embryonic or non-neural ectoderm does not induce the expression neural markers (Streit et al., 1998; Streit and Stern, 1999a, b) and grafted protein sources of BMP do not prevent neural development in the future neural plate (Streit et al., 1998), assuming that inhibition of BMP signalling alone is not sufficient for the specification of neural tissue. In support to this data, mouse mutants lacking the endogenous BMP antagonists Cerberus, Noggin and/or Chordin still develop a nervous system (Bachiller et al., 2000; Belo et al., 2000; McMahon et al., 1998; Mukhopadhyay et al., 2001). It is worth noting that the loss of BMP signalling in mouse mutants missing the BMP receptor 1a (*Bmpr1a*) resulted in an early neural differentiation, implicating a role of BMP signalling in timing of neural induction (Di-Gregorio et al., 2007). The outcome of this study also suggests that neural induction appears earlier in development than thought. Indeed, gene expression analysis in chick embryos revealed that neural induction seems to be already activated before gastrulation as *Erni*, a marker for neural induction, is expressed before the organizer region has formed (Streit et al., 2000).

BMP antagonists appeared not to be sufficient to induce neural cells, indicating that signals distinct from BMP antagonists are required for induction of neural fate. It has been proposed that FGFs and WNTs are involved in this process. Indeed, recent studies demonstrated that both FGF and WNT signalling can regulate BMP signalling (Baker et al., 1999; Eivers et al., 2008; Gomez-Skarmeta et al., 2001; Pera et al., 2003). Whether these pathways have independent functions in neural induction, beside their effects on BMP signalling, remains elusive.

Several studies indicated that the organiser itself is not required for neural induction because *Foxa2* mouse mutants lacking the node are still able to form a neural plate (Ang and

Rossant, 1994; Episkopou et al., 2001; Klingensmith et al., 1999). Reinforcing this hypothesis; a neural plate is still formed after the gastrula organizer is surgically removed in chick, frog, zebrafish and mouse embryos (Davidson et al., 1999; Shih and Fraser, 1996; Smith and Schoenwolf, 1989). It has been proposed that the embryo possesses more than one organizer. Indeed, the anterior visceral endoderm (AVE) might be involved in the formation of neural tissue as it exists at the right time to induce neural tissue, being present shortly after implantation (Thomas et al., 1998). Recent results show that the AVE plays mainly a role in the formation of the anterior neural tissue, since embryos where the AVE is removed display a dramatic loss of anterior neural tissue (Martinez-Barbera and Beddington, 2001; Thomas and Beddington, 1996). However, anterior neural induction is still initiated in *Nodal* mutants in the absence of the AVE (Camus et al., 2006) suggesting the AVE might not always be required for anterior neural induction and is likely to play an indirect or secondary role.

1.2.2 Neural patterning – regionalisation and specification of midbrain dopaminergic neurons

After initial neural induction, the neural plate folds and fuses at the midline to generate the neural tube. During this process of neurulation, cells of the neuroectoderm become patterned along the anterior-posterior and dorsal-ventral axis. The major mechanism underlying patterning is based on the actions of inductive signals that direct the fate of neural progenitors in a concentration dependent manner. There are three local signalling centres which establish the antero-posterior axis: the anterior neural ridge (ANR) at the anterior end of the neural plate (Houart et al., 1998; Shimamura and Rubenstein, 1997), the zona limitans intrathalamica (ZLI) in the middle of the diencephalon (Echevarria et al., 2003; Kiecker and Lumsden, 2004; Vieira et al., 2005) and the isthmic organiser (IsO) at the midbrain hindbrain border (MHB) (Martinez et al., 1991). These domains are characterised by their complex expression of sonic hedgehog (*Shh*, in ZLI), the fibroblast growth factor 8 (*Fgf8*, in ANR, ZLI, and IsO), the BMP antagonists *Chordin* and *Noggin* (in ANR), and *Wnt1*

(in IsO) (Figure 1.1). As a result of their combined actions, the most anterior end of the neural tube gives rise to the forebrain, while more posterior regions form the midbrain, the hindbrain and the spinal cord.

The establishment of the dorsal-ventral axis is a consequence of the antagonistic interaction between the ventralising factor, SHH, emanating from the notochord and the ventral midline of the neural tube and the dorsalising factors WNT and BMP from the roof plate (Chizhikov and Millen, 2005; Lee et al., 2000a; Lee and Jessell, 1999). Cells along the dorsal-ventral axis are subdivided into the floor plate at the ventral side, the basal plate, the alar plate, and the roof plate in the dorsal most region of the neural tube by their expression of specific genes.

DA neurons of the midbrain arise ventrally and rostrally to the midbrain-hindbrain border (MHB) as consequence of the morphogenetic gradient between SHH and FGF8. SHH secreted from the ventral midline cells of the floorplate induces mDA neurons in the ventral region of the neural tube, whereas the isthmic secretion of FGF8 determines the position and size of the mDA neuron field along the anterior-posterior axis (Figure 1.1) (Burbach and Smidt, 2006; Prakash and Wurst, 2006; Ye et al., 1998). Additionally, members of the WNT family of secreted glycoproteins are expressed in the midbrain close to the MHB and may indirectly enhance the production or the survival of mDA neurons (Figure 1.1) (Castelo-Branco et al., 2003; Danielian and McMahon, 1996; Smidt and Burbach, 2007). The induction and positioning of mDA progenitors in the neural tube occur between embryonic days (E) 7.5 and E9 of mouse development (Gale and Li, 2008).

As cell proliferation and differentiation progress during the formation of the brain, the developing ventral midbrain becomes thicker and layered into a ventricular zone, an intermediate zone, and a marginal zone based on their regional traits and expression of combinations of specific genes. In the ventricular zone, the cells are marked by the expression of *Lmx1a*, *Lmx1b*, *Ngn2*, *Msx1*, *Fox2a*, and *Dmrt5* (Andersson et al., 2006a; Andersson et al., 2006b; Ferri et al., 2007; Gennet et al., 2011; Kele et al., 2006; Smidt et

al., 2000). These cells retain their proliferative neural stem cell properties. As soon as the cells become part of the intermediate zone, they exit the cell cycle and start the post-mitotic differentiation into mDA neurons (E11.5-15). As they differentiate, the cells migrate ventrally into the mantle zone and then laterally. In contrast to mDA progenitors, these cells express the mDA neuronal markers *Nurr1*, *Pitx3*, and *TH* (Maxwell et al., 2005; Saucedo-Cardenas et al., 1998; Smidt et al., 1997; Zetterstrom et al., 1997).

1.2.3 Isthmus assiociated factors

The IsO is located at the border between the expression domains of the transcription factors *Otx2*, expressed in the presumptive fore- and midbrain, and *Gbx2*, expressed in the presumptive hindbrain and spinal cord (Joyner et al., 2000). This organizer is required for the specification of all cells in the posterior midbrain and in the anterior hindbrain. When the IsO was transplanted into naive diencephalic tissue then these presumptive forebrain cells differentiated into midbrain cells (Martinez et al., 1991) whereas the transplantation of IsO into the posterior hindbrain resulted in the formation of an ectopic cerebellum (Marin and Puelles, 1994). Based on these observations the IsO was identified as signaling centre.

OTX2

OTX2 is a homeodomain-containing transcription factor. At E6, it is detected in the visceral endoderm, the presumptive AVE implicated in the formation of anterior neural tissue, and the entire epiblast (Ang et al., 1994; Simeone et al., 1993). As gastrulation proceeds, *Otx2* expression becomes restricted to the anterior end of the embryo covering all three germ layers (Ang et al., 1994; Simeone et al., 1993; Simeone et al., 1995). In the neuroectoderm, it is later confined to the presumptive forebrain and midbrain with a sharp boundary at the MHB (Acampora et al., 1995; Ang et al., 1994; Millet et al., 1996; Simeone et al., 1992).

The evidence that OTX2 has an important role in anterior neural patterning derives from studies on mice lacking *Otx2*. These embryos die early during embryogenesis having lost the anterior neuroectoderm (Acampora et al., 1995; Ang et al., 1996; Matsuo et al., 1995). In

addition, mouse mutant embryos where *Otx2* was replaced by the *lacZ* reporter gene displayed a loss of *lacZ* expression in the epiblast indicating that *Otx2* itself is required for its induction in the epiblast (Acampora et al., 1995). Moreover, OTX2 seems to be involved in anteriorising the visceral endoderm as it remained to the distal region in these mutant embryos (Acampora et al., 1995). Chimeric embryos containing $Otx2^{-/-}$ epiblast and wild-type visceral endoderm rescued the induction of the early anterior neural plate in the mutant embryos, but failed to develop fore- and midbrain tissue (Rhinn et al., 1998). Altogether, the results of these experiments emphasise the necessity of OTX2 for the induction and regionalization of the anterior neuroectoderm.

As early as E7.5, *Gbx2* is expressed in the anterior hindbrain adjacent to the posterior end of the *Otx2* expression domain. The border of these mutually exclusive expression domains marks the prospective midbrain hindbrain border where the IsO is located (Joyner et al., 2000). An important function of OTX2 is to control proper positioning of the MHB as well as the IsO. *In vivo* studies revealed that ectopic expression of *Gbx2* or reduced *Otx2* expression in the midbrain shifts the IsO to a more anterior position and subsequently ablates the midbrain section of mDA neurons (Acampora et al., 1997; Millet et al., 1999; Puelles et al., 2003); whereas overexpression of *Otx2* or loss of *Gbx2* in the hindbrain results in an expansion of the midbrain caused by the caudal shift of the IsO (Broccoli et al., 1999; Sunmonu et al., 2011; Wassarman et al., 1997).

It was demonstrated that in the ventral midbrain (E11.5) *Otx2* is a direct downstream target of WNT1/β-catenin signalling as Chip-qPCR analysis uncovered a direct association of the β-catenin complex to the *Otx2* promotor (Chung et al., 2009). Additionally, detailed analysis of mouse embryos at E11.5 in that Otx2 was inserted into the gene locus of Engrailed 1 (*En1*, $En1^{+/Otx2}$), which is expressed in the midbrain region from E8, showed an expansion of the *Wnt1* expression domain while lack of *Otx2* in $En1^{+/Cre}$; $Otx2^{flox/flox}$ embryos (E12.5) resulted in a loss of *Wnt1* expression in the ventral midbrain (Prakash et al., 2006) indicating

a positive regulatory feedback loop between OTX2 and WNT1 to maintain their expression in the ventral midbrain.

OTX2 may also play a role during neurogenesis of mDA neurons. Mouse mutants in which *Otx2* was conditionally inactivated by *Cre* recombinase under the transcriptional control of *En1* (*En1*$^{+/Cre}$; *Otx2*$^{flox/flox}$) showed a reduced number of TH positive cells in the midbrain (Puelles et al., 2004). Consistent to this finding, mouse mutants overexpressing (ov) *Otx2* by *En1-Cre* activity (*En1*$^{+/Cre}$*; Otx2*$^{ov/+}$) displayed an increased number of TH positive cells throughout the ventral midbrain due to an enhanced proliferation of mDA progenitor cells (Omodei et al., 2008). Moreover, OTX2 controls the identity and fate of neural mDA progenitors by suppressing the expression of the transcription factor *Nkx2.2* which has been shown to be sufficient to repress the mDA neuronal fate and to induce serotonergic 5HT positive neurons in the ventral midbrain (Prakash et al., 2006; Puelles et al., 2004).

Recent findings demonstrated a specific role for OTX2 in a subtype of mDA neurons as in the adult mouse brain OTX2 is restricted to the VTA neurons and excluded from SN neurons (Di Salvio et al., 2010a; Di Salvio et al., 2010b). Two VTA specific functions of OTX2 have been uncovered: firstly, OTX2 reduces the DA uptake in VTA neurons and, secondly, it antagonizes vulnerability to the Parkinsonian toxin MPTP (1-methyl-4-phenyl-1,2,3,6-tetrahydropyridine) (Di Salvio et al., 2010a; Di Salvio et al., 2010b).

FGF8

The fibroblast growth factor 8 (FGF8) is an important diffusible signalling molecule of the IsO. FGF8 containing beads can mimic the isthmic transplant's ability to induce midbrain and cerebellum characteristics in the diencephalon or cerebellum properties in the posterior hindbrain (Crossley and Martin, 1995; Crossley et al., 1996; Irving and Mason, 2000; Martinez et al., 1999). From E8.5, *Fgf8* is expressed in the caudal, *Gbx2*-positive expression domain of the MHB, a region that will form the isthmus and anterior hindbrain (Crossley and Martin, 1995). Genetic studies in mice have demonstrated the crucial role of *Fgf8* in the development of the midbrain as homozygous *Fgf8* mouse mutants lack the posterior

midbrain where mDA neurons arise (Meyers et al., 1998). *Fgf8* is in a cross-regulatory network with *Wnt1*, *En1*, *En2*, *Pax2*, and *Pax5* which establishes and maintains the IsO (Wurst and Bally-Cuif, 2001; Ye et al., 2001). FGF8 is required to maintain the expression of these early midbrain-hindbrain regulatory factors and additionally stable expression of *Fgf8* is controlled by the correct expression of *Wnt1*, *En1*, *En2*, *Pax2*, and *Pax5* (Lee et al., 1997; Lun and Brand, 1998; McMahon et al., 1992; Meyers et al., 1998; Reifers et al., 1998; Schwarz et al., 1997; Wurst et al., 1994; Wurst and Bally-Cuif, 2001; Ye et al., 2001; Ye et al., 1998).

FGF8 has further been suggested to stimulate cell proliferation in the midbrain and play a role in mDA development. In embryos where *Fgf8* was ectopically expressed under the control of the *Wnt1* enhancer the midbrain expanded in size. The self-renewability of mDA neural progenitors was supported *in vitro* by addition of FGF8 (Chung et al., 2011; Lee et al., 1997). Additionally, mDA neurons in E9 midbrain explants are only generated in the presence of FGF8 indicating a requirement of FGF8 in the specification mDA neurons (Ye et al., 1998).

WNTs

Members of the WNT family are secreted palmitoylated glycoproteins (Willert et al., 2003). In the nervous system, they are involved in cell proliferation (Castelo-Branco et al., 2003; Chenn and Walsh, 2002; Megason and McMahon, 2002; Taipale and Beachy, 2001), fate decision (Baker et al., 1999; Castelo-Branco et al., 2003; Dorsky et al., 1998; Wilson et al., 2001), neuronal differentiation (Hall et al., 2000; Krylova et al., 2002; Patapoutian and Reichardt, 2000), and neuroprotection (Alvarez et al., 2004; De Ferrari et al., 2003; Fuentealba et al., 2004; L'Episcopo et al., 2011; Zhang and Carthew, 1998). So far, 19 *Wnt* ligands have been identified in the mouse genome. Thirteen of these were shown to be expressed in the developing midbrain (Rawal et al., 2006). Among them, *Wnt1* and *Wnt5a* have been demonstrated to play an important role in the development of mDA neurons (Castelo-Branco et al., 2006; Castelo-Branco et al., 2003; Prakash et al., 2006; Schulte et

al., 2005). WNT proteins have been postulated to activate three different pathways: the canonical WNT pathway, ß-catenin mediated, the non-canonical WNT pathway and the WNT/Ca^{2+} pathway. Much work has been done to understand WNT/β-catenin signalling (Barker, 2008; Logan and Nusse, 2004). Briefly, WNT ligand binds to the receptor protein Frizzled (FZD) and the co-receptor low-density lipoprotein receptor related protein 5/6 (LRP5/6) (Figure 1.3 B). The formation of this complex leads to the intracellular phosphorylation of LRP5/6 and thus mediates the WNT signal into the cell which activates Dishevelled (DVL) by phosphorylation and subsequently inactivates glycogen-synthase-kinase-3β (GSK3β), a key modulator of this pathway. In the absence of WNT signals, GSK3β forms a complex with Axin, adenomatous polyposis coli (APC) and Diversin resulting in the phosphorylation and degradation of β-catenin. When cells receive WNT signals, the degradation of β-catenin is inhibited by physically displacing GSK3β from the destruction complex. Stabilised β-catenin enters the nucleus and interacts with T-cell factor/lymphoid enhancer binding factor (TCF/LEF) to affect transcription of WNT target genes such as *Cyclin D1*, *Axin2*, and *Myc*.

Wnt1 is detected as early as E8.5 in the mouse embryo rostral and adjacent to the *Fgf8* expression domain at the MHB (Davis and Joyner, 1988; Wilkinson et al., 1987). In the midbrain, its expression continues until E14 and becomes restricted to the roofplate, the dorsal midline, and the floorplate (Davis and Joyner, 1988; Parr et al., 1993; Wilkinson et al., 1987). *Wnt1* is crucial for the establishment of the MHB as mouse embryos homozygous for *Wnt1* null alleles display a loss of the midbrain and anterior hindbrain by E9.5 (Bally-Cuif et al., 1995; McMahon and Bradley, 1990; McMahon et al., 1992; Thomas and Capecchi, 1990). In this context it is worth noting that *Wnt1* is not required to induce *Fgf8* expression because in mice lacking *Wnt1, Fgf8* expression is initially induced and later lost (McMahon and Bradley, 1990; McMahon et al., 1992). In addition, the expression pattern of *Fgf8* is not changed in embryos where *Wnt1* is expressed under the control of the endogenous *En1* promotor, a gene which is expressed in the midbrain and hindbrain domain from E8

(Panhuysen et al., 2004). More likely, *Wnt1* plays an important role in stabilising and maintaining *Fgf8* expression at the MHB as it was shown in chick embryos (Canning et al., 2007).

WNT1 signalling is also important in maintaining *En1* expression as in *Wnt1*-null mutant mice its expression is lost (Danielian and McMahon, 1996; McMahon et al., 1992). Since *En1* and *En1/2* knock-outs display a similar phenotype to the *Wnt1*-null in mice (Simon et al., 2001; Wurst et al., 1994) and overexpression of *En1* in *Wnt*$^{-/-}$ mice rescued the mid–hindbrain phenotype (Danielian and McMahon, 1996), *En1* is thought to be a target of *Wnt1*.

WNT1 is generally considered a canonical WNT as it co-localizes with β-catenin in the ventral midbrain (Castelo-Branco et al., 2003). Reinforcing this link, inhibition of GSK3β or overexpression of *β-catenin*, which are downstream targets of the canonical WNT pathway, resulted in similar phenotypes in the ventral midbrain as *Wnt1* activation (Castelo-Branco et al., 2004; Castelo-Branco et al., 2003; Danielian and McMahon, 1996; Prakash et al., 2006; Tang et al., 2010). In the development of mDA neurons, WNT1 appears to have multiple roles. WNT1 regulates the expression of *Lmx1a*, a key transcription factor of mDA neurons, (Chung et al., 2009) and activates *Otx2* that in turn inhibits *Nkx2.2* expression, a suppressor of the DA lineage (Prakash et al., 2006). Several independent studies further demonstrated a role of WNT1 in the proliferation of DA neural precursors (Castelo-Branco et al., 2003; Megason and McMahon, 2002; Panhuysen et al., 2004; Rimerman et al., 2000). Treatment of neural stem cells with WNT1 yields an increase of proliferating NURR1 positive precursors and an upregulation of *Cyclin D1* and *D3* which are involved in regulating cell cycle progression (Castelo-Branco et al., 2003). Confirming the importance of WNT1 in the proliferation of mDA precursors *in vivo*, mouse embryos display an expansion of the caudal midbrain when *Wnt1* is ectopically expressed in the *En1* expression domain (Panhuysen et al., 2004).

At E9.5, *Wnt5* is detected in the floor plate and basal plate of the developing midbrain (Andersson et al., 2008; Blakely et al., 2011; Yamaguchi et al., 1999). From E12.5 until

E14.5, *Wnt5a* expression is extended from the ventricular zone into the intermediate and marginal zone of the ventral midbrain (Andersson et al., 2008; Blakely et al., 2011). Later on, in the postnatal mouse, *Wnt5* expression is lost in SN neurons while neurons of the VTA still show a low expression of *Wnt5a* (Andersson et al., 2008).

Several studies investigated the molecular mechanism of WNT5a in the cells of the developing ventral midbrain and they found that WNT5a activates specific components of the non-canonical WNT pathway: Casein kinase 1, DVL and the small GTPase RAC1 (Andersson et al., 2008; Blakely et al., 2011; Bryja et al., 2007; Schulte et al., 2005). WNT5A plays an important role in the terminal differentiation of mDA neurons as it increases the number of TH positive neurons by promoting DA differentiation of NURR1 positive precursors (Andersson et al., 2008; Bryja et al., 2007; Castelo-Branco et al., 2003). Moreover, when ventral midbrain explants were exposed to WNT5a, the axons of DA neurons were significantly elongated whereas mice lacking *Wnt5a* showed a reduced length of mDA neurites (Blakely et al., 2011) demonstrating the importance of WNT5a in axon outgrowth of DA neurons.

Engrailed genes

Engrailed 1 and 2 (EN1/2) are homeobox transcription factors. They are expressed across the MHB in the caudal midbrain and rostral hindbrain during early neural development from about E8 (Davidson et al., 1988; Davis and Joyner, 1988; Davis et al., 1988; McMahon et al., 1992; Wurst et al., 1994). The expression of both genes is maintained in adult SN and VTA (Davis and Joyner, 1988; Davis et al., 1988; Sgado et al., 2006; Simon et al., 2001). Mutant mice homozygous null for *En1/2* (*En1*$^{-/-}$*; En2*$^{-/-}$) completely lack the mid-hindbrain region, a region where mDA neurons arise. Interestingly, neither single mutants show a completely loss of the mid-hindbrain region (Liu and Joyner, 2001; Simon et al., 2001) implying a functional compensation for each other. EN1/2 have at least two distinct functions during the development of mDA neurons. Firstly, they take part in the regionalisation of the MHB as they are essential to maintain the expression of the isthmic related factors *Wnt1* and

Fgf8 (Liu and Joyner, 2001). Secondly, as development progresses, EN1/2 are required for the survival of mDA neurons. These neurons are initially generated in *En1/2* double mutant mice but soon thereafter die through an activation of Caspase-3, a crucial factor of apoptosis (Alberi et al., 2004; Sgado et al., 2006; Simon et al., 2001). In this context it was recently reported that infusion of EN1/2 into the SN of mice treated with MPTP, a mitochondrial complex I toxin which is commonly used for PD models, resulted in a rescue of mDA neurons against cell death through upregulation of translation of the two mitochondrial complex I proteins NDUFS1 and NDUFS3 (Alvarez-Fischer et al., 2011).

LMX1B

Ever since the LIM homeodomain transcription factor LMX1B was detected in DA neurons of the adult SN and VTA as well as in mDA progenitors (Guo et al., 2008; Smidt et al., 2000), LMX1B has been suggested to be required for mDA development. At E8.5, *Lmx1b* is expressed at the MHB (Guo et al., 2007). Mouse embryos lacking *Lmx1b* show a loss of *Fgf8* expression and isthmus regulatory genes *Wnt1*, *En1/2*, *Pax2*, and *Gbx2* revealing a role for *Lmx1b* in the development of the IsO (Guo et al., 2007). In these mouse mutant embryos, all mDA neurons are lost by E15.5. This phenotype is most likely caused by an increased cell death (Guo et al., 2007) as a consequence of abolished *En1/2* expression. However, conditional knock-out of *Lmx1b* in DA neurons (using *TH-Cre* mice) has no effect on terminal differentiation and survival of mDA neurons. It is worth noting that *Lmx1a*, another member of the LIM homeodomain transcription factor family, is also expressed in mDA neurons (Andersson et al., 2006b) and might compensate the loss of *Lmx1b* at later stages (Nakatani et al., 2010; Yan et al., 2011).

1.2.4 Floorplate associated factors

SHH

In the early stages of development, *Shh* is expressed in the notochord and the floor plate of the neural tube. It is one of the first factors involved in inducing the ventral cell types,

including DA neurons (Bayly et al., 2007; Blaess et al., 2006; Fedtsova and Turner, 2001; Hynes et al., 1995; Ye et al., 1998). Mechanisms underlying SHH signal transduction have not been fully elucidated. Broadly, secreted SHH binds to the twelve-pass membrane hedgehog receptor patched (PTC) to relieve inhibition of the seven-membrane spanning G-protein smoothened (SMO) by PTC (Figure 1.3 C). As soon as SMO inhibition is relieved, the GLI zinc finger transcription factors are modified so that GLI2 and GLI1 are activated while GLI3 is inactivated (Blaess et al., 2006; Fuccillo et al., 2006).

Analysis of *Shh*-null mutant mice revealed a defect in the developing midbrain and forebrain by E11.5 (Chiang et al., 1996), confirming its requirement. In the absence of *Shh*, floor plate cells were not present, suggesting that *Shh* is required for the induction of the floor plate (Chiang et al., 1996). Several studies have postulated an antagonistic effect between the canonical WNT signalling and the SHH pathway in mDA development. *Shh* expression is maintained in the ventral midbrain when *ß-catenin* was conditionally abolished by *Shh-Cre* (Joksimovic et al., 2009) whereas in mouse embryos with *Shh-Cre*-mediated expression of stabilized *ß-catenin* resulted in a reduction of *Shh* and its target genes (Tang et al., 2010). In contrast, Chung et al (2009) recently reported that overexpression of the WNT and SHH target genes *Oxt2*, *Lmx1a*, and *Foxa2* significantly promoted the generation of mDA neurons during *in vitro* differentiation assuming a synergistic interaction of the SHH and WNT pathways (Chung et al., 2009).

FOXA2

FOXA2 is a forkhead/winged helix transcription factor. During embryonic development, it is expressed within the central nervous system in the node, the notochord and floor plate (Sasaki and Hogan, 1993). The expression of *Foxa2* can be induced by SHH via activation of GLI1 (Hynes et al., 1997; Ruiz i Altaba, 1998; Sasaki and Hogan, 1994; Sasaki et al., 1997). Mouse embryos where *Foxa2* expression is abolished show an absence of the node and notochord (Ang and Rossant, 1994; Weinstein et al., 1994). As a consequence of the missing notochord, the SHH signalling is absent therefore the floor plate is not formed (Ang

and Rossant, 1994). Two independent studies on conditional *Foxa1* and *Foxa2* double mutant mouse embryos have demonstrated that *Foxa1/2* regulate the expression of midbrain-specific developmental factors such as *Lmx1a/b*, *Nurr1*, *TH*, and *Ngn2* (Ferri et al., 2007; Lin et al., 2009). Moreover, it was reported that forced expression of *Foxa2* in differentiating mouse ES cells and NPCs resulted in a significant increase of TH positive neurons (Kittappa et al., 2007; Lee et al., 2010). Together, these data suggest a central role of FOXA2 in mDA development.

1.2.5 Genes regulating midbrain dopaminergic development

LMX1A

LMX1A is a member of the LIM homeodomain transcription factor family. The expression of *Lmx1a* is initiated at around E9.5 and maintained in differentiated NURR1 and LMX1B double positive DA neurons (Andersson et al., 2006b). In the chick, *Lmx1a* appears to be crucial for mDA development, as knock-down of *Lmx1a* using siRNA reduces the number of postmitotic NURR1/LMX1B double positive DA neurons (Andersson et al., 2006b). In contrast, loss of *Lmx1a* in mice results in only minor mDA defects (Ono et al., 2007). Additionally, forced expression of *Lmx1a* in stably transformed mouse ES cells increases the number of mDA neurons during *in vitro* differentiation shown by the mDA neuronal identity seen in 75-95% of the derived neurons (Friling et al., 2009).

SHH appeared to be an inducer of *Lmx1a* since chick midbrain explants exposed to SHH show an increase of LMX1A positive cells (Andersson et al., 2006b). However, a recent study reported an induction of *Lmx1a* by WNT signalling, independent of SHH signalling (Chung et al., 2009).

LMX1A induces the expression of *Msx1* which inhibits expression of negative regulators of neurogenesis, such as *Nkx6.1*, and induces the neurogenic factor, *Ngn2* (Andersson et al., 2006b). Notably, the same study showed that Msx1 is neither necessary nor sufficient for mDA generation. Additional pathways may function downstream of LMX1A. Indeed, Chung

et al. (2009) showed a direct regulation of *Otx2*, *Pitx3*, and *Nurr1* by LMX1A (Chung et al., 2009).

NURR1

NURR1 is an orphan nuclear receptor which belongs to the conserved family of ligand-activated transcription factors (Aranda and Pascual, 2001; Giguere, 1999; Perlmann and Wallen-Mackenzie, 2004). At E10.5, it is expressed in the ventral midbrain before the onset expression of the DA marker TH (E11.5). Its expression continues into adulthood in mDA neurons (Saucedo-Cardenas et al., 1998; Smidt et al., 1997; Wallen et al., 1999; Zetterstrom et al., 1997). Analysis of *Nurr1* knock-out mice revealed that NURR1 has multiple roles during mDA development.

Firstly, it regulates the transcription of genes involved in maintenance and survival of mDA neurons such as the receptor tyrosine kinase (*Ret*) which in turn responds to trophic factors such as glial cell line-derived neurotrophic factor (GDNF) (Galleguillos et al., 2010; Kadkhodaei et al., 2009; Perlmann and Wallen-Mackenzie, 2004; Saucedo-Cardenas et al., 1998; Smits et al., 2003; Zetterstrom et al., 1997). Secondly, it regulates the transcription of the genes which determine the DA neuron transmitter phenotype such as *TH*, the vesicular dopamine transporter 2 (*Vmat2*), and the DA transporter (*Dat*). In this context, overexpression of *Nurr1* in immortalized neural stem cells and in ESCs during differentiation specifies cells towards DA lineage (Chung et al., 2002; Kim et al., 2002; Kim et al., 2003; Lee et al., 2010; Sakurada et al., 1999). This leads to the suggestion that other factors are required to direct the DA precursor cells into mature mDA neurons.

PITX3

The paired-like homeodomain transcription factor *Pitx3* has a tightly regulated expression in the SN and VTA in the brain where it is first detected at E11.5 (Smidt et al., 1997). Furthermore, DA cells in the SN express PITX3 prior to TH, whilst it sequence is reversed for

DA cells of the VTA (Maxwell et al., 2005). Accordingly, *Pitx3* deficiency resulted in the preferential loss of SN TH positive neurons during foetal development (Smidt et al., 2004).

1.3 Strategies for neural differentiation *in vitro* of pluripotent stem cells

So far, there are three types of protocols being used for differentiating ES cells towards a neuronal fate. These protocols are typically used to initiate a general differentiation programme and in recent years have been modified to include instructive factors that direct more lineage-specific neuronal differentiation, including the DA phenotype.

1.3.1 Embryoid body differentiation

This approach is based on the formation of embryoid bodies (EB) that are similar to the ICM of a blastocyst as it consists of an outer hypoblast-like layer and an epiblast-like core which is capable of differentiation into tissue of all three germlayers (Coucouvanis and Martin, 1995; Keller, 2005; Keller, 1995). The EB differentiation protocol can be divided into four main steps: 1) Differentiation of ES cells into EBs containing all three germ layers. 2) Enrichment of the neuroectodermal fate by inhibiting mesodermal cells using selection medium. 3) Expansion and maintenance of neural precursor cells in the presence of FGF2 followed by an induction of DA neural cell fate using Ascorbic acid and the two morphogens SHH and FGF8. 4) Induction of neuronal differentiation in serum free medium. It has been demonstrated that over 30% of neurons express TH (Lee et al., 2000b). However, it is still unclear to what extent these cells represent a midbrain DA phenotype.

1.3.2 Stromal co-culture system

Neural differentiation of ESCs has been shown to be induced by the stromal derived inducing activity (SDIA). This method involves the use of the skull bone marrow derived

stromal cell line PA6 (Kodama et al., 1986) that efficiently induces neuronal differentiation of ESCs with a high proportion of TH positive neurons (Kawasaki et al., 2000). About 30 % neurons were TH positive of which only 10-15% displayed a midbrain DA phenotype (Kawasaki et al., 2000; Kawasaki et al., 2002; Zhao et al., 2004). The nature of SDIA is still not known. It was suggested that SDIA may be a secreted factor that is secondarily bound to the cell surface, as treatment with Heparin removes the neural inducing activity and neural differentiation is still induced in the absence of physical contact to ESC.

1.3.3 Monolayer differentiation

In this method, undifferentiated ES cells are dissociated and plated at a low density onto gelatinised culture plates in chemical-defined N2B27 medium (Ying and Smith, 2003; Ying et al., 2003b). Through this method, it was demonstrated that about 75% cells express the neuroepithelial marker SOX1 by day 3 and 4 (Ying and Smith, 2003; Ying et al., 2003b). Only few TH positive cells are generated but the number of DA neurons can be significantly increased by the addition of SHH and FGF8 (Ying and Smith, 2003; Ying et al., 2003b). The serum-free chemical-defined condition of this protocol allows studies of the role of signalling molecules in neural differentiation.

1.4 FGF pathway

Fibroblast growth factor ligands and receptors are involved in diverse processes of early brain development including antero-posterior patterning, cell proliferation, survival and migration (Oki et al., 2010; Partanen, 2007; Sun et al., 1999).

1.4.1 FGF ligands

Fibroblast growth factors (FGF) are secreted glycoproteins. They are structurally related as they share a central core of ~120 amino acids and a high affinity for Heparin and Heparan

sulphate proteoglycans (Itoh and Ornitz, 2004; Ornitz and Itoh, 2001). The family includes 23 members (FGF1-23) of which FGF19 has not been identified in mouse yet (Itoh and Ornitz, 2004; Ornitz, 2000; Ornitz and Itoh, 2001). FGFs can be divided into 7 groups by phylogenetic and gene-location analysis (Table 1). In terms of their manner of action, they can be further sorted into hormone-like (FGF19: FGF19/21/23), intracellular (FGF11: FGF11-14) and canonical FGFs (FGF1: FGF1-2; FGF4: FGF4-6; FGF7: FGF3/7/22; FGF9: FGF9/16/20; FGF8: FGF8/17/18) whereby the canonical FGFs mediate the signal into the cell by binding Fibroblast growth factor receptors (FGFR) (Itoh and Ornitz, 2004, 2008).

1.4.2 FGF receptors

The FGFRs are single transmembrane proteins. The extracellular region contains the Ig-like domain that is required for binding the FGF ligands. The intracellular domain of FGFRs holds the domain responsible for the tyrosine kinase activity. There are five FGFRs (FGFR1-5). It is worth noting that FGFR5 does not have a tyrosine kinase domain and therefore might be involved in other processes (Wiedemann and Trueb, 2000). The FGFRs undergo alternative splicing in their extracellular domain in order to achieve a large variety of receptors with diverse affinities and specificities for their ligands (Powers et al., 2000; Zhang et al., 2006). After receptor-ligand binding, the receptors dimerise and mediate the signal into the cell by structural alterations that in turn activate the intracellular kinase domain and result in phosphorylated tyrosine residues inducing downstream signalling pathways such as Mitogen-activated protein kinases (MAPK/ERK), Phosphatidylinositol-3 kinase (PI3K) and Phospholipase C gamma (PLC-γ) (Figure 1.3 A) (Beenken and Mohammadi, 2009; Eswarakumar et al., 2005; Powers et al., 2000; Turner and Grose, 2010).

1.4.3 FGF signalling

The PLC-γ pathway is induced when phospholipase C-γ binds to the intracellular phosphorylated domain of FGFR (Burgess et al., 1990; Mohammadi et al., 1992; Mohammadi et al., 1991; Peters et al., 1992). Activated PLC-γ then hydrolyses

Phosphatidyl-inositol-4,5-bisphosphate to inositol trisphosphate (IP3) and Diacylglycerol (DAG) (Klint and Claesson-Welsh, 1999). IP3 cause the release of calcium from the endoplasmic reticulum, while DAG stimulates protein kinase C (PKC). In Xenopus, this pathway has been suggested to be involved in the caudalization of neural tissue by fgfr4 (Umbhauer et al., 2000).

Before activation of PI3K, FGFR substrate 2 (FRS2 also known as SNT1) binds to the phosphorylated FGFR allowing the phosphorylation of FRS2 (Hadari et al., 2001; Xu et al., 1998). As a consequence, Growth factor receptor-bound 2 (GRB2) recognise the phosphorylated sites of FRS2 and forms a complex in order to recruit the GRB2 associated binding protein 1 (GAB1) and subsequently induces the PI3K pathway (Hadari et al., 2001; Kim et al., 1994; Kim et al., 1998; Kouhara et al., 1997; Ong et al., 2000; Ong et al., 2001; Rodrigues et al., 2000; Xu et al., 1998). Activated PI3K leads to the generation of Phosphatidylinositol -3, 4, 5-tripphosphate (PIP3) via phosphorylation of Phosphatindylinositol-4,5-diphosphate (PIP2) (Denley et al., 2009; Rodriguez-Escudero et al., 2005; Whitman et al., 1988; Whitman et al., 1987). PIP3 mediates the translocation of the serine/threonine kinase AKT1 (also called protein kinase B) to its membrane-bound activator, the Phosphoinositide-dependent kinase (PDK1) (Fayard et al., 2010; Rodriguez-Escudero et al., 2005).

The MAPK/ERK pathway also requires the activation of the multi-protein complex FGFR-FRS2-GRB2. To induce the GTP binding protein RAS, GRB2 binds the adopter protein Son of sevenless (SOS) which drives the exchange of GDP for GTP in RAS (Clark et al., 1992; Kouhara et al., 1997; Lowenstein et al., 1992; Schlessinger, 1994). RAS then stimulates the MAPK/ERK pathway consisting of RAF1, RAC1, MEKKs (also called MAPKKK), MEK (also known as MAPKK), and ERK1/2 (extra-cellular signal-regulated kinases, alias MAPK) (Gardner et al., 1994; Kouhara et al., 1997; Marshall, 1995). This cascade controls the phosphorylation of target transcription factors which initiate expression of genes such as *c-*

Myc or *Cyclin D1* (Balmanno and Cook, 1999; Chuang and Ng, 1994; Lavoie et al., 1996; Sears et al., 1999; Terada et al., 1999).

1.4.4 FGF modulation

Initial studies in Zebrafish and Xenopus identified several Fgf target genes that share the same expression pattern as Fgf activity and are supposed to be in a negative feedback loop with FGF signalling (Gawantka et al., 1998; Kudoh et al., 2001): Sprouty (*spry1-4*) (Furthauer et al., 2001; Kramer et al., 1999), Sprouty related EVH1 domain proteins (s*preds1-3*) (Wakioka et al., 2001), Map kinase phosphatase 3 (*mkp3*) (Groom et al., 1996), *sef* (Furthauer et al., 2002; Lin et al., 2002; Tsang et al., 2002) and Fibronectin-leucine-rich transmembrane protein 3 (*flrt3*) (Bottcher et al., 2004).

Gain of function studies in mouse showed an antagonistic role of *Spry* in FGF signalling (Mailleux et al., 2001; Minowada et al., 1999). It was shown that SPRY is able to interfere with the FGF signalling in two different ways: 1) Inactivation of GRB2 (Hanafusa et al., 2002) or 2) Inhibition of RAF and consequently preventing the activation of the MAPK/ERK pathway (Sasaki et al., 2003).

SPRY and SPRED proteins share a cisteine-rich domain at the C terminus (Kato et al., 2003; Wakioka et al., 2001). However, the mechanism of SPREDs in inhibition of FGF signalling has not been identified yet. Most likely SPRED proteins interfere with FGF activity by binding RAF and/or RAS (Sasaki et al., 2003; Wakioka et al., 2001).

In agreement with the initial results for fgf target genes in Zebrafish and Xenopus, studies in mouse confirmed that MPK3 (also called PYST1 or DUSP6) also has an antagonistic role in FGF signalling (Urness et al., 2008). Moreover, it has been demonstrated that MKP3 inhibits the MAPK/ERK pathway via inactivation of ERK1/2 (Urness et al., 2008). Its expression pattern is very similar to that of the *Fgf8* indicating a regulatory effect of FGF8 on *Mkp3* expression (Eblaghie et al., 2003; Kawakami et al., 2003; Vieira and Martinez, 2005).

The transmembrane protein SEF, one of the other feedback regulators of FGF originally identified in zebrafish, prevents FGF signalling via FGFR1 as overexpression of *Sef* resulted in a reduced phosphorylation of FGFR1 (Kovalenko et al., 2006; Kovalenko et al., 2003).

1.4.5 Multiple roles of the FGF pathway during neural development

FGF signalling has been shown to be involved in neural induction (Alvarez et al., 1998; Hudson and Lemaire, 2001; Inazawa et al., 1998; Kengaku and Okamoto, 1995; Kudoh et al., 2004; Lamb and Harland, 1995; Rodriguez-Gallardo et al., 1997; Storey et al., 1998) but whether FGF signalling is necessary to initiate the neuroepithelium fate is still controversial ((Alvarez et al., 1998; Kengaku and Okamoto, 1995; Lamb and Harland, 1995; Storey et al., 1998; Streit et al., 2000) vs (Ribisi et al., 2000; Wills et al., 2010)). In the stem cell model, a blockade of FGF signalling via the MAPK/ERK pathway is required for maintaining mESCs in a pluripotent state (Silva et al., 2008a; Ying et al., 2008) and thus activation of this pathway drives ESCs into differentiation (Kunath et al., 2007; Stavridis et al., 2007). In this context, Kunath et al. (Kunath et al., 2007) suggest that ERK dependent FGF signalling is required for the exit from an ICM-like state toward epiblast ectoderm, whereas Stavridis et al. (2007, 2010) argue that this signalling acts in the transition of epiblast-like cells to neural progenitors. Additionally, other studies demonstrated that FGF signalling modulates BMP signalling which in turn promotes neural induction (Marchal et al., 2009; Pera et al., 2003; Stuhlmiller and Garcia-Castro, 2011). However, beyond the controversial role of FGF signalling in neural induction, a consensus is emerging that FGF signalling does play an important role during the induction of the posterior nervous system (Cox and Hemmati-Brivanlou, 1995; Doniach, 1995; Holowacz and Sokol, 1999; Kengaku and Okamoto, 1995; Lamb and Harland, 1995; Rentzsch et al., 2004; Ribisi et al., 2000; Wills et al., 2010). Several independent studies demonstrated that, FGF2 or FGF8 induce hindbrain characteristics in explants of forebrain tissue (Cox and Hemmati-Brivanlou, 1995; Crossley

and Martin, 1995; Crossley et al., 1996; Irving and Mason, 2000; Kengaku and Okamoto, 1995; Lamb and Harland, 1995; Martinez et al., 1999). Reinforcing the link that FGF signalling is involved in caudalisation of the neuroectoderm, mouse embryos at E~7.5 lacking *Fgf8* or exposed to small molecules blocking FGF signalling show an increase of the anterior tissue markers *Otx2* and *Six3* and a reduction of the hindbrain marker *Gbx2* (Oki et al., 2010; Sun et al., 1999).

Analysis of the spatial and temporal patterns of phosphorylated ERK during early mouse development uncovered an activation of ERK midbrain-hindbrain boundary at E8.5-10.5 which coincides with the expression of *Fgf8* (Crossley and Martin, 1995). When the embryos were exposed to FGFR specific inhibitors the phosphorylated ERK domain at the MHB was lost (Corson et al., 2003) implying that FGF acts via the MAPK/ERK pathway in mDA development.

So far only five FGF ligands have been shown to be expressed in embryos at gastrulation: FGF3 (Niswander and Martin, 1992; Wilkinson et al., 1988); FGF4 (Hebert et al., 1990; Niswander and Martin, 1992); FGF5 (Goldfarb et al., 1991; Haub and Goldfarb, 1991; Hebert et al., 1991); FGF8 (Crossley and Martin, 1995; Mahmood et al., 1995) and FGF17 (Maruoka et al., 1998). Of these ligands, *Fgf3*, *Fgf5*, and *Fgf17* null mutant mice are viable and fertile (Hebert et al., 1994; Mansour et al., 1993; Xu et al., 2000) whereas homozygous *Fgf4* mutant mouse embryos die shortly before gastrulation starts (Feldman et al., 1995). Mouse embryos lacking *Fgf8* are also not viable and die around E9.5 (Sun et al., 1999). As already mentioned above, besides the defects in the mesoderm and endoderm, *Fgf8* null embryos display an expansion of factors that are expressed in the anterior region of the developing embryo such as *Otx2* and *Six3* and a reduction of *Gbx2*, a marker for the presumptive hindbrain (Sun et al., 1999).

Furthermore, *Fgfr1* and *Fgfr2* are expressed and required at gastrulation stage shown by the death of gastrulating embryos lacking one of these genes (Arman et al., 1998; Deng et al., 1994; Orr-Urtreger et al., 1991; Yamaguchi et al., 1992; Yamaguchi et al., 1994). As the

phenotypes of *Fgf8* and *Fgfr1* mutants are similar, FGFR1 is considered to be the receptor of FGF8.

1.5 Hypthesis and aims

Effective induction of mDA neurons from stem cells is fundamental for realising their potential in biomedical applications for neurodegenerative diseases such as PD. This thesis focuses on the temporal actions of FGF signalling in mDA neuron fate specification of mouse PSCs. During early stages of neural development, FGF is involved in the formation of the hindbrain and forebrain. Therefore we supposed that inhibition of FGF activity guides PSCs into midbrain fate including the cell population from where mDA neurons arise. To study the effects of FGF blockade during DA neuron differentiation *in vitro*, I used mouse EpiSCs. I supposed that these cells potentially offer a better and more synchronised *in vitro* differentiation model than mouse ESCs. Therefore, I firstly validated mouse EpiSCs as an alternative model to study neural differentiation *in vitro*. Secondly, I investigated the effects of FGF/ERK inhibition during mDA neural differentiation of EpiSCs. Lastly, I demonstrate the functional capability of mouse EpiSC-derived mDA neurons *in vitro* and *in vivo*.

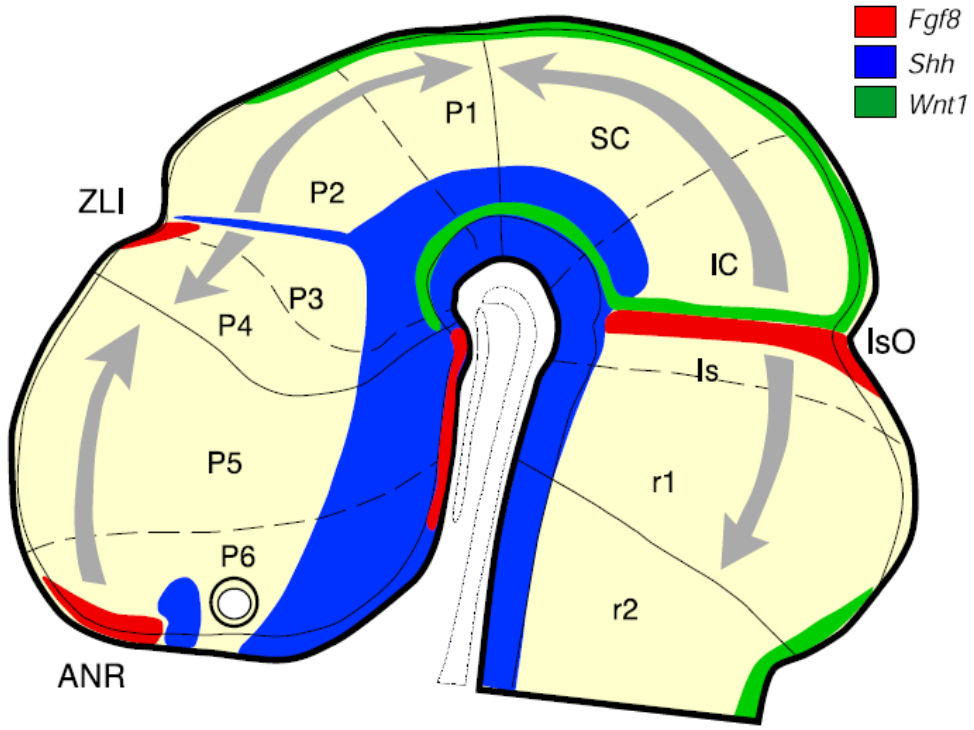


Figure 1.1 Schematic illustration of the signalling centres which establish the antero-posterior axis.

These centres are characterised by their complex expression of *Shh*, marked in blue, *Fgf*8, labelled in red, the BMP antagonists *Chordin* and *Noggin* (in ANR, not shown), and *Wnt1*, displayed in green. (Echevarria et al., 2003)

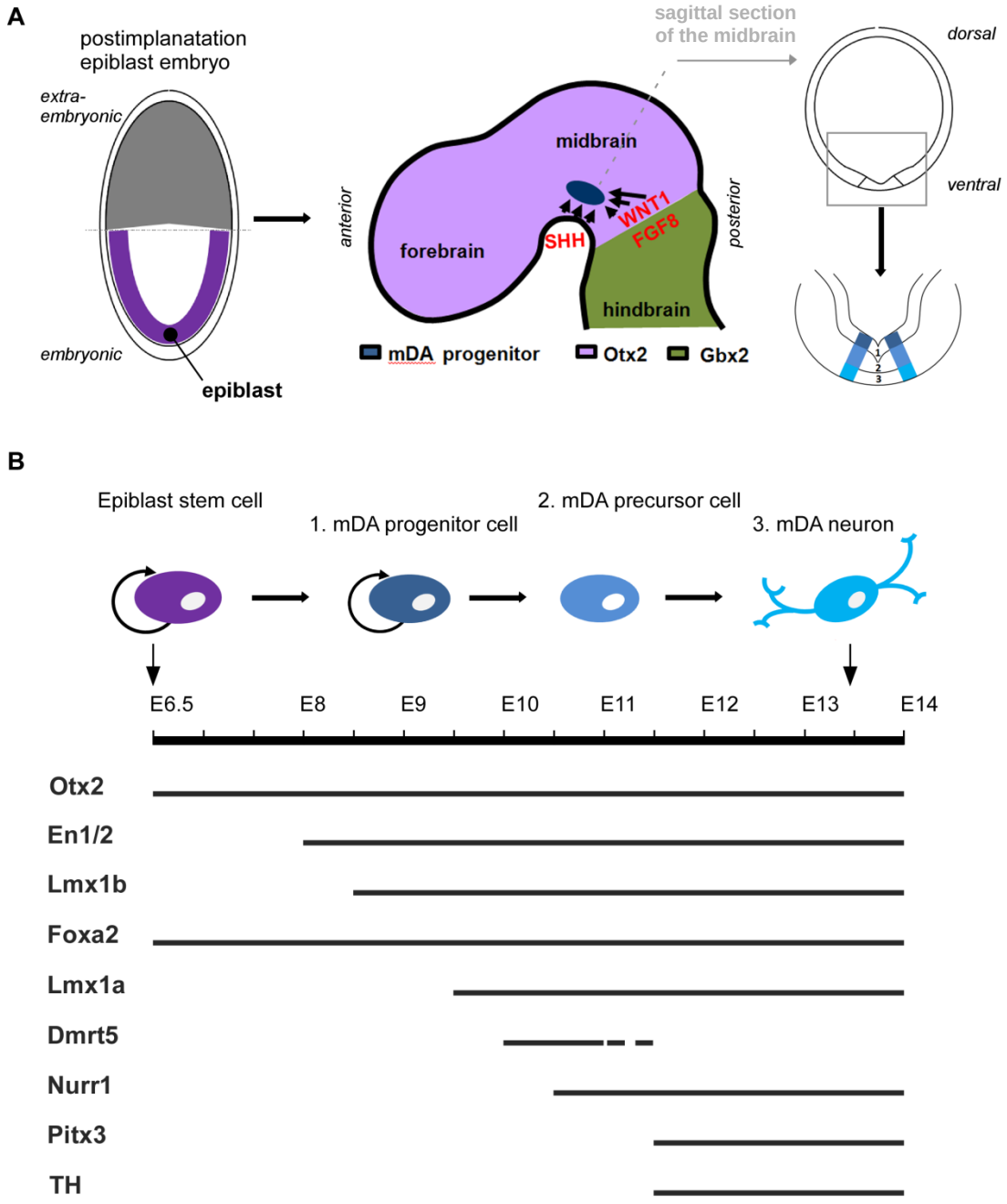


Figure 1.2 Drawing of midbrain DA neural development

(A) Cell lineage specification into the three germlayers takes place during gastrulation from E~6.5. From E8.5-11, patterning factors such as FGF8, WNT1, and SHH are essential to induce the gene expression of transcription factors that guide the cells into mDA neurons. First mDA neurons are born around E11.5 when TH expression is initiated. (B) Timescale showing the expression of factors related to development of mDA neurons. Dashed lines for Dmrt5 indicate that this gene isnot expressed in cells becoming mDA neurons.

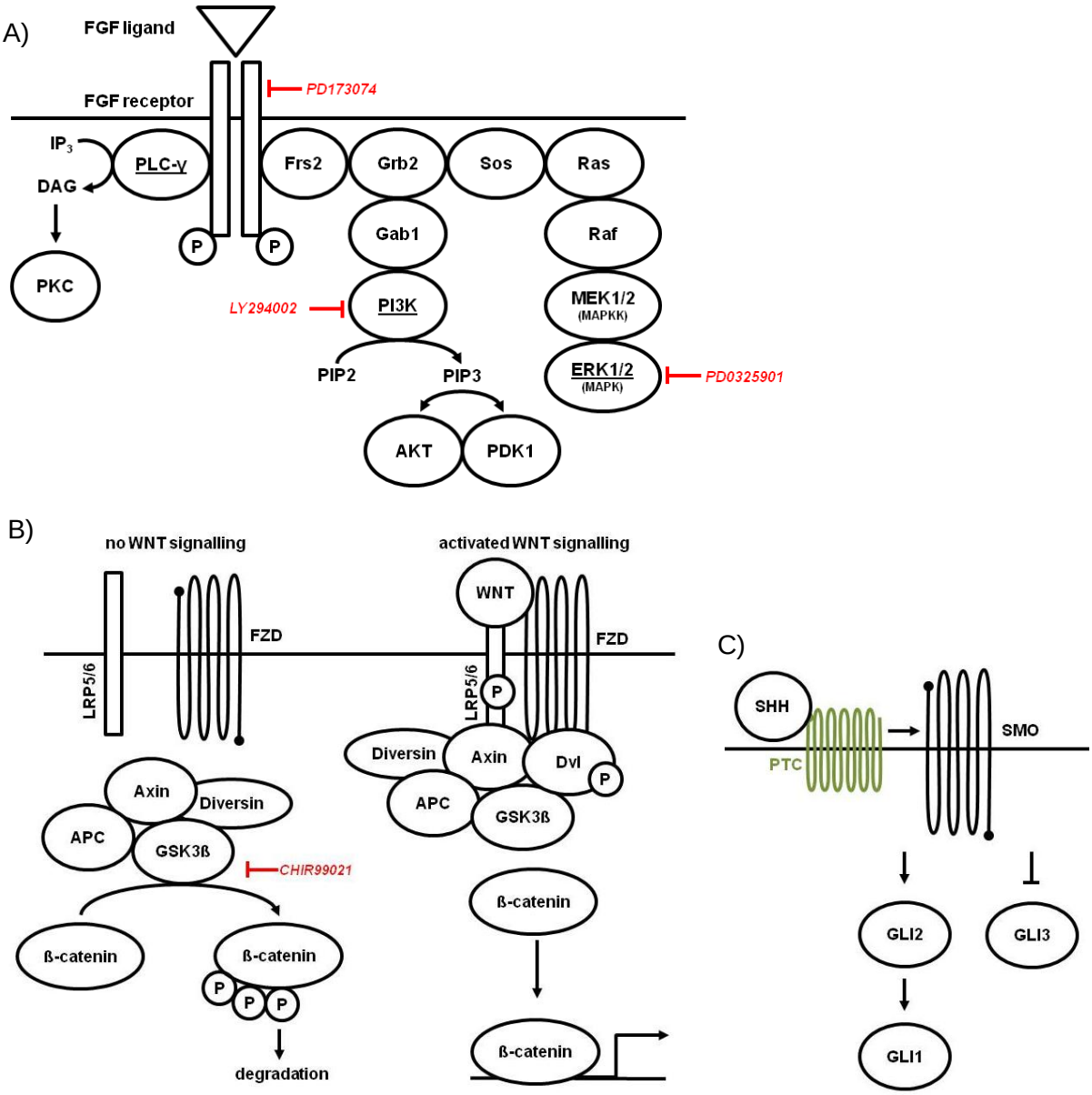


Figure 1.3 Schematic illustration of the pathways implicated in the generation of mDA neurons.

(A) FGF pathway. **(B)** WNT/ß-catenin pathway. **(C)** SHH pathway. PD0325901, PD173074 and CHIR99021 are small molecules that modulate the pathways by specific inhibition of the indicated enzymes.

Table 1.1 The 23 members of the FGF family can be divided into 7 groups according their evolutionary relationship and and gene-location analysis.

Family	Members
FGF1	FGF1, FGF2
FGF4	FGF4, FGF5, FGF6
FGF7	FGF3, FGF7, FGF22
FGF9	FGF9, FGF16, FGF20
FGF8	FGF8, FGF17, FGF18
FGF19	FGF19, FGF21, FGF23
FGF11	FGF11, FGF12, FGF13, FGF14

2 Materials and Methods

2.1 Cell Culture

Unless stated otherwise reagents and materials for tissue culture were purchased from Invitrogen, Nunc, or Sigma.

All steps were carried out inside a laminar flow sterile hood (Nuaire) to avoid contamination. Cells were incubated at 37°C with 5% CO_2 in a humidified incubator (Sanyo).

2.1.1 Routine ESC and iPSC culture

Culture dishes were coated for at least 30 min with 0.1% Gelatine in PBS at room temperature. ESCs and iPSCs were propagated on gelatinized culture dishes in 1x Glasgow minimum essential medium (GMEM) supplemented with 10% (v/v) foetal calf serum (FCS), 1 mM sodium pyruvate, 1x non-essential amino acid (NEAA), 2 mM l-glutamine, 0.1 mM ß-mercaptoethanol, and 100 units/ml leukaemia inhibitory factor (LIF) which was prepared in house by transfecting COS-7 cells with a human LIF expression plasmid. The culture was passaged every 2 to 3 days.

ESCs and iPSCs used in this thesis can be found in Table 2.1.

2.1.2 Derivation of EpiSC from ESC

ESCs were plated at three different cell densities on gelatinized culture dishes in ESC medium ($1x10^4$, $1x10^5$, and $1x10^6$ cells/cm²). The day after, ESCs were washed twice with PBS and cultured in retinol-free N2B27 medium with 10 ng/ml FGF2 (Peprotech) and 20 ng/ml Activin A (R&D). The composition of N2B27 was 50% DMEM/F12 and 50% Neurobasal supplemeted with 1:200 N2 and 1:100 B27 supplements. Cells were passaged every 2-3 days as EpiSCs. After ~5 passages, cultures should become more homogenous and EpiSC-like.

2.1.3 Routine EpiSC culture

EpiSCs were routinely passaged every 2 days. Cells were incubated in PBS without magnesium and calcium for ~3 min at room temperature. PBS was then gently replaced by retinol-free N2B27 medium with 10 ng/ml FGF2 (Peprotech) and 20 ng/ml Activin A (R&D). EpiSCs were mechanically dissociated and seeded into plates which were coated either with FCS or 15 µg/ml Fibronectin (Millipore) for 30 min at 37°C and washed twice with PBS. After 2 days in culture, the surviving EpiSCs formed large compact, flattened colonies.

2.1.4 Freezing ESCs, iPSCs and EpiSCs

Cells in tissue culture dishes were harvested as described above and centrifuged for 5 min at 1000 rpm. Cells were resuspended in freezing medium consisting of 10% dimethyl sulphoxide (DMSO) and culture medium and transferred into a cryotube. Tubes were placed in a styropor box at -20°C for ~3 hours and then at -80°C for overnight. The next day, cells were transferred to a liquid nitrogen cell bank.

2.1.5 Thawing ESCs, iPSCs and EpiSCs

Frozen cryotubes were retrieved from liquid nitrogen storage and placed immediately into 37°C water bath. Once the cells were thawed, they were transferred into 9.5 ml warm media to dilute out the DMSO. The cell suspension was then centrifuged for 5 min at 1000 rpm and the cells were gently resuspended in the appropriate media and transferred to suitable culture plates. The media was then refreshed about 10 hours later to remove any dead cells and dilute out the remaining DMSO.

2.2 Neural differentiation

Monolayer differentiations (MD) from ESCs and iPSCs were carried out as decribed by Ying et al. (2003). Briefly, MD of ES cells was performed on 0.1% Gelatine pre-coated plates. Routinely, 0.5-1.5x10^4 cells/cm^2 were plated in retinol-free N2B27 medium that consisted of

50% DMEM/F12 and 50% Neurobasal and was completed with 1:200 N2 and 1:100 B27 supplements. Medium was changed every other day. According to their characteristic morphology, first neurons could be seen around day (d) 5 of differentiation. During the course of differentitiation the number of cells highly increases. Therefore, cells were replated between d5 and d8 of differentiation on poly-L-Lysine and Laminin coated dishes to obtain an optimal yield of neurons. Plates were incubated in 0.002% solution of poly-L-Lysine for 2 hours at 37°C, rinsed twice with PBS and then covered with 10 µg/ml Laminin for 1 hour at 37°C.

For neural differentiation of EpiSCs, EpiSCs were plated on Fibronectin-coated plates and cultured in EpiSC media until cells reached a confluency of 60-80%. If the densitiy was too low, cells differentiated into non-neuronal cells with a big flat morphology which persisted and increased during the whole course of differentiation. Cells were rinsed twice with PBS and cultured in retinol-free N2B27. The day cells were switched to retinol-free N2B27 is designated as d0 MD. Due to the initial high number of EpiSCs at d0, half of the medium was replaced by fresh medium at d1. As a result of the high cell densitiy and continuing proliferation, cells formed a 3-dimensional layer by d2 of differentiation. At this stage, cells were gently rinsed and incubated for few seconds in PBS. Cells were mechanically dissociated in retinol-free N2B27 medium and seeded onto Fibronectin pre-coated plates at different dilutions from 1:3 to 1:6. The optimal plating densitiy for the generation of mDA neurons is 1:6 but this can slightly vary between cell lines. Medium was changed every other day, as with ESC differentiation. Cells were not further replated during differentiation as this might reduce the already existing neuronal cell population.

Factors and chemicals used for MD as indicated elsewhere in the chapters can be found in Table 2.2.

2.3 Flow cytometry

I used flow cytometry sorting to establish GFP profiles at different stages during neural differentiation. Cells were trypsinised and resuspended in PBS with 10% FCS. Cells were washed twice in PBS. Then, cells were immediately resuspended in 2% paraformaldehyde (PFA) and fixed for 15 min at 4°C. After washing with high volume of PBS, cells were resuspended in sorting buffer (1 mM EDTA, 25 mM HEPES pH7, 1% FCS in PBS without Ca^{2+} and Mg^{2+}). To ensure that the cells are single cells, the cell suspension was transferred into tubes by passing through cell-strainer caps (BD Falcon). Cells were kept on ice and analysed with BD LSRII (Becton Dickison Biosciences), BD FACS Divaaria software (Becton Dickison Biosciences) and FlowJo v7.6.5 (TreeStar). The analysis was supervised by Phil Huxley in Flow Cytometry of MRC Clinical Sciences Centre, London.

2.4 Electophysiological studies

D14-16 MD cultures derived from Pitx3-GFP EpiSCs were placed on a recording chamber and viewed using an Olympus BX51WI microscope with a 40x water immersion lens and DIC optics. Cells were bathed in a solution containing: 140 mM NaCl, 3.5 mM KCl, 1.25 mM NaH_2PO4, 2 mM $CaCl_2$, 1 mM $MgCl_2$, 10 mM Glucose, and 10 mM HEPES. For whole-cell electrophysiological recordings, low resistance recording pipettes (9-12 MΩ) were pulled from capillary glass (Harvard Apparatus Ltd.) and coated with ski wax to reduce pipette capacitance. Recording pipettes were filled with a solution containing: 140 mM K-gluconate, 5 mM NaCl, 2 mM Mg-ATP, 0.5 mM LiGTP, 0.1 mM CaCl2, 1 mM MgCl2, 1 mM ethylene glycol-bis (b-aminoethyl ether) -N,N,N',N'-tetraacetic acid (EGTA), and 10 mM HEPES. Osmolarity and pH of both solutions were adjusted before experiments. Prior to recording, the GFP positive neurons were identified for recording using fluorescence via a GFP selective filter (X-Cite series 120, EXFO). Data were acquired at room temperature (20 -

22°C) using an Axon Multiclamp 700B amplifier and a Digidata 1440a acquisition system, with pClamp 10 software (Molecular Devices). Data analysis was carried out using Clampfit 10.2 software (Axon Instruments), OriginPro 8.1 (OriginLab Corporation), and Spike2v5 software (Cambridge Electronic Design). Data are presented as the mean ± sem (standard error of the mean). This work was performed and analysed by Dr. Jessica Risner-Janiczek from our group.

2.5 Animal work

The studies on mice were carried out by Andreas Heuer and Dr. Sophie Precious from the research group of Prof. Steve Dunnett at the Cardiff University.

2.5.1 Animals

Male adult mice of the C57/Black 6 strain (Charles River, UK) were used that were 20-25 g at the start of the experiment. All animals were housed in standard laboratory cages in groups of 4-6 with access to food and water ad libitum. All procedures were in accordance to the UK Scientific Procedures (1986) Act and to local ethical review.

2.5.2 Lesion surgery

Animals were placed into an induction box where anaesthesia was induced by 5% isoflurane using oxygen as carrier gas. Subsequently the head of the animal was shaved and cleaned and the mouse was placed into a sterotaxic frame (Kopf instruments) with the incisior bar set to 0.0mm on the intra-aural line. Anaesthesia was maintained via a nose mask delivering 1-2% isoflurane in a 2:1 mixture of O_2/NO.

Lesions were performed by unilateral infusions of the neurotoxin 6-hydroxydopamine, also called 6-OHDA, at a concentration of 6 µg/µl calculated from free-base weight (hydrobromide salt, Sigma Chemicals, UK) in a solution of 0.9% sterile saline in 0.2 mg/ml Ascorbic acid. Lesions were aimed at the medial forebrain bundle at the sterotaxic

coordinates AP: -1.2, ML: -1.2, DV: -4.75. 1 µl of 6-OHDA was delivered via a 30-gauge stainless steel cannula connected via polyethylene tubing to a 10 µl Hamilton syringe which was mounted on a microdrive pump. The infusion rate of the toxin was 0.5 µl/min and the injection needle was left in place for an additional 3 min to allow for diffusion of the toxin before careful retraction of the needle. At the end of each surgical session the wound was cleaned and sutured and the animal was given a subcutaneous injection of 0.5 ml 0.9% sterile saline containing 4% glucose and 0.03 ml Metacam as analgesic.

For 14 days post lesion the animals' body weights were recorded and all lesioned animals received injections of glucose-saline (0.5 ml) three times daily in addition to wet palletable food during the post-lesion recovery period.

2.5.3 Graft surgery

Preparation for the surgery was as described above. Graft placement was performed at coordinates AP: +0.8, ML: -1.9, DV: -3.0 and -2.8. Cells were implanted via injection through a 10 µl Hamilton syringe at a density of 300.000 cells in 2 µl at a flow rate of 1 µl/min with an additional 3 min allowed for diffusion.

For grafting of the primary fetal tissue, pregnant C57/Bl6 dams were sacrificed and the embryos (E12.5) removed from the amniotic sack. The ventral mesencephalic area was dissected and pooled from all pups that were dissected. Cells were ezymatically dissociated by incubation in trypsin for 10 min at 37°C followed by mechanical dissociation into a quasi-single cell suspension. After inhibition of trypsin, the cells were centrifugated and resuspended to the required concentration of 150.000 cells per microliter.

2.5.4 Drug-induced rotations

Mice were injected with methamphetamine (2.5 mg/kg; Sigma) before they were placed into automated rotometer bowls, designed after the model by Ungerstedt (Ungerstedt and Arbuthnott, 1970). The machine recorded the rotations over a period of 60 min. Data were expressed as average net number of rotations per min.

2.6 Molecular biology methods

Unless otherwise stated analytical grade chemicals were obtained from Sigma, Fisher or BDH Laboratory Supplies (Merck Ltd). Stock solutions were prepared with reverse osmosis purified water and filtered or autoclaved as necessary. Agarose for electrophoresis was supplied by Invitrogen. Synthetic oligonucleotides were synthesised by Sigma.

2.6.1 Quantitative PCR

Total RNA was extracted using TRIReagent (Sigma) and reverse transcribed using the Quantitect RT kit (Qiagen). Remaining RNA was removed afterwards by RNase H (2 units/µl, Invitrogen). qPCR was performed using iQ™SYBR®Green Supermix (Biorad) on a Chromo4-detection system (Biorad). To validate the primers, I included five serial dilutions (in steps of 2-fold) of a positive control cDNA from a whole mouse embryo at E12. Synthetic oligonucleotides were synthesised by Sigma (Genosys, Table 4). All PCR data were normalized to the average of the reference genes *Cyclophillin* and *Hmbs*. In addition to normalisation to reference genes, a reference sample was chosen as the calibrator. The relative expression of all samples in the assay was given in relation to the calibrator.

Primers used to study neural differentiation can be found in Table 2.3.

2.6.2 Protein extraction and quantification

Cells were washed twice with PBS (137 mM NaCl, 2.7 mM KCl, 4.3 mM Na_2HPO_4 x$7H_2O$, 1.4 mM KH_2PO_4, pH 7.4) and lysed in lysis buffer containing 10 mM Tris-HCl (pH8.0, Fisher), 50 mM EDTA (Fisher), 100 mM NaCl (BDH) and 0.5% sodium dodecyl sulfate (SDS, Fisher). RC DC Protein Assay kit from Biorad was used to measure the protein concentration. Albumin from bovine serum (BSA, Sigma) was used as protein standard.

2.6.3 Western Blot analysis

The SDS PAGE was carried out using the Mini-PROTEAN®3 system from Biorad following manufacture's instructions. 10% polyacrylamide separating gel and a 4.3% polyacrylamide stacking gel were used in a discontinuous buffer system. Protein was loaded into the well of a SDS-gel and ran for 45 min at 150 V in running buffer consisting of 0.025 M Tris, 0.25 M glycine, and 0.1% SDS.

Separated proteins in SDS-gel were transferred using semidry transfer cell (Trans-Blot SD, Biorad) in transfer buffer (3.9 mM glycine, 4.8 mM Tris, 0,037% SDS, 20% methanol) to nitrocellulose membrane (GE healthcare) for 1 hour at 15 V and constant 0.27 A (for two gels á 9x6 cm). Then membrane was blocked in PBS (137 mM NaCl, 2.7 mM KCl, 4.3 mM $Na_2HPO_4x7H_2O$, 1.4 mM KH_2PO_4, pH 7.4) containing 0.1% Tween 20 (hereafter called PBST) and 3% dried non-fat milk (blocking solution) for 1 hour at room temperature on a rotator. The membrane was incubated with primary antibody in the appropriate dilution in blocking solution at 4°C for over night. After washing with PBST, the membrane was incubated with horseradish peroxidase (HRP)-conjugated secondary antibody for 1 hour at room temperature. The signals were then detected with enhanced chemiluminescence (Roche) and Hyperfilm ECL (GE Healthcare). Primary antibodies used for Western Blot were rabbit anti-pERK (1:1000, Cell Signalling) and rabbit-anti ERK1/2 (1:500, Cell Signalling). Secondary antibodies were donkey anti-rb IgG-HRP (1:2000, Santa Crusz).

2.6.4 Immunofluorescence staining

Cells were washed twice with PBS (137 mM NaCl, 2.7 mM KCl, 4.3 mM Na_2HPO_4 x$7H_2O$, 1.4 mM KH_2PO_4, pH 7.4) and fixed in 4% PFA at room temperature for 10 min. Then, they were washed with PBS-0.3% TritonX-100 (PBST) three times for 5 min each. Fixed cells were blocked in blocking solution consisting of PBST and 5% normal serum for 10 till 20 min followed by incubation over night with primary antibodies. Cells were washed three times with PBST followed by incubation for 1 hour with fluorescence-labelled secondary antibodies

(1:200, Invitrogen). Again, cells were washed with PBST three times and counterstained with DAPI (1:1000, Molecular Probes).

Primary antibodies used for immunochemical analysis can be found in Table 2.4.

2.6.5 Quantitative analysis of immunocytochemistry

Coverslips were examined using a Leica TCS SP5 confocal microscope equipped with 405 Diode, Argon, DPSS 561, HeNe 594 and HeNe 633 lasers. To compare each set of experiment, pictures were taken with the same parameters on the confocal software. The number of positively stained cells was quantified by counting randomly selected fields from at least 3 independent experiments. To determine the number of TH positive, PITX3/TH double positive, and FOXA2/TH double positive cells, all positively stained cells were counted manually. To evaluate the proportion of OTX2, LMX1A, FOXA2 or DMRT5 positive cells, a custom written Image J macro was used (rsb.info.nih.gov/ij/download/). Tresholds were applied to each channel independently to select clearly labeled cells and to avoid detection of unspecific background staining. Binarised images were merged and the proportion of OTX2, LMX1A, FOXA2 or DMRT5 positive cells were determined by the total number of pixels of these positive labeled cells to the total pixel number of DAPI labeled cells. Statistical significance was determined using two tailed student t-test. The values of $p<0.01$ were considered significant. Analysis was performed using GraphPad software (www.graphpad.com, Dr. Harvey Motulsky, San Diego, California, USA)). Each set of values was expressed as means ± standard deviation.

Table 2.1 Pluripotent stem cell lines used for the investigations of this thesis.

Cell lines	
E14TG2a	(Hooper et al., 1987)
Lmx1a-GFP	(Dr. Johan Ericson and Dr. Thomas Perlmann lab)
Pitx3-GFP	(Zhao et al., 2004)
Sox1-GFP	(Ying et al., 2003b)
NSAOK6	mouse iPSCs were reprogrammed by Oct4 and Klf4 from Neural Stem Cells as described by Jose Silva et al. (Silva et al., 2008a)

Table 2.2 List of factors used for neural differentiation.

Factors	Supplier	Final Concentration
Ascorbic acid	Sigma	200 µM
BDNF	Preprotech	10 ng/ml
Cyclopamine	Sigma	10 µM
CHIR99021	Miltenyi Biotec	0.5 µM and 2 µM
FGF8b, human	Preprotech	100 ng/ml
GDNF	Preprotech	10 ng/ml
LY294002	Cambridge Bioscience	2 µM
PD173074	Sigma	50 ng/ml
PD0325901	Axon	1 µM
SHH (C25 II-N)	R&D	200 ng/mL

Table 2.3 List of gene specific primers for qPCR.

Gene	Forward primer	Reverse primer
Cyclophilin	GGCAAATGCTGGACCAAACAC	TTCCTGGACCCAAAACGCTC
Hmbs	ACTGGTGGAGTCTGGAGTCTAGATGGC	GCCAGGCTGATGCCCAGGTT
Axin2	GGTTGGCTTGTCCAGACAAAACT	GCTGGTGGCTGGTGCAAAGAC
Dmbx1	ACTCCCTGCACGCTATGAACT	GGCCTCCAAGATGATGTCAGCTAG
Dmrt5	GAGAGCCGAGGCGCGAGCCGAGCT	GTCCCGTCGCTGTCGCTGCTGCTGT
En1	CAAGACTGACTCACAGCAACC	ACTCCGCCTTGAGTCTCTGC
En2	ACTGCACGCGCTATTCTGAC	TGTTGCCCGTGGCTTTCTTG
Foxa2	CTGGGAGCCGTGAAGATGGA	ATTCCAGCGCCCACATAGGA
Foxg1	GACCCGTCGAGCGACGACG	GGACAGGAAGGGCGACATGG
Gad1	CGCAGGCACGACTGTTTACG	CCAGGTGACTGAATTGGCCC
Gata2	TCACCCCTAAGCAGAGAAGC	CGCCATAAGGTGGTGGTTGTC
Gbx2	AGAGAGAAGCTCTCCTCCTTG	CGGCAACTTCGACAAAGCCG
Gli1	TCAGGGTCCCAGGGTTATGG	CGAGGCTGGCATCAGAAAGG
Helt	GGAGGGACCGAATTAACCGC	CATGCACTCCGTGGTAACCGT
Lmx1a	GGACCATAAGCGACCCAAAC	CCTGAACCACACGGACACTC
Mash1	CCCTGAAACTGGGTTGATGT	AAAGGCTGTCCGAGAACTGA
Msx1	GCCTCTCGGCCATTTCTCAG	CGGTTGGTCTTGTGCTTGCG
Nanog	CTTACAAGGGTCTGCTACTGAGATGC	TGCTTCCTGGCAAGGACCTT
Ncam	TGAGCCTGAGAGTATCGACTG	AGTTTGCCGTTCCTGAACC
Nestin	TGAGAACTCTCGCTTGCAGACAC	GGTCCTCTGGTATCCCAAGGAAATG
Ngn2	GCTGTGGGAATTTCACCTGT	AAATTTCCACGCTTGCATTC
Oct4	CACGAGTGGAAAGCAACTCA	AGATGGTGGTCTGGCTGAAC
Otx2	TCGAAGAGCTAAGTGCCGCC	GGCAATGGTTGGGACTGAGG
Shh	AGCATCCCTGCAGCGCAATC	GCTGGACTTGACCGCCATTC
Six3	GGTTTAAGAACCGGCGACAG	TACCGAGAGGATCGAAGTGC
Sox1	GGGCGCCCTCGGATCTCTGGTCAA	GCCCTGGTAGTGCTGTGGCAGCGAGT
Tubb3	ATCAGCAAGGTGCGTGAGGAG	ATGGACAGGGTGGCGTTGTAG
Wnt1	TGAGCCGCAAGCAGCGGCGA	TGGGGCCCCGGAGCAGTGGG

Table 2.4 List of primary antibodies for immunocytochemistry.

Antigen	Species	Supplier	dilution
5HT	mouse	Abcam	1:50
DMRT5	rabbit	Custom-made antibody	1:1000
FOXA2	goat	Santa Cruz	1:200
GAD67	mouse	Millipore 5406	1:300
GFP	rabbit	Invitrogen	1:500
GFP	mouse	Invitrogen	1:500
LMX1A	ginuin pig	Custom-made antibody	1:500
Nestin	chicken	Neuromics	1:500
Nestin	mouse	DSHB	1:200
NEUN	mouse	Chemicon	1:200
NURR1	rabbit	Santa Cruz	1:200
OCT4	goat	Santa Cruz	1:500
OTX2	rabbit	Millipore	1:300
OTX2	goat	R&D	1:500
PAX6	mouse	DSHB	1:1000
PITX3	rabbit	gift of M.Smidt, University of Amsterdam	1:500
SOX2	rabbit	Chemicon	1:500
TH	rabbit	Pelfreeze	1:500
TH	mouse	Millipore	1:500
TH	sheep	Pelfreeze	1:300
TUBB3	rabbit	Covance	1:1000
TUBB3	mouse	Covance	1:500
TUBB3	mouse	Sigma	1:1000
VMAT2	rabbit	Santa Cruz	1:500

3 Epiblast stem cells as an alternative model to study neural differentiation *in vitro*

Pluripotent stem cells are capable of differentiating into cells from all three germ layers. Knowledge gained from *in vivo* studies about the mechanisms controlling the fate choice of stem cells during development has been used to design protocols directing differentiation of PSCs *in vitro*. Although efficient methods for directed differentiation of ESCs towards neuronal subtypes have been established (Eiraku et al., 2008; Gaspard et al., 2009; Gaspard et al., 2008; Lee et al., 2000b; Murashov et al., 2005; Salero and Hatten, 2007; Su et al., 2006; Wataya et al., 2008; Wichterle et al., 2002), ESC differentiation *in vitro* is asynchronised and heterogeneous in nature. During differentiation, progenitors of various spatial and temporal developmental stages co-exist and response differently to given inductive signals according to their distinct cellular properties.

Furthermore, to study FGF signalling in neural differentiation, mouse EpiSCs may be a better cell source than ESCs for the following reasons: Firstly, the transition from ESCs to EpiSCs requires the activation of FGF signalling (Kunath et al., 2007). Secondly, EpiSCs are developmentally primed PSCs and may potentially offer a more accelerated and synchronised *in vitro* differentiation model than ESCs. Lastly, human ESCs seem to be more similar to mouse EpiSCs than mouse ESCs (Brons et al., 2007; Rossant, 2008; Tesar et al., 2007; Vallier et al., 2009; Xu et al., 2008).

To validate EpiSCs as an alternative *in vitro* differentiation model, I performed comparative neural differentiation from mouse ESCs and mouse EpiSCs. I used the monolayer differentiation (MD) protocol described by Ying et al. (2003), because it represents a well defined system ideally for studying the effect of molecular manipulations on cell lineage choice. I found that neural differentiation occurs more homogeneously and faster in EpiSCs than in ESCs. Furthermore, EpiSCs differentiated into multiple neuronal subtypes demonstrating their capacity of making neurons is not restricted to a specific subtype.

3.1 Comparison of neural induction in ESCs cell and EpiSCs

To gain insight into the progress of *in vitro* neural differentiation in ESCs and EpiSCs, MD of ESCs and EpiSCs were analysed for pluripotent and neural lineage markers by immunocytochemistry and qPCR.

Immunostaining for OCT4 demonstrated the pluripotent state of ESC and EpiSC cultures as the majority of the cells express OCT4 (Figure 3.1 B). In agreement with the published data, the expression level of *Oct4* was similar in ESCs and EpiSCs whereas expression of *Nanog* was reduced in EpiSCs when compared to ESCs (Figure 3.1 A) (Greber et al., 2010; Han et al., 2010; Najm et al., 2011). In MD cultures of EpiSC, *Nanog* expression was already substantially decreased at day (d) 2 MD and extinguished at d4 MD. In contrast, the loss of *Nanog* mRNA was delayed in ESCs to d6 MD (Figure 3.1 A). *Oct4* was significantly downregulated in EpiSC MD cultures by d2 whereas in ESC MD the expression level of *Oct4* decreased at d4 MD (Figure 3.1 A). Consistent with this gene expression analysis, an antibody against OCT4 detected few OCT4 positive cells at d4 in MD of EpiSCs whereas at the same time a high number of OCT4 positive cells were still present in MD cultures of ESCs. Furthermore, SOX2, which is expressed in both pluripotent stem cells and neuroepithelial stem cells, was detected in the majority of OCT4 negative cells at d4 in EpiSC MD, indicating neural lineage commitment.

The neuroepithelial markers SOX1 and Nestin were used to analyse the kinetics of neural lineage conversion from the pluripotent stem cells, EpiSCs and ESCs. SOX1 is specifically expressed in the neuroectoderm at the headfold stage (Wood and Episkopou, 1999) and Nestin is an intermediate filament protein found to be expressed in neuroepithelial stem cells (Cattaneo and McKay, 1990; Lendahl et al., 1990). A robust upregulation of *Sox1* was observed in MD of EpiSCs at d2, followed by a high increase of *Nestin* expression at d6 MD (Figure 3.1 A). In addition, the expression of the pro-neural genes, mammalian achaete-scute homolog 1 (*Mash1*) (Guillemot and Joyner, 1993; Sommer et al., 1995; Verma-Kurvari

et al., 1996) and Neurogenin2 (*Ngn2*) (Sommer et al., 1996), started to increase at d2 and d4 MD respectively in EpiSC cultures. In comparison to the observation of neural lineage markers in EpiSC MD, upregulation of *Sox1*, *Nestin*, *Mash1*, and *Ngn2* transcription was delayed by 2 days in MD of ESCs (Figure 3.1 A). An accelerated neural differentiation of EpiSCs was further confirmed by immunocytochemistry, EpiSC cultures at d4 contained numerous SOX1 and Nestin positive cells whereas there were significantly fewer in ESC MD. As a consequence of a more rapid neural differentiation in EpiSC MD, the neuronal marker genes *Ncam* and *Tubb3* were markedly increased at d6 in MD of EpiSC compared to ESC MD (Figure 3.1 A,B). However, by d12 of MD, the mRNA levels of the neuronal marker genes in ESC MD were similar to those of EpiSCs (Figure 3.1 A), suggesting the efficiency of neural conversion is similar between the two protocols. Immunostaining for TUBB3 further confirmed that the quantitative conversion to a neuronal phenotype was comparable at d12 MD in ESC and EpiSC cultures (Figure 3.1 B). It is worth noting that at d12 MD, SOX1 positive neural progenitor cells were still present in MD cultures of ESCs and EpiSCs. I also observed a variety of neuronal subtypes in d14 MD cultures of EpiSCs verified by the expression of the serotonergic marker 5HT, the GABAergic marker GAD67 or the DA marker TH (Figure 3.1 C), as was previously demonstrated for MD of ESCs (Ying et al., 2003b),

Interestingly, antibody for TUBB3 revealed neurons of mature morphology with long axons as well as cells with less pronounced neuronal morphology at d6 of ESC MD while in d6 EpiSC MD all TUBB3 positive cells displayed an immature neuronal morphology indicating a more synchronised neuronal differentiation of EpiSCs. To strengthen this observation, I used the reporter cell line 46C in which GFP is inserted into the *Sox1* locus (Ying et al., 2003b). EpiSCs were derived from 46C ESCs by culturing ESCs in N2B27 supplemented with 20 ng/ml Activin A and 12 ng/ml FGF2 (Guo et al., 2009). 46C-ESCs and 46C-EpiSCs were subjected to MD and Sox1-GFP expression was detected by flow cytometry. Sox1-GFP was undetectable in 46C-ESCs and 46C-EpiSCs, but as cells differentiated, Sox1-GFP reporter expression was activated in both types of MD culture (Figure 3.2). *In vivo* data indicates that

as neural development progresses, *Sox1* expression is switched off in most neurons and remains only expressed in the lens and subgranular layer of the hippocampus (Aubert et al., 2003). In 46C-EpiSC MD the number of Sox1-GFP positive cells was dramatically increased by d4 of MD. In agreement with the *in vivo* data, I observed that most of the cells lost Sox1-GFP by d6 of MD and only a small subset of cells maintained Sox1-GFP expression (Figure 3.2). In contrast, MD of ESCs did not show a strong increase of Sox1-GFP positive cells until d6 of MD. Furthermore, although the neural differentiation of ESCs was successful which was observed by the presence of Sox1-GFP cells, the flow cytometry profile at d6 of ESC MD displayed the presence of a large Sox1-GFP negative cell population (Figure 3.2). These results indicate that EpiSCs progress more uniformly toward the neural lineage than ESCs.

Taken together, the analysis of neural lineage markers by qPCR and immunocytochemistry as well as the detection of Sox1-GFP during differentiation revealed that EpiSCs commit to neuronal lineage more rapidly and in a more synchronised manner than ESCs. Furthermore, neural marker genes are upregulated at d2-4 in MD of EpiSCs, indicating the time window when neural induction is activated.

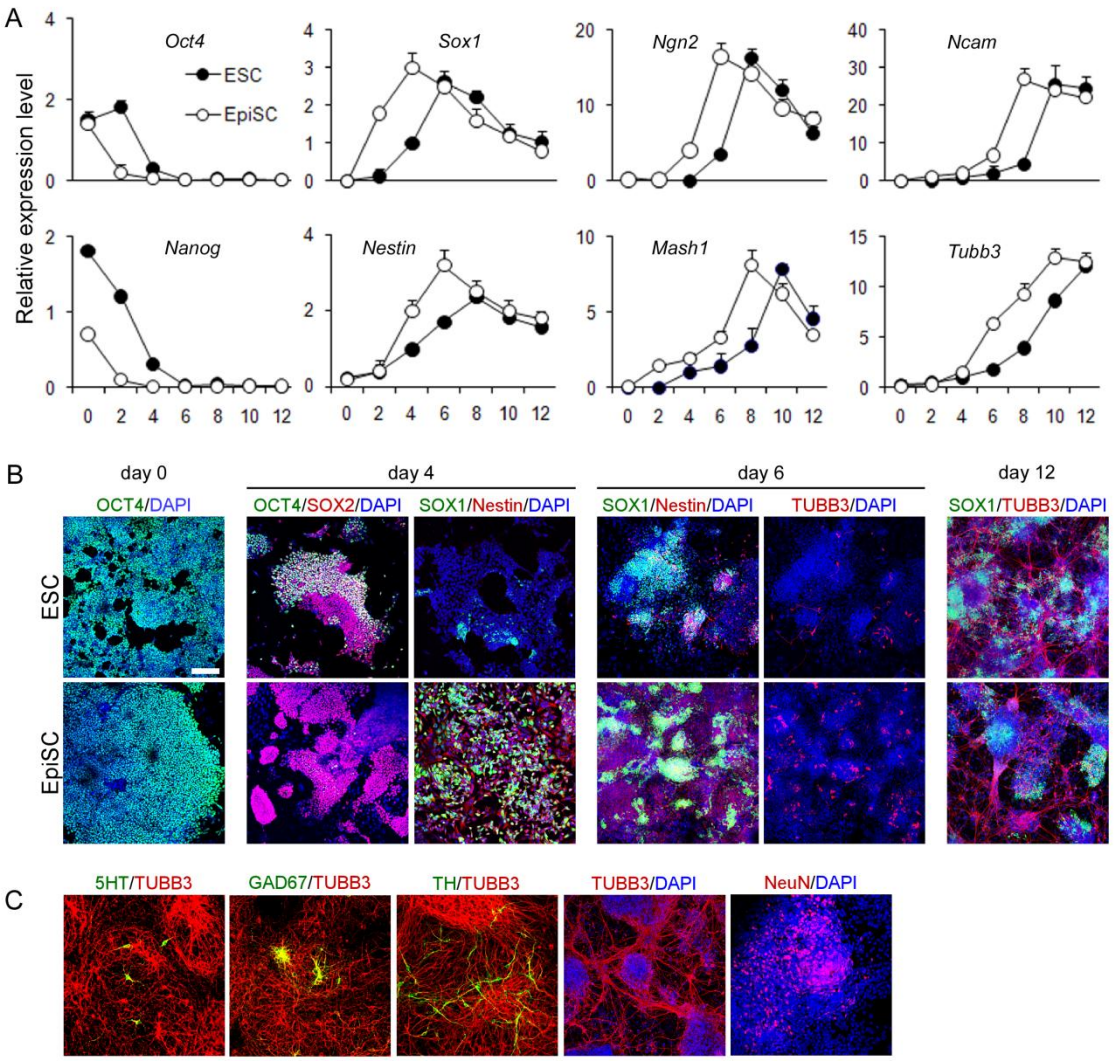


Figure 3.1 Accelerated neural differentiation potential of EpiSCs.

(A) qPCR analysis for the expression of pluripotency and neural lineage genes over 12-days MD cultures of ESCs and EpiSCs. Data represent mean±s.e.m. from triplicate cultures of a single experiment. **(B)** Mouse ESC and EpiSC cultures at d0, d4, d6 and d12 MD immunostained for the pluripotent marker OCT4, the pluripotent and neuroepithelial marker SOX2, and the neural lineage marker proteins SOX2, SOX1, Nestin, and TUBB3. DAPI labeling is in blue. **(C)** At day 14 of neural differentiation from EpiSCs, cultures were stained for the serotonergic marker 5HT, GABAergic marker GAD67, dopaminergic marker TH, all labelled in green, and the neuronal markers, TUBB3 and NeuN, shown in red. DAPI labeling is in blue. Scale bars: 100 µm

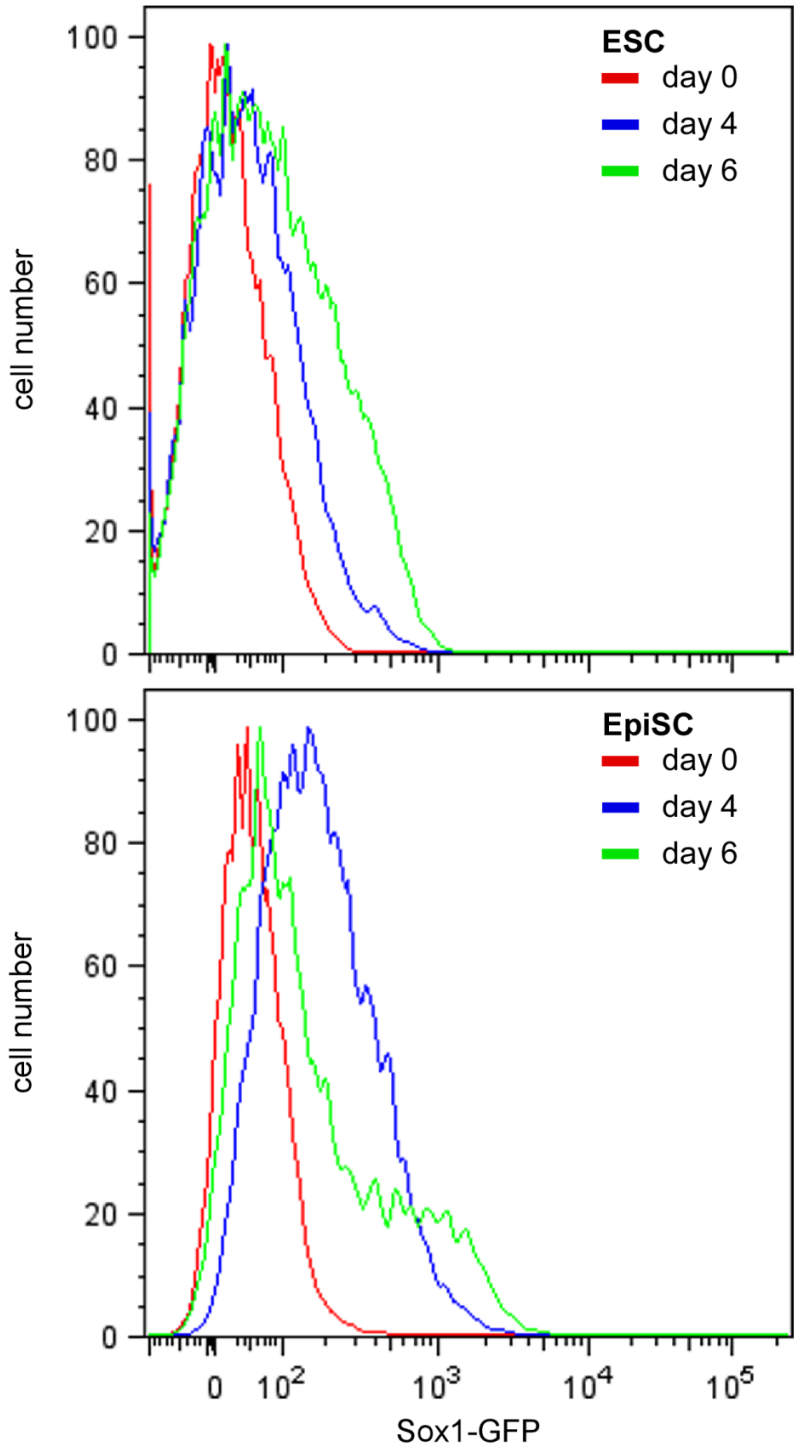


Figure 3.2 Synchronised neuroectodermal differentiation from EpiSCs.

Flow cytometry profiles of Sox1-GFP ESCs and EpiSCs MD cultures.

3.2 Discussion

Realising the potential of human ESCs in regenerative medicine requires an in-depth understanding of the mechanisms that control the fate choice of stem cells during differentiation. Recent studies reported that hESCs appear to be functionally more akin to mouse EpiSCs than mouse ESCs (Brons et al., 2007; Rossant, 2008; Tesar et al., 2007; Vallier et al., 2009). Therefore, mouse EpiSCs are an attractive model system for studying neuroectodermal specification *in vitro.* Knowledge gained from neural differentiation of mouse EpiSCs may provide a better understanding of neural commitment in hESCs and improve techniques for the generation of particular neuronal subtypes from hESCs for biomedical applications. Mouse EpiSCs have been shown to be capable of multilineage differentiation *in vitro* (Bernemann et al., 2011; Brons et al., 2007; Tesar et al., 2007; Vallier et al., 2009) and to form teratomas when grafted into adult mice (Brons et al., 2007; Tesar et al., 2007). However, a direct comparison of mouse EpiSCs and mouse ESCs in neural differentiation has not been described.

In this chapter, I report that EpiSCs are competent to commit efficiently to a neuronal fate. It was demonstrated that neuronal cells derived from ESCs are not restricted to a specific neuronal fate (Ying and Smith, 2003; Ying et al., 2003b) which was also the case for EpiSC-derived neurons. I observed a more rapid loss of pluripotent markers in neural differentiation of EpiSCs when compared to ESC in MD (Figure 3.1). This observation might be explained by the developmentally advanced stage of EpiSCs (Brons et al., 2007; Tesar et al., 2007). EpiSCs are developmentally equivalent to cells from the postimplantation epiblast at E~6.5 while ESCs are isolated from E3.5 embryos. Though EpiSCs express the pluripotent marker genes and readily form teratomas upon injection into immunocompromised mice, they make minimal contribute to the formation of chimeras (Brons et al., 2007; Tesar et al., 2007). In conclusion, ESCs represent a more immature stage of differentiation than EpiSCs which are poised to differentiate more readily.

The rapid exit of EpiSCs from a pluripotent stage was accompanied by an early, synchronised conversion into a neuroectodermal lineage whereas neural induction in ESC MD seemed to be a more heterogeneous progress (Figure 3.2). Consistent with this finding, it has been reported that ESC cultures are composed of cells with different pluripotency levels (Chambers et al., 2007; Furusawa et al., 2004; Hayashi et al., 2008; Toyooka et al., 2008), consequently resembling different stages of development *in vivo*. Therefore, the asynchronous neural differentiation observed in ESCs might be due to the presence of distinct cell subpopulations within ESC cultures that when exposed to a given activation stimuli respond differently according their developmental stages. In this respect, MD of EpiSCs appeared as a more coordinated process, indicating that EpiSCs are more homogeneous in nature. The relative synchronous nature of EpiSCs during neural differentiation provides a more precise system to study the mechanisms of neural induction and specification than ESC MD.

However, MD of ESCs and EpiSCs at d12 displayed comparable amounts of TUBB3 and Sox1-GFP positive cells (Figure 3.1). The Sox1-GFP positive cells are mostly seen in areas of high cell density concomitant with less TUBB3 positive cells. Since these areas seem to create a “niche” where neural precursors are maintained and neuronal differentiation is suppressed, dissociation of the cells might disrupt the niches with their cell-cell contacts and subsequently improve neuronal differentiation. It needs to be taken into consideration that replating of cells at this stage has a negative impact on the survival of the existing neuronal cell population.

4 Temporally controlled modulation of FGF/ERK signalling directs a midbrain dopaminergic fate

Extrinsic signals, such as FGF, WNT, BMP, and SHH, are essential for governing stem cell fate decision and lineage specification. This chapter focuses on FGF signalling which plays multiple roles during development depending on the time and the tissue.

During gastrulation, FGFs are involved in the posteriorisation of the neuroepithelium (Cox and Hemmati-Brivanlou, 1995; Doniach, 1995; Holowacz and Sokol, 1999; Kengaku and Okamoto, 1995; Lamb and Harland, 1995; Rentzsch et al., 2004; Ribisi et al., 2000; Wills et al., 2010). At E~6.5, loss of *Fgf8* expression in mouse embryos results in an expansion of *Otx2* and *Six3* positive anterior tissue accompanied with the loss of posterior tissue marked by *Gbx2* (Sun et al., 1999). Consistent with this finding, Oki et al (2010) demonstrated that potent FGFR inhibitors block posteriosation of mouse embryos during gastrulation. The same study further reported that MAPK/ERK inhibitor could mainly replace the FGFR inhibitor whereas antagonists of PLC-γ or PI3K pathway had no effect, implying FGF signalling acts via the MAPK/ERK pathway in this context.

If *in vitro* differentiation of ESCs resembles the developmental process, inhibition of FGF/ERK pathway during early stages of *in vitro* neural differentiation should induce the production of cells with anterior characteristics (*Otx*2), including the cells from which mDA neurons arise, at the expense of posterior neuroepithelial cells (*Gbx2*). We proposed that a direct induction of early region-specific progenitors should improve the production of DA neurons. I therefore tested this hypothesis using EpiSCs *in vitro* differentiation model because they have already completed the transition from ESCs which involves the activation of FGF signalling (Kunath et al., 2007). Additionally, EpiSCs are more advantageous than ESCs because their *in vitro* differentiation towards neuroectoderm is more synchronously as shown in Chapter 3. In this chapter I show that regulating the level of FGF/ERK activity

during distinct phases of neural differentiation *in vitro* is crucial for efficient generation of mDA neurons.

4.1 Blockade of FGF/ERK signalling upon exit of epiblast pluripotent state accelerates neural fate commitment

Self-renewal of EpiSCs *in vitro* is maintained by FGF2 and Activin A. I proposed that, in the absence of Activin A, inhibition of FGF signalling promotes differentiation. To investigate whether early blockade of FGF/ERK promotes differentiation into neuroectoderm, MD of EpiSC was performed with either the FGFR inhibitor PD173074 (Stavridis et al., 2007) or the potent MEK (MAPKK) blocker PD0325901 (Ying et al., 2008), which prevents ERK activation and is referred as ERK inhibitor hereafter. As shown by Western Blot, phosphorylated ERK was diminished in cultures treated with PD173074 or PD0325901 (Figure 4.1 A).

To determine whether FGF/ERK inhibition promotes the exit from the pluripotent stage, immunostaining for the pluripotent marker OCT4 was performed on MD cultures at d1-3 with and without PD0325901. As expected, less OCT4 positive cells were seen in cultures exposed to the FGF/ERK inhibitor when compared to control cultures from d2 MD and onward (Figure 4.1 B).

The patterns of stage-specific gene expression observed in Chapter 3 suggest that neural induction in MD of EpiSCs occurred during the first 2-4 days of differentiation. In order to examine whether inhibition of FGF/ERK signalling further promotes the transition of EpiSCs into neuroectodermal cell fate, EpiSCs were cultured with PD0325901 and the expression of the pro-neural genes *Ngn2* and *Mash1* and the neuronal marker gene *Tubb3* were analysed by qPCR (Figure 4.2 A). The levels of *Mash1* were increased from d3 MD with or without PD0325901. However, *Mash1* expression level was higher in cultures with PD0325901. Interestingly, the expression of the pro-neural gene *Ngn2* was already highly upregulated at

d3 MD in PD0325901 treated cultures whereas in no-PD0325901 control cultures an increase of *Ngn2* expression was not observed until d4 of differentiation. Moreover, in cultures that were exposed to PD0325901, the elevation of *Tubb3* mRNA was shifted forward to d3 of differentiation when compared with no-PD0325901 controls.

To strengthen the observation that inhibition of the FGF/ERK pathway causes a more rapid neuroectodermal differentiation, I used Sox1-GFP knock-in (46C) reporter EpiSCs (Ying et al., 2003b) to monitor differentiation. *Sox1* is specifically expressed in the neuroectoderm from the headfold stage onwards (Wood and Episkopou, 1999), thus it is commonly used as a marker gene for neural progenitors. To gain insight into the kinetics of neural induction, Sox1-GFP positive cells were detected by flow cytometry and the percentage of Sox1-GFP positive cells was determined between d1 and d6 MD. As shown, Sox1-GFP was undetectable before differentiation (Figure 4.2 C, D). At d2 of differentiation, a high proportion of Sox1-GFP positive cells (44.15%±1.2) were already detected in cultures with PD0325901, compared to control cultures without PD0325901 (7.55%±0.64). Furthermore and consistent with the observation above, immunocytochemical staining of PLZF, a marker of neuroectodermal cells (Avantaggiato et al., 1995), indicated that PD0325901 treatment accelerated and enhanced the generation of PLZF positive cells compared to controls cultures (Figure 4.2 B).

Taking together, the results from the analysis of the flow cytometry data, immunostaining and gene expression demonstrate that inactivation of FGF/ERK signalling accelerates the transition from a pluripotent epiblast stage toward neuroectoderm.

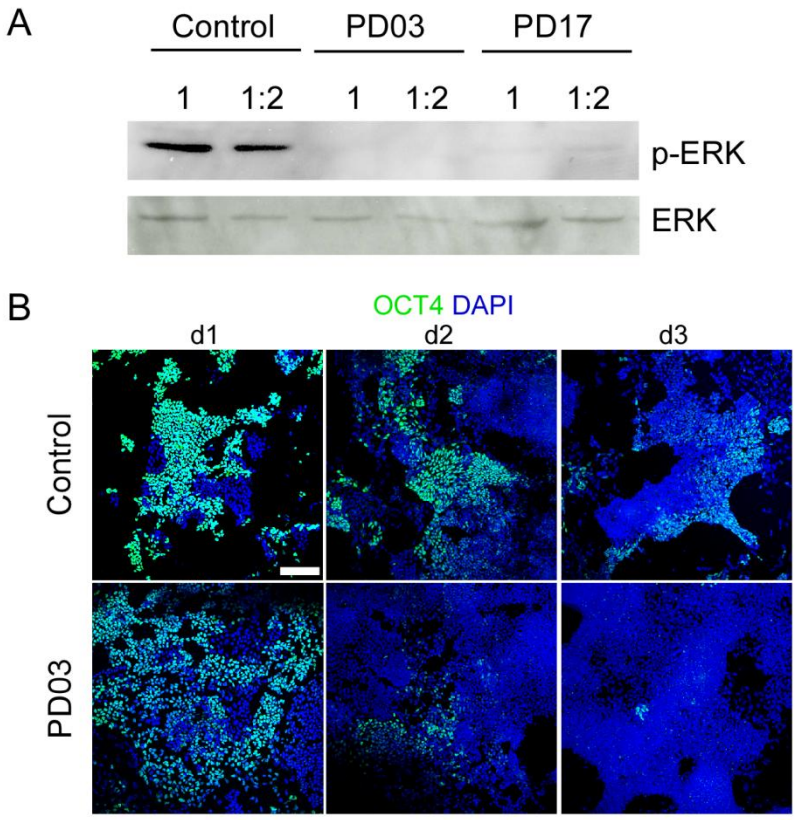


Figure 4.1 Inhibition of FGF/ERK activity accelerates the exit of EpiSCs from a pluripotent stage.

(A) Western blot analysis for phosphorylated ERK in d2 mouse EpiSC differentiation cultures treated with PD0325901 (PD03) or PD173074 (PD17). Samples were loaded undiluted (1; 30 µg) or diluted 1:2 in loading buffer. **(B)** Antibody staining for the pluripotent marker OCT4, labelled with green, in d1, d2 and d3 MD cultures with or without PD0325901 (PD03). DAPI labelling is in blue. Scale bars: 100 µm.

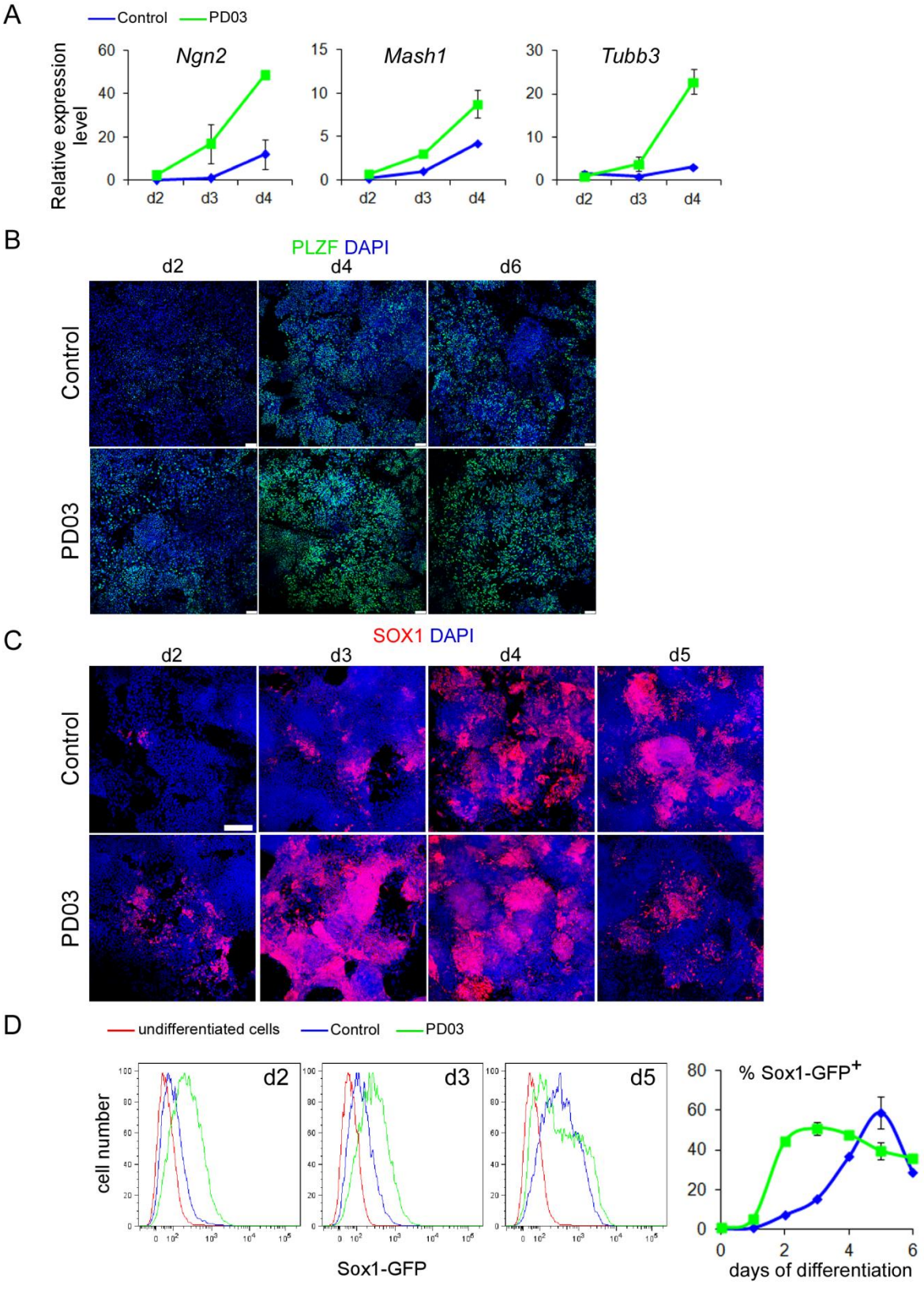

A
Control
PD03
Relative expression level
Ngn2
Mash1
Tubb3
d2
d3
d4
B
PLZF DAPI
d2
d4
d6
Control
PD03
C
SOX1 DAPI
d2
d3
d4
d5
Control
PD03
D
undifferentiated cells
Control
PD03
cell number
d2
d3
d5
Sox1-GFP
% Sox1-GFP+
days of differentiation

Figure 4.2 Inhibition of FGF/ERK activity accelerates neural fate conversion of EpiSCs.

(A) qPCR analysis for the expression of neural lineage marker genes over 4 days MD cultures of EpiSCs. Data represent mean±s.e.m. from triplicate cultures of a single experiment. **(B)** Immunostaining for the neural rosette marker PLZF, shown in green, at d2, d4 and d6 MD with or without PD0325901 (PD03). DAPI labelling is in blue. Scale bars: 100 μm. **(C)** Antibody staining for a neuroepithelium marker SOX1, red, in d2-5 MD cultures with or without PD0325901 (PD03). DAPI labelling is in blue. Scale bars: 100 μm. **(D)** MD cultures of Sox1-GFP EpiSCs in the presence or absence of PD0325901 (PD03). Sox1-GFP reporter expression was analyzed by flow cytometry and the percentage of Sox1-GFP positive cells was determined from three independent cultures. Error bars indicate s.e.m.

4.2 Inhibition of FGF/ERK activity at the onset of EpiSC differentiation promotes mDA progenitor characteristics

To investigate the effect of early FGF/ERK inhibition on the generation of mDA neurons from EpiSCs, cells were exposed for 2 days with either PD173074 or PD0325901 at the onset of neural differentiation and the expression of mDA regulatory genes, *Foxa2*, *Lmx1a*, and *Dmrt5*, were tested. Compared to no-factor controls, the expression levels of *Lmx1a*, *Foxa2*, and *Dmrt5* were already upregulated at d2 MD in cultures that experienced FGF/ERK blockade. Moreover, the increase of *Lmx1a*, *Foxa2*, and *Dmrt5* continued after withdrawal of FGF/ERK inhibitor (Figure 4.3 B, C).

To determine whether longer exposure to the ERK inhibitor could further enhance the expression of mDA regulatory genes, I compared the effects of 5 days PD0325901 treatment (d0-5) to that of 2 days (d0-2) during MD. Contrary to short exposure of PD0325901, no increase of *Foxa2* and *Dmrt5* was observed after 5 days PD0325901 treatment. Moreover, the transcript level of *Lmx1a* was reduced in cultures continuously exposed to PD0325901 when compared with the no-PD0325901 culture at d5. Notably, detection of p-ERK by Western Blot analysis demonstrated the presence of FGF/ERK signalling at d4 MD in cultures which had been treated with PD0325901 for 2 days (d0-2) (Figure 4.3 A). These results indicate that although FGF/ERK inhibition at early stages initiates EpiSC differentiation, endogenous FGF/ERK signalling is necessary from d3 to acquire mDA progenitor characteristics.

To confirm the results of qPCR analysis, EpiSC cultures at d5 MD were stained for LMX1A, FOXA2, and DMRT5. The proportion of cells expressing either one of the mDA progenitor marker in the total cell population was determined by pixel-analysis. At d5, when the majority of cells are Nestin positive, the percentage of neural progenitors expressing LMX1A, FOXA2, or DMRT5 increased greatly in PD0325901 treated cultures (LMX1A: 12±4.3%; FOXA2: 59±10.82%; DMRT5: 35±7.65%) compared to cultures without PD0325901

treatment (LMX1A: 3±1.27%; FOXA2: 24±8.6%; DMRT5: 6±2.45%) (Figure 4.3 E). As treatment with either PD0325901 or PD173074 displayed similar results, PD0325901 was used for further studies unless stated otherwise.

Gene expression analysis by qPCR further revealed an increased expression of *Shh* and *Wnt1* in PD0325901 treated cultures when compared to control cultures. SHH and WNT1 are signalling molecules which were shown to be required for the induction of mDA progenitor cells by forming regulatory loops with LMX1A and FOXA2 (Andersson et al., 2006b; Chung et al., 2009; Echelard et al., 1993; Mavromatakis et al., 2010). At d2 MD, the expression level rose 1.5-fold and 4-fold in cultures with PD173074 and PD0325901, respectively, when compared to no-factor control. The expression of *Shh* was further upregulated between d3 and d5 after withdrawal of PD173074 and PD0325901. However, long exposure of PD0325901 displayed similar transcript levels of *Shh* as in cultures without PD0325901 (Figure 4.3 B). *Wnt1* expression was already highly upregulated at d1 and d2 MD in PD173074- or PD0325901-treated cultures whereas in control cultures the transcript levels of *Wnt1* were low (Figure 4.3 B,C). In contrast to the observed *Shh* expression pattern during the first day of differentiation, *Wnt1* expression decreased from d3 and onward even after withdrawal of the small molecule ERK inhibitor, implying the activation of a pathway negatively regulating *Wnt1* expression. Consistent with a previous study (Chung et al., 2009), I observed similar expression pattern of *Wnt1* and *Lmx1a* at d1 and d2 MD. Furthermore, the kinetics of *Shh* expression correlates with the pattern of *Foxa2* expression, supporting published results of a regulatory relationship between SHH and FOXA2 (Ang and Rossant, 1994; Mavromatakis et al., 2010).

The FGF family can activate 3 different signalling pathways: Mitogen-activated protein kinase (MAPK/ERK), Phosphatidylinositol-3 kinase (PI3K) and Phospholipase C gamma (PLC-γ) (Figure 1.3 A). To address whether the induction of mDA regulators is specific to the blockade of FGF/ERK pathway, neural differentiation of EpiSC was carried out in the presence of the PI3K inhibitor LY294002 (2 µM) from d0-2 MD (Figure 4.4 A). RNA was

collected every day during d1-3 of MD, and the expression levels of *Wnt1*, *Shh*, *Foxa2*, *Dmrt5, Lmx1a*, and *Msx1*, a downstream target of LMX1A (Andersson et al., 2006b), were assessed by qPCR (Figure 4.4 B). I found similar level of mRNA for *Wnt1*, *Shh*, *Dmrt5,* and *Msx1* between LY2949002 treated cultures and control cultures. The expression of *Foxa2* and *Lmx1a* dropped below control levels at d2-3. These findings indicate that early inhibition of FGF/PI3K signalling is not involved in mDA neural specification.

Taking together, blockade of FGF/ERK activity at the onset of the epiblast pluripotent state induces the expression of *Shh* and *Wnt1*, signalling molecules essential for mDA generation, and enhances the generation of mDA progenitor cells marked by FOXA2, LMX1A, and DMRT5. However, these newly converted neural progenitors require endogenous FGF/ERK activity to maintain and stabilise mDA neural progenitor fate.

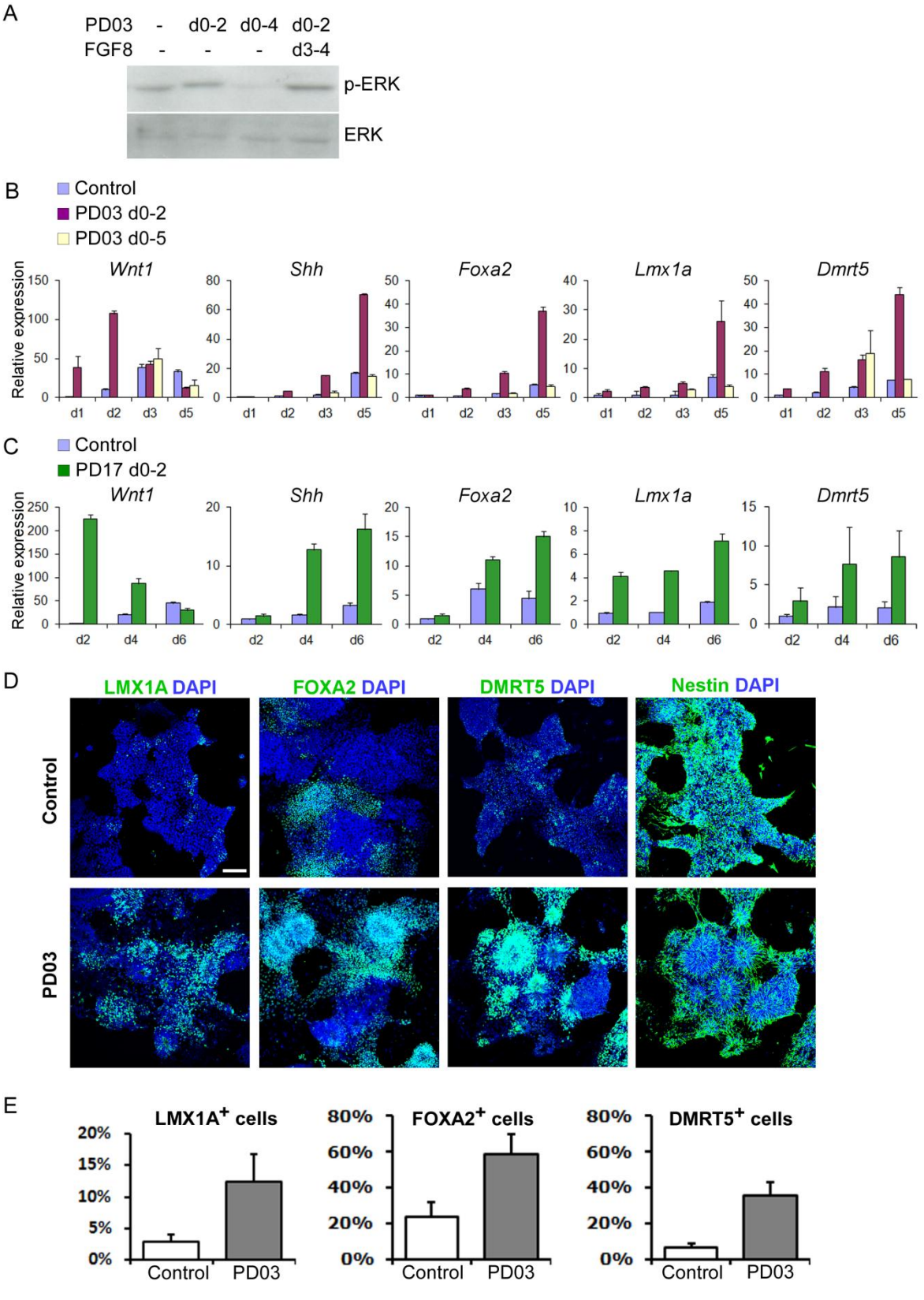

A
PD03 - d0-2 d0-4 d0-2
FGF8 - - - d3-4
p-ERK
ERK
B
Control
PD03 d0-2
PD03 d0-5
Wnt1
Shh
Foxa2
Lmx1a
Dmrt5
Relative expression
d1 d2 d3 d5
C
Control
PD17 d0-2
Wnt1
Shh
Foxa2
Lmx1a
Dmrt5
Relative expression
d2 d4 d6
D
LMX1A DAPI
FOXA2 DAPI
DMRT5 DAPI
Nestin DAPI
Control
PD03
E
LMX1A+ cells
FOXA2+ cells
DMRT5+ cells
Control
PD03

Figure 4.3 Inhibition of FGF/ERK on the exit of the epiblast pluripotent stage promotes the generation of mDA progenitor cells.

(A) Western blot analysis for phosphorylated ERK (p-ERK) and total ERK in d4 mouse EpiSC differentiation cultures treated with PD0325901 (PD03) and FGF8 (15 µg protein). **(B)** E14tg2a mouse EpiSC MD cultures were exposed to PD0325901 from d0 MD for either 2 days (PD03 d0-2) or 5 days (PD03 d0-5). Cultures were harvested at d1, d2, d3 and d5 MD for qPCR analysis. Gene expressions of *Wnt1, Shh*, *Lmx1a*, *Foxa2*, and *Dmrt5* were tested. The value of the d1 MD control was set as 1. Error bars indicate s.e.m. of two sets of experiments performed in duplicate. **(C)** E14tg2a mouse EpiSC MD cultures were exposed to PD173074 from d0 MD for 2 days (PD17 d0-2) and cultures were harvested at d2, d4 and d6 MD. qPCR analysis of *Wnt1, Shh, Lmx1a,Foxa2*, and *Dmrt5*. The value of the d2 MD control was set as 1. Error bars indicate mean±s.e.m. of two sets of experiments performed in duplicate. **(D)** MD of EpiSCs exposed to PD0325901 (PD03) from d0 MD for 2 days were immunostained at d5 for LMX1A, FOXA2, and DMRT5 and counterstained with DAPI. Scale bar: 100 µm. **(E)** Quantification of immunostaining in D showing the percentage of cells expressing each mDA progenitor marker protein.

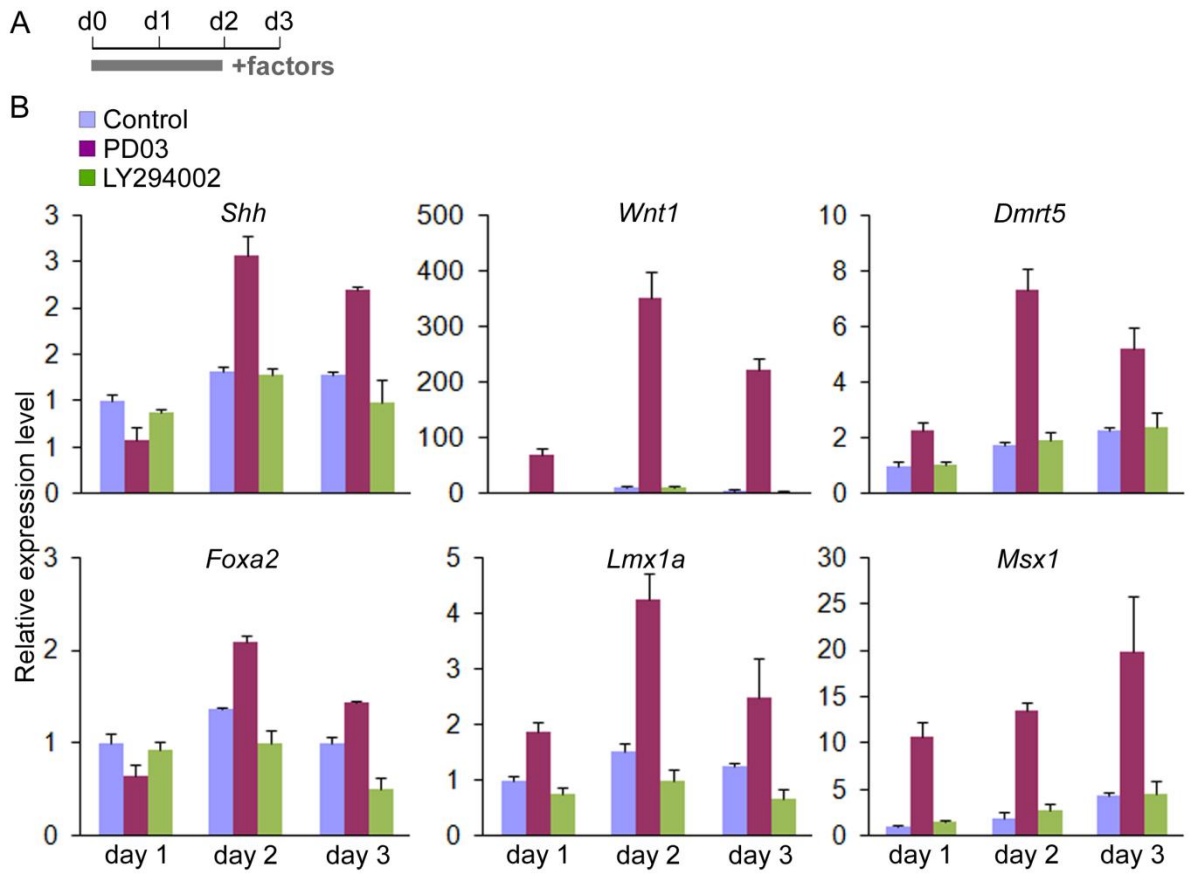


Figure 4.4 Blockade of FGF/PI3K signalling does not induce expression of mDA regulatory genes.

(A) Experimental scheme of neural differentiation with E14tg2a mouse EpiSCs. MD cultures were exposed to PD0325901 (PD03) or LY294002 from d0 MD for 2 days. **(B)** Cultures were harvested at d1, d2, and d3 MD for qPCR analysis. Gene expressions of *Shh, Wnt1, Lmx1a, Foxa2, Dmrt5* and *Msx1* were tested. The value of the d1 MD control was set as 1. Error bars indicate s.e.m. of two sets of experiments performed in duplicate.

4.3 FGF/ERK inhibition affects anterior-posteriorisation and the maintenance of OTX2 in nascent neural progenitors

It has been shown in mouse embryos that blockade of FGF signalling during gastrulation results in an expansion of anterior and a reduction of posterior tissue (Oki et al., 2010; Sun et al., 1999). Therefore, it is possible that inhibition of FGF/ERK promotes the generation of ventral midbrain progenitor cells via modulating anterior–posterior characteristics of neural progenitor cells. To verify whether early blockade of FGF/ERK signalling maintains anterior neural character during neural differentiation, EpiSC MD cultures were analysed for anterior-posterior markers.

In order to examine the anterior character of EpiSC MD, cultures were analysed by immunostaining for OTX2 which is an anteriorly expressed homeobox protein (Acampora et al., 1995; Ang et al., 1994; Millet et al., 1996; Simeone et al., 1992; Simeone et al., 1995). As expected, EpiSC cultures exposed to PD0325901 on exit of the pluripotent stage exhibited an enlarged OTX2 positive cell population when compared to control cultures at d3-5 MD (control, d5: 11.75±4.25%; PD0325901, d5: 69.48±17.89%) (Figure 4.5 A, B). Consistent with the immunostaining for OTX2, transcript levels of *Gbx2*, expressed *in vivo* in areas becoming the anterior hindbrain and spinal cord, increased from d1 until d3 of MD in cultures without PD0325901 whereas the expression decreased with PD0325901 (Figure 4.5 C). Together, these data indicate that early FGF/ERK blockade promotes and/or maintains an anterior character of neural progenitor cells.

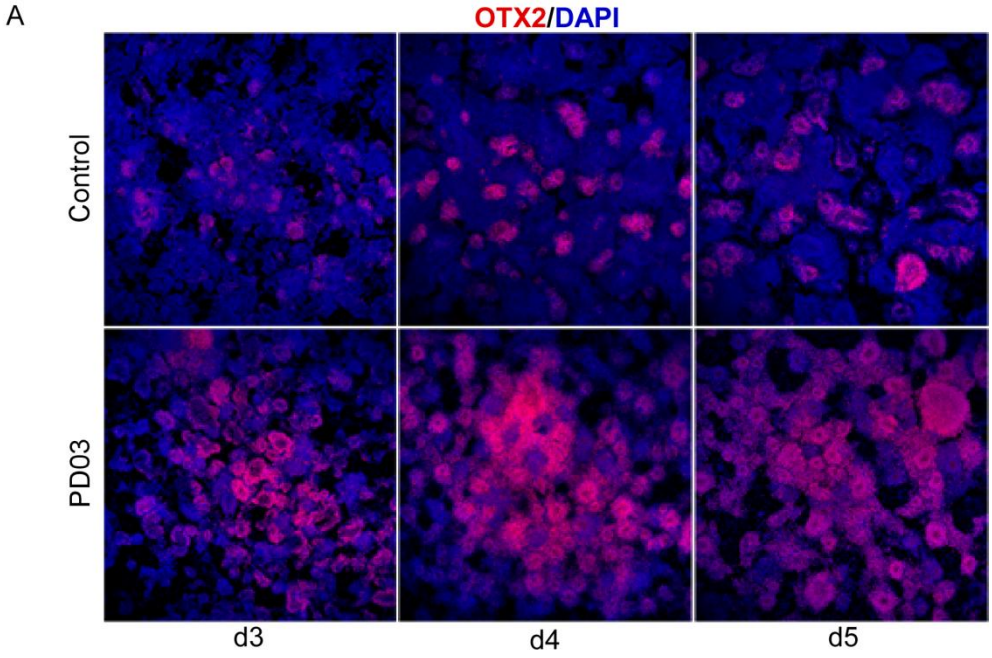
However, FGFs are expressed in the anterior neural ridge where they are involved in the formation of the forebrain (Paek et al., 2009; Shimamura and Rubenstein, 1997). To investigate whether the generation of cells with forebrain characteristic is affected by inhibition of FGF/ERK activity, the expressions of the forebrain marker genes *Six3* and *Foxg1* were tested in MD cultures with or without PD0325901 at d0-2 (Figure 4.5 D) (Hebert and McConnell, 2000; Jeong et al., 2008; Lavado et al., 2008). The transcript level of *Six3*

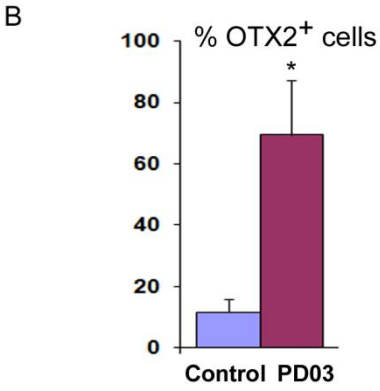
and *Foxg1* were similar at d2 MD in both conditions. Interestingly, in cultures exposed to PD0325901 the expression of *Six3* and *Foxg1* decreased after PD0325901 was withdrawn. Furthermore, their expression levels were reduced at d3-4 when compared to control MD, suggesting that early inhibition of FGF/ERK activity suppress the commitment of newly born neural progenitor cells toward anterior forebrain fate.

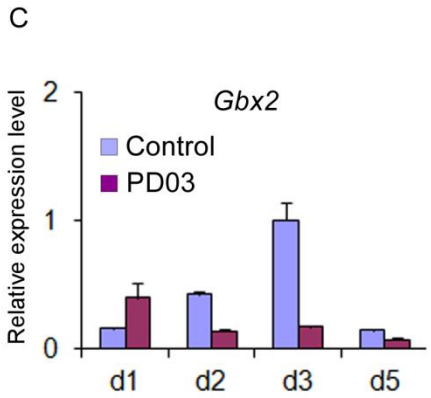
The *Otx2* positive domain in the neuroepithelium spans the prospective forebrain and midbrain. Following the observation on decreased forebrain marker gene expression in PD0325901-treated cultures, I examined the expression of midbrain marker genes *En2* and *Dmbx1* (Davidson et al., 1988; Davis et al., 1988; Gogoi et al., 2002; Ohtoshi and Behringer, 2004). The transcript level of *En2* increased steadily in both culture conditions from d2 until d5 of MD. However, a greater increase was observed in PD0325901-treated cultures compared to the control. An increase of *Dmbx1* was already evident from d1 MD with PD0325901 treatment when compared to control, although its level in the control cultures catched up at d5 MD.

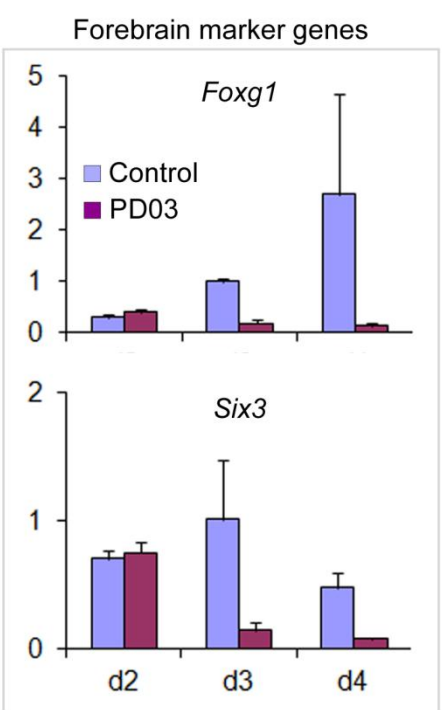
To test whether FGF/PI3K pathway plays a role in anterior-posterior modulation of neural progenitor, EpiSC cultures at d5 MD treated with or without PD0325901 or LY294002 were assessed by immunocytochemistry for OTX2. An increase of the OTX2 positive cell population was only observed in PD0325901-treated cultures while LY294002-treated cultures had a similar proportion of OTX2 positive cells as those in the control.

Taken together, these results suggest that early inhibition of FGF/ERK activity primes cells for a midbrain progenitor cell fate by blocking forebrain and hindbrain cell fate.


A
OTX2/DAPI
Control
PD03
d3
d4
d5


B
% OTX2+ cells
100
80
60
40
20
0
*
Control
PD03


C
Gbx2
Relative expression level
2
1
0
Control
PD03
d1
d2
d3
d5


D
Forebrain marker genes
Foxg1
5
4
3
2
1
0
Control
PD03
Six3
2
1
0
d2
d3
d4

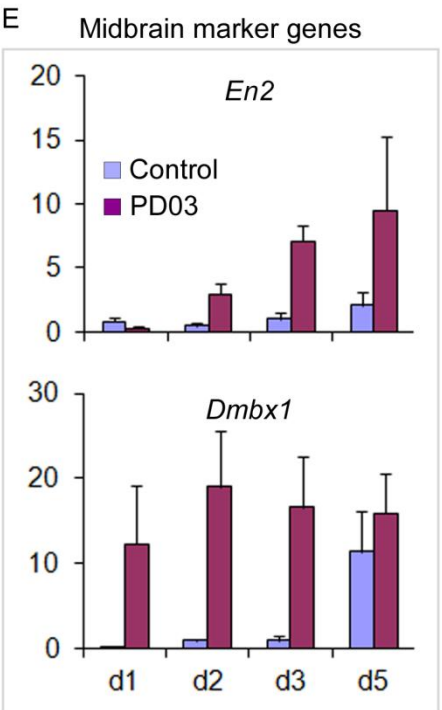

E
Midbrain marker genes
En2
20
15
10
5
0
Control
PD03
Dmbx1
30
20
10
0
d1
d2
d3
d5

Figure 4.5 Early blockade of FGF/ERK activity modulates anterior –posterior characteristics of neural progenitor cells.

(A) Antibody staining for the anterior marker OTX2 shown in red in d3, d4 and d5 MD cultures with or without PD0325901 (PD03). DAPI is labelled in blue. **(B)** Quantification of immunostaining in A illustrating the percentage of cells expressing OTX2. Mean±s.e.m. of ten fields from two independent experiments. *, P<0.01 relative to no-PD0325901 control (Student's t-test). **(C)** Mouse E14tg2a EpiSC MD cultures were exposed to PD0325901 (PD03) from d0 MD for 2 days. Cultures were harvested at d1, d2, d3 or d5 for qPCR analysis of *Gbx2*. **(D)** E14tg2a EpiSC MD cultures were treated with PD0325901 cultures were harvested at d2-4 for qPCR analysis of the forebrain marker genes *Foxg1* and *Six3.* **(E)** EpiSCs were differentiated in the presence of PD0325901 from d0 MD for 2 days, collected as in C and tested for the midbrain marker genes *En2* and *Dmbx1* by qPCR. The value of the d3 MD control was set as 1. Error bars indicate s.e.m. of two sets of experiments performed in triplicates.

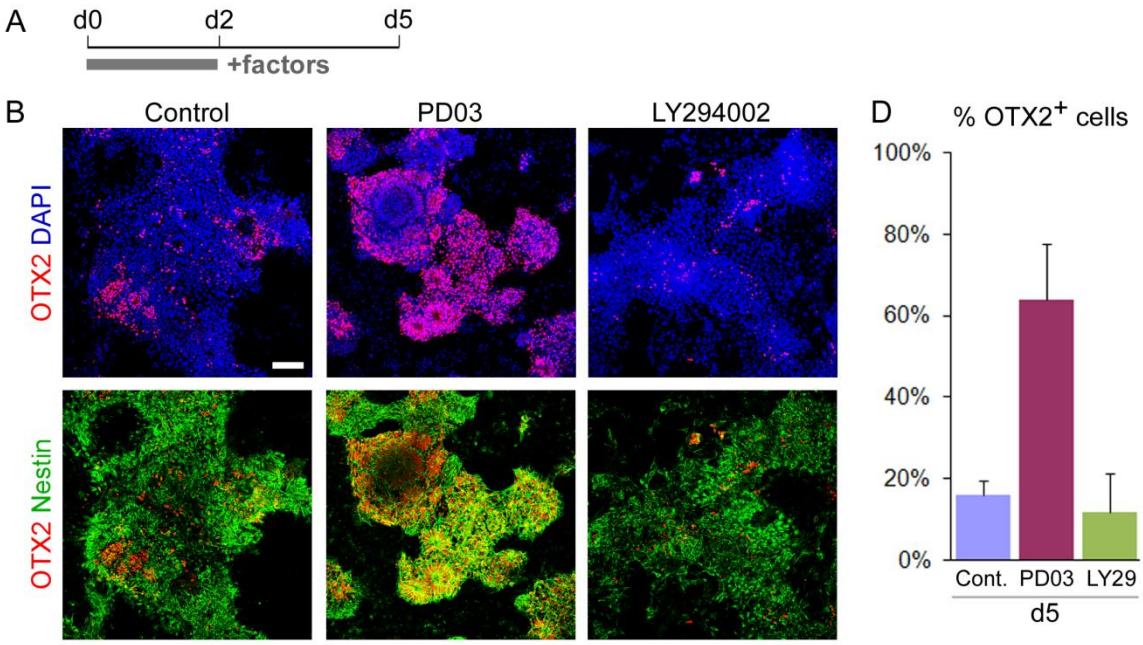


Figure 4.6 Early blockade of FGF/PI3K activity does not promote the generation of neural progenitors with anterior characteristics.

(A) Antibody staining for the anterior marker OTX2 shown in red in d5 MD cultures with or without the small molecule inhibitors PD0325901 (PD03) or LY294002 (LY29). DAPI is labelled in blue. Scale bars: 100 µm. **(B)** Quantification of immunostaining in A illustrating the percentage of cells expressing OTX2. Mean±s.e.m. of ten fields from two independent experiments.

4.4 Highly reliable and efficient production of mDA neurons by ERK inhibitor-primed neural progenitors

To investigate whether the primed mDA progenitor cells generated above can terminally differentiate into DA neurons (TH positive cells) with midbrain-specific identity, SHH and FGF8 were applied to induce DA differentiation in MD cultures at d5 when the majority of cells were Nestin positive as they are used in standard mDA differentiation protocols (Figure 4.7 A) (Barberi et al., 2003; Kawasaki et al., 2000; Kim et al., 2002; Lee et al., 2000b; Parmar and Li, 2007; Perrier et al., 2004). D14 MD cultures were then analysed in detail for mDA neuronal markers by immunocytochemistry (Figure 4.7 B-D). I found that MD cultures exposed to PD0325901 at d0-2 followed by SHH and FGF8 at d5-9 contained 4-fold more TH positive neurons than no-PD0325901 cultures (PD, 52.3±8%; control, 13.5±9%) (Figure 4.7 B, C).

In order to examine the midbrain-specific characteristics of the derived DA neurons, EpiSC were derived from Pitx3-GFP knock-in ESCs (Maxwell et al., 2005; Zhao et al., 2004). During midbrain development, *Pitx3* expression starts at E11.5 and is restricted to SN and VTA (Smidt et al., 1997). Therefore, co-expression of TH and PITX3 is used as a marker for mDA neurons. Pitx3-GFP EpiSCs were subjected to neural differentiation as illustrated in Figure 4.7 A. Cultures were assessed by immunstaining for TH and GFP at d14 MD. A high proportion (73.8±10.2%) of TH positive neurons co-expressed Pitx3-GFP in cultures received PD0325901 at d0-2 and SHH and FGF8 at d5-9 (Figure 4.7 B, C). In addition, these TH positive neurons also co-expressed midbrain transcription factors, LMX1A (88.5±3.9%) and FOXA2 (99.5±1.2%), and pan-dopaminergic-neuronal markers, NURR1 (also known as NR4A2, 85.4±4%) and VMAT (known as SLC18A1, 85.6±12%). In contrast, 37.1±9.5% of TH positive neurons co-expressed Pitx3-GFP in control cultures exposed to SHH and FGF8 only. In conclusion, midbrain progenitor cells induced by FGF/ERK inhibition can efficiently generate authentic mDA neurons.

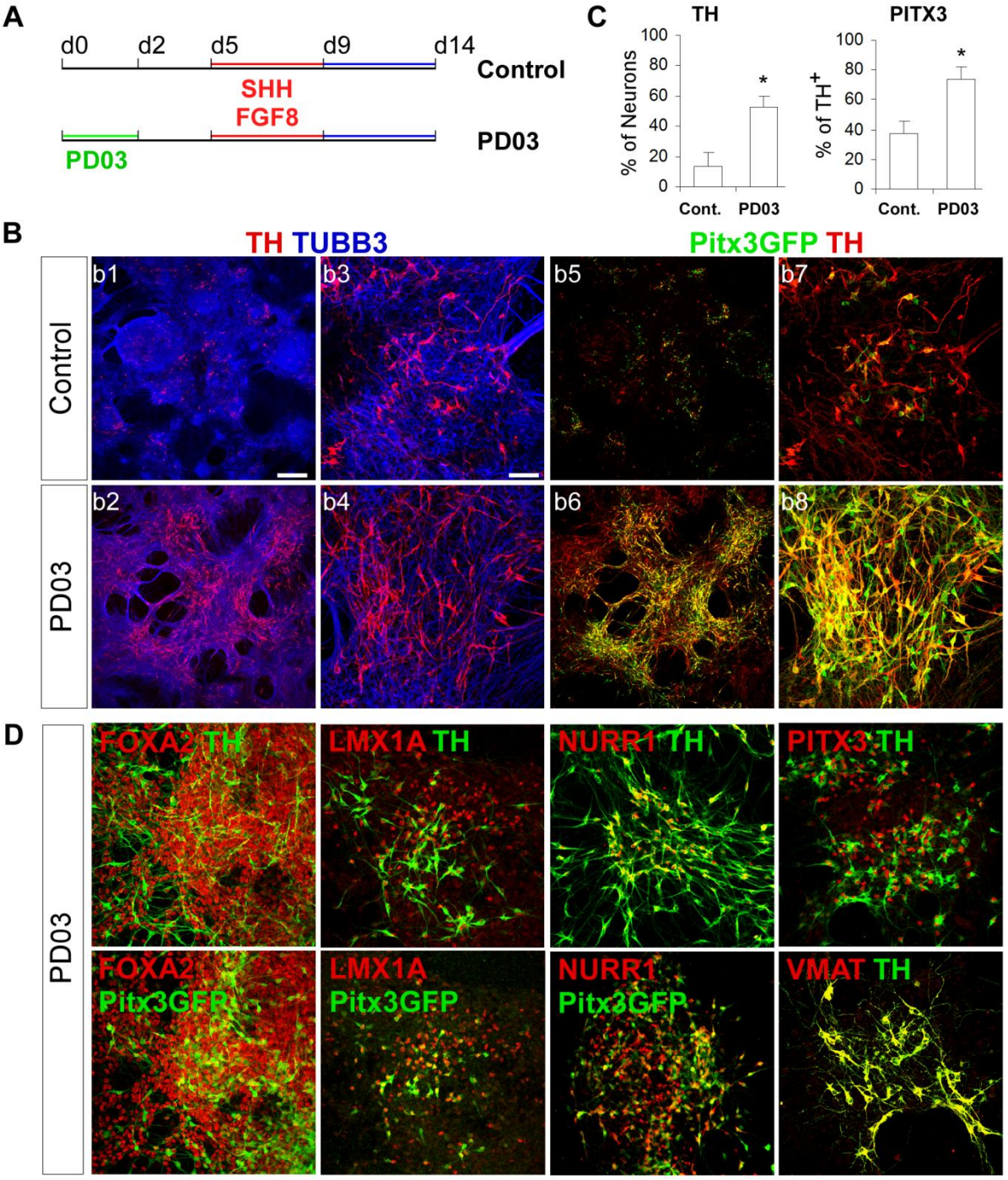

A
d0
d2
d5
d9
d14
Control
SHH
FGF8
PD03
PD03
C
TH
PITX3
% of Neurons
% of TH+
100
80
60
40
20
0
*
Cont.
PD03
B
TH TUBB3
Pitx3GFP TH
Control
PD03
b1
b2
b3
b4
b5
b6
b7
b8
D
PD03
FOXA2 TH
LMX1A TH
NURR1 TH
PITX3 TH
FOXA2 Pitx3GFP
LMX1A Pitx3GFP
NURR1 Pitx3GFP
VMAT TH

Figure 4.7 Temporally controlled FGF/ERK activity promotes the production of functional, authentic mDA neurons.

(A) Experimental scheme of neural differentiation with Pitx3-GFP EpiSCs. MD cultures were exposed to PD0325901 (PD03) from d0 MD for 2 days. SHH and FGF8 were applied from d5 until d9. Medium was then changed to N2B27 plus GDNF, BDNF and ascorbic acid and cultured for another 5 days. **(B)** MD cultures at d14 were double stained for (b1-4) TH, red, and TUBB3, blue, as well as (b5-8) TH, red, and Pitx3-GFP labelled in green. **(C)** Quantification of the immunostaining in B, showing the percentage of TH positive neurons and TH positive neurons co-expressing Pitx3-GFP. Mean±s.e.m. *, $P<0.01$ relative to no-PD0325901 control (Student's t-test). **(D)** Immunostaining of mouse d14 MD cultures for TH and mDA neural markers. Scale bars: 200 µm for B (b1,2,5,6) and 50 µm for B (b2,3,7,8), D.

4.5 Dopaminergic neuron differentiation of mouse iPSCs in response to ERK inhibition

Next I wanted to test whether this protocol can be applied to mouse induced pluripotent stem cells. Considering that inhibition of FGF/ERK signalling maintains ESCs in the naïve pluripotent state (Silva et al., 2008a; Ying et al., 2008) and activation of FGF signalling is necessary to drive ESCs toward the primitive ectoderm/epiblast stage (Kunath et al., 2007), PD0325901 was applied for 2 days either during d1-3 or d2-4 of MD. To support the generation of mDA neurons, SHH and FGF8 were added from d6 until d10 of MD (see Figure 4.8 A). Immunostaining for TUBB3, TH and FOXA2 was carried out at d14 MD to observe the generation of mDA neurons. During development, the specification of mDA neurons, which are TH positive, starts in the medial domain of the *Foxa2*-expressing floor plate (Ferri et al., 2007). Consequently, co-expression of TH and FOXA2 can be used as a marker for mDA neurons. Consistent with the observation in EpiSC MD, mDA neurons (TH and FOXA2 double positive) neurons were also efficiently generated in MD cultures of iPSCs exposed to PD0325901 either at d1-3 or d2-4 MD when compared to control (Figure 4.8 B), supporting our hypothesis that early blockade of FGF signalling during neural induction primes a midbrain regional fate in derived neural progenitors, which subsequently differentiate into DA neurons exhibiting midbrain characteristics.

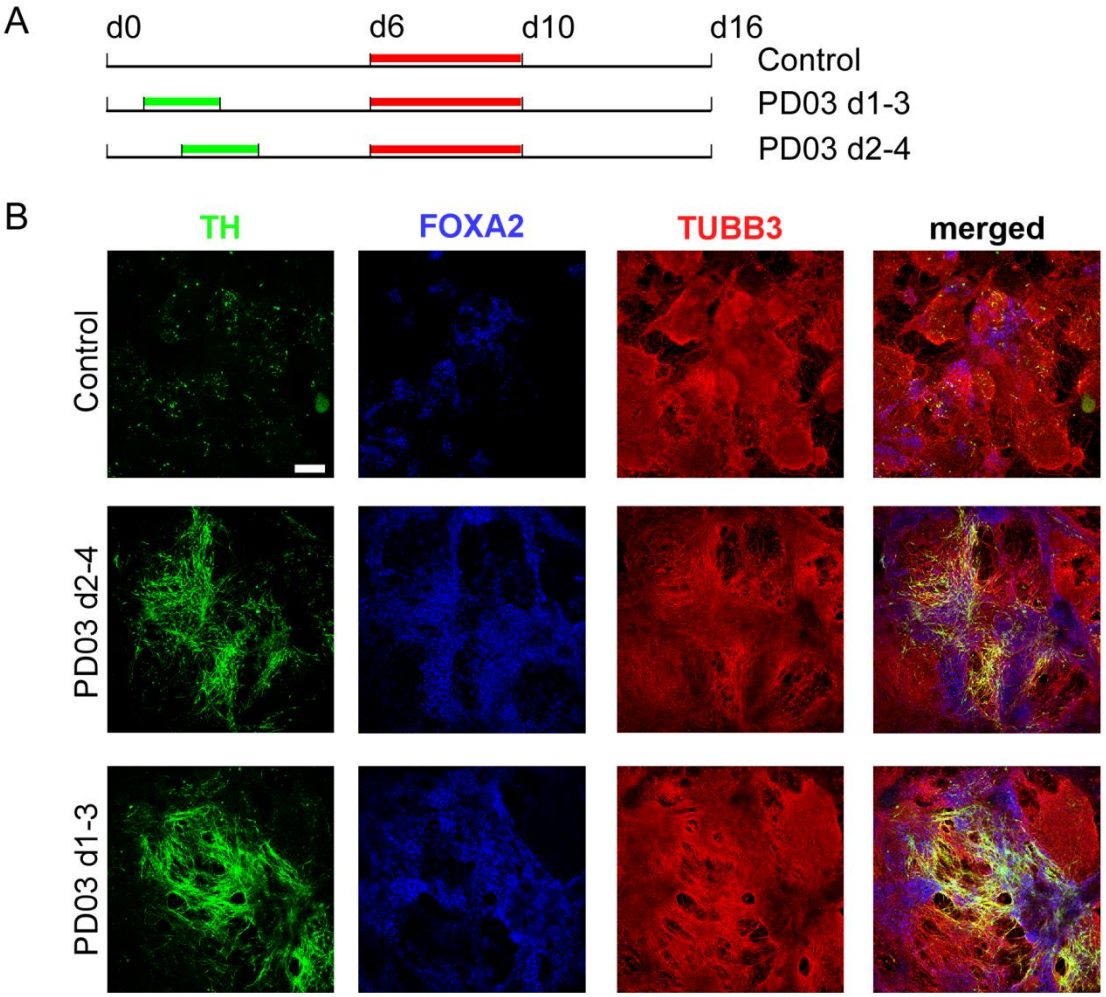


Figure 4.8 Efficient generation of mDA neurons from mouse iPSCs.

(A) Experimental scheme of neural differentiation with mouse iPSCs. MD cultures were exposed to PD0325901 (PD03, green) at either d1-3 or d2-4 of MD. SHH and FGF8 (red) were applied from d6 until d10 of MD. Medium was then changed to N2B27 plus GDNF, BDNF and ascorbic acid and cultured for another 4 days. **(B)** MD cultures at d14 were double stained for TH shown in green, FOXA2, blue, and TUBB3, red. Scale bar: 200 µm.

4.6 Differential activity of SHH and FGF8 in mDA fate specification and differentiation

Ye and colleagues reported (1998) that only the combinatorial treatment of SHH and FGF8 can induce DA fate in E9 ventral caudal forebrain rat explants. In agreement with this study, I also observed a robust generation of TH positive neurons at d14 MD in PD0325901-treated cultures exposed to SHH and FGF8 from d5 until d9 whereas few TH positive cells were detected in cultures treated with PD0325901 alone (Figure 4.9). A large number of TH positive cells were also detected in MD cultures which received PD0325901 at d0-2 followed by SHH alone at d5-9. However, these DA neurons showed a low expression of TH with immature neuronal morphology. In contrast, TH positive neurons in d14 MD cultures treated with PD0325901 followed by FGF8 alone displayed a more mature morphology. The number of TH positive cells in this condition was comparable with control MD cultures exposed to SHH and FGF8 in the absence of PD0325901.

I next analysed the expression of gene markers associated with GABAergic phenotype by qPCR. The RNA levels of *Helt*, *Gata2*, and *Gad1* were determined at d5 and d8 and the data was presented as the fold change to the level of d5 in control MD cultures with no added factors. I detected the highest fold increase of these GABAergic marker genes in control cultures without exogenous stimuli (*Gata2,* 38-fold; *Helt*, 293-fold; *Gad1*, 401-fold) (Figure 4.10) whereas in cultures with SHH the expression of these genes was substantially repressed. In cultures exposed to PD0325901 followed by SHH, the mRNA levels of *Helt* and *Gad1* were only 10% of the level of MD cultures treated with SHH alone and were less than 1% of the level of no-factor controls.

To further elucidate how SHH and FGF8 may shape neural progenitor cell fate, SHH and FGF8, either alone or in combination, were applied at d3-6 of EpiSCs, a stage when neural progenitor arise (Figure 3.1 and Figure 4.2), and changes in the expression levels of mDA regulator genes were monitored at d6 of differentiation when the majority of cells is Nestin

positive (Figure 4.3 D). The expression levels of *Dmrt5*, *Foxa2*, and *Msx1* were upregulated in cultures exposed to SHH at d3-6 while the mRNA transcript levels of *Lmx1a* and *Shh* were not enhanced (Figure 4.11 B, C). In contrast, adding FGF8 alone or with SHH abolished the increased expression of *Dmrt5*, *Foxa2*, *Msx1*, *Lmx1a*, and *Shh* caused by PD0325901 or PD0325901-SHH. Moreover, activation of FGF signalling by FGF8 resulted in an increase of isthmus associated genes *Wnt1*, *En1*, and *En2,* in agreement with previously published data (Lee et al., 1997; Liu and Joyner, 2001; Liu et al., 1999).

The results shown in chapter 4.2 indicated that a period of autocrine FGF/ERK signalling is essential for newly born neural progenitor cell to become specified into a ventral midbrain fate characterised by DMRT5, LMX1A, and FOXA2. However, enhancement of FGF signalling by FGF8 in newly born neural progenitors eliminated the PD0325901-mediated upregulation of mDA regulatory genes *Dmrt5*, *Lmx1a*, *Foxa2*, *Shh* and *Msx1*. These data demonstrate the importance of temporally controlled modulation of FGF/ERK signalling in the specification of neural progenitors towards a ventral midbrain fate. Furthermore, SHH and FGF8 co-operatively direct the conversion of PD0325901-generated d5 neural progenitors into mDA neurons where SHH signalling specifies a DA phenotype and FGF8 facilitates progenitor differentiation.

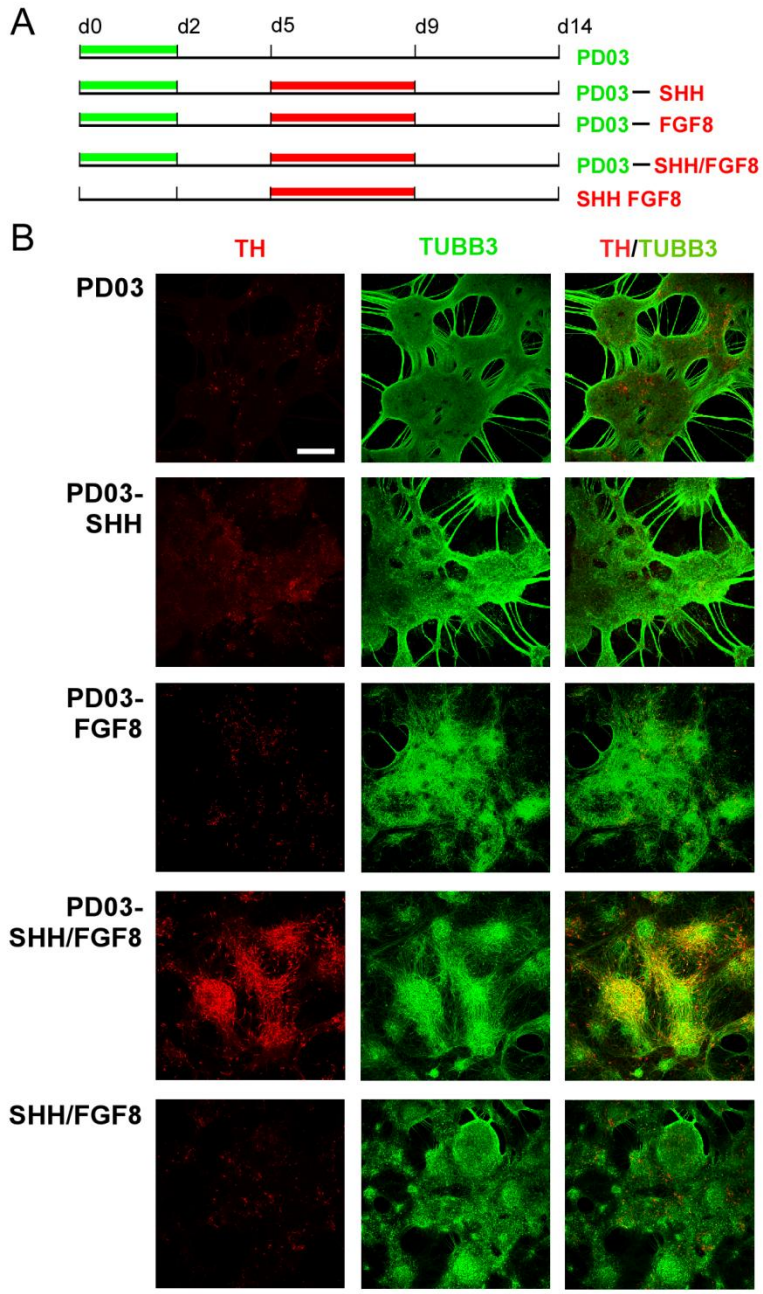


Figure 4.9 Temporally controlled FGF/ERK activity in combination with SHH and FGF8 promotes the production of DA neurons.

(A) Experimental schemes for data in B. **(B)** MD cultures of EpiSCs at d14 were double stained for TH, shown in red, and TUBB3, labelled with green. Scale bar: 200 µm.

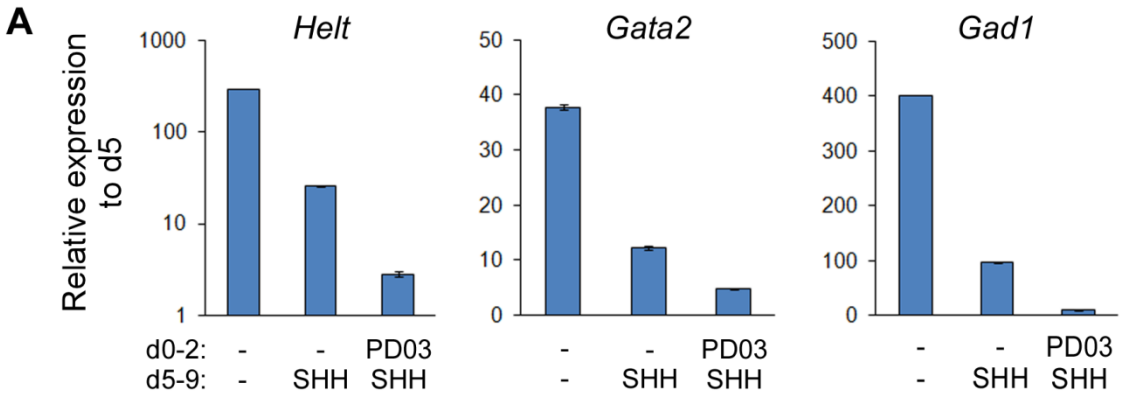


Figure 4.10 Activation of SHH signalling promotes the production of DA neurons by repressing the transcript level of genes for a GABAergic neuronal fate.

(A) Gene expression analysis of *Helt, Gata2*, and *Gad1* of d5 and d9 MD cultures by qPCR. Fold change analysis is used to determine the difference of gene expression between d5 and d9 in control MD cultures with no added factors, control cultures treated with SHH, and cultures exposed to PD0325901 at d0-2 followed by SHH. Error bars indicate s.e.m. of triplicate cultures from one representative experiment.

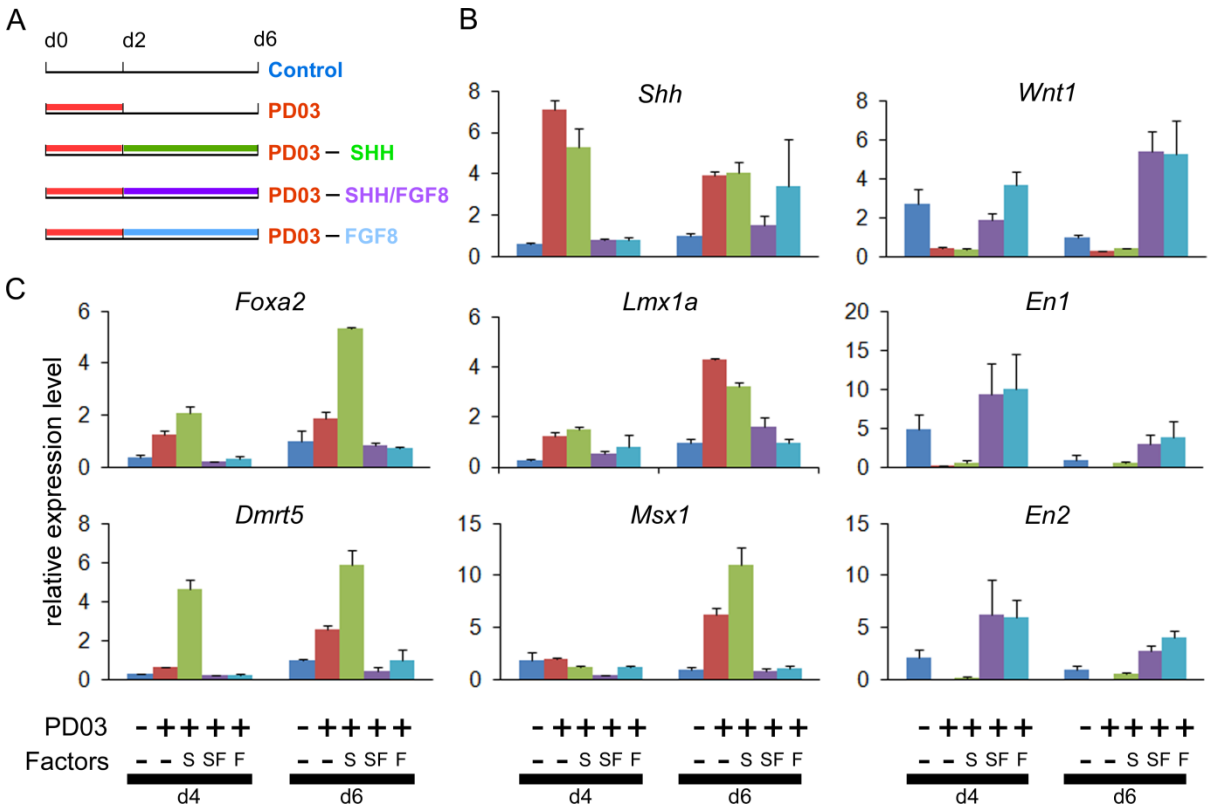


Figure 4.11 Effect of SHH and/or FGF8 in EpiSC MD.

(A) Experimental schemes for data in B. **(B+C)** Mouse E14tg2a EpiSC MD cultures were exposed to PD0325901 (PD03) from d0 MD for 2 days. Cultures were harvested at d4 and d6 for qPCR analysis of the mDA fate inducing signalling molecules *Shh* and *Wnt1* (B) and the midbrain genes *Lmx1a, Foxa2, Msx1, En1,* and *En2* (C). The value of the d6 MD control was set as 1. Error bars indicate s.e.m. of two sets of experiments performed in duplicate.

4.7 WNT alone or in combination with SHH cannot replace ERK inhibitor in inducing midbrain progenitor cell fate

The induction of signalling molecules *Shh* and *Wnt1* by either PD173074 or PD0325901 and the concomitant induction of their target genes *Foxa2* and *Lmx1a*, respectively (Figure 4.3 B, C), prompted me to investigate whether SHH and WNT1 are the mediators of early FGF/ERK blockade that led to induced efficient mDA fate specification and differentiation.

4.7.1 The effects of early SHH activation on mDA induction

In order to investigate the contribution of an early activation of SHH signalling, MD differentiation was firstly carried out in the presence of SHH, PD0325901+SHH, or PD0325901 alone from d0. RNA was collected from d1-3 of MD and analysed for the expression of *Shh*, the SHH downstream targets *Gli1* and *Foxa2* and the mDA regulator genes *Dmrt5, Lmx1a*, and *Msx1* (Figure 4.12). As expected, in MD cultures exposed to SHH alone (d0-2) showed an increased mRNA level of *Gli1* and *Foxa2* from d2 or d3 respectively when compared to control cultures. However, the transcript levels of the mDA regulator genes *Lmx1a*, *Msx1*, and *Dmrt5* were similar to the expression levels in control cultures.

Next I wanted to determine whether the observed induction of mDA marker gene expression is SHH dependent. To this end I performed an additional MD in the presence of the SHH inhibitor cyclopamine with or without PD0325901 (Figure 4.13). MD cultures exposed to cyclopamine (10 µM) in the presence or absence of PD0325901 displayed a reduction in the expression levels of the SHH downstream target genes *Gli1* at d1-3 and *Foxa2* at d2-3 to control cultures, confirming its SHH inhibitory activity. Cyclopamine had little effect on the expression of *Shh, Msx1*, and *Dmrt5*. Interestingly, PD0325901-induced expression of *Dmrt5* and *Msx1* was further enhanced by cyclopamine, suggesting a SHH-independent mechanism. However, cyclopamine treatment attenuated PD0325901-mediated induction of *Foxa2* and *Lmx1a* (Fig 4.7.2).

Because SHH treatment alone could increase the expression of *Foxa2* and *Lmx1a* from d3 onward, we asked whether an early addition of SHH is sufficient to direct MD cultures towards a midbrain neural progenitor fate. I first tested the expression of the hindbrain marker gene *Gbx2* and midbrain marker genes *En1* and *Dmbx1* during 3 days of differentiation (Figure 4.14 A). The data revealed that, unlike PD0325901, SHH did not suppress the hindbrain marker gene *Gbx2* and upregulated the midbrain marker genes *En1* and *Dmbx1*. Consistent with the qPCR data, I did not observe an increase of OTX2 positive cells at d5 and d9 in cultures exposed to early SHH (Figure 4.14 B). As shown in Figure 4.14 C, only cultures exposed to PD0325901 had a significant proportion of OTX2 positive cells at d9 MD (PD0325901, 43.88±5.32%; SHH, 6.75±2.75%; control, 7.25±2.29%). Surprisingly, at d9, no obvious difference was seen in the number of FOXA2 and LMX1A positive neural progenitors in PD0325901-, SHH-treated and no-factor cultures. However, a high proportion of TH positive neurons were only obtained in PD0325901-treated cultures (Figure 4.15 B). Taken together, these results suggest that SHH is not sufficient to replace PD0325901 at d0-2 for complete mDA induction.

4.7.2 The effects of GSK3ß inhibition on mDA induction

Early inhibition of FGF/ERK activity also induced the expression of *Wnt1*. This factor is generally considered a canonical WNT because it co-localizes with β-catenin in the ventral midbrain and mutation of *Wnt1 in vivo* lead to a similar phenotype as *ß-catenin* mutations (Castelo-Branco et al., 2004; Castelo-Branco et al., 2003; Danielian and McMahon, 1996; Prakash et al., 2006; Tang et al., 2010). To test whether activation of WNT signalling can bring about similar effects to PD0325901, I used the small molecule CHIR99021, a selective inhibitor of the Glycogen synthase kinase-3 (GSK3ß) with an IC_{50} less than 10 nM (Bain et al., 2007; Murray et al., 2004; Ring et al., 2003). In the absence of WNT, ß-catenin is phosphorylated by a GSK3ß containing destruction protein complex inducing its degradation. In the presence of WNT, GSK3ß is physically displaced from the complex of

regulatory binding partners preventing the phosphorylation and degradation of ß-catenin. Thus, inhibition of GSK3ß by CHIR99021 results in the maintenance and accumulation of ß-catenin mimicking WNT signalling (Ring et al., 2003). As a transcriptional readout of active canonical WNT signalling, I analysed the expression of the downstream target *Axin2* by qPCR (Jho et al., 2002). As expected, the expression level of *Axin2* increased when CHIR99021 was added at d0-2 of MD confirming the stimulation of ß-catenin/TCF signalling (Figure 4.16 B). The effect of CHIR99021 on *Axin2* expression was dose-dependent, as MD cultures exposed to 2 µM CHIR99021 showed an enhanced mRNA level of *Axin2* when compared to cultures that experienced only 0.5 µM. The expression level of *Axin2* dropped to the transcript level of control cultures at d3 MD after withdrawal of CHIR99021. PD0325901 treatment resulted in upregulation of *Axin2* (2.5 to 3.7x fold compared to control cultures), suggesting that activation of canonical WNT signalling may be involved (Figure 4.16 B).

It has been reported that LMX1A is in a autoregulatory loop with the WNT pathway in the context of mDA neurogenesis (Chung et al., 2009). I therefore asked whether CHIR99021 could mimic PD0325901 in upregulating of *Lmx1a*. The expression of *Lmx1a* in cultures exposed to CHIR99021 was similar to control cultures at d1 whereas *Lmx1a* induction was already evident in PD0325901-treated cultures (Figure 4.16 B). However, at d2 MD, the mRNA level of *Lmx1a* visibly increased in CHIR99021-treated cultures compared to cultures without factor. Furthermore, expression of *Dmrt5* was not affected by CHIR99021. These findings suggest that other pathway(s) may contribute to the induction of the mDA neural progenitor fate.

It has been reported that in the developing midbrain OTX2 and WNT1 are in a positive regulatory feedback loop (Chung et al., 2009; Prakash et al., 2006). To investigate whether the observed *Otx2* upregulation is mediated by WNT1, I examined OTX2 and *Gbx2* by immunocytochemistry and qPCR (Figure 4.16 C-E). No increase of OTX2 positive cells was observed at d5 MD with any concentrations of CHIR990221 (0.5 µM: 6±2.02%; 2.0 µM:

16±6.02%) when compared to control cultures (16±3.57%), whereas in PD0325901-treated sister cultures the majority of cells were OTX2 positive neural progenitors (64±13.64%) (Figure 4.16 C, D). In addition, no reduction of *Gbx2* expression was seen in cultures experienced early inhibition of GSK3ß (Figure 4.16 E).

4.7.3 The effects of combined treatment of SHH and CHIR99021 on mDA induction

Because SHH and CHIR99021 only partially induced mDA neural progenitor characteristics (↑*Foxa2*, ↑*Lmx1a*), I next studied their combination in mDA induction. In the presence of both CHIR99021 and SHH at d0-2 MD, the expression of *Lmx1a* and *Foxa2* at d2 MD increased up to ~3 times compared to control cultures, similar to that observed in cultures exposed to PD0325901 (Figure 4.17 B). However, unlike PD0325901 treatment, no upregulation of *Dmrt5* was observed (Figure 4.17 B). Furthermore, the proportion of OTX2 positive cells in cultures with SHH and CHIR99021 (SHH & 0.5 µM CHIR99021: 5.56±2.5%; SHH & 2µM CHIR99021: 0.35±0.22%) was even below the percentage observed in control cultures at d5 MD (16±3.57%) (Figure 4.17 C, D). In keeping with this observation, a downregulation of *Gbx2*, as in PD0325901 treated cultures, was not detected in cultures exposed to SHH and CHIR99021 (Figure 4.17 E). Nonetheless, I performed terminal neural differentiation with PD0325901, CHIR99021 alone or with SHH and no-factor, as illustrated in Figure 4.18 A, and tested whether robust induction of the mDA regulators *Lmx1a* and *Foxa2* potentiate mDA neuronal production. I applied immunofluorescent staining at d14 MD to examine the generation of DA neurons with midbrain character, marked by TH and FOXA2 double positive cells. As anticipated, most of FOXA2 and TH double positive cells were detected in cultures treated with PD0325901 at d0-2 (Figure 4.18 B). Only few TH positive cells were observed in MD cultures with CHIR99021, CHIR99021-SHH or without factors. Most of these TH positive cells did not co-express FOXA2, suggesting that they might be a different subpopulation of DA cells. On the other hand, the cell population of FOXA2 positive cells was slightly but consistently increased in cultures exposed to CHIR99021 alone or its

combination with SHH. It is possible that CHIR99021 treated cells respond more efficiently to secreted SHH.

Taken together, neither SHH, canonical WNT signalling nor their combination can replace early inhibition of FGF/ERK activity in the generation of mDA neurons, indicating that other pathways are involved in this process.

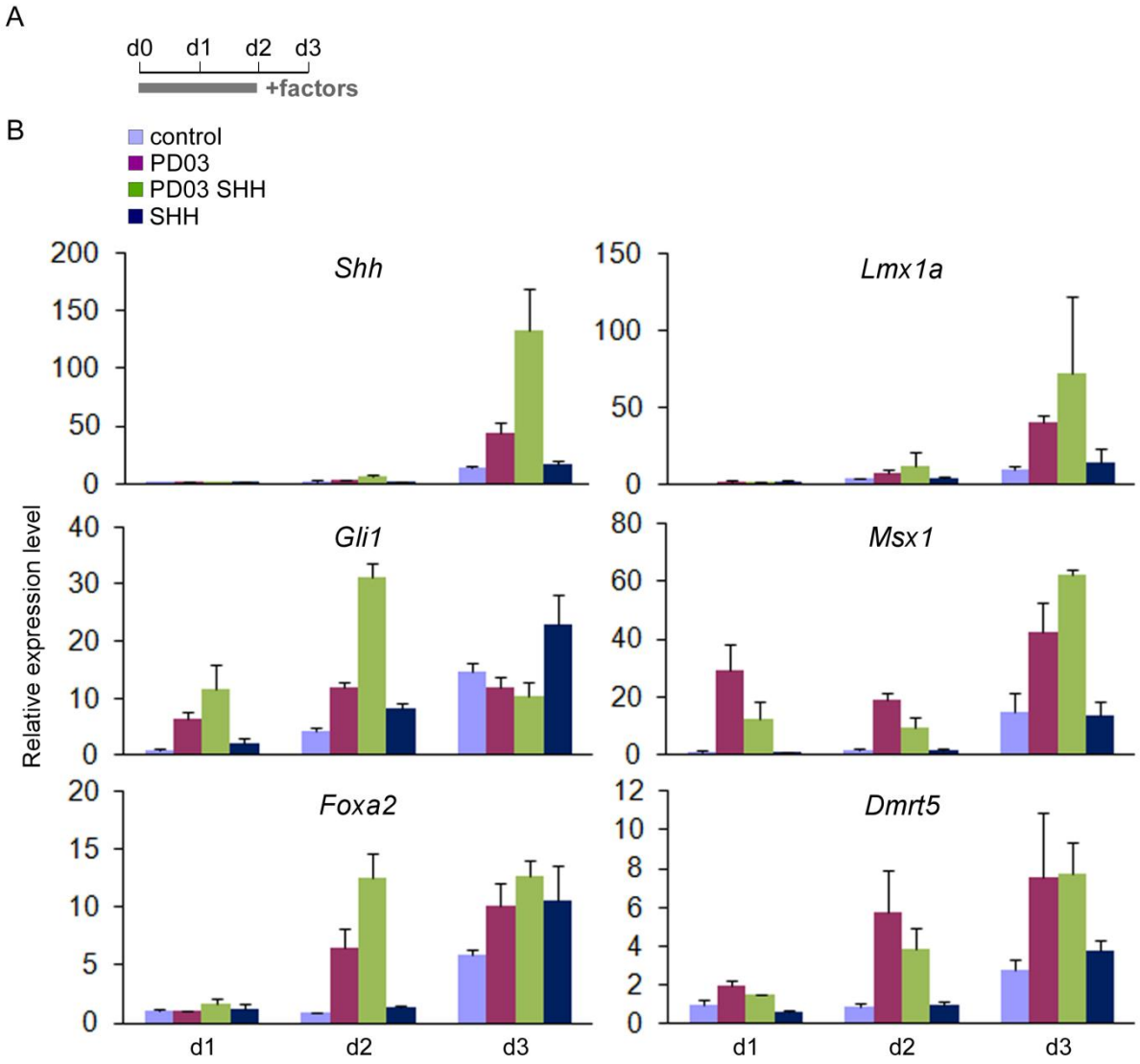


Figure 4.12 Activation of SHH pathway is not sufficient for complete mDA induction.

(A) Experimental schemes for data in B. **(B)** Mouse E14tg2a EpiSC MD cultures were exposed to PD0325901 (PD03) and/or SHH from d0 MD for 2 days. Cultures were harvested at d1-3 for qPCR analysis of the mDA fate inducing signalling molecule *Shh* and its downstream target genes *Gli1* and *Foxa2* as well as the midbrain genes *Lmx1a, Msx1,* and *Dmrt5*. The value of the d1 MD control was set as 1. Error bars indicate s.e.m. of two sets of experiments performed in triplicate.

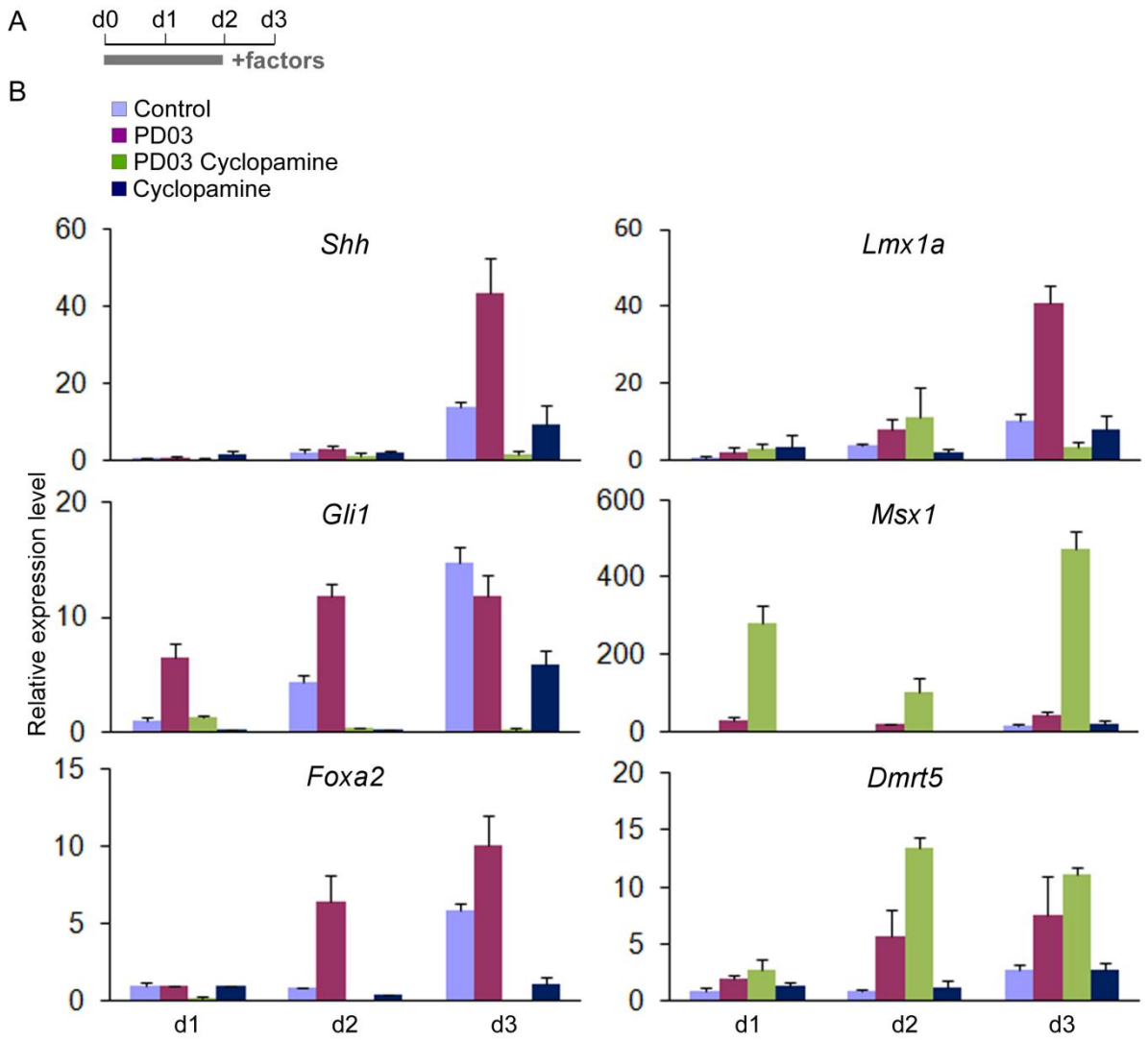


Figure 4.13 Early inhibition of FGF/ERK acts partly via the SHH pathway.

(A) Experimental schemes for data in B. **(B)** Mouse E14tg2a EpiSC MD cultures were treated with PD0325901 (PD03), the SHH antagonist cyclopamine or a combination of the two as indicated. Cultures were harvested at d1, d2, and d3 for qPCR analysis of the mDA fate inducing signalling molecule *Shh* and its downstream target genes *Gli1* and *Foxa2* as well as the midbrain progenitor genes *Lmx1a, Msx1*, and *Dmrt5*. The value of the d1 MD control was set as 1. Error bars indicate s.e.m. of two sets of experiments performed in triplicate.

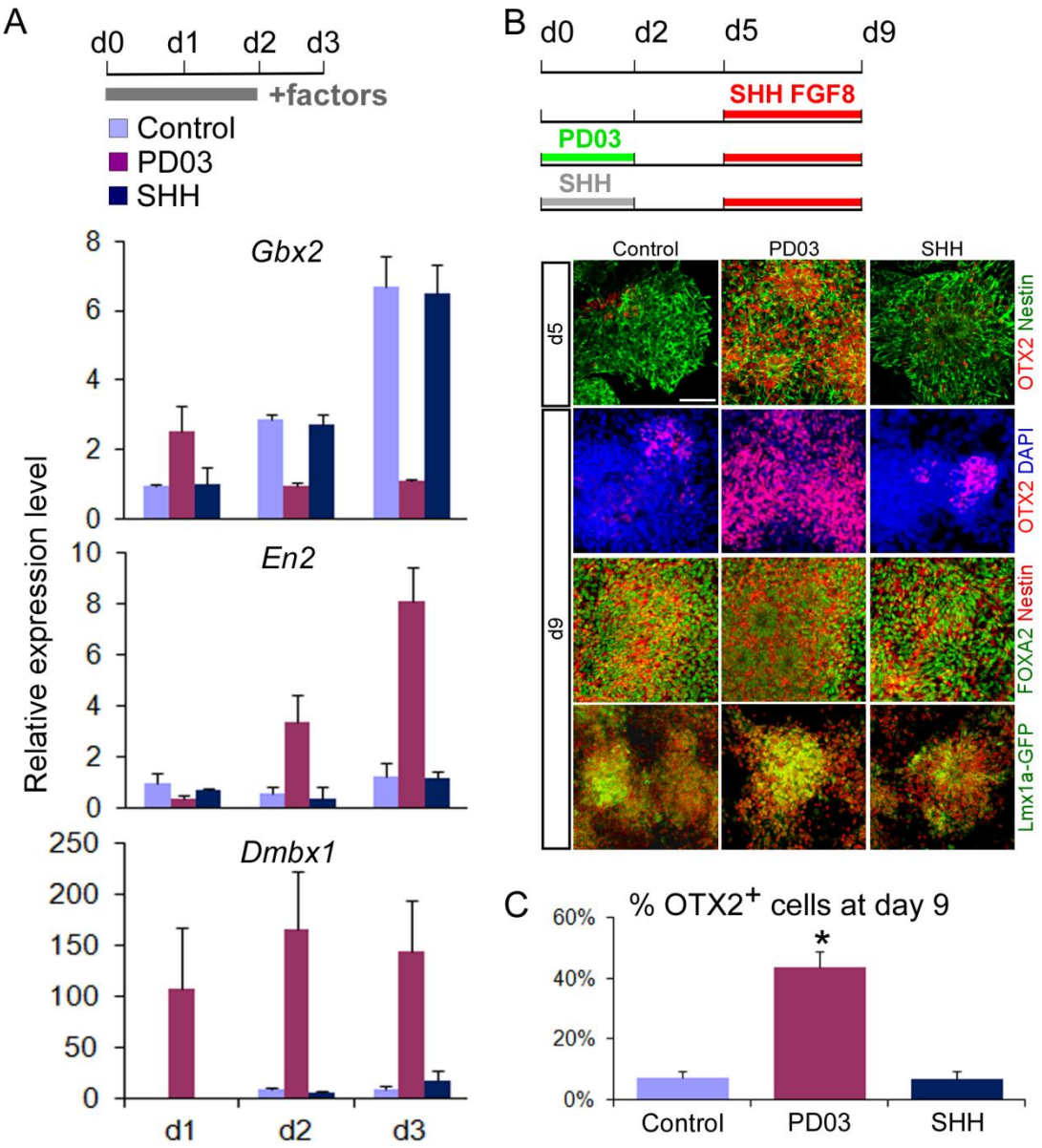

A
d0
d1
d2
d3
+factors
Control
PD03
SHH
Relative expression level
Gbx2
En2
Dmbx1
d1
d2
d3
B
d0
d2
d5
d9
SHH FGF8
PD03
SHH
Control
PD03
SHH
d5
d9
OTX2 Nestin
OTX2 DAPI
FOXA2 Nestin
Lmx1a-GFP
C
% OTX2+ cells at day 9
60%
40%
20%
0%
*
Control
PD03
SHH

Figure 4.14 SHH treatment cannot induce midbrain neural progenitor fate.

(A) Mouse E14tg2a EpiSC MD cultures were exposed to PD0325901 (PD03), SHH or to no-factor control from d0 MD for 2 days. Cultures were harvested at d1, d2, and d3 for qPCR analysis of the hindbrain marker gene *Gbx2* and the midbrain genes *En1* and *Dmbx1*. The value of the d1 MD control was set as 1. Error bars indicate mean±s.e.m. of two sets of experiments performed in triplicate. **(B)** EpiSC MD cultures were treated with PD0325901 (PD03), SHH, or without a factor (Control) at d0-2 and exposed to SHH and FGF8 from d5 for 4 days. MD cultures were fixed at d5 and d9 for analysis by immuncytochemistry. Immunostaining of d5 and d9 MD E14tg2a EpiSCs (top two rows) and Lmx1a-GFP EpiSCs (bottom two rows). Antibodies against OTX2, red, and Nestin, green, or OTX2 alone, red, were used in E14tg2a EpiSCs. FOXA2 and GFP, green, and Nestin, red, were used in the Lmx1a-GFP panels. Scale bar: 100 μm. **(C)** Quantification of OTX2 immunostaining at d9 in E illustrating the percentage of cells expressing OTX2. Mean±s.e.m. of ten fields from two independent experiments. *, P<0.01 relative to no-PD0325901 control (Student's t-test).

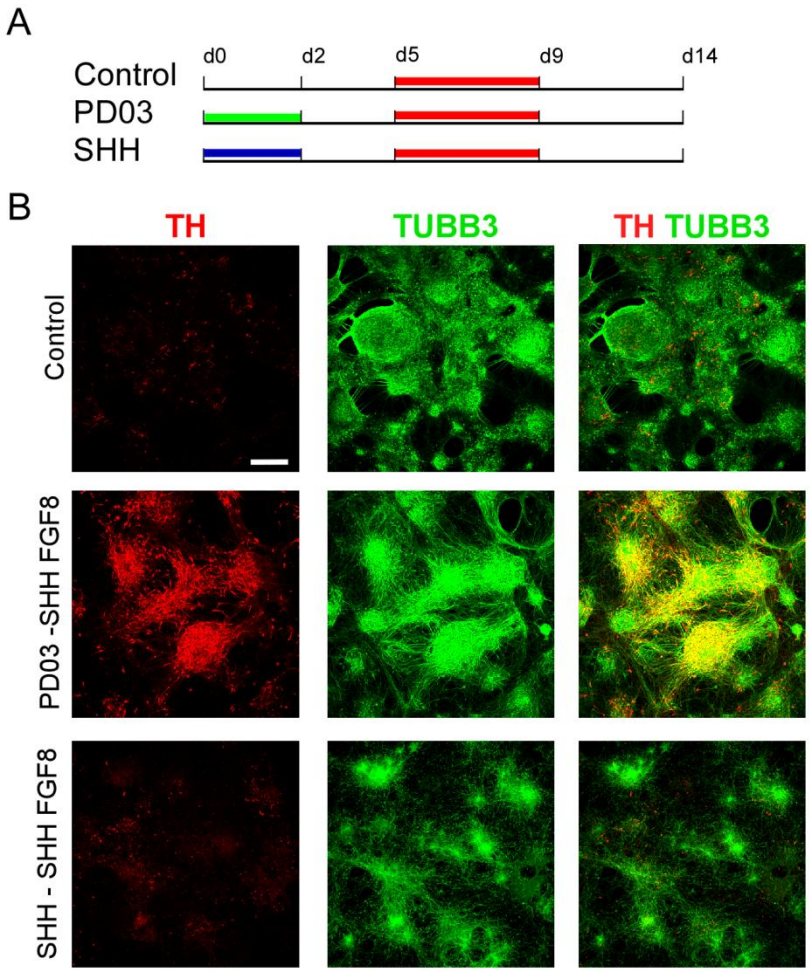


Figure 4.15 Activation of SHH alone cannot replace early blockade of FGF/ERK pathway in the generation of DA neurons.

(A) Experimental schemes for data in B. **(B)** MD cultures of EpiSCs at d14 were double stained for TH, red, and TUBB3, green. Scale bar: 200 µm.

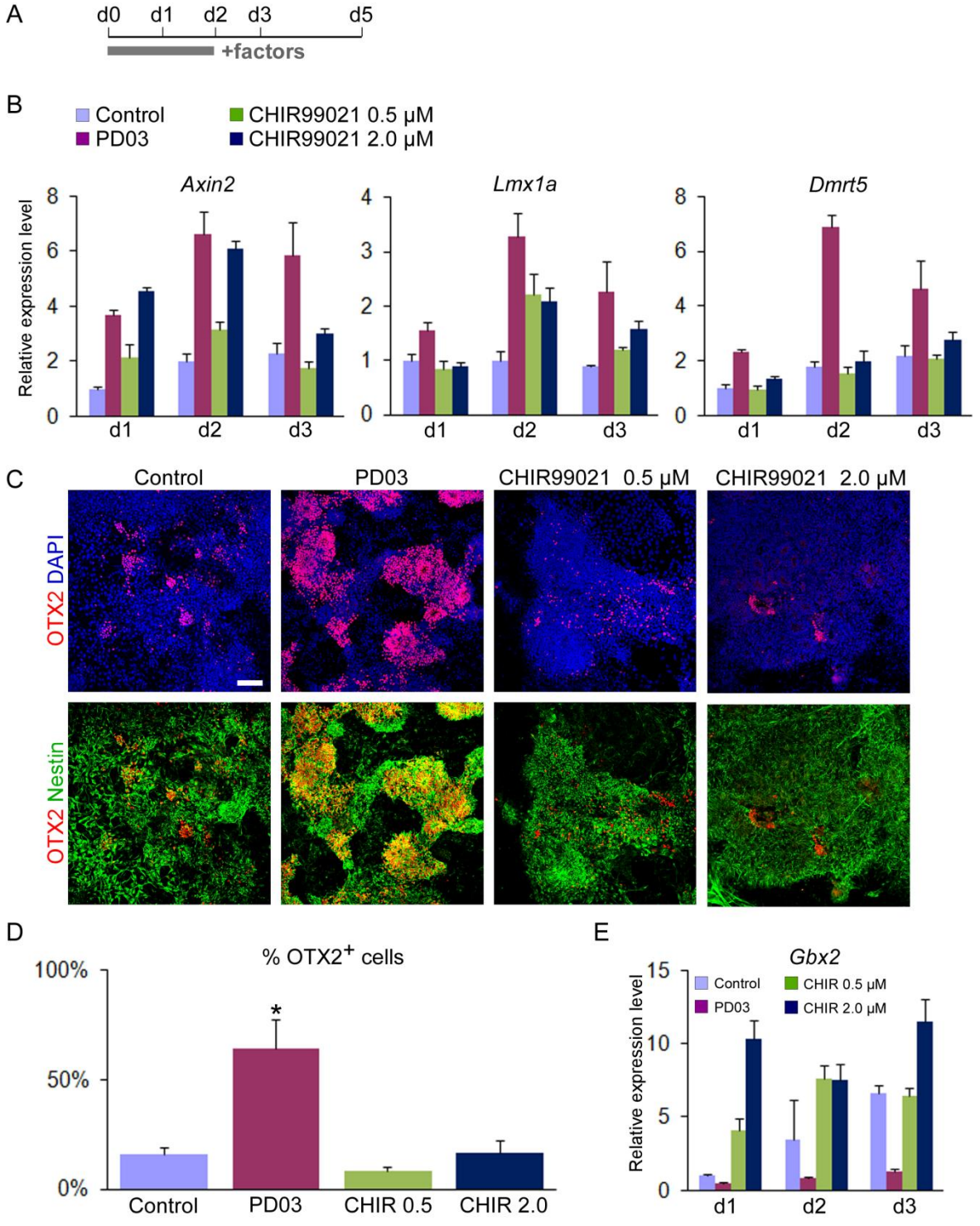

A
d0
d1
d2
d3
d5
+factors
B
Control
PD03
CHIR99021 0.5 µM
CHIR99021 2.0 µM
Axin2
Lmx1a
Dmrt5
Relative expression level
d1
d2
d3
C
Control
PD03
CHIR99021 0.5 µM
CHIR99021 2.0 µM
OTX2 DAPI
OTX2 Nestin
D
% OTX2+ cells
100%
50%
0%
Control
PD03
CHIR 0.5
CHIR 2.0
E
Gbx2
Control
PD03
CHIR 0.5 µM
CHIR 2.0 µM
Relative expression level
d1
d2
d3

Figure 4.16 Activation of the WNT pathway does not mirror the effects of early ERK inhibition in neural differentiation.

(A) Experimental schemes for data in B-E. **(B)** EpiSCs were differentiated in the presence of PD0325901 (PD03), 0.5μM or 2.0μM CHIR99021 from d0 MD for 2 days. RNA was collected at d1-3 and tested for *Axin2, Lmx1a*, and *Dmrt5* by qPCR. The value of the d1 MD control was set as 1. Error bars indicate mean±s.e.m. of two sets of experiments performed in duplicates. **(C)** Antibody staining for the anterior marker OTX2 labelled with red in d5 MD cultures with or without PD0325901 or CHIR99021. DAPI is labelled in blue (top row) and Nestin is coloured in green (bottom row). Scale bars: 100 μm. **(D)** Quantification of immunostaining in C illustrating the percentage of cells expressing OTX2. Mean±s.e.m. of ten fields from two independent experiments. *, P<0.01 relative to no-PD0325901 control (Student's t-test). **(E)** Mouse E14tg2a EpiSC MD cultures were exposed to PD0325901 (PD03), 0.5 μM or 2.0 μM CHIR99021 or no-factor control from d0 MD for 2 days. Cultures were harvested and analysed as in B for qPCR analysis of *Gbx2*.

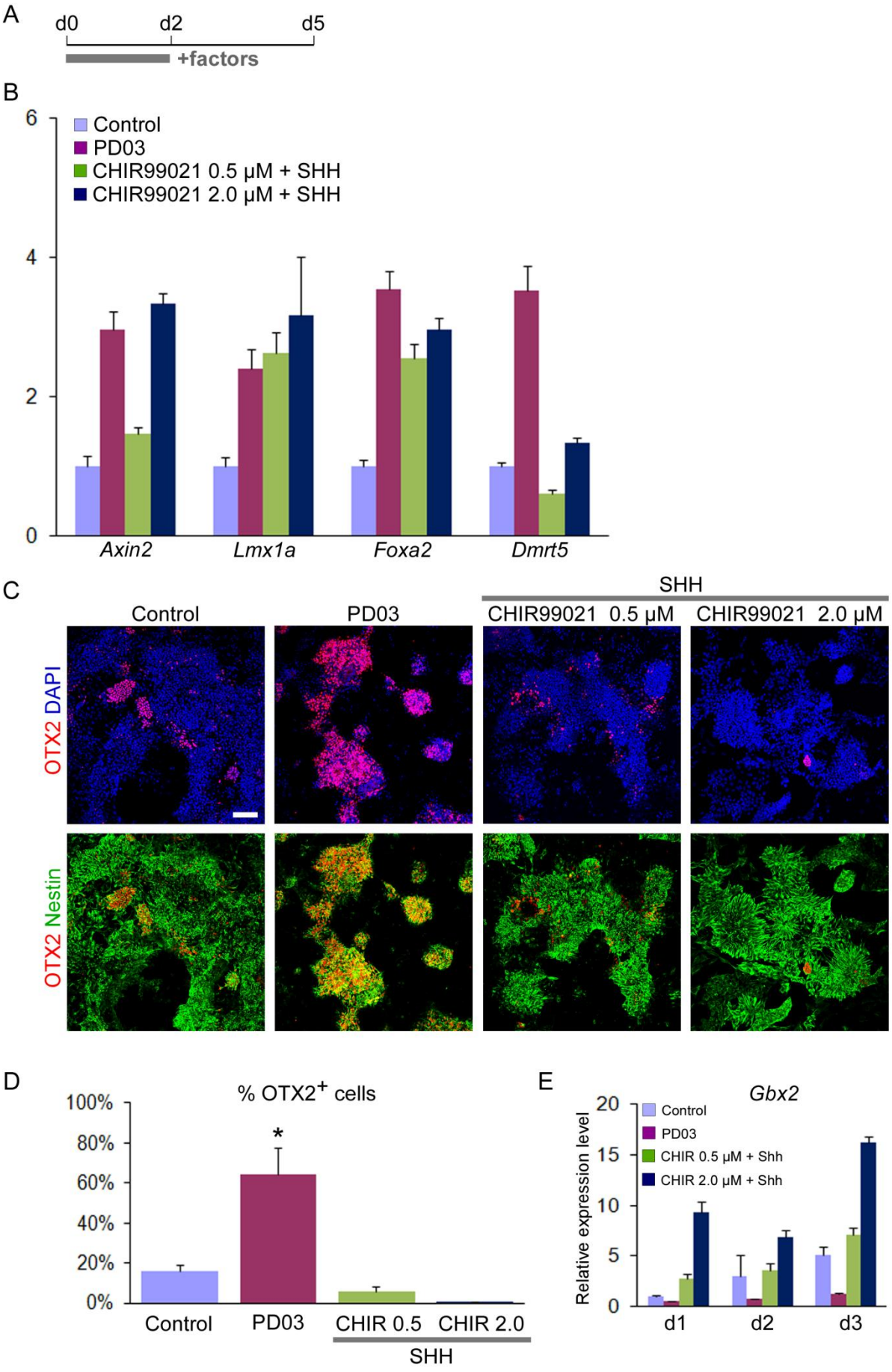

A
d0
d2
d5
+factors
B
Control
PD03
CHIR99021 0.5 µM + SHH
CHIR99021 2.0 µM + SHH
6
4
2
0
Axin2
Lmx1a
Foxa2
Dmrt5
C
SHH
Control
PD03
CHIR99021 0.5 µM
CHIR99021 2.0 µM
OTX2 DAPI
OTX2 Nestin
D
% OTX2+ cells
100%
80%
60%
40%
20%
0%
*
Control
PD03
CHIR 0.5
CHIR 2.0
SHH
E
Gbx2
Relative expression level
20
15
10
5
0
Control
PD03
CHIR 0.5 µM + Shh
CHIR 2.0 µM + Shh
d1
d2
d3

Figure 4.17 SHH and CHIR99021 treatment partly mimics early ERK inhibition.

(A) Experimental schemes for data in B-E. **(B)** EpiSCs were differentiated in the presence of no factors, PD0325901 (PD03), and CHIR99021 together with SHH from d0 until d2 of MD. RNA was collected at d2 and tested for *Axin2, Lmx1a, Foxa2*, and *Dmrt5* by qPCR. The value of control was set as 1. Error bars indicate s.e.m. of two sets of experiments performed in duplicates. **(C)** Antibody staining for the anterior marker OTX2 labelled with red in d5 MD cultures without or with factors as indicated. DAPI is labelled in blue (top row) and Nestin is coloured in green (bottom row). Scale bars: 100 μm. **(D)** Quantification of immunostaining in C illustrating the percentage of cells expressing OTX2. Mean±s.e.m. of ten fields from two independent experiments. *, P<0.01 relative to no-PD0325901 control (Student's t-test). **(E)** EpiSCs were differentiated in the presence of no factors, PD0325901 (PD03), and CHIR99021 together with SHH at d0-2 MD RNA was collected at d1, d2 and d3 MD and analysed for *Gbx2* by qPCR. The value of the d1 MD control was set as 1. Error bars indicate mean±s.e.m. of two sets of experiments performed in duplicates.

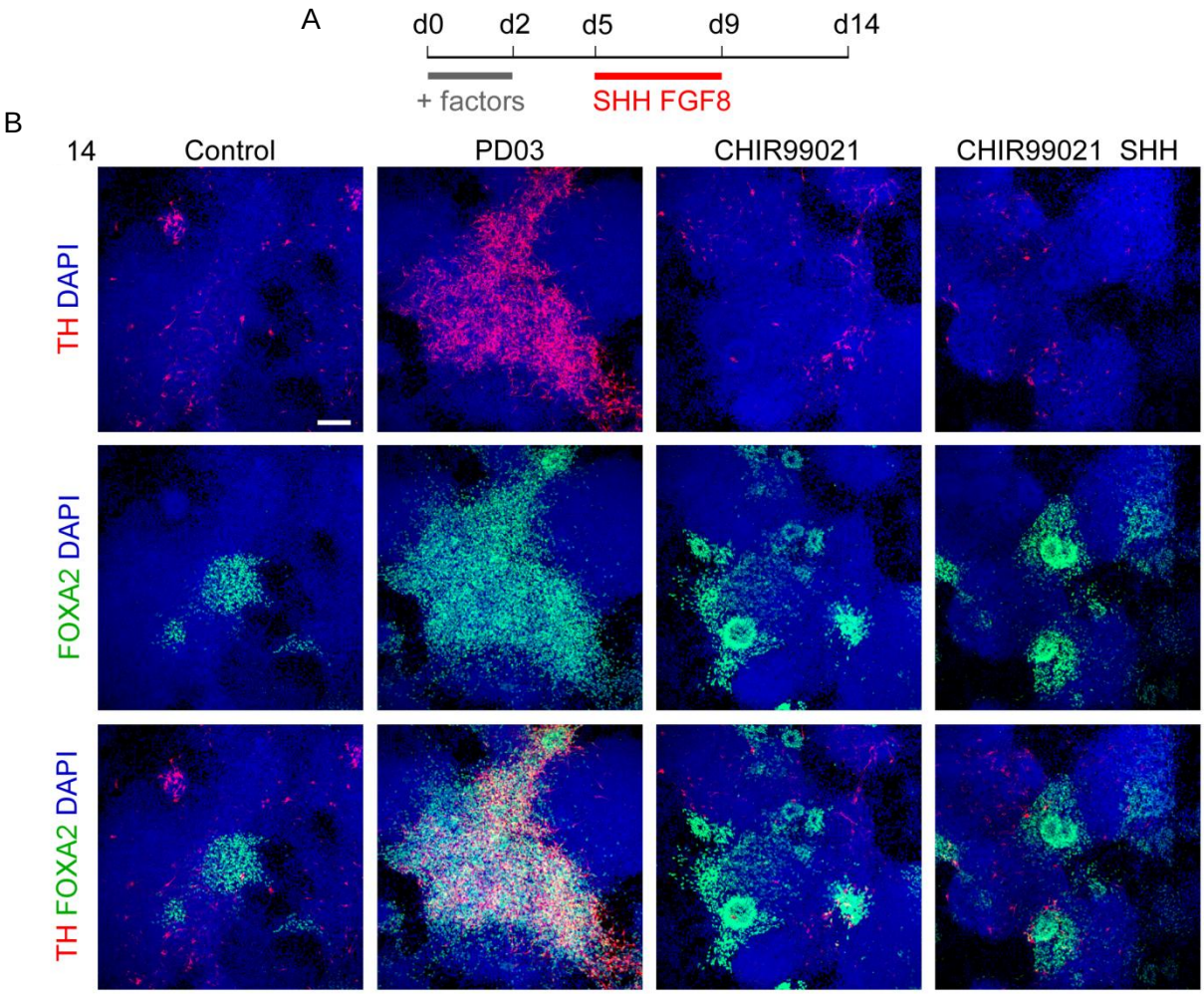


Figure 4.18 Early stimulation of SHH and WNT pathway cannot substitute ERK inhibition in the generation of DA neurons.

(A) Experimental scheme of neural differentiation with mouse EpiSCs. MD cultures were exposed to PD0325901 (PD03), CHIR99021 and SHH or to no-factor control at d0-2 MD. SHH and FGF8 were applied from d5 until d9 of MD. Medium was then changed to N2B27 plus GDNF, BDNF and ascorbic acid and cultured for another 4 days. **(B)** MD cultures at d14 were double stained for TH, red, and FOXA2, green. DAPI is labelled in blue. Scale bar: 200 µm.

4.8 Discussion

Midbrain characteristic DA neurons derived from stem cells provides a unique opportunity in cell therapy and drug discovery for developing novel strategies for brain repair in PD. However, the generation of 'authentic' mDA neurons in a robust and reproducible manner requires an in-depth understanding of the mechanisms that control the fate choice of stem cells during differentiation. The data of the present chapter revealed that a stepwise control of FGF/ERK activity during specific stages of neural differentiation can effectively promote the generation of authentic mDA neurons from mouse PSCs.

Regulation of mDA differentiation by controlling FGF signalling

Compared to ESCs, EpiSCs, the *in vitro* counterpart of postimplantation epiblast stem cells, have already completed the transition from a naive pluripotent stage toward a primed stage of lineage commitment which involves the activation of FGF signalling (Kunath et al., 2007; Ying et al., 2008). As described in chapter 3, EpiSCs are more synchronised in the process of neural induction than ESCs. I found that inactivation of FGF/ERK pathway by either FGFR or ERK inhibitor upon the exit of the epiblast pluripotent stage specifies nascent neural progenitor cells towards mDA progenitor fate. Notable, our strategy appears to induce region-specific gene expression almost at the same time when neural induction occurs, implying that coupling neural induction and regionalisation may be crucial for generating specific neuronal cell types *in vitro*.

To maintain the mDA neural progenitor characteristics, these cells require endogeneous FGF signalling (Figure 4.3 A). Addition of FGF8 or continued PD0325901-treatment after the onset of a ventral midbrain fate abolished the early increased expression levels of mDA key regulator genes (*Foxa2, Lmx1a, Dmrt5*) caused by early FGF/ERK blockade (Figure 4.3 B and 4.11), suggesting that the level of FGF signalling is important. Previous *in vivo* studies revealed that high levels of FGF8 specify cells of the presumptive midbrain to a hindbrain fate (Liu and Joyner, 2001; Liu et al., 2003; Sato et al., 2001) whereas reduction of FGF

signalling in the midbrain instructs cells toward anterior cell fates (Basson et al., 2008; Lahti et al., 2012). In keeping with these findings, an increase or decrease of FGF8 in the prospective diencephalon or hindbrain respectively induce a midbrain identity (Crossley et al., 1996; Lee et al., 1997; Liu et al., 1999; Martinez et al., 1999; Sato et al., 2001; Sato and Nakamura, 2004; Shamim et al., 1999). I also found that increase of FGF signalling resulted in an upregulation of the isthmus organizer related genes, *Wnt1, En1*, and *En2* (Figure 4.11), supporting previously reported cross-regulatory network between these molecules (Wurst and Bally-Cuif, 2001; Ye et al., 2001). Furthermore, these genes have been shown to be essential for the differentiation and survival of DA neurons (Prakash et al., 2006; Simon et al., 2001; Tang et al., 2009). However, it has been reported that SHH and canonical WNT signalling have opposing roles in mDA neurogenesis (Joksimovic et al., 2009; Tang et al., 2010). Thus, for an efficient generation of mDA neurons, it might be crucial to allow SHH-dependent progenitor specification and expansion before activating FGF signalling by FGF8 which indirectly stimulates WNT signalling (Andersson et al., 2006b; Hynes et al., 1997; Sasaki et al., 1997). These findings point out the importance of precise temporal control of FGF signalling to orchestrate mDA midbrain induction and neurogenesis.

Early inhibition of FGF/ERK signalling promotes acquisition of a midbrain neural progenitor identity

I found that blocking specifically FGF/ERK signalling at the onset of EpiSC MD directs a midbrain fate in the anterior-posterior axis by suppressing both hindbrain (*Gbx2* expression) and the forebrain fates (*Foxg1* and *Six3* expression) (Figure 4.5) whereas blockade of FGF/PI3K did not modulate anterior-posterior characteristics (Figure 4.6). However, it is unclear whether blockade of the FGF/PLC-γ pathway instruct cells toward a midbrain fate.

Recent reports demonstrated that forced expression of any of the mDA regulator genes (*Lmx1a, Otx2, Dmrt5, Foxa2*) lead to an increased production of DA neurons (Chung et al., 2009; Friling et al., 2009; Gennet et al., 2011; Kittappa et al., 2007) and combined overexpression of *Oxt2*, *Lmx1a*, and *Foxa2* significantly improved the generation of mDA

neurons (Chung et al., 2009). My results showed that a complete set of the key mDA progenitor transcription factors (FOXA2, LMX1A, DMRT5 and OTX2) was already induced at d5 MD in PD0325901-treated neural progenitor cells (Figure 4.3 and 4.5). These cells exposed to SHH and FGF8 differentiated efficiently into mDA neurons. Although, untreated neural progenitors exposed to SHH and FGF8 for 4 days (d5-9) showed an increase in the number of FOXA2 and LMX1A positive cells at d9 MD (Figure 4.14 B), their efficiency to convert into mDA neurons was low compared to PD0325901-treated MD cultures (Figure 4.7 and 4.9). These data suggest that an early induction of *Lmx1a* and *Foxa2* is required for highly efficient production of mDA neurons.

Implications of SHH and WNT1

SHH and WNT1 are required for the expression of *Otx2* (Chung et al., 2009; Prakash et al., 2006; Puelles et al., 2004), *Lmx1a* (Andersson et al., 2006b; Chung et al., 2009) and *Foxa2* (Hynes et al., 1997; Sasaki et al., 1997). These factors form a network that coordinates mDA differentiation (Chung et al., 2009; Lin et al., 2009; Nakatani et al., 2010; Prakash et al., 2006; Tang et al., 2010). The results of this chapter revealed a robust induction of *Shh* and *Wnt* when exposed to FGF/ERK inhibitor (Figure 4.3). One might ask whether the effect of early FGF/ERK inhibition is based on the initiation of these signalling molecules. However, MD of EpiSCs in the presence of either SHH or canonical Wnt pathway or both only partially mimicked PD0325901 effect on nascent neural progenitors (↑*Foxa2*, ↑*Lmx1*, ↓*Dmrt5*, ↓*Otx2*) and failed to produce a high number of DA neurons (Figures 4.12 and 4.16-17), suggesting that a fully correct region-specific identity is essential for efficient generation of mDA neurons.

It was demonstrated that SHH establishes the dorso-ventral axis and subsequently controlling the positioning and generation of DA neurons in the ventral midbrain (Andersson et al., 2006b; Ye et al., 1998). The same studies showed that SHH has no effect on the formation of the anteror-posterior axis. Our results also revealed that SHH applied at d0-2

had no effect on anterior-posterior identity (*Gbx2*, *Otx2*) (Figure 4.14). Thus, other factors are needed to synchronise and modulate the cell fate of distinct anteror-posterior identities during differentiation of EpiSC. Chung et al. (2009) demonstrated that WNT1 positively regulates expression of *Otx2* via the canonical pathway, making it a good candidate to shift the cell fate toward an anterior character during neural *in vitro* differentiation. However, mimicking the canonical WNT signalling via the GSK3ß inhibitor at d0-2 did neither increase the percentage of OTX2 positive cells. In addition, expression of *Dmrt5* was neither induced by activation of canonical WNT or SHH signalling indicating the involvement of other unknown pathways/factors.

Although activation of canonical WNT pathway resulted in an upregulation of *Lmx1a* expression (Chung et al., 2009), in PD0325901-treated neural differentiation the expression of *Lmx1a* steadily increased even after *Wnt1* expression dropped below the levels observed in control EpiSC MD cultures (Figure 4.3 B, C). A previous study indicated that *Lmx1a* is induced by SHH (Andersson et al., 2006b) as midbrain explants from chick embryos displayed LMX1A positive cells only after SHH treatment. In PD0325901 treated MD cultures, *Shh* expression increased continuously until d5 of differentiation as seen for *Lmx1a* expression (Figure 4.3 B, C), which was enhanced by the addition of SHH to PD0325901 at d0-2 and when SHH signalling was blocked by cyclopamine *Lmx1a* expression dropped at d3 after an initial burst of upregulation, implying a role of SHH in the regulation of *Lmx1a* expression. These findings lead to an interesting question whether *Lmx1a* is initially induced by canonical WNT pathway and later on maintained and stabilised by SHH signalling.

Efficient generation of mDA neurons from PD0325901-treated EpiSCs

Differentiation protocols using growth factors to control the process have so far been highly variable and limited in the generation of DA neurons (Kawasaki et al., 2000; Lee et al., 2000b; Ying and Smith, 2003). Cells derived by these strategies represented a mixed population containing neural cells at different developmental stages, or other embryonic germ layer lineages and undifferentiated ESCs which used in cell replacement therapy can

cause the formation of tumour or transplant-induced diseases such as dyskinesia. Although overexpression of mDA transcription factors increases markedly the efficacy of ESC-derived DA neurons (Chung et al., 2009; Chung et al., 2002; Friling et al., 2009; Kittappa et al., 2007; Maxwell et al., 2005), the genetic manipulations are a burden for the production of DA neurons for clinical trials. Therefore, there is a pressing need to develop a robust chemically defined condition that can rapidly convert stem cells into DA neurons of midbrain identity in a synchronised manner. In this chapter, I have presented a novel strategy of highly reliable nature that allows producing mDA neurons in high yield and fully chemical defined condition free from genetic manipulation. The presence of the FGF/ERK inhibitor at the onset of EpiSC MD resulted in a remarkably increase of TH positive cells. A common problem of DA differentiation protocols is the sub-specification into distinct DA cell phenotype. The majority of DA neurons generated by my new method are mDA specific as confirmed by co-expression of the marker genes LMX1A, FOXA2, NURR1, TH, PITX3, and VMAT.

It is worth to note that, even without FGF/ERK inhibitor treatment, nearly 40% of TH positive neurons were immunopositive for PITX3 in MD of EpiSCs which is much higher than that from ESCs (Andersson et al., 2006b; Friling et al., 2009; Parmar and Li, 2007). This suggests that using the more synchronised nature of EpiSC differentiation is important for the effective enrichment of mDA-competent progenitors.

5 Functional analysis of *in vitro* derived midbrain dopaminergic neurons

A major goal of *in vitro* derived mDA neurons will be their use for disease modeling and cell therapy. Thus, it is essential to test the functional properties of these cells and their functional integration to the surrounding host tissue. I therefore set up collaborations to investigate whether the cells I generated and described in Chapter 4 exhibit electrophysiological properties similar to those of mDA neurons *in vivo* as well as their ability to integrate into the striatum of a 6-hydroxy-dopamine-lesioned mouse model PD.

5.1 *In vitro* generated mDA neurons exhibit functional neuronal characteristics

Electrophysiological characterisation of mDA neurons was carried out in collaboration with Dr. Jessica Risner-Janiczek in our laboratory, using facilities of Dr. Mark Ungless at the MRC Clinical Sciences Centre in London. For this study, I employed a reporter cell line in which GFP is inserted into the Pitx3 locus allowing specific labelling of mDA neurons (Zhao et al., 2004). Pitx3-GFP EpiSCs were first cultured for two days with or without PD0325901. From d5 until d9 of MD the cultures were treated with SHH and FGF8 and were then further differentiated in the presence of BDNF, GDNF, and ascorbic acid. GFP positive neurons were analysed by whole-cell recordings at d14-16 MD. Neurons derived from EpiSC-MD cultures with or without PD0325901 exhibited a negative resting membrane potential which is a characteristic feature of neurons (control, –67±1.3 mV, n=6; PD0325901, –45±4.7, n=13; $P<0.05$). Neurons generated with PD0325901 treatment showed a slightly more depolarized resting membrane potential when compared to those in no-PD0325901 control cultures. The input resistance was similar for neurons generated under both conditions (control, 422±198

MΩ, n=8; PD0325901, 558±79 MΩ, n=15; P>0.05). Furthermore, no difference was seen between the groups in whole-cell capacitance (control, 9.6±1 pF, n=8; PD0325901, 12±5 pF, n=15; P>0.05). As we did not observe any changes in the input resistance and whole-cell capacitance in neurons from PD0325901-treated MD cultures, we assume that PD0325901 treatment had no affect on the cell size. 14% of Pitx3-GFP positive neurons showed multiple spontaneous potentials (n=14) (Figure 5.1 B). Stimulation with a depolarizing current pulse resulted in an overshooting action potential in all cells (n=14) of which 19% (3/14) responded by firing multiple action potentials with a low frequency (0.95±0.14 Hz; n=3) and in an irregular pattern (CV-ISI, 1.19±0.24; n=3). When cells were cultured in medium containing BDNF, GDNF, and ascorbic acid until d40, we observed 67% (PD0325901, 6/9) of cells firing spontaneous action potentials (3.54±0.8 Hz; CV-ISI, 0.49±0.08; n=6). These cells displayed a pacemaker-like activity typical of mDA neurons (Figure 5.1 E). Moreover, all Pitx3-GFP positive neurons demonstrated a large outward current in voltage–clamp mode, typical of a delayed-rectifier K+ current (2.19±0.28 nA, n=15; P>0.05) (Figure 5.1 D, left panel). The cells exhibited fast activating, fast-inactivating inward currents that is a typical feature of Na+ currents (1.69±0.25 nA, n=15; P>0.05) (Figure 5.1 D, right panel).

In summary, these results provide evidence that the mouse EpiSC-derived Pitx3-GFP positive neurons acquired functional, neuron-like properties that were similar to those of mDA neurons *in vivo*.

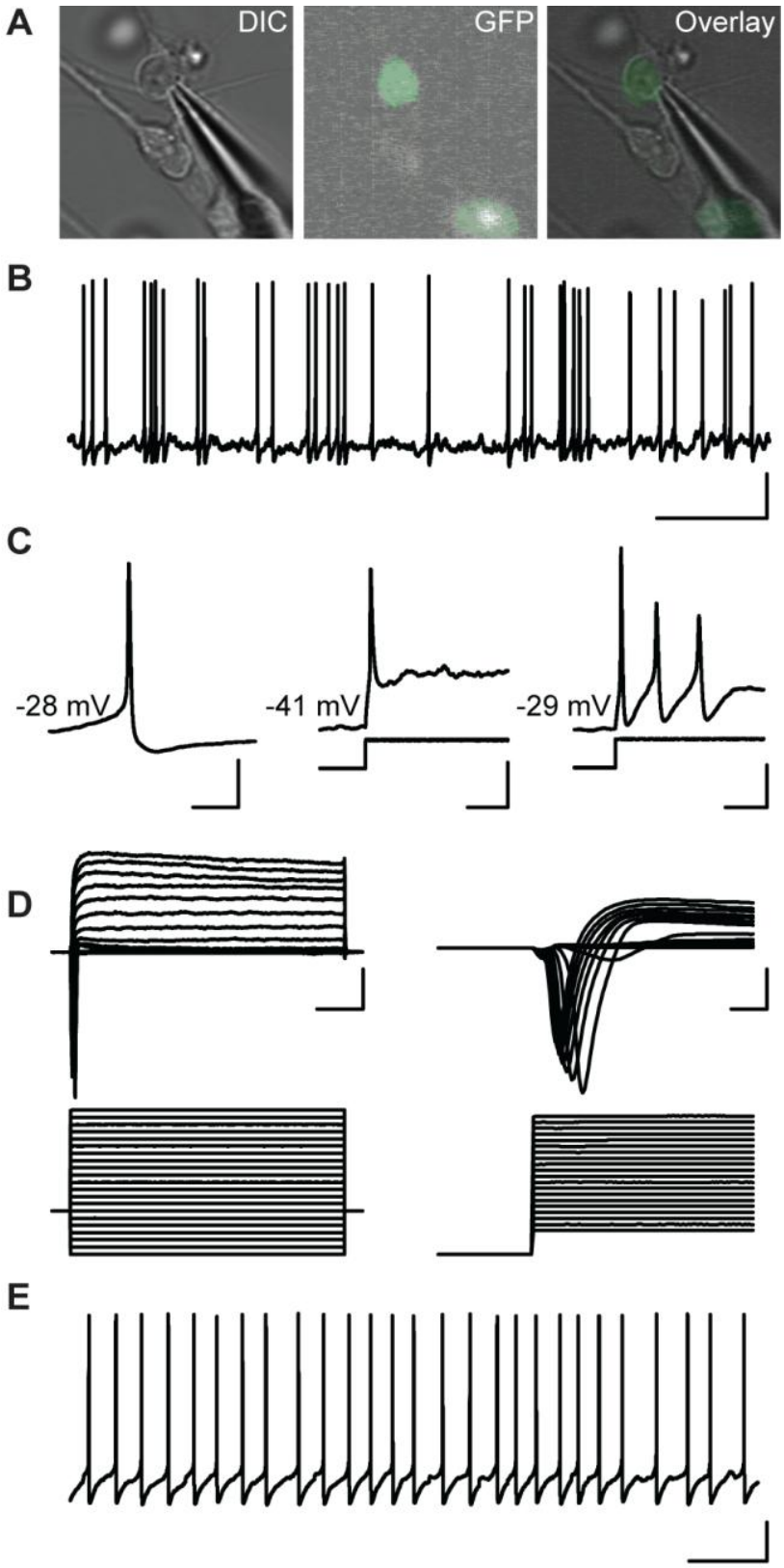

A
DIC
GFP
Overlay
B
C
-28 mV
-41 mV
-29 mV
D
E

Figure 5.1 Pitx3-GFP positive cells exhibit functional neuron-like electrophysiological properties. (kindly provided by Dr. Jessica Risner-Janiczek).

(A) DIC and GFP image showing a recording pipette patched onto a mouse Pitx3-GFP positive cell. **(B)** Spontaneous action potentials fired by a d14 neuron. Vertical scale bar, 20 mV; horizontal scale bar, 5 ms. **(C)** A single spontaneous action potential (left). A single action potential fired in response to a 50 pA depolarizing current pulse (middle). Multiple action potentials fired in response to a 50 pA depolarizing current pulse (right). Vertical bars, 20 mV; horizontal bars, 50, 100, and 100 ms, respectively. **(D)** Outward current evoked by a serious of voltage steps (left). Fast inward current evoked by a series of voltage steps (right). Vertical bars, 1 nA; horizontal bars, 50 ms. **(E)** Pacemaker-like spontaneous firing a d41 neuron. Vertical bar, 20 mV; horizontal bar, 1 second.

5.2 Transplantation of *in vitro* generated mDA progenitors in a mouse model of Parkinson's disease

I then investigated whether DA neurons generated by the present protocol can functionally integrate in the brain of a mouse PD model. This part of the work was carried out in collaboration with Prof. Steve Dunnett's laboratory at Cardiff University.

5.2.1 Modification of differentiation protocol

Many lines of previous studies demonstrated that the developmental stage of the donor cells is pivotal for survival and efficient functional integration in animal models of PD0325901. The most suitable donor cells appear to be those that are mDA specified and yet to leave the cell cycle (Brundin et al., 1988; Das et al., 1980; Finger and Dunnett, 1989; Torres et al., 2007). From a practical standpoint, a shorter differentiation time prior to transplantation may benefit cell survival during transportation of the cells. Therefore, I sought to modify the protocol to accelerate and possibly enhance mDA lineage commitment. SHH is a well known ventralising factor that induces the generation of floorplate cells including cells from which mDA neurons derive (Bayly et al., 2007; Blaess et al., 2006; Fedtsova and Turner, 2001; Hynes et al., 1995; Ye et al., 1998). I therefore proposed that SHH added at d2-5 straight after PD0325901 treatment would enhance the induction of ventral midbrain progenitor cells and subsequently the conversion into mDA neurons. MD cultures were stained at d5 MD for OTX2, LMX1A, FOXA2, and DMRT5, and the percentage of cells expressing one of these markers were quantified by pixel analysis (Figure 5.2 B, C). I found that early SHH treatment, either alone or following PD0325901 treatment, significantly increased the number of FOXA2 positive cells (control: 24±9%; SHH: 77±6%; PD0325901-SHH: 40±18%) by d5 MD (Figure 5.2 C). Furthermore, early SHH following PD0325901 also resulted in an increase of LMX1A positive cells compared to with PD0325901 alone cultures (PD0325901: 12±4%; PD0325901-SHH: 17±4%) (Figure 5.2 C). However, SHH had no effect on the generation of DMRT5 and OTX2 positive cells (Figure 5.2 C).

To see how above changes might impact on the generation of DA cells, progenitors in all four MD cultures were allowed to differentiate till d14 of MD (Figure 5.3 A). Immunostaining for TH revealed that cultures with the earlier SHH treatment following PD0325901 generated the most numbers of TH positive cells (Figure 5.3 B). Interestingly, no-PD0325901 MD cultures treated with SHH at d3-5 also generated more TH positive cells compared to the basal control condition. This number is still lower than those original plus PD0325901 condition. This data indicates that enhanced induction of FOXA2 alone by SHH at d5 is not sufficient for DA commitment.

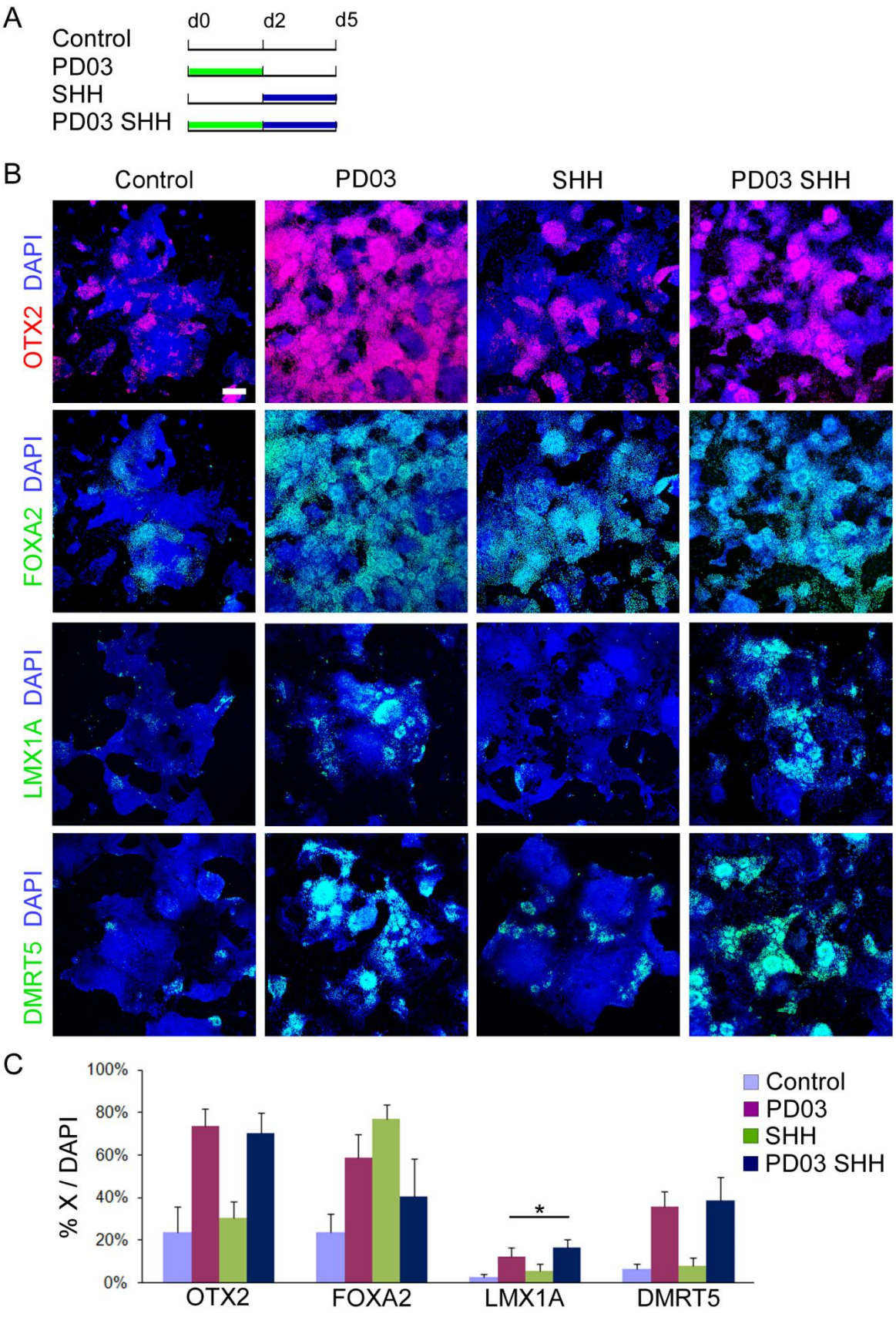

A
d0
d2
d5
Control
PD03
SHH
PD03 SHH
B
Control
PD03
SHH
PD03 SHH
OTX2 DAPI
FOXA2 DAPI
LMX1A DAPI
DMRT5 DAPI
C
% X / DAPI
100%
80%
60%
40%
20%
0%
OTX2
FOXA2
LMX1A
DMRT5
*
Control
PD03
SHH
PD03 SHH

Figure 5.2 Early blockade of FGF signalling and postliminary enhancement of SHH signalling support generation of ventral midbrain progenitor cells.

(A) Experimental schemes for data in B. **(B)** Mouse E14tg2a EpiSC MD cultures were treated with PD0325901 (PD03) at d0-2 or SHH at d2-5 or a combination of the two as indicated in A. At d5, cultures were analysed by immunocytochemistry for the anterior marker OTX2, red, and the midbrain progenitor markers LMX1A, FOXA2, and DMRT5, all shown in green. DAPI is labelled in blue. Scale bars: 200 μm. **(C)** Quantification of immunostaining in B illustrating the percentage of cells expressing OTX2, FOXA2, LMX1A, or DMRT5. Mean±s.e.m. of ten fields from two independent experiments. *, $P<0.05$ relative to no-PD0325901 control (Student's t-test).

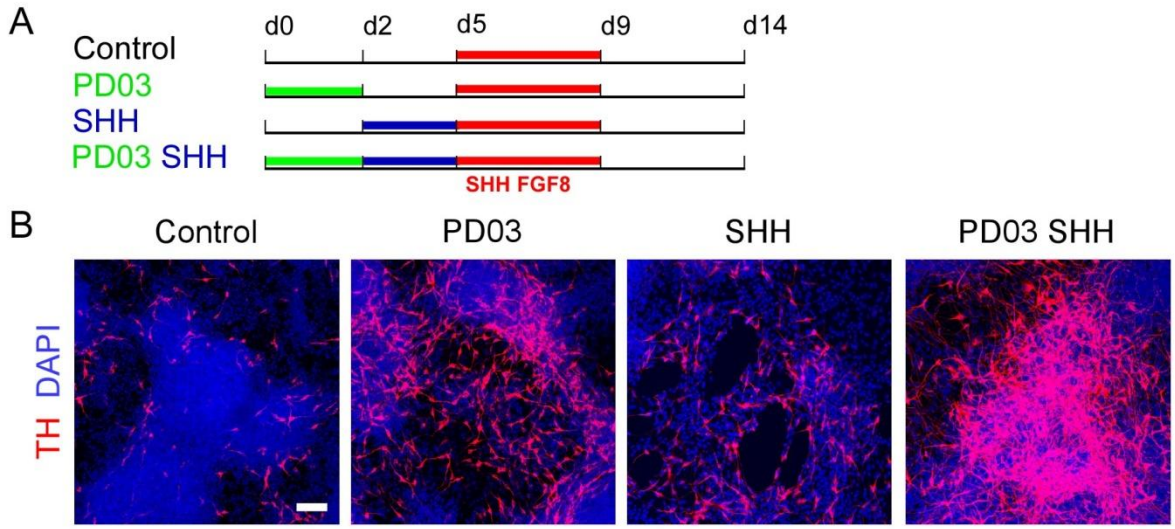


Figure 5.3 ERK inhibition followed by stimulation of the SHH signalling promotes the generation of DA neurons.

(A) Experimental schemes for data in B. **(B)** Mouse E14tg2a EpiSC MD cultures were treated with PD0325901 (PD03) at d0-2 or SHH at d2-5 or a combination of the two as indicated in A. From d5 until d9 of MD, all cultures were exposed to SHH and FGF8. Cultures were stained for the DA marker TH labelled with at d14 MD. DAPI is labelled in blue. Scale bars: 100 µm.

5.2.2 Transplantation of EpiSC-derived mDA progenitors; pilot study

The pathophysiology of PD is the preferential loss of a specific DA neuronal subpopulation, those in the Substantia Nigra (SN). These cells project to the striatum and form the dopaminergic nigrostriatal pathway which controls motor functions. Embryonic midbrain cells transplanted into the striatum has been shown to differentiate into DA neurons, survive longterm, re-innervate the striatum and improve motor control (Bjorklund et al., 1980; Bolam et al., 1987; Doucet et al., 1989; Dunnett et al., 1983; Dunnett et al., 1987; Lindvall and Bjorklund, 1989; Madrazo et al., 1988; Mendez et al., 2005; Schmidt et al., 1983). These findings demonstrate the functionality of cell derived from embryonic midbrain tissue. To test whether the cells generated by the present protocol have the potential to replace the loss of mDA neurons, we have used 6-hydroxydopamine (6-OHDA) treated mouse models of PD. Injection of the catecholaminergic neurotoxin 6-OHDA into the area where the ascending DA fibres is at its most compact, the medial forebrain bundle, results in a robust degeneration of the dopaminergic nigrostriatal pathway. In order to reduce health problems of the animals, unilateral depletion was carried out which in addition allows a variety of behavioural tests (Heuer et al., 2012). Cells transplanted into the SN do not reconnect with the striatum (Collier et al., 2002; Mukhida et al., 2001; Nikkhah et al., 1994; Starr et al., 1999). Therefore, cells are generally placed within the striatal target region.

Previous transplantation studies demonstrate that maximum functional integration is achieved with ventral midbrain progenitors prior to neurogenesis (Brundin et al., 1988; Das et al., 1980; Finger and Dunnett, 1989; Torres et al., 2007). In my culture system, active neuronal differentiation occurs from d7 MD. We therefore transplanted cells of d5 and d7 MD into striatum of mice that had been lesioned with 6-OHDA. Both d5 and d7 cultures were exposed to PD0325901 at d0-2 followed by SHH treatment from d2 till transplantation. D7 cultures received two days exposure of FGF8. At the time of transplantation most of the cells were Nestin positive (Figure 5.4 A). Immunostaining and pixel analysis revealed a similar

proportion of cells positive for OTX2, FOXA2, LMX1, and DMRT5 in d5 and d7 MD cultures (Figure 5.4 A, B).

To investigate the integration, differentiation, and neuronal function, drug-induced behavioral rotation tests were performed. Here we used the DA agonist amphetamine which induces typical body rotations in unilateral 6-OHDA lesioned mice to the side of the DA-depletion. Consequently, any recovery by the transplanted cells will be observed by a significant reduction in rotational behaviour. *In vivo* DA neurons of the SN are part of the Basal Ganglia which forms a circuit that controls their activity in the striatum. Grafts that are transplanted within the target side, the striatum, are not under the control of this regulatory network. Therefore, grafts that are enriched with DA neurons display an overcompensatory response which correlates with the induced Dopamine level.

Eight weeks after transplantation, animals grafted with d7 MD cultures showed a significant reduction in amphetamine-induced rotation scores and over-compensatory response in 6-OHDA lesioned mice (Figure 5.5). However, mice that received d5 MD cultures showed no recovery compared to lesion control group. (Figure 5.5).

To verify whether the observed difference in recovery correlates with DA neuronal differentiation and survival after transplantation, immunostaing for TH was carried out on brain sections with grafted cells of d5 and d7 MD cultures after 8 weeks of transplantation. The loss of DA fibres in the striatum was clearly visible in these sections, demonstrating the unilateral depletion of the DA nigrostial pathway by 6-OHDA (Figure 5.6 A). TH positive neurons were observed in both d5 and d7 MD grafts, demonstrating their potential for DA lineage commitment *in vivo*. However, d7 MD grafts had significantly more TH positive neurons than d5 MD grafts (Figure 5.6 B-E), which could explain the difference of the amphetamine-induced rotation behavioural test (Figure 5.5).

One of the concerns for cell replacement therapy in PD is the formation of tumours and neural overgrowth. Strikingly, none of the animals exhibited tumour formation or extensive overgrowths in the surviving grafts.

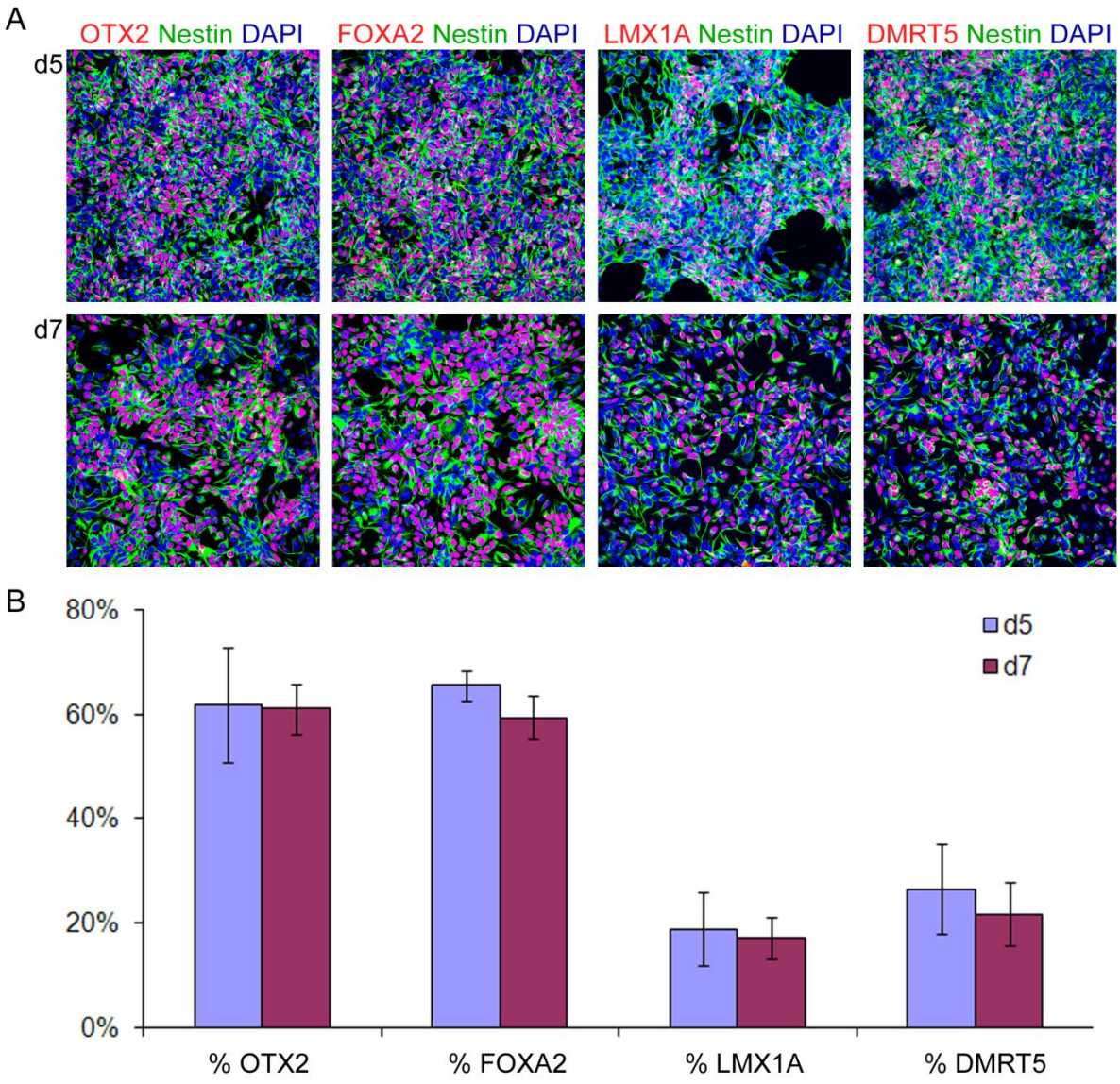


Figure 5.4 EpiSC-derived cells display robust induction of ventral midbrain progenitor fate at the day of transplantation.

(A) Mouse Pitx3-GFP EpiSC MD cultures were treated with PD0325901 at d0-2 and SHH at d2-5. D7 cultures were exposed to FGF8 and SHH from d5 for 2 days of differentiation. At the day of transplantation, cells were fixed and analysed by immunocytochemistry for anterior marker OTX2 and the midbrain progenitor markers FOXA2, LMX1A, and DMRT5. DAPI is labelled in blue and Nestin is shown in green. **(B)** Quantification of immunostaining in B illustrating the percentage of cells expressing OTX2, FOXA2, LMX1A, or DMRT5. Mean±s.e.m. of ten fields from two independent experiments.

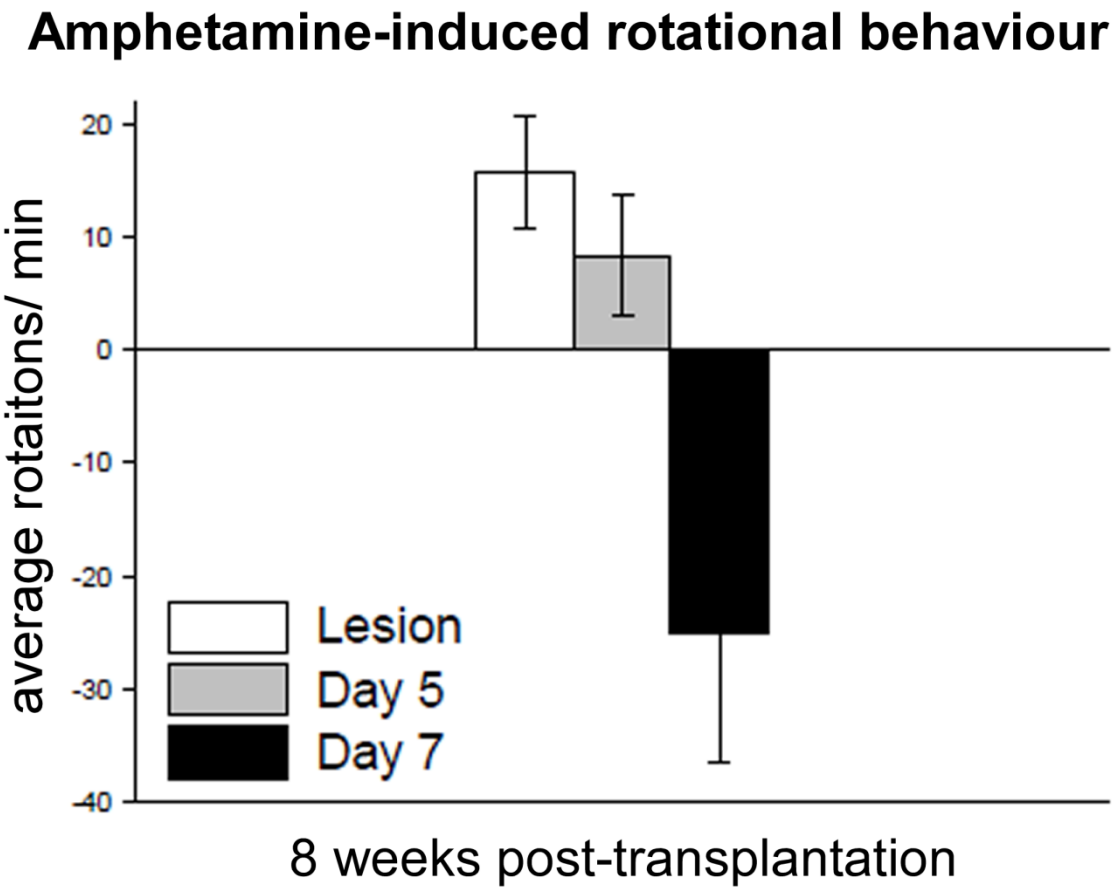


Figure 5.5 Bar graph of amphetamine-induced rotational behaviour 8 weeks after transplantation of lesioned, d5 and d7 MD cultures mice (kindly provided by Dr. Sophie Precious and Andreas Heuer).

Eight weeks after transplantation, amphetamine-induced rotations in unilateral 6-OHDA lesioned mice with or without grafts were determined by the number of rotations per minute. The black line displays the rotational behaviour of control mice without any lesion. Recovery by d7 MD grafts was observed by a significant reduction in the number of rotations to the the side of DA-depletion, an overcompensatory response which correlates with the induced Dopamine level. The bar graphs represent 11 mice for lesion control group, 16 mice for d5 MD cell group and 15 mice that received cells of d7 MD cultures. Data represent mean ± SEM.

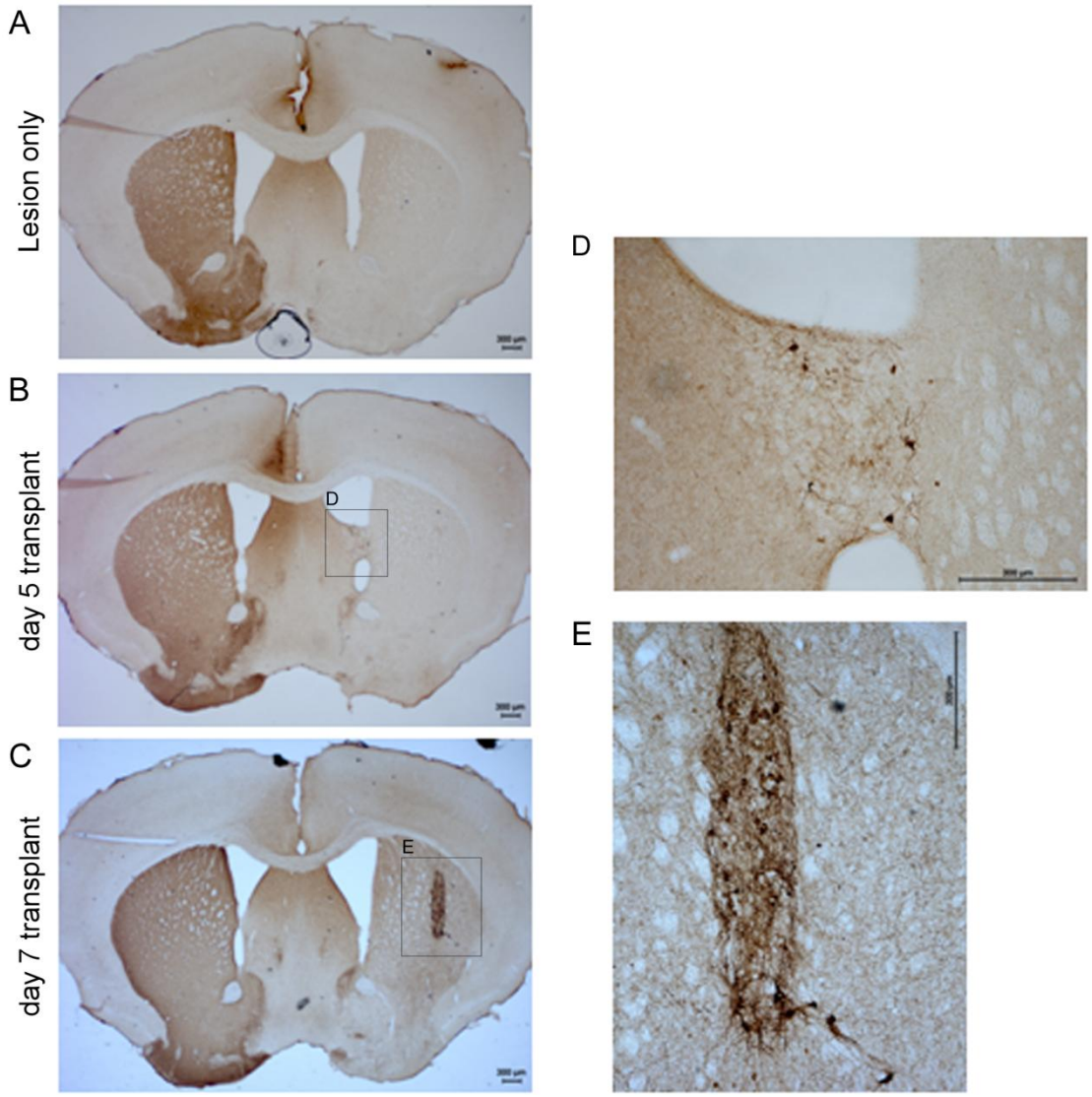


Figure 5.6 Substantial graft-derived reinnervation of the lesioned striatum 8 weeks after transplantation of d5 and d7 MD cultures (kindly provided by Dr. Sophie Precious and Andreas Heuer).

(A) Immunohistochemistry for TH illustrates the typical dense staining of DA fibers in the intact striatum (left) and almost complete loss of TH fibers is seen in 6-OHDA lesioned striatum (right). **(B+C)** Graft-derived re-innervation of the lesioned striatum 8 weeks after transplantation (boxed area, graft core). The graft cores in B+C contain stained TH positive neurons. **(D+E)** The boxed area in B+C is shown at larger magnification.

5.2.3 Head to head comparison of EpiSC-derived mDA grafts with ventral midbrain tissue in 6-OHDA-lesioned mouse models of PD

Transplantation of embryonic ventral midbrain (VM) tissue into dopamine-depleted animals has been studied in detail. In summary, embryonic VM cells have been demonstrated to survive, reinnervate into the host striatum, make synaptic connections onto the appropriate neuronal populations, and reduce many of the motor deficits caused by dopamine depleting lesions (Bjorklund et al., 1980; Bjorklund and Stenevi, 1979; Bjorklund et al., 1983; Dunnett et al., 1981; Dunnett et al., 1988; Freed et al., 1980; Perlow et al., 1979; Schmidt et al., 1983; Schmidt et al., 1982; Schultz, 1982; Schultzberg et al., 1984; Stromberg et al., 1985; Wuerthele et al., 1981). These very promising results led to clinical trials started in 1987 where cells of the human fetal mesencephalic tissue were transplanted to the striatum of PD patients. However, the use of fetal tissue involves ethical concerns. Pluripotent stem cells (PSC) offer a promising alternative to obtain mDA neurons *in vitro* but to date it has been a challenge to generate PSC-derived mDA neurons that functionally engraft *in vivo* as successfully as embryonic VM cells.

In the section above (5.2.2), I showed that d7 MD cultures were able to reduce drug-induced rotational behaviour in 6-OHDA lesioned mice after 8 weeks of tranplantation. To valuate d7 MD cultures for cell replacement in PD, we transplanted the d7 MD cells side-by-side with ventral E12.5 foetal ventral midbrain cells. Amphetamine-induced rotational test was performed before transplantation and at 4, 8, and 16 weeks after transplantation. As expected, VM graft goups displayed a decrease in rotations and an over-compensated rotational response by 4 weeks post-grafting which was maintained until 16 weeks after transplantation (the latest time point examined) (Figure 5.7). The group of mice that received d7 MD cultures also showed a decrease in the rotational behaviour but the score was less when compared to VM grafts (Figure 5.7). However, the level of over-compensatory response increased over the time in d7 MD grafted animals, indicating an increased level of Dopamine.

Following the functional assessment, graft survival and neuron cell differentiation was evaluated by immunostaining. Both groups displayed good TH positive cell survival within the transplanted striatum after 16 weeks of transplantation (Figure 5.8 A). Counting analysis of immunohistochemistry data further revealed large numbers of TH positive cells within the grafts wich received VM or d7 MD cells (Figure 5.8 A, C), indicating therapeutical potential of d7 MD cultures in the treatment of PD.

A negative side effect of cell replacement in PD is the appearance of graft-induced dyskineasia, showing abnormal involuntary movements and postures. The presence of serotonergic neurons within grafts is thought to play an important role in graft-induced dyskinesia (Braak and Del Tredici, 2008; Carta et al., 2007). Therefore, we performed an immunostaing for 5HT to detect serotonergic neurons. As shown in Figure 5.8 B, both the VM and d7 MD grafts contained 5HT positive neurons. It has been suggested that the ratio of DA neurons to serotonergic neurons may be inversely correlated to the development of graft-induced dyskineasia. In this study, the TH/5HT ratio of d7 MD grafts was higher than the one of VM grafts (Figure 5.8 C), suggesting that animals which received d7 MD grafts might be less likely to develop graft-induced dyskineasia.

In summary, these data demonstrate that the cells produced by the present protocol may potentially provide a useful therapeutic source for cell replacement therapy in PD.

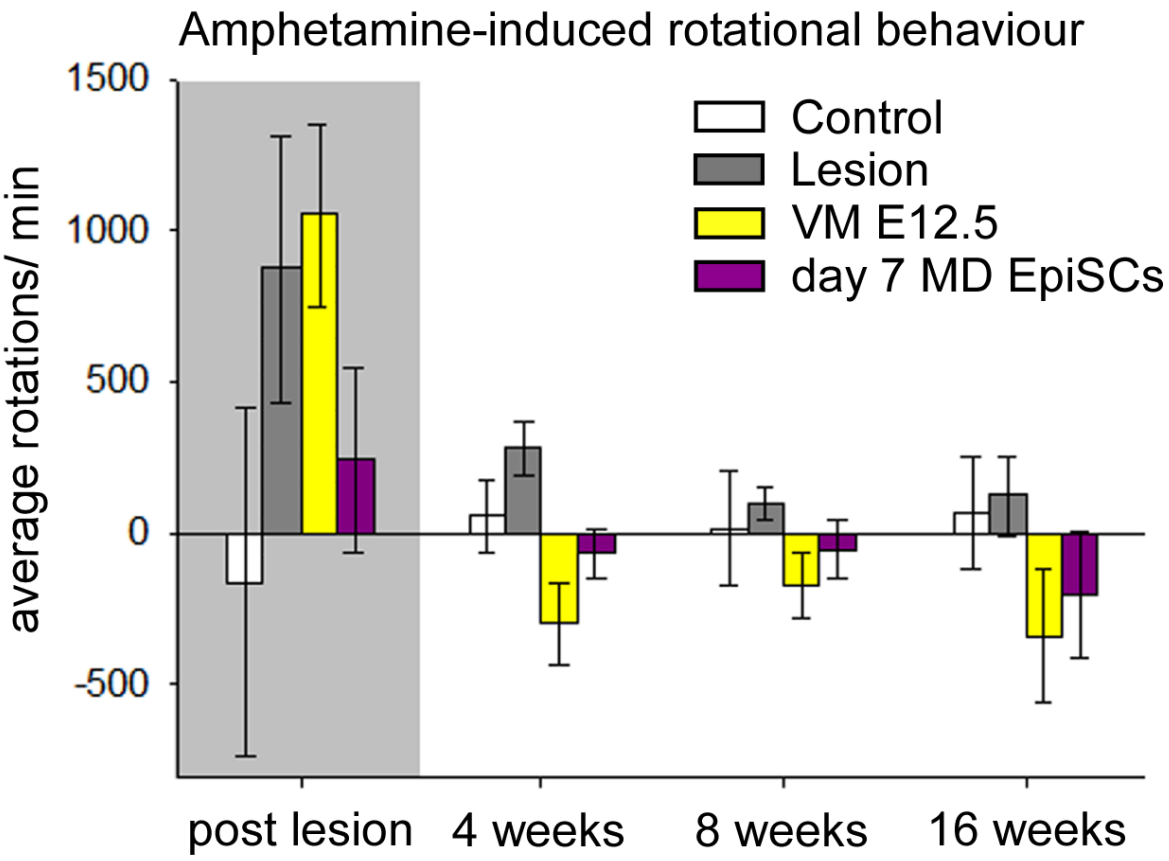
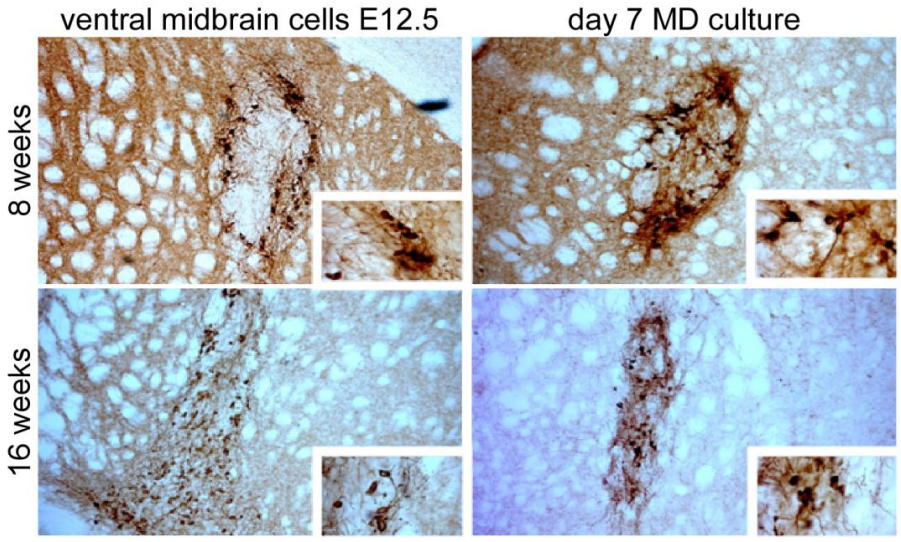


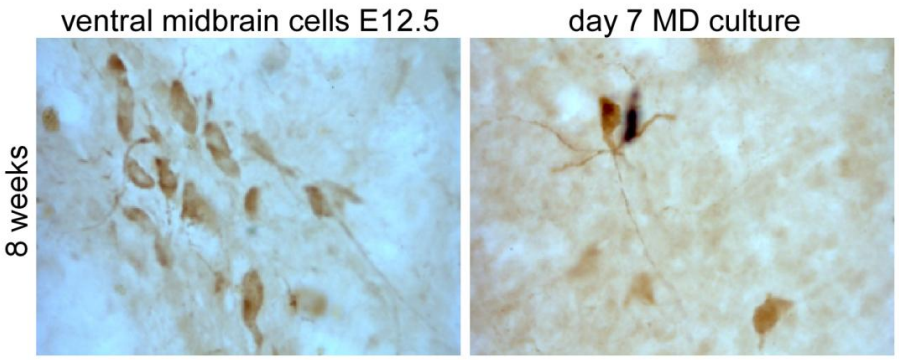
Figure 5.7 Behavioural analysis in E12.5 VM- versus d7 MD-grafted mice (kindly provided by Dr. Sophie Precious and Andreas Heuer).

Amphetamine-induced rotational test of no-lesion control (12 mice), lesioned (12 mice), VM- (29 mice) and d7 MD grafted mice (12 mice) in response to amphaetamine. Bars underlain by a grey background show drug induced rotations after 6-OHDA treatment (post lesion). Test was performed 4, 8 (control: n=12; lesion: n=12; VM: n=29; d7 MD EpiSC: n=28) and 16 weeks after transplantation (control: n=12; lesion: n=12; VM: n=21; d7 MD EpiSC: n=20).

A


ventral midbrain cells E12.5
day 7 MD culture
8 weeks
16 weeks

B


ventral midbrain cells E12.5
day 7 MD culture
8 weeks

C

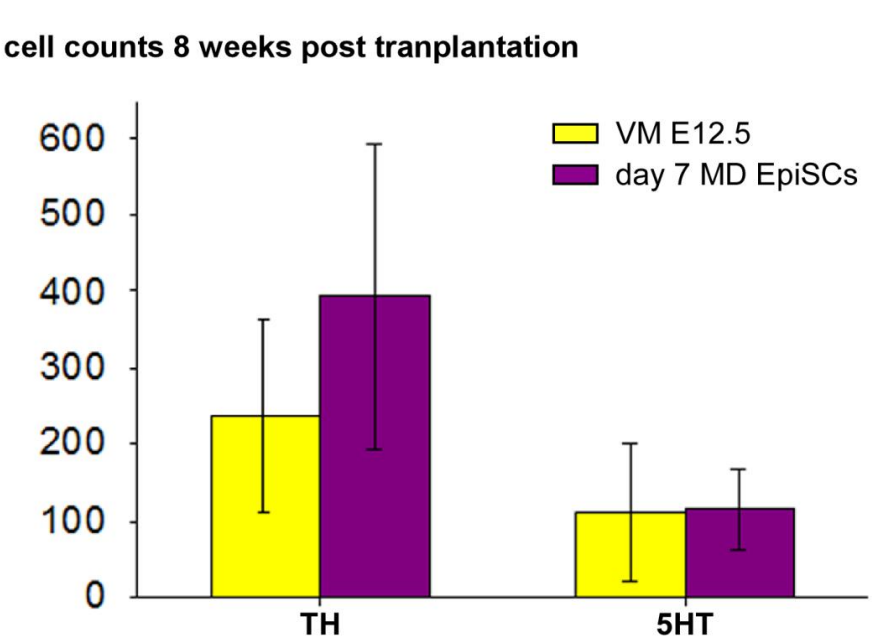

cell counts 8 weeks post tranplantation
600
500
400
300
200
100
0
VM E12.5
day 7 MD EpiSCs
TH
5HT

Figure 5.8 Characterisation of neurons in 6-OHDA lesioned mouse models of PD grafted with either d7 MD or VM cells (kindly provided by Dr. Sophie Precious and Andreas Heuer).

(A) Immunohistochemistry for TH on coronal sections illustrating TH positive cell survival and striatal reinnervation on the lesioned and grafted striatum with cells of d7 MD cultures or VM (E12.5) after 8 and 16 weeks of Transplantation. **(B)** Immunohistochemistry for the serotonergic marker 5HT in 6-OHDA lesioned mice 8 weeks posttransplantation. **(C)** The total number of TH positive and 5HT positive neurons oin the lesioned and grafted striatum shown in A and B.

5.3 Discussion

In this chapter, I show that EpiSC-derived mDA neurons exhibit electrophysiological properties typical of primary mDA neurons. Moreover, after transplantation into 6-OHDA lesioned mouse striatum, the mDA progenitor cells survived and differentiated into DA neurons, and mediated behavioural improvements. Thus, neural progenitors with ventral midbrain characteristics may represent a valuable source for functional and transplantable mDA neurons in clinical applications for the treatment of PD.

Although cells of d5 and d7 MD display the same profile for the molecular markers examined (Figure 5.4), only d7 MD cells markedly restored amphetamine-induced behaviour which correlates with the observed increase of TH positive cells in the grafts. D7 MD cultures received 2 days of FGF8 whereas d5 MD cultures did not, suggesting that the activation of FGF signalling is essential for the acquisition of DA properties. These results point towards an important point for FGF8 in mDA neural progenitor cells.

During development of the midbrain and hindbrain region, FGF8 has been reported to be involved in patterning (Basson et al., 2008; Crossley et al., 1996; Sato and Joyner, 2009), proliferation (Lahti et al., 2011; Xu et al., 2000), and cell survival (Basson et al., 2008; Chi et al., 2003). I found that when FGF8 was added during differentiation, the expression of the *En1/2* was highly increased (Figure 4.11). EN1/2 are implicated in regionalisation of the midbrain and hindbrain (Crossley et al., 1996; Liu and Joyner, 2001; Simon et al., 2001) and in the survival of mDA neurons (Alberi et al., 2004; Alvarez-Fischer et al., 2011; Sgado et al., 2006; Simon et al., 2001). Thus, the increase of TH positive cells in grafts with d7 MD cultures may be a result of FGF-induced upregulation of *En* expression, which in turn result in decreased cell death and/or proper induction of DA neuronal phenotype.

To reinforce the importance of FGF8 for the specification of mDA neurons (Ye et al., 1998), only EpiSC MD cultures exposed to SHH and FGF8 efficiently produced DA neurons (Figure 4.7 and 4.9). In addition, I observed that DA neurons exposed to FGF8 displayed a

morphologically more mature phenotype compared to cultures with SHH alone (Figure 4.9). These data suggest an integral role for FGF8 in the maturation of functional mDA neurons.

Torres et al (2007) reported that the developmental age of the donor cells has a significant impact in cell replacement of DA neurons. Cells derived from ventral midbrain of rat embryos (E~12) at a stage, when no DA neurons are present, differentiated into DA neurons after transplantation. These cells survived and integrated into the host striatum of 6-OHDA-lesioned rat PD models. However, foetal ventral midbrain cells taken from E~11 rat embryos failed to generate DA neurons post-implantation. Therefore, the possibility cannot be excluded that the stage of maturation might also be a reason for the difference in TH positive cells in d5 and d7 MD grafts.

Taken together, temporally controlled modulation of FGF signalling during MD of pluirpotent stem cells is crucial for obtaining functional authentic mDA neurons. Furthermore, it provides a fully chemically defined system that resembles an attractive tool for biomedical applications.

6 Concluding remarks and future directions

The characteristics of pluripotent stem cells in broad differentiation potential and self-renewal represent a remarkable model to study development *in vitro* and further offer an attractive tool for biomedical application such as cell therapy, disease modelling and drug screening. Several studies have demonstrated that ESC-derived mDA neurons transplanted into animal PD models can survive and alleviate behaviour deficits (Bjorklund et al., 2002; Cho et al., 2008; Friling et al., 2009; Hargus et al., 2010; Kim et al., 2002; Kriks et al., 2011; Rodriguez-Gomez et al., 2007; Roy et al., 2006; Sanchez-Pernaute et al., 2008; Tabar et al., 2008; Takagi et al., 2005). However, due to pluripotent nature of ESCs, the generation of a desired cell type is often accompanied by other cells that may negatively interfere with the benefits of biomedical applications. In order to achieve a pure mDA cell population, it is essential to understand the molecular mechanisms responsible for the generation of mDA neurons that in turn enable us to commad stem cell fate specification and differentiation.

The work presented in this thesis is focused on the role of FGF signalling in mDA neuronal differentiation using mouse pluripotent stem cells. In summary (Figure 6.1), the findings demonstrate a previously unrecognized inhibitory role of FGF/ERK in the institution of a midbrain progenitor cell fate and the induction of *Wnt* and *Shh*. I show that a period of endogenous FGF activity is essential to confer a ventral midbrain progenitor fate and that later in differentiation activation of FGF signalling is required to generate mDA neurons. EpiSC-derived mDA neurons exhibit functional, neuron-like properties and when implanted into the striatum of mouse PD model strongly restored amphetamine-induced rotation behaviour without any signs of overgrowth. Thus, a stepwise control of FGF/ERK activation during specific stages of neural differentiation from mouse stem cells is crucial for generation of authentic, functional mDA neurons. Importantly, this small-molecular-based protocol is fully chemically defined, free from genetic manipulation and represents a method for

significantly improved efficiency and high reproducibility compared to previously reported transgene-free protocols.

In collaboration with the group of Steve Dunnett we have begun detailed analysis of the potential of the mDA precursor cells generated by the current protocol. These studies will involve the validation of a midbrain specific DA phenotype in grafts and the precise characterisation of grafted non-DA neuronal cells. It cannot be excluded that the observed reduced rotation behaviour was caused by cells releasing neurotrophic factors which have the ability to regulate the survival of specific neuronal populations in the central nervous system. One potential candidate is the glial cell line-derived neurotrophic factor (GDNF) which has been demonstrated to protect and restore mDA neurons (Behrstock et al., 2006; Dezawa et al., 2004; Redmond et al., 2007). Moreover, by using behaviour tests, we will further investigate the consequences of the presence of serotonergic neurons in grafts which are assumed to be in causative relationship with graft induced dyskinesia (Carlsson et al., 2007; Politis et al., 2011; Politis et al., 2010). However, for future therapies of PD, the results obtained on mouse cells have to be confirmed on human ESCs.

Charlie Arber in our group has addressed this point and has obtained encouraging results. Briefly, human ESCs were exposed to PD0325901 at d3 MD, a time point when the primitive ectoderm/epiblast marker *FGF5* was peaked. Indeed, blockade of FGF/ERK signalling after initial neurectodermal induction resulted in a direct and early induction of the midbrain characteristics at the expense of forebrain and caudal neural fates. Exposure of these cells to SHH and FGF8 led to the robust production of DA neurons expressing marker genes for correct, ventral midbrain-specific identity. We are currently in the process of validating the potential of these hESC-derived ventral midbrain neuronal cells to restore parkinsonian symptoms in a rat model of PD.

Given the similarities in the response to early Erk inhibition during differentiation, cell fate decisions of human ESC and mouse EpiSC may be instructed by the same signalling pathways. Yet, Kriks et al. (2011) recently reported that early stimulation of SHH and FGF

signalling followed by activation of WNT signalling, using the GSK3ß inhibitor CHIR99021, can direct human ESC toward an mDA specific fate (↑FOXA2, ↑LMX1A, ↑OTX2). It is worth noting that FGF signalling activates the expression of the FGF signalling inhibitors *MPK3, SPRY* and *SEF* (Eblaghie et al., 2003; Kawakami et al., 2003; Kovalenko et al., 2006; Kovalenko et al., 2003; Urness et al., 2008; Vieira and Martinez, 2005). It might be therefore possible that such a negative feedback regulation of FGF signalling results in a reduction of FGF activity at a time when regional specification occurs. However, this controversy raises the need for more direct *in vitro* analysis of FGF regulation during differentiation toward mDA neurons.

The results of this thesis also revealed that neither stimulation of SHH pathway nor activation of canonical WNT signalling or their combination could replace early inhibition of FGF/ERK activity in the specification of mouse EpiSCs toward a ventral midbrain progenitor cell fate. This observation opens up the possibility that early FGF/ERK inhibition allows the activation of other pathways that promote midbrain induction. For example, although expression of *Lmx1a* and *Foxa2* were increased by SHH treatment and/or activation of canonical WNT signalling, the number of OTX2 positive cells and the expression of *Dmrt5* were not altered. In order to identify pathways that are activated or blocked in a FGF/ERK deficient environment, I have recently performed a microarray gene expression assay of d3 MD EpiSC cultures with and without PD0325901. The outcome of this study would widen our knowledge in the molecular interactions between signalling pathways during the process of regional specification. Furthermore, the microarray might identify novel surface markers specific for ventral midbrain progenitor fate which in turn allows the purification of mDA progenitors by fluorescence-activated cell sorting.

Previous studies indicated that *Msx1* is directly induced by LMX1A (Andersson et al., 2006a; Chung et al., 2009). In the developing midbrain *Msx1* is expressed in the ventral and dorsal midline as *Lmx1a* (Andersson et al., 2006b; Bach et al., 2003; Mishima et al., 2009; Yan et al., 2011) strentghten that *Msx1* is a downstream target of LMX1A. Andersson et al. (2006)

recently reported that SHH can induce the expression of *Lmx1a* and *Msx1* in neural tube explants of chick embryos. However, my findings presented in chapter 4.7 show that expression of *Msx1* was not increased by SHH (Figure 4.12) and treatment with the SHH antagonist cyclopamine did not reduce PD0325901-induced *Msx1* mRNA level (Figure 4.13), implying a SHH-independent activation of *Msx1* expression. Interstingly, induction of *Lmx1a* by PD0325901 was abolished at d3 of MD in cultures with cyclopamine. Another study demonstrated that WNT1 and LMX1A form a regulatory loop in the gerenation of mDA neurons (Chung et al., 2009). However the same study showed that overexpression of *Wnt1* during neural differentiation did not significantly alter the expression of *Msx1* while the level of *Lmx1* expression was highly induced. These observations raise the question of which other extrinsic or intrinsic factors regulate *Msx1*. In other tissues, Msx1 was demonstrated to be a downstream target of BMP (Furuta et al., 1997; Liu et al., 2004; Suzuki et al., 1997; Timmer et al., 2002) which, in the developing midbrain, is expressed in the roofplate (Bach et al., 2003). Therefore, for detailed analysis of the molecular mechanisms during mDA neural differentiation, further anaylsis should be carried out to elucidate whether EpiSC-derived midbrain cell population by early ERK inhibition contain cells of a dorsal midbrain progenitor identity.

The results of chapter 4 pointed out further an important role of DMRT5 in the generation of mDA neurons. *Dmrt5* is one of the genes upregulated by Erk inhibition, implying a crucial role of DMRT5 in the differentiation of mDA neurons as previously suggested (Gennet et al., 2011). Our lab has recently generated a conditional *Dmrt5* KO allele in mouse ES cells for elucidating the role of DMRT5 in this process. This model should facilitate the identification of factors that are regulated by DMRT5 and to unreveal the precise mechanism in which this factor is involved.

Here, we have focused on the inhibition of FGF signaling via ERK. It would be of importance to verify whether FGF/ERK inhibition has an effect on the other two FGF mediated pathways, FGF/PI3K and FGF/PLC-γ. I would also like to investigate whether modulation of

FGF/PLC-γ has any role in the promotion of mDA neurons by using the PLC-γ inhibitor U73122.

Previous studies demonstrated that dopaminergic neurons of the midbrain targeting the striatum are implicated in drug addiction (Reading et al., 1991; Robbins et al., 1990; White, 1989). In this context, electophysiological studies on Pitx3-GFP positive cells revealed features similar to adult dopamine neurons observed *in vivo* midbrain DA system; even more than *ex vivo* brainslices (unpublished observation by Dr. Jessica Risner-Janiczek). Thus, EpiSC-derived mDA neurons represent an attractive model to study in detail the impacts of drug exposure: firstly, the desired neurons are easily accessible *in vitro* for electrophysiological studies and, secondly, this strategy allows a powerful high-throughput screening of mDA neurons.

Finally, using the knowledge obtained from *in vivo* developmental studies, it might be interesting to test whether the strategy of early specification can be applied for the generation towards other disease-relevant neurons such as medium spiny GABAergic neurons lost in Huntington's disease, basal forebrain cholinergic neurons implicated in Alzheimer's disease or motor neurons affected in spinal cord injury, amyotrophic lateral sclerosis, and spinal muscular atrophy.

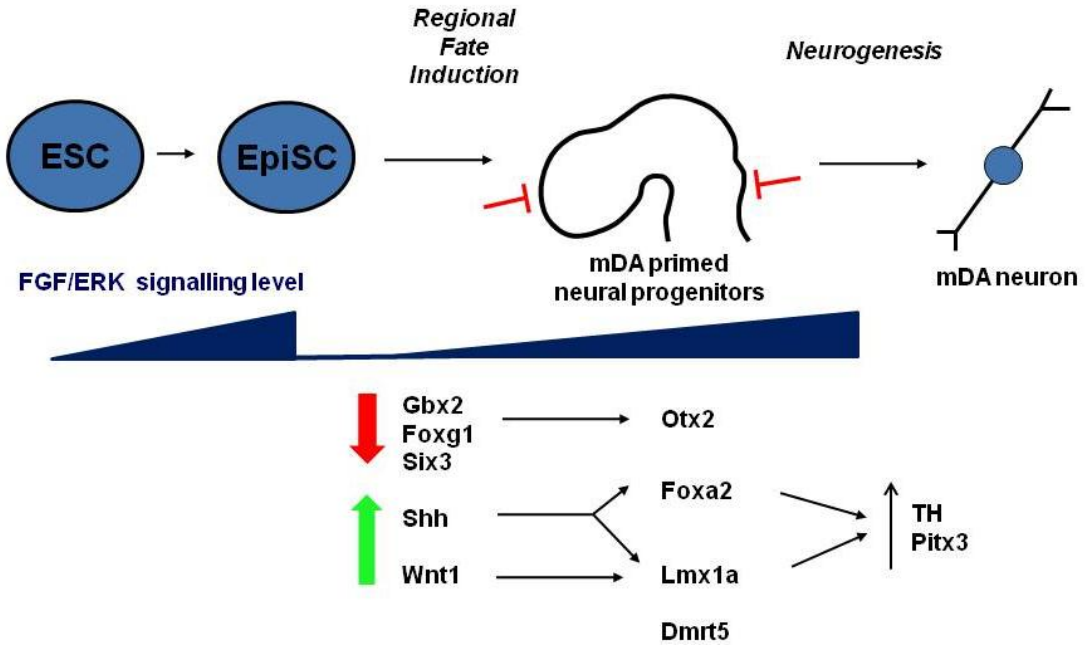


Figure 6.1 Proposed model of FGF signalling in mDA neural differentiation.

7 Bibliography

Aasen, T., Raya, A., Barrero, M.J., Garreta, E., Consiglio, A., Gonzalez, F., Vassena, R., Bilic, J., Pekarik, V., Tiscornia, G.*, et al.* (2008). Efficient and rapid generation of induced pluripotent stem cells from human keratinocytes. Nat Biotechnol *26*, 1276-1284.

Acampora, D., Avantaggiato, V., Tuorto, F., and Simeone, A. (1997). Genetic control of brain morphogenesis through Otx gene dosage requirement. Development *124*, 3639-3650.

Acampora, D., Mazan, S., Lallemand, Y., Avantaggiato, V., Maury, M., Simeone, A., and Brulet, P. (1995). Forebrain and midbrain regions are deleted in Otx2-/- mutants due to a defective anterior neuroectoderm specification during gastrulation. Development *121*, 3279-3290.

Adachi, K., Suemori, H., Yasuda, S.Y., Nakatsuji, N., and Kawase, E. (2010). Role of SOX2 in maintaining pluripotency of human embryonic stem cells. Genes Cells *15*, 455-470.

Alberi, L., Sgado, P., and Simon, H.H. (2004). Engrailed genes are cell-autonomously required to prevent apoptosis in mesencephalic dopaminergic neurons. Development *131*, 3229-3236.

Alvarez-Fischer, D., Fuchs, J., Castagner, F., Stettler, O., Massiani-Beaudoin, O., Moya, K.L., Bouillot, C., Oertel, W.H., Lombes, A., Faigle, W.*, et al.* (2011). Engrailed protects mouse midbrain dopaminergic neurons against mitochondrial complex I insults. Nat Neurosci *14*, 1260-1266.

Alvarez, A.R., Godoy, J.A., Mullendorff, K., Olivares, G.H., Bronfman, M., and Inestrosa, N.C. (2004). Wnt-3a overcomes beta-amyloid toxicity in rat hippocampal neurons. Exp Cell Res *297*, 186-196.

Alvarez, I.S., Araujo, M., and Nieto, M.A. (1998). Neural induction in whole chick embryo cultures by FGF. Dev Biol *199*, 42-54.

Andersson, E., Jensen, J.B., Parmar, M., Guillemot, F., and Bjorklund, A. (2006a). Development of the mesencephalic dopaminergic neuron system is compromised in the absence of neurogenin 2. Development *133*, 507-516.

Andersson, E., Tryggvason, U., Deng, Q., Friling, S., Alekseenko, Z., Robert, B., Perlmann, T., and Ericson, J. (2006b). Identification of intrinsic determinants of midbrain dopamine neurons. Cell *124*, 393-405.

Andersson, E.R., Prakash, N., Cajanek, L., Minina, E., Bryja, V., Bryjova, L., Yamaguchi, T.P., Hall, A.C., Wurst, W., and Arenas, E. (2008). Wnt5a regulates ventral midbrain morphogenesis and the development of A9-A10 dopaminergic cells in vivo. PLoS One *3*, e3517.

Ang, S.L., Conlon, R.A., Jin, O., and Rossant, J. (1994). Positive and negative signals from mesoderm regulate the expression of mouse Otx2 in ectoderm explants. Development *120*, 2979-2989.

Ang, S.L., Jin, O., Rhinn, M., Daigle, N., Stevenson, L., and Rossant, J. (1996). A targeted mouse Otx2 mutation leads to severe defects in gastrulation and formation of axial mesoderm and to deletion of rostral brain. Development *122*, 243-252.

Ang, S.L., and Rossant, J. (1994). HNF-3 beta is essential for node and notochord formation in mouse development. Cell *78*, 561-574.

Aoi, T., Yae, K., Nakagawa, M., Ichisaka, T., Okita, K., Takahashi, K., Chiba, T., and Yamanaka, S. (2008). Generation of pluripotent stem cells from adult mouse liver and stomach cells. Science *321*, 699-702.
Aranda, A., and Pascual, A. (2001). Nuclear hormone receptors and gene expression. Physiol Rev *81*, 1269-1304.
Arman, E., Haffner-Krausz, R., Chen, Y., Heath, J.K., and Lonai, P. (1998). Targeted disruption of fibroblast growth factor (FGF) receptor 2 suggests a role for FGF signaling in pregastrulation mammalian development. Proc Natl Acad Sci U S A *95*, 5082-5087.
Aubert, J., Stavridis, M.P., Tweedie, S., O'Reilly, M., Vierlinger, K., Li, M., Ghazal, P., Pratt, T., Mason, J.O., Roy, D.*, et al.* (2003). Screening for mammalian neural genes via fluorescence-activated cell sorter purification of neural precursors from Sox1-gfp knock-in mice. Proc Natl Acad Sci U S A *100 Suppl 1*, 11836-11841.
Avantaggiato, V., Pandolfi, P.P., Ruthardt, M., Hawe, N., Acampora, D., Pelicci, P.G., and Simeone, A. (1995). Developmental analysis of murine Promyelocyte Leukemia Zinc Finger (PLZF) gene expression: implications for the neuromeric model of the forebrain organization. J Neurosci *15*, 4927-4942.
Bach, A., Lallemand, Y., Nicola, M.A., Ramos, C., Mathis, L., Maufras, M., and Robert, B. (2003). Msx1 is required for dorsal diencephalon patterning. Development *130*, 4025-4036.
Bachiller, D., Klingensmith, J., Kemp, C., Belo, J.A., Anderson, R.M., May, S.R., McMahon, J.A., McMahon, A.P., Harland, R.M., Rossant, J.*, et al.* (2000). The organizer factors Chordin and Noggin are required for mouse forebrain development. Nature *403*, 658-661.
Bain, J., Plater, L., Elliott, M., Shpiro, N., Hastie, C.J., McLauchlan, H., Klevernic, I., Arthur, J.S., Alessi, D.R., and Cohen, P. (2007). The selectivity of protein kinase inhibitors: a further update. Biochem J *408*, 297-315.
Baker, J.C., Beddington, R.S., and Harland, R.M. (1999). Wnt signaling in Xenopus embryos inhibits bmp4 expression and activates neural development. Genes Dev *13*, 3149-3159.
Bally-Cuif, L., Cholley, B., and Wassef, M. (1995). Involvement of Wnt-1 in the formation of the mes/metencephalic boundary. Mech Dev *53*, 23-34.
Balmanno, K., and Cook, S.J. (1999). Sustained MAP kinase activation is required for the expression of cyclin D1, p21Cip1 and a subset of AP-1 proteins in CCL39 cells. Oncogene *18*, 3085-3097.
Barberi, T., Klivenyi, P., Calingasan, N.Y., Lee, H., Kawamata, H., Loonam, K., Perrier, A.L., Bruses, J., Rubio, M.E., Topf, N.*, et al.* (2003). Neural subtype specification of fertilization and nuclear transfer embryonic stem cells and application in parkinsonian mice. Nat Biotechnol *21*, 1200-1207.
Barker, N. (2008). The canonical Wnt/beta-catenin signalling pathway. Methods Mol Biol *468*, 5-15.
Basson, M.A., Echevarria, D., Ahn, C.P., Sudarov, A., Joyner, A.L., Mason, I.J., Martinez, S., and Martin, G.R. (2008). Specific regions within the embryonic midbrain and cerebellum require different levels of FGF signaling during development. Development *135*, 889-898.
Bayly, R.D., Ngo, M., Aglyamova, G.V., and Agarwala, S. (2007). Regulation of ventral midbrain patterning by Hedgehog signaling. Development *134*, 2115-2124.
Beddington, R.S. (1994). Induction of a second neural axis by the mouse node. Development *120*, 613-620.

Beenken, A., and Mohammadi, M. (2009). The FGF family: biology, pathophysiology and therapy. Nat Rev Drug Discov *8*, 235-253.
Behrstock, S., Ebert, A., McHugh, J., Vosberg, S., Moore, J., Schneider, B., Capowski, E., Hei, D., Kordower, J., Aebischer, P.*, et al.* (2006). Human neural progenitors deliver glial cell line-derived neurotrophic factor to parkinsonian rodents and aged primates. Gene Ther *13*, 379-388.
Belo, J.A., Bachiller, D., Agius, E., Kemp, C., Borges, A.C., Marques, S., Piccolo, S., and De Robertis, E.M. (2000). Cerberus-like is a secreted BMP and nodal antagonist not essential for mouse development. Genesis *26*, 265-270.
Bernemann, C., Greber, B., Ko, K., Sterneckert, J., Han, D.W., Arauzo-Bravo, M.J., and Scholer, H.R. (2011). Distinct developmental ground states of epiblast stem cell lines determine different pluripotency features. Stem Cells *29*, 1496-1503.
Bjorklund, A., Dunnett, S.B., Stenevi, U., Lewis, M.E., and Iversen, S.D. (1980). Reinnervation of the denervated striatum by substantia nigra transplants: functional consequences as revealed by pharmacological and sensorimotor testing. Brain Res *199*, 307-333.
Bjorklund, A., and Stenevi, U. (1979). Reconstruction of the nigrostriatal dopamine pathway by intracerebral nigral transplants. Brain Res *177*, 555-560.
Bjorklund, A., Stenevi, U., Schmidt, R.H., Dunnett, S.B., and Gage, F.H. (1983). Intracerebral grafting of neuronal cell suspensions. II. Survival and growth of nigral cell suspensions implanted in different brain sites. Acta Physiol Scand Suppl *522*, 9-18.
Bjorklund, L.M., Sanchez-Pernaute, R., Chung, S., Andersson, T., Chen, I.Y., McNaught, K.S., Brownell, A.L., Jenkins, B.G., Wahlestedt, C., Kim, K.S.*, et al.* (2002). Embryonic stem cells develop into functional dopaminergic neurons after transplantation in a Parkinson rat model. Proc Natl Acad Sci U S A *99*, 2344-2349.
Blaess, S., Corrales, J.D., and Joyner, A.L. (2006). Sonic hedgehog regulates Gli activator and repressor functions with spatial and temporal precision in the mid/hindbrain region. Development *133*, 1799-1809.
Blakely, B.D., Bye, C.R., Fernando, C.V., Horne, M.K., Macheda, M.L., Stacker, S.A., Arenas, E., and Parish, C.L. (2011). Wnt5a regulates midbrain dopaminergic axon growth and guidance. PLoS One *6*, e18373.
Blum, M., Gaunt, S.J., Cho, K.W., Steinbeisser, H., Blumberg, B., Bittner, D., and De Robertis, E.M. (1992). Gastrulation in the mouse: the role of the homeobox gene goosecoid. Cell *69*, 1097-1106.
Boettger, T., Knoetgen, H., Wittler, L., and Kessel, M. (2001). The avian organizer. Int J Dev Biol *45*, 281-287.
Bolam, J.P., Freund, T.F., Bjorklund, A., Dunnett, S.B., and Smith, A.D. (1987). Synaptic input and local output of dopaminergic neurons in grafts that functionally reinnervate the host neostriatum. Exp Brain Res *68*, 131-146.
Bottcher, R.T., Pollet, N., Delius, H., and Niehrs, C. (2004). The transmembrane protein XFLRT3 forms a complex with FGF receptors and promotes FGF signalling. Nat Cell Biol *6*, 38-44.
Bouwmeester, T., Kim, S., Sasai, Y., Lu, B., and De Robertis, E.M. (1996). Cerberus is a head-inducing secreted factor expressed in the anterior endoderm of Spemann's organizer. Nature *382*, 595-601.
Braak, H., and Del Tredici, K. (2008). Assessing fetal nerve cell grafts in Parkinson's disease. Nat Med *14*, 483-485.

Broccoli, V., Boncinelli, E., and Wurst, W. (1999). The caudal limit of Otx2 expression positions the isthmic organizer. Nature *401*, 164-168.
Brons, I.G., Smithers, L.E., Trotter, M.W., Rugg-Gunn, P., Sun, B., Chuva de Sousa Lopes, S.M., Howlett, S.K., Clarkson, A., Ahrlund-Richter, L., Pedersen, R.A.*, et al.* (2007). Derivation of pluripotent epiblast stem cells from mammalian embryos. Nature *448*, 191-195.
Brundin, P., Strecker, R.E., Widner, H., Clarke, D.J., Nilsson, O.G., Astedt, B., Lindvall, O., and Bjorklund, A. (1988). Human fetal dopamine neurons grafted in a rat model of Parkinson's disease: immunological aspects, spontaneous and drug-induced behaviour, and dopamine release. Exp Brain Res *70*, 192-208.
Bryja, V., Schulte, G., Rawal, N., Grahn, A., and Arenas, E. (2007). Wnt-5a induces Dishevelled phosphorylation and dopaminergic differentiation via a CK1-dependent mechanism. J Cell Sci *120*, 586-595.
Burbach, J.P., and Smidt, M.P. (2006). Molecular programming of stem cells into mesodiencephalic dopaminergic neurons. Trends Neurosci *29*, 601-603.
Burgess, W.H., Dionne, C.A., Kaplow, J., Mudd, R., Friesel, R., Zilberstein, A., Schlessinger, J., and Jaye, M. (1990). Characterization and cDNA cloning of phospholipase C-gamma, a major substrate for heparin-binding growth factor 1 (acidic fibroblast growth factor)-activated tyrosine kinase. Mol Cell Biol *10*, 4770-4777.
Camus, A., Perea-Gomez, A., Moreau, A., and Collignon, J. (2006). Absence of Nodal signaling promotes precocious neural differentiation in the mouse embryo. Dev Biol *295*, 743-755.
Canning, C.A., Lee, L., Irving, C., Mason, I., and Jones, C.M. (2007). Sustained interactive Wnt and FGF signaling is required to maintain isthmic identity. Dev Biol *305*, 276-286.
Carlsson, T., Carta, M., Winkler, C., Bjorklund, A., and Kirik, D. (2007). Serotonin neuron transplants exacerbate L-DOPA-induced dyskinesias in a rat model of Parkinson's disease. J Neurosci *27*, 8011-8022.
Carta, M., Carlsson, T., Kirik, D., and Bjorklund, A. (2007). Dopamine released from 5-HT terminals is the cause of L-DOPA-induced dyskinesia in parkinsonian rats. Brain *130*, 1819-1833.
Carvajal-Vergara, X., Sevilla, A., D'Souza, S.L., Ang, Y.S., Schaniel, C., Lee, D.F., Yang, L., Kaplan, A.D., Adler, E.D., Rozov, R.*, et al.* (2010). Patient-specific induced pluripotent stem-cell-derived models of LEOPARD syndrome. Nature *465*, 808-812.
Castelo-Branco, G., Rawal, N., and Arenas, E. (2004). GSK-3beta inhibition/beta-catenin stabilization in ventral midbrain precursors increases differentiation into dopamine neurons. J Cell Sci *117*, 5731-5737.
Castelo-Branco, G., Sousa, K.M., Bryja, V., Pinto, L., Wagner, J., and Arenas, E. (2006). Ventral midbrain glia express region-specific transcription factors and regulate dopaminergic neurogenesis through Wnt-5a secretion. Mol Cell Neurosci *31*, 251-262.
Castelo-Branco, G., Wagner, J., Rodriguez, F.J., Kele, J., Sousa, K., Rawal, N., Pasolli, H.A., Fuchs, E., Kitajewski, J., and Arenas, E. (2003). Differential regulation of midbrain dopaminergic neuron development by Wnt-1, Wnt-3a, and Wnt-5a. Proc Natl Acad Sci U S A *100*, 12747-12752.
Cattaneo, E., and McKay, R. (1990). Proliferation and differentiation of neuronal stem cells regulated by nerve growth factor. Nature *347*, 762-765.

Chambers, I., Silva, J., Colby, D., Nichols, J., Nijmeijer, B., Robertson, M., Vrana, J., Jones, K., Grotewold, L., and Smith, A. (2007). Nanog safeguards pluripotency and mediates germline development. Nature *450*, 1230-1234.
Chenn, A., and Walsh, C.A. (2002). Regulation of cerebral cortical size by control of cell cycle exit in neural precursors. Science *297*, 365-369.
Chenoweth, J.G., and Tesar, P.J. (2010). Isolation and maintenance of mouse epiblast stem cells. Methods Mol Biol *636*, 25-44.
Chi, C.L., Martinez, S., Wurst, W., and Martin, G.R. (2003). The isthmic organizer signal FGF8 is required for cell survival in the prospective midbrain and cerebellum. Development *130*, 2633-2644.
Chiang, C., Litingtung, Y., Lee, E., Young, K.E., Corden, J.L., Westphal, H., and Beachy, P.A. (1996). Cyclopia and defective axial patterning in mice lacking Sonic hedgehog gene function. Nature *383*, 407-413.
Chizhikov, V.V., and Millen, K.J. (2005). Roof plate-dependent patterning of the vertebrate dorsal central nervous system. Dev Biol *277*, 287-295.
Cho, M.S., Lee, Y.E., Kim, J.Y., Chung, S., Cho, Y.H., Kim, D.S., Kang, S.M., Lee, H., Kim, M.H., Kim, J.H.*, et al.* (2008). Highly efficient and large-scale generation of functional dopamine neurons from human embryonic stem cells. Proc Natl Acad Sci U S A *105*, 3392-3397.
Chuang, C.F., and Ng, S.Y. (1994). Functional divergence of the MAP kinase pathway. ERK1 and ERK2 activate specific transcription factors. FEBS Lett *346*, 229-234.
Chung, S., Leung, A., Han, B.S., Chang, M.Y., Moon, J.I., Kim, C.H., Hong, S., Pruszak, J., Isacson, O., and Kim, K.S. (2009). Wnt1-lmx1a forms a novel autoregulatory loop and controls midbrain dopaminergic differentiation synergistically with the SHH-FoxA2 pathway. Cell Stem Cell *5*, 646-658.
Chung, S., Moon, J.I., Leung, A., Aldrich, D., Lukianov, S., Kitayama, Y., Park, S., Li, Y., Bolshakov, V.Y., Lamonerie, T.*, et al.* (2011). ES cell-derived renewable and functional midbrain dopaminergic progenitors. Proc Natl Acad Sci U S A *108*, 9703-9708.
Chung, S., Sonntag, K.C., Andersson, T., Bjorklund, L.M., Park, J.J., Kim, D.W., Kang, U.J., Isacson, O., and Kim, K.S. (2002). Genetic engineering of mouse embryonic stem cells by Nurr1 enhances differentiation and maturation into dopaminergic neurons. Eur J Neurosci *16*, 1829-1838.
Clark, S.G., Stern, M.J., and Horvitz, H.R. (1992). C. elegans cell-signalling gene sem-5 encodes a protein with SH2 and SH3 domains. Nature *356*, 340-344.
Collier, T.J., Sortwell, C.E., Elsworth, J.D., Taylor, J.R., Roth, R.H., Sladek, J.R., Jr., and Redmond, D.E., Jr. (2002). Embryonic ventral mesencephalic grafts to the substantia nigra of MPTP-treated monkeys: feasibility relevant to multiple-target grafting as a therapy for Parkinson's disease. J Comp Neurol *442*, 320-330.
Corson, L.B., Yamanaka, Y., Lai, K.M., and Rossant, J. (2003). Spatial and temporal patterns of ERK signaling during mouse embryogenesis. Development *130*, 4527-4537.
Coucouvanis, E., and Martin, G.R. (1995). Signals for death and survival: a two-step mechanism for cavitation in the vertebrate embryo. Cell *83*, 279-287.
Cox, W.G., and Hemmati-Brivanlou, A. (1995). Caudalization of neural fate by tissue recombination and bFGF. Development *121*, 4349-4358.

Crossley, P.H., and Martin, G.R. (1995). The mouse Fgf8 gene encodes a family of polypeptides and is expressed in regions that direct outgrowth and patterning in the developing embryo. Development *121*, 439-451.
Crossley, P.H., Martinez, S., and Martin, G.R. (1996). Midbrain development induced by FGF8 in the chick embryo. Nature *380*, 66-68.
Danielian, P.S., and McMahon, A.P. (1996). Engrailed-1 as a target of the Wnt-1 signalling pathway in vertebrate midbrain development. Nature *383*, 332-334.
Das, G.D., Hallas, B.H., and Das, K.G. (1980). Transplantation of brain tissue in the brain of rat. I. Growth characteristics of neocortical transplants from embryos of different ages. Am J Anat *158*, 135-145.
Davidson, B.P., Kinder, S.J., Steiner, K., Schoenwolf, G.C., and Tam, P.P. (1999). Impact of node ablation on the morphogenesis of the body axis and the lateral asymmetry of the mouse embryo during early organogenesis. Dev Biol *211*, 11-26.
Davidson, D., Graham, E., Sime, C., and Hill, R. (1988). A gene with sequence similarity to Drosophila engrailed is expressed during the development of the neural tube and vertebrae in the mouse. Development *104*, 305-316.
Davis, C.A., and Joyner, A.L. (1988). Expression patterns of the homeo box-containing genes En-1 and En-2 and the proto-oncogene int-1 diverge during mouse development. Genes Dev *2*, 1736-1744.
Davis, C.A., Noble-Topham, S.E., Rossant, J., and Joyner, A.L. (1988). Expression of the homeo box-containing gene En-2 delineates a specific region of the developing mouse brain. Genes Dev *2*, 361-371.
De Ferrari, G.V., Chacon, M.A., Barria, M.I., Garrido, J.L., Godoy, J.A., Olivares, G., Reyes, A.E., Alvarez, A., Bronfman, M., and Inestrosa, N.C. (2003). Activation of Wnt signaling rescues neurodegeneration and behavioral impairments induced by beta-amyloid fibrils. Mol Psychiatry *8*, 195-208.
Deng, C.X., Wynshaw-Boris, A., Shen, M.M., Daugherty, C., Ornitz, D.M., and Leder, P. (1994). Murine FGFR-1 is required for early postimplantation growth and axial organization. Genes Dev *8*, 3045-3057.
Denley, A., Gymnopoulos, M., Kang, S., Mitchell, C., and Vogt, P.K. (2009). Requirement of phosphatidylinositol(3,4,5)trisphosphate in phosphatidylinositol 3-kinase-induced oncogenic transformation. Mol Cancer Res *7*, 1132-1138.
Dezawa, M., Kanno, H., Hoshino, M., Cho, H., Matsumoto, N., Itokazu, Y., Tajima, N., Yamada, H., Sawada, H., Ishikawa, H.*, et al.* (2004). Specific induction of neuronal cells from bone marrow stromal cells and application for autologous transplantation. J Clin Invest *113*, 1701-1710.
Di-Gregorio, A., Sancho, M., Stuckey, D.W., Crompton, L.A., Godwin, J., Mishina, Y., and Rodriguez, T.A. (2007). BMP signalling inhibits premature neural differentiation in the mouse embryo. Development *134*, 3359-3369.
Di Salvio, M., Di Giovannantonio, L.G., Acampora, D., Prosperi, R., Omodei, D., Prakash, N., Wurst, W., and Simeone, A. (2010a). Otx2 controls neuron subtype identity in ventral tegmental area and antagonizes vulnerability to MPTP. Nat Neurosci *13*, 1481-1488.
Di Salvio, M., Di Giovannantonio, L.G., Omodei, D., Acampora, D., and Simeone, A. (2010b). Otx2 expression is restricted to dopaminergic neurons of the ventral tegmental area in the adult brain. Int J Dev Biol *54*, 939-945.
Dionne, M.S., Skarnes, W.C., and Harland, R.M. (2001). Mutation and analysis of Dan, the founding member of the Dan family of transforming growth factor beta antagonists. Mol Cell Biol *21*, 636-643.

Doniach, T. (1995). Basic FGF as an inducer of anteroposterior neural pattern. Cell *83*, 1067-1070.
Dorsky, R.I., Moon, R.T., and Raible, D.W. (1998). Control of neural crest cell fate by the Wnt signalling pathway. Nature *396*, 370-373.
Doucet, G., Murata, Y., Brundin, P., Bosler, O., Mons, N., Geffard, M., Ouimet, C.C., and Bjorklund, A. (1989). Host afferents into intrastriatal transplants of fetal ventral mesencephalon. Exp Neurol *106*, 1-19.
Dunnett, S.B., Bjorklund, A., Schmidt, R.H., Stenevi, U., and Iversen, S.D. (1983). Intracerebral grafting of neuronal cell suspensions. V. Behavioural recovery in rats with bilateral 6-OHDA lesions following implantation of nigral cell suspensions. Acta Physiol Scand Suppl *522*, 39-47.
Dunnett, S.B., Bjorklund, A., Stenevi, U., and Iversen, S.D. (1981). Behavioural recovery following transplantation of substantia nigra in rats subjected to 6-OHDA lesions of the nigrostriatal pathway. I. Unilateral lesions. Brain Res *215*, 147-161.
Dunnett, S.B., Hernandez, T.D., Summerfield, A., Jones, G.H., and Arbuthnott, G. (1988). Graft-derived recovery from 6-OHDA lesions: specificity of ventral mesencephalic graft tissues. Exp Brain Res *71*, 411-424.
Dunnett, S.B., Whishaw, I.Q., Rogers, D.C., and Jones, G.H. (1987). Dopamine-rich grafts ameliorate whole body motor asymmetry and sensory neglect but not independent limb use in rats with 6-hydroxydopamine lesions. Brain Res *415*, 63-78.
Ebert, A.D., Yu, J., Rose, F.F., Jr., Mattis, V.B., Lorson, C.L., Thomson, J.A., and Svendsen, C.N. (2009). Induced pluripotent stem cells from a spinal muscular atrophy patient. Nature *457*, 277-280.
Eblaghie, M.C., Lunn, J.S., Dickinson, R.J., Munsterberg, A.E., Sanz-Ezquerro, J.J., Farrell, E.R., Mathers, J., Keyse, S.M., Storey, K., and Tickle, C. (2003). Negative feedback regulation of FGF signaling levels by Pyst1/MKP3 in chick embryos. Curr Biol *13*, 1009-1018.
Echelard, Y., Epstein, D.J., St-Jacques, B., Shen, L., Mohler, J., McMahon, J.A., and McMahon, A.P. (1993). Sonic hedgehog, a member of a family of putative signaling molecules, is implicated in the regulation of CNS polarity. Cell *75*, 1417-1430.
Echevarria, D., Vieira, C., Gimeno, L., and Martinez, S. (2003). Neuroepithelial secondary organizers and cell fate specification in the developing brain. Brain Res Brain Res Rev *43*, 179-191.
Eggan, K. (2007). Short-circuiting epiblast development. Cell Stem Cell *1*, 131-132.
Eimon, P.M., and Harland, R.M. (2001). Xenopus Dan, a member of the Dan gene family of BMP antagonists, is expressed in derivatives of the cranial and trunk neural crest. Mech Dev *107*, 187-189.
Eiraku, M., Watanabe, K., Matsuo-Takasaki, M., Kawada, M., Yonemura, S., Matsumura, M., Wataya, T., Nishiyama, A., Muguruma, K., and Sasai, Y. (2008). Self-organized formation of polarized cortical tissues from ESCs and its active manipulation by extrinsic signals. Cell Stem Cell *3*, 519-532.
Eivers, E., Fuentealba, L.C., and De Robertis, E.M. (2008). Integrating positional information at the level of Smad1/5/8. Curr Opin Genet Dev *18*, 304-310.
Eminli, S., Utikal, J., Arnold, K., Jaenisch, R., and Hochedlinger, K. (2008). Reprogramming of neural progenitor cells into induced pluripotent stem cells in the absence of exogenous Sox2 expression. Stem Cells *26*, 2467-2474.
Episkopou, V., Arkell, R., Timmons, P.M., Walsh, J.J., Andrew, R.L., and Swan, D. (2001). Induction of the mammalian node requires Arkadia function in the extraembryonic lineages. Nature *410*, 825-830.

Eswarakumar, V.P., Lax, I., and Schlessinger, J. (2005). Cellular signaling by fibroblast growth factor receptors. Cytokine Growth Factor Rev *16*, 139-149.
Evans, M.J., and Kaufman, M.H. (1981). Establishment in culture of pluripotential cells from mouse embryos. Nature *292*, 154-156.
Fainsod, A., Deissler, K., Yelin, R., Marom, K., Epstein, M., Pillemer, G., Steinbeisser, H., and Blum, M. (1997). The dorsalizing and neural inducing gene follistatin is an antagonist of BMP-4. Mech Dev *63*, 39-50.
Fayard, E., Xue, G., Parcellier, A., Bozulic, L., and Hemmings, B.A. (2010). Protein kinase B (PKB/Akt), a key mediator of the PI3K signaling pathway. Curr Top Microbiol Immunol *346*, 31-56.
Fedtsova, N., and Turner, E.E. (2001). Signals from the ventral midline and isthmus regulate the development of Brn3.0-expressing neurons in the midbrain. Mech Dev *105*, 129-144.
Feldman, B., Poueymirou, W., Papaioannou, V.E., DeChiara, T.M., and Goldfarb, M. (1995). Requirement of FGF-4 for postimplantation mouse development. Science *267*, 246-249.
Ferri, A.L., Lin, W., Mavromatakis, Y.E., Wang, J.C., Sasaki, H., Whitsett, J.A., and Ang, S.L. (2007). Foxa1 and Foxa2 regulate multiple phases of midbrain dopaminergic neuron development in a dosage-dependent manner. Development *134*, 2761-2769.
Finger, S., and Dunnett, S.B. (1989). Nimodipine enhances growth and vascularization of neural grafts. Exp Neurol *104*, 1-9.
Freed, W.J., Perlow, M.J., Karoum, F., Seiger, A., Olson, L., Hoffer, B.J., and Wyatt, R.J. (1980). Restoration of dopaminergic function by grafting of fetal rat substantia nigra to the caudate nucleus: long-term behavioral, biochemical, and histochemical studies. Ann Neurol *8*, 510-519.
Friling, S., Andersson, E., Thompson, L.H., Jonsson, M.E., Hebsgaard, J.B., Nanou, E., Alekseenko, Z., Marklund, U., Kjellander, S., Volakakis, N.*, et al.* (2009). Efficient production of mesencephalic dopamine neurons by Lmx1a expression in embryonic stem cells. Proc Natl Acad Sci U S A *106*, 7613-7618.
Fuccillo, M., Joyner, A.L., and Fishell, G. (2006). Morphogen to mitogen: the multiple roles of hedgehog signalling in vertebrate neural development. Nat Rev Neurosci *7*, 772-783.
Fuentealba, R.A., Farias, G., Scheu, J., Bronfman, M., Marzolo, M.P., and Inestrosa, N.C. (2004). Signal transduction during amyloid-beta-peptide neurotoxicity: role in Alzheimer disease. Brain Res Brain Res Rev *47*, 275-289.
Furthauer, M., Lin, W., Ang, S.L., Thisse, B., and Thisse, C. (2002). Sef is a feedback-induced antagonist of Ras/MAPK-mediated FGF signalling. Nat Cell Biol *4*, 170-174.
Furthauer, M., Reifers, F., Brand, M., Thisse, B., and Thisse, C. (2001). sprouty4 acts in vivo as a feedback-induced antagonist of FGF signaling in zebrafish. Development *128*, 2175-2186.
Furthauer, M., Thisse, B., and Thisse, C. (1999). Three different noggin genes antagonize the activity of bone morphogenetic proteins in the zebrafish embryo. Dev Biol *214*, 181-196.
Furusawa, T., Ohkoshi, K., Honda, C., Takahashi, S., and Tokunaga, T. (2004). Embryonic stem cells expressing both platelet endothelial cell adhesion molecule-1 and stage-specific embryonic antigen-1 differentiate predominantly into epiblast cells in a chimeric embryo. Biol Reprod *70*, 1452-1457.

Furuta, Y., Piston, D.W., and Hogan, B.L. (1997). Bone morphogenetic proteins (BMPs) as regulators of dorsal forebrain development. Development *124*, 2203-2212.
Gale, E., and Li, M. (2008). Midbrain dopaminergic neuron fate specification: Of mice and embryonic stem cells. Mol Brain *1*, 8.
Galleguillos, D., Fuentealba, J.A., Gomez, L.M., Saver, M., Gomez, A., Nash, K., Burger, C., Gysling, K., and Andres, M.E. (2010). Nurr1 regulates RET expression in dopamine neurons of adult rat midbrain. J Neurochem *114*, 1158-1167.
Gardner, A.M., Vaillancourt, R.R., Lange-Carter, C.A., and Johnson, G.L. (1994). MEK-1 phosphorylation by MEK kinase, Raf, and mitogen-activated protein kinase: analysis of phosphopeptides and regulation of activity. Mol Biol Cell *5*, 193-201.
Gardner, R.L. (1998). Contributions of blastocyst micromanipulation to the study of mammalian development. Bioessays *20*, 168-180.
Gaspard, N., Bouschet, T., Herpoel, A., Naeije, G., van den Ameele, J., and Vanderhaeghen, P. (2009). Generation of cortical neurons from mouse embryonic stem cells. Nat Protoc *4*, 1454-1463.
Gaspard, N., Bouschet, T., Hourez, R., Dimidschstein, J., Naeije, G., van den Ameele, J., Espuny-Camacho, I., Herpoel, A., Passante, L., Schiffmann, S.N.*, et al.* (2008). An intrinsic mechanism of corticogenesis from embryonic stem cells. Nature *455*, 351-357.
Gawantka, V., Pollet, N., Delius, H., Vingron, M., Pfister, R., Nitsch, R., Blumenstock, C., and Niehrs, C. (1998). Gene expression screening in Xenopus identifies molecular pathways, predicts gene function and provides a global view of embryonic patterning. Mech Dev *77*, 95-141.
Gennet, N., Gale, E., Nan, X., Farley, E., Takacs, K., Oberwallner, B., Chambers, D., and Li, M. (2011). Doublesex and mab-3-related transcription factor 5 promotes midbrain dopaminergic identity in pluripotent stem cells by enforcing a ventral-medial progenitor fate. Proc Natl Acad Sci U S A *108*, 9131-9136.
Giguere, V. (1999). Orphan nuclear receptors: from gene to function. Endocr Rev *20*, 689-725.
Giorgetti, A., Montserrat, N., Aasen, T., Gonzalez, F., Rodriguez-Piza, I., Vassena, R., Raya, A., Boue, S., Barrero, M.J., Corbella, B.A.*, et al.* (2009). Generation of induced pluripotent stem cells from human cord blood using OCT4 and SOX2. Cell Stem Cell *5*, 353-357.
Godsave, S.F., and Slack, J.M. (1989). Clonal analysis of mesoderm induction in Xenopus laevis. Dev Biol *134*, 486-490.
Gogoi, R.N., Schubert, F.R., Martinez-Barbera, J.P., Acampora, D., Simeone, A., and Lumsden, A. (2002). The paired-type homeobox gene Dmbx1 marks the midbrain and pretectum. Mech Dev *114*, 213-217.
Goldfarb, M., Bates, B., Drucker, B., Hardin, J., and Haub, O. (1991). Expression and possible functions of the FGF-5 gene. Ann N Y Acad Sci *638*, 38-52.
Gomez-Skarmeta, J., de La Calle-Mustienes, E., and Modolell, J. (2001). The Wnt-activated Xiro1 gene encodes a repressor that is essential for neural development and downregulates Bmp4. Development *128*, 551-560.
Greber, B., Wu, G., Bernemann, C., Joo, J.Y., Han, D.W., Ko, K., Tapia, N., Sabour, D., Sterneckert, J., Tesar, P.*, et al.* (2010). Conserved and divergent roles of FGF signaling in mouse epiblast stem cells and human embryonic stem cells. Cell Stem Cell *6*, 215-226.

Groom, L.A., Sneddon, A.A., Alessi, D.R., Dowd, S., and Keyse, S.M. (1996). Differential regulation of the MAP, SAP and RK/p38 kinases by Pyst1, a novel cytosolic dual-specificity phosphatase. EMBO J *15*, 3621-3632.
Grunz, H., and Tacke, L. (1989). Neural differentiation of Xenopus laevis ectoderm takes place after disaggregation and delayed reaggregation without inducer. Cell Differ Dev *28*, 211-217.
Guillemot, F., and Joyner, A.L. (1993). Dynamic expression of the murine Achaete-Scute homologue Mash-1 in the developing nervous system. Mech Dev *42*, 171-185.
Guo, C., Qiu, H.Y., Huang, Y., Chen, H., Yang, R.Q., Chen, S.D., Johnson, R.L., Chen, Z.F., and Ding, Y.Q. (2007). Lmx1b is essential for Fgf8 and Wnt1 expression in the isthmic organizer during tectum and cerebellum development in mice. Development *134*, 317-325.
Guo, C., Qiu, H.Y., Shi, M., Huang, Y., Johnson, R.L., Rubinstein, M., Chen, S.D., and Ding, Y.Q. (2008). Lmx1b-controlled isthmic organizer is essential for development of midbrain dopaminergic neurons. J Neurosci *28*, 14097-14106.
Guo, G., Yang, J., Nichols, J., Hall, J.S., Eyres, I., Mansfield, W., and Smith, A. (2009). Klf4 reverts developmentally programmed restriction of ground state pluripotency. Development *136*, 1063-1069.
Hadari, Y.R., Gotoh, N., Kouhara, H., Lax, I., and Schlessinger, J. (2001). Critical role for the docking-protein FRS2 alpha in FGF receptor-mediated signal transduction pathways. Proc Natl Acad Sci U S A *98*, 8578-8583.
Hall, A.C., Lucas, F.R., and Salinas, P.C. (2000). Axonal remodeling and synaptic differentiation in the cerebellum is regulated by WNT-7a signaling. Cell *100*, 525-535.
Han, D.W., Tapia, N., Joo, J.Y., Greber, B., Arauzo-Bravo, M.J., Bernemann, C., Ko, K., Wu, G., Stehling, M., Do, J.T.*, et al.* (2010). Epiblast stem cell subpopulations represent mouse embryos of distinct pregastrulation stages. Cell *143*, 617-627.
Hanafusa, H., Torii, S., Yasunaga, T., and Nishida, E. (2002). Sprouty1 and Sprouty2 provide a control mechanism for the Ras/MAPK signalling pathway. Nat Cell Biol *4*, 850-858.
Hansen, C.S., Marion, C.D., Steele, K., George, S., and Smith, W.C. (1997). Direct neural induction and selective inhibition of mesoderm and epidermis inducers by Xnr3. Development *124*, 483-492.
Hargus, G., Cooper, O., Deleidi, M., Levy, A., Lee, K., Marlow, E., Yow, A., Soldner, F., Hockemeyer, D., Hallett, P.J.*, et al.* (2010). Differentiated Parkinson patient-derived induced pluripotent stem cells grow in the adult rodent brain and reduce motor asymmetry in Parkinsonian rats. Proc Natl Acad Sci U S A *107*, 15921-15926.
Hatta, K., and Takahashi, Y. (1996). Secondary axis induction by heterospecific organizers in zebrafish. Dev Dyn *205*, 183-195.
Haub, O., and Goldfarb, M. (1991). Expression of the fibroblast growth factor-5 gene in the mouse embryo. Development *112*, 397-406.
Hay, D.C., Sutherland, L., Clark, J., and Burdon, T. (2004). Oct-4 knockdown induces similar patterns of endoderm and trophoblast differentiation markers in human and mouse embryonic stem cells. Stem Cells *22*, 225-235.
Hayashi, K., Lopes, S.M., Tang, F., and Surani, M.A. (2008). Dynamic equilibrium and heterogeneity of mouse pluripotent stem cells with distinct functional and epigenetic states. Cell Stem Cell *3*, 391-401.

Hebert, J.M., Basilico, C., Goldfarb, M., Haub, O., and Martin, G.R. (1990). Isolation of cDNAs encoding four mouse FGF family members and characterization of their expression patterns during embryogenesis. Dev Biol *138*, 454-463.
Hebert, J.M., Boyle, M., and Martin, G.R. (1991). mRNA localization studies suggest that murine FGF-5 plays a role in gastrulation. Development *112*, 407-415.
Hebert, J.M., and McConnell, S.K. (2000). Targeting of cre to the Foxg1 (BF-1) locus mediates loxP recombination in the telencephalon and other developing head structures. Dev Biol *222*, 296-306.
Hebert, J.M., Rosenquist, T., Gotz, J., and Martin, G.R. (1994). FGF5 as a regulator of the hair growth cycle: evidence from targeted and spontaneous mutations. Cell *78*, 1017-1025.
Hemmati-Brivanlou, A., Kelly, O.G., and Melton, D.A. (1994). Follistatin, an antagonist of activin, is expressed in the Spemann organizer and displays direct neuralizing activity. Cell *77*, 283-295.
Heuer, A., Smith, G.A., Lelos, M.J., Lane, E.L., and Dunnett, S.B. (2012). Unilateral nigrostriatal 6-hydroxydopamine lesions in mice I: motor impairments identify extent of dopamine depletion at three different lesion sites. Behav Brain Res *228*, 30-43.
Hoffman, L.M., and Carpenter, M.K. (2005). Characterization and culture of human embryonic stem cells. Nat Biotechnol *23*, 699-708.
Holowacz, T., and Sokol, S. (1999). FGF is required for posterior neural patterning but not for neural induction. Dev Biol *205*, 296-308.
Hooper, M., Hardy, K., Handyside, A., Hunter, S., and Monk, M. (1987). HPRT-deficient (Lesch-Nyhan) mouse embryos derived from germline colonization by cultured cells. Nature *326*, 292-295.
Houart, C., Westerfield, M., and Wilson, S.W. (1998). A small population of anterior cells patterns the forebrain during zebrafish gastrulation. Nature *391*, 788-792.
Hsu, D.R., Economides, A.N., Wang, X., Eimon, P.M., and Harland, R.M. (1998). The Xenopus dorsalizing factor Gremlin identifies a novel family of secreted proteins that antagonize BMP activities. Mol Cell *1*, 673-683.
Hudson, C., and Lemaire, P. (2001). Induction of anterior neural fates in the ascidian Ciona intestinalis. Mech Dev *100*, 189-203.
Hynes, M., Porter, J.A., Chiang, C., Chang, D., Tessier-Lavigne, M., Beachy, P.A., and Rosenthal, A. (1995). Induction of midbrain dopaminergic neurons by Sonic hedgehog. Neuron *15*, 35-44.
Hynes, M., Stone, D.M., Dowd, M., Pitts-Meek, S., Goddard, A., Gurney, A., and Rosenthal, A. (1997). Control of cell pattern in the neural tube by the zinc finger transcription factor and oncogene Gli-1. Neuron *19*, 15-26.
Inazawa, T., Okamura, Y., and Takahashi, K. (1998). Basic fibroblast growth factor induction of neuronal ion channel expression in ascidian ectodermal blastomeres. J Physiol *511 (Pt 2)*, 347-359.
Irving, C., and Mason, I. (2000). Signalling by FGF8 from the isthmus patterns anterior hindbrain and establishes the anterior limit of Hox gene expression. Development *127*, 177-186.
Itoh, N., and Ornitz, D.M. (2004). Evolution of the Fgf and Fgfr gene families. Trends Genet *20*, 563-569.
Itoh, N., and Ornitz, D.M. (2008). Functional evolutionary history of the mouse Fgf gene family. Dev Dyn *237*, 18-27.

Jeong, Y., Leskow, F.C., El-Jaick, K., Roessler, E., Muenke, M., Yocum, A., Dubourg, C., Li, X., Geng, X., Oliver, G.*, et al.* (2008). Regulation of a remote Shh forebrain enhancer by the Six3 homeoprotein. Nat Genet *40*, 1348-1353.
Jho, E.H., Zhang, T., Domon, C., Joo, C.K., Freund, J.N., and Costantini, F. (2002). Wnt/beta-catenin/Tcf signaling induces the transcription of Axin2, a negative regulator of the signaling pathway. Mol Cell Biol *22*, 1172-1183.
Joksimovic, M., Yun, B.A., Kittappa, R., Anderegg, A.M., Chang, W.W., Taketo, M.M., McKay, R.D., and Awatramani, R.B. (2009). Wnt antagonism of Shh facilitates midbrain floor plate neurogenesis. Nat Neurosci *12*, 125-131.
Joyner, A.L., Liu, A., and Millet, S. (2000). Otx2, Gbx2 and Fgf8 interact to position and maintain a mid-hindbrain organizer. Curr Opin Cell Biol *12*, 736-741.
Kadkhodaei, B., Ito, T., Joodmardi, E., Mattsson, B., Rouillard, C., Carta, M., Muramatsu, S., Sumi-Ichinose, C., Nomura, T., Metzger, D.*, et al.* (2009). Nurr1 is required for maintenance of maturing and adult midbrain dopamine neurons. J Neurosci *29*, 15923-15932.
Kato, R., Nonami, A., Taketomi, T., Wakioka, T., Kuroiwa, A., Matsuda, Y., and Yoshimura, A. (2003). Molecular cloning of mammalian Spred-3 which suppresses tyrosine kinase-mediated Erk activation. Biochem Biophys Res Commun *302*, 767-772.
Kaufman, M.H., Robertson, E.J., Handyside, A.H., and Evans, M.J. (1983). Establishment of pluripotential cell lines from haploid mouse embryos. J Embryol Exp Morphol *73*, 249-261.
Kawakami, Y., Rodriguez-Leon, J., Koth, C.M., Buscher, D., Itoh, T., Raya, A., Ng, J.K., Esteban, C.R., Takahashi, S., Henrique, D.*, et al.* (2003). MKP3 mediates the cellular response to FGF8 signalling in the vertebrate limb. Nat Cell Biol *5*, 513-519.
Kawasaki, H., Mizuseki, K., Nishikawa, S., Kaneko, S., Kuwana, Y., Nakanishi, S., Nishikawa, S.I., and Sasai, Y. (2000). Induction of midbrain dopaminergic neurons from ES cells by stromal cell-derived inducing activity. Neuron *28*, 31-40.
Kawasaki, H., Suemori, H., Mizuseki, K., Watanabe, K., Urano, F., Ichinose, H., Haruta, M., Takahashi, M., Yoshikawa, K., Nishikawa, S.*, et al.* (2002). Generation of dopaminergic neurons and pigmented epithelia from primate ES cells by stromal cell-derived inducing activity. Proc Natl Acad Sci U S A *99*, 1580-1585.
Kele, J., Simplicio, N., Ferri, A.L., Mira, H., Guillemot, F., Arenas, E., and Ang, S.L. (2006). Neurogenin 2 is required for the development of ventral midbrain dopaminergic neurons. Development *133*, 495-505.
Keller, G. (2005). Embryonic stem cell differentiation: emergence of a new era in biology and medicine. Genes Dev *19*, 1129-1155.
Keller, G.M. (1995). In vitro differentiation of embryonic stem cells. Curr Opin Cell Biol *7*, 862-869.
Kengaku, M., and Okamoto, H. (1995). bFGF as a possible morphogen for the anteroposterior axis of the central nervous system in Xenopus. Development *121*, 3121-3130.
Khokha, M.K., Hsu, D., Brunet, L.J., Dionne, M.S., and Harland, R.M. (2003). Gremlin is the BMP antagonist required for maintenance of Shh and Fgf signals during limb patterning. Nat Genet *34*, 303-307.
Kiecker, C., and Lumsden, A. (2004). Hedgehog signaling from the ZLI regulates diencephalic regional identity. Nat Neurosci *7*, 1242-1249.

Kim, H.H., Sierke, S.L., and Koland, J.G. (1994). Epidermal growth factor-dependent association of phosphatidylinositol 3-kinase with the erbB3 gene product. J Biol Chem *269*, 24747-24755.
Kim, H.H., Vijapurkar, U., Hellyer, N.J., Bravo, D., and Koland, J.G. (1998). Signal transduction by epidermal growth factor and heregulin via the kinase-deficient ErbB3 protein. Biochem J *334 (Pt 1)*, 189-195.
Kim, J.B., Zaehres, H., Wu, G., Gentile, L., Ko, K., Sebastiano, V., Arauzo-Bravo, M.J., Ruau, D., Han, D.W., Zenke, M.*, et al.* (2008). Pluripotent stem cells induced from adult neural stem cells by reprogramming with two factors. Nature *454*, 646-650.
Kim, J.H., Auerbach, J.M., Rodriguez-Gomez, J.A., Velasco, I., Gavin, D., Lumelsky, N., Lee, S.H., Nguyen, J., Sanchez-Pernaute, R., Bankiewicz, K.*, et al.* (2002). Dopamine neurons derived from embryonic stem cells function in an animal model of Parkinson's disease. Nature *418*, 50-56.
Kim, J.Y., Koh, H.C., Lee, J.Y., Chang, M.Y., Kim, Y.C., Chung, H.Y., Son, H., Lee, Y.S., Studer, L., McKay, R.*, et al.* (2003). Dopaminergic neuronal differentiation from rat embryonic neural precursors by Nurr1 overexpression. J Neurochem *85*, 1443-1454.
Kintner, C.R., and Dodd, J. (1991). Hensen's node induces neural tissue in Xenopus ectoderm. Implications for the action of the organizer in neural induction. Development *113*, 1495-1505.
Kittappa, R., Chang, W.W., Awatramani, R.B., and McKay, R.D. (2007). The foxa2 gene controls the birth and spontaneous degeneration of dopamine neurons in old age. PLoS Biol *5*, e325.
Klingensmith, J., Ang, S.L., Bachiller, D., and Rossant, J. (1999). Neural induction and patterning in the mouse in the absence of the node and its derivatives. Dev Biol *216*, 535-549.
Klint, P., and Claesson-Welsh, L. (1999). Signal transduction by fibroblast growth factor receptors. Front Biosci *4*, D165-177.
Kodama, H., Hagiwara, H., Sudo, H., Amagai, Y., Yokota, T., Arai, N., and Kitamura, Y. (1986). MC3T3-G2/PA6 preadipocytes support in vitro proliferation of hemopoietic stem cells through a mechanism different from that of interleukin 3. J Cell Physiol *129*, 20-26.
Kouhara, H., Hadari, Y.R., Spivak-Kroizman, T., Schilling, J., Bar-Sagi, D., Lax, I., and Schlessinger, J. (1997). A lipid-anchored Grb2-binding protein that links FGF-receptor activation to the Ras/MAPK signaling pathway. Cell *89*, 693-702.
Kovalenko, D., Yang, X., Chen, P.Y., Nadeau, R.J., Zubanova, O., Pigeon, K., and Friesel, R. (2006). A role for extracellular and transmembrane domains of Sef in Sef-mediated inhibition of FGF signaling. Cell Signal *18*, 1958-1966.
Kovalenko, D., Yang, X., Nadeau, R.J., Harkins, L.K., and Friesel, R. (2003). Sef inhibits fibroblast growth factor signaling by inhibiting FGFR1 tyrosine phosphorylation and subsequent ERK activation. J Biol Chem *278*, 14087-14091.
Kramer, S., Okabe, M., Hacohen, N., Krasnow, M.A., and Hiromi, Y. (1999). Sprouty: a common antagonist of FGF and EGF signaling pathways in Drosophila. Development *126*, 2515-2525.
Kriks, S., Shim, J.W., Piao, J., Ganat, Y.M., Wakeman, D.R., Xie, Z., Carrillo-Reid, L., Auyeung, G., Antonacci, C., Buch, A.*, et al.* (2011). Dopamine neurons derived from human ES cells efficiently engraft in animal models of Parkinson's disease. Nature *480*, 547-551.

Krylova, O., Herreros, J., Cleverley, K.E., Ehler, E., Henriquez, J.P., Hughes, S.M., and Salinas, P.C. (2002). WNT-3, expressed by motoneurons, regulates terminal arborization of neurotrophin-3-responsive spinal sensory neurons. Neuron *35*, 1043-1056.
Kudoh, T., Concha, M.L., Houart, C., Dawid, I.B., and Wilson, S.W. (2004). Combinatorial Fgf and Bmp signalling patterns the gastrula ectoderm into prospective neural and epidermal domains. Development *131*, 3581-3592.
Kudoh, T., Tsang, M., Hukriede, N.A., Chen, X., Dedekian, M., Clarke, C.J., Kiang, A., Schultz, S., Epstein, J.A., Toyama, R.*, et al.* (2001). A gene expression screen in zebrafish embryogenesis. Genome Res *11*, 1979-1987.
Kunath, T., Saba-El-Leil, M.K., Almousailleakh, M., Wray, J., Meloche, S., and Smith, A. (2007). FGF stimulation of the Erk1/2 signalling cascade triggers transition of pluripotent embryonic stem cells from self-renewal to lineage commitment. Development *134*, 2895-2902.
L'Episcopo, F., Serapide, M.F., Tirolo, C., Testa, N., Caniglia, S., Morale, M.C., Pluchino, S., and Marchetti, B. (2011). A Wnt1 regulated Frizzled-1/beta-Catenin signaling pathway as a candidate regulatory circuit controlling mesencephalic dopaminergic neuron-astrocyte crosstalk: Therapeutical relevance for neuron survival and neuroprotection. Mol Neurodegener *6*, 49.
Lahti, L., Peltopuro, P., Piepponen, T.P., and Partanen, J. (2012). Cell-autonomous FGF signaling regulates anteroposterior patterning and neuronal differentiation in the mesodiencephalic dopaminergic progenitor domain. Development *139*, 894-905.
Lahti, L., Saarimaki-Vire, J., Rita, H., and Partanen, J. (2011). FGF signaling gradient maintains symmetrical proliferative divisions of midbrain neuronal progenitors. Dev Biol *349*, 270-282.
Lamb, T.M., and Harland, R.M. (1995). Fibroblast growth factor is a direct neural inducer, which combined with noggin generates anterior-posterior neural pattern. Development *121*, 3627-3636.
Lamb, T.M., Knecht, A.K., Smith, W.C., Stachel, S.E., Economides, A.N., Stahl, N., Yancopolous, G.D., and Harland, R.M. (1993). Neural induction by the secreted polypeptide noggin. Science *262*, 713-718.
Lavado, A., Lagutin, O.V., and Oliver, G. (2008). Six3 inactivation causes progressive caudalization and aberrant patterning of the mammalian diencephalon. Development *135*, 441-450.
Lavoie, J.N., L'Allemain, G., Brunet, A., Muller, R., and Pouyssegur, J. (1996). Cyclin D1 expression is regulated positively by the p42/p44MAPK and negatively by the p38/HOGMAPK pathway. J Biol Chem *271*, 20608-20616.
Lee, G., Papapetrou, E.P., Kim, H., Chambers, S.M., Tomishima, M.J., Fasano, C.A., Ganat, Y.M., Menon, J., Shimizu, F., Viale, A.*, et al.* (2009). Modelling pathogenesis and treatment of familial dysautonomia using patient-specific iPSCs. Nature *461*, 402-406.
Lee, H.S., Bae, E.J., Yi, S.H., Shim, J.W., Jo, A.Y., Kang, J.S., Yoon, E.H., Rhee, Y.H., Park, C.H., Koh, H.C.*, et al.* (2010). Foxa2 and Nurr1 synergistically yield A9 nigral dopamine neurons exhibiting improved differentiation, function, and cell survival. Stem Cells *28*, 501-512.
Lee, K.J., Dietrich, P., and Jessell, T.M. (2000a). Genetic ablation reveals that the roof plate is essential for dorsal interneuron specification. Nature *403*, 734-740.
Lee, K.J., and Jessell, T.M. (1999). The specification of dorsal cell fates in the vertebrate central nervous system. Annu Rev Neurosci *22*, 261-294.

Lee, S.H., Lumelsky, N., Studer, L., Auerbach, J.M., and McKay, R.D. (2000b). Efficient generation of midbrain and hindbrain neurons from mouse embryonic stem cells. Nat Biotechnol *18*, 675-679.
Lee, S.M., Danielian, P.S., Fritzsch, B., and McMahon, A.P. (1997). Evidence that FGF8 signalling from the midbrain-hindbrain junction regulates growth and polarity in the developing midbrain. Development *124*, 959-969.
Lendahl, U., Zimmerman, L.B., and McKay, R.D. (1990). CNS stem cells express a new class of intermediate filament protein. Cell *60*, 585-595.
Li, X.J., Du, Z.W., Zarnowska, E.D., Pankratz, M., Hansen, L.O., Pearce, R.A., and Zhang, S.C. (2005). Specification of motoneurons from human embryonic stem cells. Nat Biotechnol *23*, 215-221.
Lin, W., Furthauer, M., Thisse, B., Thisse, C., Jing, N., and Ang, S.L. (2002). Cloning of the mouse Sef gene and comparative analysis of its expression with Fgf8 and Spry2 during embryogenesis. Mech Dev *113*, 163-168.
Lin, W., Metzakopian, E., Mavromatakis, Y.E., Gao, N., Balaskas, N., Sasaki, H., Briscoe, J., Whitsett, J.A., Goulding, M., Kaestner, K.H.*, et al.* (2009). Foxa1 and Foxa2 function both upstream of and cooperatively with Lmx1a and Lmx1b in a feedforward loop promoting mesodiencephalic dopaminergic neuron development. Dev Biol *333*, 386-396.
Lindvall, O., and Bjorklund, A. (1989). Transplantation strategies in the treatment of Parkinson's disease: experimental basis and clinical trials. Acta Neurol Scand Suppl *126*, 197-210.
Liu, A., and Joyner, A.L. (2001). EN and GBX2 play essential roles downstream of FGF8 in patterning the mouse mid/hindbrain region. Development *128*, 181-191.
Liu, A., Li, J.Y., Bromleigh, C., Lao, Z., Niswander, L.A., and Joyner, A.L. (2003). FGF17b and FGF18 have different midbrain regulatory properties from FGF8b or activated FGF receptors. Development *130*, 6175-6185.
Liu, A., Losos, K., and Joyner, A.L. (1999). FGF8 can activate Gbx2 and transform regions of the rostral mouse brain into a hindbrain fate. Development *126*, 4827-4838.
Liu, Y., Helms, A.W., and Johnson, J.E. (2004). Distinct activities of Msx1 and Msx3 in dorsal neural tube development. Development *131*, 1017-1028.
Logan, C.Y., and Nusse, R. (2004). The Wnt signaling pathway in development and disease. Annu Rev Cell Dev Biol *20*, 781-810.
Lowenstein, E.J., Daly, R.J., Batzer, A.G., Li, W., Margolis, B., Lammers, R., Ullrich, A., Skolnik, E.Y., Bar-Sagi, D., and Schlessinger, J. (1992). The SH2 and SH3 domain-containing protein GRB2 links receptor tyrosine kinases to ras signaling. Cell *70*, 431-442.
Lun, K., and Brand, M. (1998). A series of no isthmus (noi) alleles of the zebrafish pax2.1 gene reveals multiple signaling events in development of the midbrain-hindbrain boundary. Development *125*, 3049-3062.
Madrazo, I., Leon, V., Torres, C., Aguilera, M.C., Varela, G., Alvarez, F., Fraga, A., Drucker-Colin, R., Ostrosky, F., Skurovich, M.*, et al.* (1988). Transplantation of fetal substantia nigra and adrenal medulla to the caudate nucleus in two patients with Parkinson's disease. N Engl J Med *318*, 51.
Maherali, N., Sridharan, R., Xie, W., Utikal, J., Eminli, S., Arnold, K., Stadtfeld, M., Yachechko, R., Tchieu, J., Jaenisch, R.*, et al.* (2007). Directly reprogrammed fibroblasts show global epigenetic remodeling and widespread tissue contribution. Cell Stem Cell *1*, 55-70.

Mahmood, R., Bresnick, J., Hornbruch, A., Mahony, C., Morton, N., Colquhoun, K., Martin, P., Lumsden, A., Dickson, C., and Mason, I. (1995). A role for FGF-8 in the initiation and maintenance of vertebrate limb bud outgrowth. Curr Biol *5*, 797-806.
Mailleux, A.A., Tefft, D., Ndiaye, D., Itoh, N., Thiery, J.P., Warburton, D., and Bellusci, S. (2001). Evidence that SPROUTY2 functions as an inhibitor of mouse embryonic lung growth and morphogenesis. Mech Dev *102*, 81-94.
Mansour, S.L., Goddard, J.M., and Capecchi, M.R. (1993). Mice homozygous for a targeted disruption of the proto-oncogene int-2 have developmental defects in the tail and inner ear. Development *117*, 13-28.
Marchal, L., Luxardi, G., Thome, V., and Kodjabachian, L. (2009). BMP inhibition initiates neural induction via FGF signaling and Zic genes. Proc Natl Acad Sci U S A *106*, 17437-17442.
Marchetto, M.C., Carromeu, C., Acab, A., Yu, D., Yeo, G.W., Mu, Y., Chen, G., Gage, F.H., and Muotri, A.R. (2010). A model for neural development and treatment of Rett syndrome using human induced pluripotent stem cells. Cell *143*, 527-539.
Marin, F., and Puelles, L. (1994). Patterning of the embryonic avian midbrain after experimental inversions: a polarizing activity from the isthmus. Dev Biol *163*, 19-37.
Marshall, M.S. (1995). Ras target proteins in eukaryotic cells. FASEB J *9*, 1311-1318.
Martinez-Barbera, J.P., and Beddington, R.S. (2001). Getting your head around Hex and Hesx1: forebrain formation in mouse. Int J Dev Biol *45*, 327-336.
Martinez, S., Crossley, P.H., Cobos, I., Rubenstein, J.L., and Martin, G.R. (1999). FGF8 induces formation of an ectopic isthmic organizer and isthmocerebellar development via a repressive effect on Otx2 expression. Development *126*, 1189-1200.
Martinez, S., Wassef, M., and Alvarado-Mallart, R.M. (1991). Induction of a mesencephalic phenotype in the 2-day-old chick prosencephalon is preceded by the early expression of the homeobox gene en. Neuron *6*, 971-981.
Maruoka, Y., Ohbayashi, N., Hoshikawa, M., Itoh, N., Hogan, B.L., and Furuta, Y. (1998). Comparison of the expression of three highly related genes, Fgf8, Fgf17 and Fgf18, in the mouse embryo. Mech Dev *74*, 175-177.
Matin, M.M., Walsh, J.R., Gokhale, P.J., Draper, J.S., Bahrami, A.R., Morton, I., Moore, H.D., and Andrews, P.W. (2004). Specific knockdown of Oct4 and beta2-microglobulin expression by RNA interference in human embryonic stem cells and embryonic carcinoma cells. Stem Cells *22*, 659-668.
Matsuda, T., Nakamura, T., Nakao, K., Arai, T., Katsuki, M., Heike, T., and Yokota, T. (1999). STAT3 activation is sufficient to maintain an undifferentiated state of mouse embryonic stem cells. EMBO J *18*, 4261-4269.
Matsuo, I., Kuratani, S., Kimura, C., Takeda, N., and Aizawa, S. (1995). Mouse Otx2 functions in the formation and patterning of rostral head. Genes Dev *9*, 2646-2658.
Mavromatakis, Y.E., Lin, W., Metzakopian, E., Ferri, A.L., Yan, C.H., Sasaki, H., Whisett, J., and Ang, S.L. (2010). Foxa1 and Foxa2 positively and negatively regulate Shh signalling to specify ventral midbrain progenitor identity. Mech Dev *128*, 90-103.
Maxwell, S.L., Ho, H.Y., Kuehner, E., Zhao, S., and Li, M. (2005). Pitx3 regulates tyrosine hydroxylase expression in the substantia nigra and identifies a subgroup of mesencephalic dopaminergic progenitor neurons during mouse development. Dev Biol *282*, 467-479.

McMahon, A.P., and Bradley, A. (1990). The Wnt-1 (int-1) proto-oncogene is required for development of a large region of the mouse brain. Cell *62*, 1073-1085.
McMahon, A.P., Joyner, A.L., Bradley, A., and McMahon, J.A. (1992). The midbrain-hindbrain phenotype of Wnt-1-/Wnt-1- mice results from stepwise deletion of engrailed-expressing cells by 9.5 days postcoitum. Cell *69*, 581-595.
McMahon, J.A., Takada, S., Zimmerman, L.B., Fan, C.M., Harland, R.M., and McMahon, A.P. (1998). Noggin-mediated antagonism of BMP signaling is required for growth and patterning of the neural tube and somite. Genes Dev *12*, 1438-1452.
Megason, S.G., and McMahon, A.P. (2002). A mitogen gradient of dorsal midline Wnts organizes growth in the CNS. Development *129*, 2087-2098.
Mendez, I., Sanchez-Pernaute, R., Cooper, O., Vinuela, A., Ferrari, D., Bjorklund, L., Dagher, A., and Isacson, O. (2005). Cell type analysis of functional fetal dopamine cell suspension transplants in the striatum and substantia nigra of patients with Parkinson's disease. Brain *128*, 1498-1510.
Meyers, E.N., Lewandoski, M., and Martin, G.R. (1998). An Fgf8 mutant allelic series generated by Cre- and Flp-mediated recombination. Nat Genet *18*, 136-141.
Millet, S., Bloch-Gallego, E., Simeone, A., and Alvarado-Mallart, R.M. (1996). The caudal limit of Otx2 gene expression as a marker of the midbrain/hindbrain boundary: a study using in situ hybridisation and chick/quail homotopic grafts. Development *122*, 3785-3797.
Millet, S., Campbell, K., Epstein, D.J., Losos, K., Harris, E., and Joyner, A.L. (1999). A role for Gbx2 in repression of Otx2 and positioning the mid/hindbrain organizer. Nature *401*, 161-164.
Minowada, G., Jarvis, L.A., Chi, C.L., Neubuser, A., Sun, X., Hacohen, N., Krasnow, M.A., and Martin, G.R. (1999). Vertebrate Sprouty genes are induced by FGF signaling and can cause chondrodysplasia when overexpressed. Development *126*, 4465-4475.
Mishima, Y., Lindgren, A.G., Chizhikov, V.V., Johnson, R.L., and Millen, K.J. (2009). Overlapping function of Lmx1a and Lmx1b in anterior hindbrain roof plate formation and cerebellar growth. J Neurosci *29*, 11377-11384.
Mohammadi, M., Dionne, C.A., Li, W., Li, N., Spivak, T., Honegger, A.M., Jaye, M., and Schlessinger, J. (1992). Point mutation in FGF receptor eliminates phosphatidylinositol hydrolysis without affecting mitogenesis. Nature *358*, 681-684.
Mohammadi, M., Honegger, A.M., Rotin, D., Fischer, R., Bellot, F., Li, W., Dionne, C.A., Jaye, M., Rubinstein, M., and Schlessinger, J. (1991). A tyrosine-phosphorylated carboxy-terminal peptide of the fibroblast growth factor receptor (Flg) is a binding site for the SH2 domain of phospholipase C-gamma 1. Mol Cell Biol *11*, 5068-5078.
Mukhida, K., Baker, K.A., Sadi, D., and Mendez, I. (2001). Enhancement of sensorimotor behavioral recovery in hemiparkinsonian rats with intrastriatal, intranigral, and intrasubthalamic nucleus dopaminergic transplants. J Neurosci *21*, 3521-3530.
Mukhopadhyay, M., Shtrom, S., Rodriguez-Esteban, C., Chen, L., Tsukui, T., Gomer, L., Dorward, D.W., Glinka, A., Grinberg, A., Huang, S.P.*, et al.* (2001). Dickkopf1 is required for embryonic head induction and limb morphogenesis in the mouse. Dev Cell *1*, 423-434.
Munoz-Sanjuan, I., and Brivanlou, A.H. (2002). Neural induction, the default model and embryonic stem cells. Nat Rev Neurosci *3*, 271-280.

Murashov, A.K., Pak, E.S., Hendricks, W.A., Owensby, J.P., Sierpinski, P.L., Tatko, L.M., and Fletcher, P.L. (2005). Directed differentiation of embryonic stem cells into dorsal interneurons. FASEB J *19*, 252-254.
Murray, J.T., Campbell, D.G., Morrice, N., Auld, G.C., Shpiro, N., Marquez, R., Peggie, M., Bain, J., Bloomberg, G.B., Grahammer, F.*, et al.* (2004). Exploitation of KESTREL to identify NDRG family members as physiological substrates for SGK1 and GSK3. Biochem J *384*, 477-488.
Najm, F.J., Chenoweth, J.G., Anderson, P.D., Nadeau, J.H., Redline, R.W., McKay, R.D., and Tesar, P.J. (2011). Isolation of epiblast stem cells from preimplantation mouse embryos. Cell Stem Cell *8*, 318-325.
Nakatani, T., Kumai, M., Mizuhara, E., Minaki, Y., and Ono, Y. (2010). Lmx1a and Lmx1b cooperate with Foxa2 to coordinate the specification of dopaminergic neurons and control of floor plate cell differentiation in the developing mesencephalon. Dev Biol *339*, 101-113.
Nichols, J., and Smith, A. (2009). Naive and primed pluripotent states. Cell Stem Cell *4*, 487-492.
Nikkhah, G., Bentlage, C., Cunningham, M.G., and Bjorklund, A. (1994). Intranigral fetal dopamine grafts induce behavioral compensation in the rat Parkinson model. J Neurosci *14*, 3449-3461.
Niswander, L., and Martin, G.R. (1992). Fgf-4 expression during gastrulation, myogenesis, limb and tooth development in the mouse. Development *114*, 755-768.
Niwa, H., Burdon, T., Chambers, I., and Smith, A. (1998). Self-renewal of pluripotent embryonic stem cells is mediated via activation of STAT3. Genes Dev *12*, 2048-2060.
Ohtoshi, A., and Behringer, R.R. (2004). Neonatal lethality, dwarfism, and abnormal brain development in Dmbx1 mutant mice. Mol Cell Biol *24*, 7548-7558.
Oki, S., Kitajima, K., and Meno, C. (2010). Dissecting the role of Fgf signaling during gastrulation and left-right axis formation in mouse embryos using chemical inhibitors. Dev Dyn *239*, 1768-1778.
Okita, K., Ichisaka, T., and Yamanaka, S. (2007). Generation of germline-competent induced pluripotent stem cells. Nature *448*, 313-317.
Omodei, D., Acampora, D., Mancuso, P., Prakash, N., Di Giovannantonio, L.G., Wurst, W., and Simeone, A. (2008). Anterior-posterior graded response to Otx2 controls proliferation and differentiation of dopaminergic progenitors in the ventral mesencephalon. Development *135*, 3459-3470.
Ong, S.H., Guy, G.R., Hadari, Y.R., Laks, S., Gotoh, N., Schlessinger, J., and Lax, I. (2000). FRS2 proteins recruit intracellular signaling pathways by binding to diverse targets on fibroblast growth factor and nerve growth factor receptors. Mol Cell Biol *20*, 979-989.
Ong, S.H., Hadari, Y.R., Gotoh, N., Guy, G.R., Schlessinger, J., and Lax, I. (2001). Stimulation of phosphatidylinositol 3-kinase by fibroblast growth factor receptors is mediated by coordinated recruitment of multiple docking proteins. Proc Natl Acad Sci U S A *98*, 6074-6079.
Ono, Y., Nakatani, T., Sakamoto, Y., Mizuhara, E., Minaki, Y., Kumai, M., Hamaguchi, A., Nishimura, M., Inoue, Y., Hayashi, H.*, et al.* (2007). Differences in neurogenic potential in floor plate cells along an anteroposterior location: midbrain dopaminergic neurons originate from mesencephalic floor plate cells. Development *134*, 3213-3225.

Ornitz, D.M. (2000). FGFs, heparan sulfate and FGFRs: complex interactions essential for development. Bioessays *22*, 108-112.
Ornitz, D.M., and Itoh, N. (2001). Fibroblast growth factors. Genome Biol *2*, REVIEWS3005.
Orr-Urtreger, A., Givol, D., Yayon, A., Yarden, Y., and Lonai, P. (1991). Developmental expression of two murine fibroblast growth factor receptors, flg and bek. Development *113*, 1419-1434.
Paek, H., Gutin, G., and Hebert, J.M. (2009). FGF signaling is strictly required to maintain early telencephalic precursor cell survival. Development *136*, 2457-2465.
Panhuysen, M., Vogt Weisenhorn, D.M., Blanquet, V., Brodski, C., Heinzmann, U., Beisker, W., and Wurst, W. (2004). Effects of Wnt1 signaling on proliferation in the developing mid-/hindbrain region. Mol Cell Neurosci *26*, 101-111.
Park, I.H., Zhao, R., West, J.A., Yabuuchi, A., Huo, H., Ince, T.A., Lerou, P.H., Lensch, M.W., and Daley, G.Q. (2008). Reprogramming of human somatic cells to pluripotency with defined factors. Nature *451*, 141-146.
Parmar, M., and Li, M. (2007). Early specification of dopaminergic phenotype during ES cell differentiation. BMC Dev Biol *7*, 86.
Parr, B.A., Shea, M.J., Vassileva, G., and McMahon, A.P. (1993). Mouse Wnt genes exhibit discrete domains of expression in the early embryonic CNS and limb buds. Development *119*, 247-261.
Partanen, J. (2007). FGF signalling pathways in development of the midbrain and anterior hindbrain. J Neurochem *101*, 1185-1193.
Patapoutian, A., and Reichardt, L.F. (2000). Roles of Wnt proteins in neural development and maintenance. Curr Opin Neurobiol *10*, 392-399.
Pearce, J.J., Penny, G., and Rossant, J. (1999). A mouse cerberus/Dan-related gene family. Dev Biol *209*, 98-110.
Pera, E.M., Ikeda, A., Eivers, E., and De Robertis, E.M. (2003). Integration of IGF, FGF, and anti-BMP signals via Smad1 phosphorylation in neural induction. Genes Dev *17*, 3023-3028.
Perlmann, T., and Wallen-Mackenzie, A. (2004). Nurr1, an orphan nuclear receptor with essential functions in developing dopamine cells. Cell Tissue Res *318*, 45-52.
Perlow, M.J., Freed, W.J., Hoffer, B.J., Seiger, A., Olson, L., and Wyatt, R.J. (1979). Brain grafts reduce motor abnormalities produced by destruction of nigrostriatal dopamine system. Science *204*, 643-647.
Perrier, A.L., Tabar, V., Barberi, T., Rubio, M.E., Bruses, J., Topf, N., Harrison, N.L., and Studer, L. (2004). Derivation of midbrain dopamine neurons from human embryonic stem cells. Proc Natl Acad Sci U S A *101*, 12543-12548.
Peters, K.G., Marie, J., Wilson, E., Ives, H.E., Escobedo, J., Del Rosario, M., Mirda, D., and Williams, L.T. (1992). Point mutation of an FGF receptor abolishes phosphatidylinositol turnover and Ca2+ flux but not mitogenesis. Nature *358*, 678-681.
Piccolo, S., Agius, E., Leyns, L., Bhattacharyya, S., Grunz, H., Bouwmeester, T., and De Robertis, E.M. (1999). The head inducer Cerberus is a multifunctional antagonist of Nodal, BMP and Wnt signals. Nature *397*, 707-710.
Piccolo, S., Sasai, Y., Lu, B., and De Robertis, E.M. (1996). Dorsoventral patterning in Xenopus: inhibition of ventral signals by direct binding of chordin to BMP-4. Cell *86*, 589-598.
Politis, M., Oertel, W.H., Wu, K., Quinn, N.P., Pogarell, O., Brooks, D.J., Bjorklund, A., Lindvall, O., and Piccini, P. (2011). Graft-induced dyskinesias in Parkinson's

disease: High striatal serotonin/dopamine transporter ratio. Mov Disord *26*, 1997-2003.
Politis, M., Wu, K., Loane, C., Quinn, N.P., Brooks, D.J., Rehncrona, S., Bjorklund, A., Lindvall, O., and Piccini, P. (2010). Serotonergic neurons mediate dyskinesia side effects in Parkinson's patients with neural transplants. Sci Transl Med *2*, 38ra46.
Powers, C.J., McLeskey, S.W., and Wellstein, A. (2000). Fibroblast growth factors, their receptors and signaling. Endocr Relat Cancer *7*, 165-197.
Prakash, N., Brodski, C., Naserke, T., Puelles, E., Gogoi, R., Hall, A., Panhuysen, M., Echevarria, D., Sussel, L., Weisenhorn, D.M.*, et al.* (2006). A Wnt1-regulated genetic network controls the identity and fate of midbrain-dopaminergic progenitors in vivo. Development *133*, 89-98.
Prakash, N., and Wurst, W. (2006). Development of dopaminergic neurons in the mammalian brain. Cell Mol Life Sci *63*, 187-206.
Puelles, E., Acampora, D., Lacroix, E., Signore, M., Annino, A., Tuorto, F., Filosa, S., Corte, G., Wurst, W., Ang, S.L.*, et al.* (2003). Otx dose-dependent integrated control of antero-posterior and dorso-ventral patterning of midbrain. Nat Neurosci *6*, 453-460.
Puelles, E., Annino, A., Tuorto, F., Usiello, A., Acampora, D., Czerny, T., Brodski, C., Ang, S.L., Wurst, W., and Simeone, A. (2004). Otx2 regulates the extent, identity and fate of neuronal progenitor domains in the ventral midbrain. Development *131*, 2037-2048.
Rawal, N., Castelo-Branco, G., Sousa, K.M., Kele, J., Kobayashi, K., Okano, H., and Arenas, E. (2006). Dynamic temporal and cell type-specific expression of Wnt signaling components in the developing midbrain. Exp Cell Res *312*, 1626-1636.
Raya, A., Rodriguez-Piza, I., Guenechea, G., Vassena, R., Navarro, S., Barrero, M.J., Consiglio, A., Castella, M., Rio, P., Sleep, E.*, et al.* (2009). Disease-corrected haematopoietic progenitors from Fanconi anaemia induced pluripotent stem cells. Nature *460*, 53-59.
Reading, P.J., Dunnett, S.B., and Robbins, T.W. (1991). Dissociable roles of the ventral, medial and lateral striatum on the acquisition and performance of a complex visual stimulus-response habit. Behav Brain Res *45*, 147-161.
Redmond, D.E., Jr., Bjugstad, K.B., Teng, Y.D., Ourednik, V., Ourednik, J., Wakeman, D.R., Parsons, X.H., Gonzalez, R., Blanchard, B.C., Kim, S.U.*, et al.* (2007). Behavioral improvement in a primate Parkinson's model is associated with multiple homeostatic effects of human neural stem cells. Proc Natl Acad Sci U S A *104*, 12175-12180.
Reifers, F., Bohli, H., Walsh, E.C., Crossley, P.H., Stainier, D.Y., and Brand, M. (1998). Fgf8 is mutated in zebrafish acerebellar (ace) mutants and is required for maintenance of midbrain-hindbrain boundary development and somitogenesis. Development *125*, 2381-2395.
Rentzsch, F., Bakkers, J., Kramer, C., and Hammerschmidt, M. (2004). Fgf signaling induces posterior neuroectoderm independently of Bmp signaling inhibition. Dev Dyn *231*, 750-757.
Rhinn, M., Dierich, A., Shawlot, W., Behringer, R.R., Le Meur, M., and Ang, S.L. (1998). Sequential roles for Otx2 in visceral endoderm and neuroectoderm for forebrain and midbrain induction and specification. Development *125*, 845-856.
Ribisi, S., Jr., Mariani, F.V., Aamar, E., Lamb, T.M., Frank, D., and Harland, R.M. (2000). Ras-mediated FGF signaling is required for the formation of posterior but not anterior neural tissue in Xenopus laevis. Dev Biol *227*, 183-196.

Rimerman, R.A., Gellert-Randleman, A., and Diehl, J.A. (2000). Wnt1 and MEK1 cooperate to promote cyclin D1 accumulation and cellular transformation. J Biol Chem *275*, 14736-14742.
Ring, D.B., Johnson, K.W., Henriksen, E.J., Nuss, J.M., Goff, D., Kinnick, T.R., Ma, S.T., Reeder, J.W., Samuels, I., Slabiak, T.*, et al.* (2003). Selective glycogen synthase kinase 3 inhibitors potentiate insulin activation of glucose transport and utilization in vitro and in vivo. Diabetes *52*, 588-595.
Robbins, T.W., Giardini, V., Jones, G.H., Reading, P., and Sahakian, B.J. (1990). Effects of dopamine depletion from the caudate-putamen and nucleus accumbens septi on the acquisition and performance of a conditional discrimination task. Behav Brain Res *38*, 243-261.
Rodrigues, G.A., Falasca, M., Zhang, Z., Ong, S.H., and Schlessinger, J. (2000). A novel positive feedback loop mediated by the docking protein Gab1 and phosphatidylinositol 3-kinase in epidermal growth factor receptor signaling. Mol Cell Biol *20*, 1448-1459.
Rodriguez-Escudero, I., Roelants, F.M., Thorner, J., Nombela, C., Molina, M., and Cid, V.J. (2005). Reconstitution of the mammalian PI3K/PTEN/Akt pathway in yeast. Biochem J *390*, 613-623.
Rodriguez-Gallardo, L., Climent, V., Garcia-Martinez, V., Schoenwolf, G.C., and Alvarez, I.S. (1997). Targeted over-expression of FGF in chick embryos induces formation of ectopic neural cells. Int J Dev Biol *41*, 715-723.
Rodriguez-Gomez, J.A., Lu, J.Q., Velasco, I., Rivera, S., Zoghbi, S.S., Liow, J.S., Musachio, J.L., Chin, F.T., Toyama, H., Seidel, J.*, et al.* (2007). Persistent dopamine functions of neurons derived from embryonic stem cells in a rodent model of Parkinson disease. Stem Cells *25*, 918-928.
Rossant, J. (2008). Stem cells and early lineage development. Cell *132*, 527-531.
Roy, N.S., Cleren, C., Singh, S.K., Yang, L., Beal, M.F., and Goldman, S.A. (2006). Functional engraftment of human ES cell-derived dopaminergic neurons enriched by coculture with telomerase-immortalized midbrain astrocytes. Nat Med *12*, 1259-1268.
Ruiz i Altaba, A. (1998). Combinatorial Gli gene function in floor plate and neuronal inductions by Sonic hedgehog. Development *125*, 2203-2212.
Sakurada, K., Ohshima-Sakurada, M., Palmer, T.D., and Gage, F.H. (1999). Nurr1, an orphan nuclear receptor, is a transcriptional activator of endogenous tyrosine hydroxylase in neural progenitor cells derived from the adult brain. Development *126*, 4017-4026.
Salero, E., and Hatten, M.E. (2007). Differentiation of ES cells into cerebellar neurons. Proc Natl Acad Sci U S A *104*, 2997-3002.
Sanchez-Pernaute, R., Lee, H., Patterson, M., Reske-Nielsen, C., Yoshizaki, T., Sonntag, K.C., Studer, L., and Isacson, O. (2008). Parthenogenetic dopamine neurons from primate embryonic stem cells restore function in experimental Parkinson's disease. Brain *131*, 2127-2139.
Sasai, Y., Lu, B., Steinbeisser, H., and De Robertis, E.M. (1995). Regulation of neural induction by the Chd and Bmp-4 antagonistic patterning signals in Xenopus. Nature *376*, 333-336.
Sasai, Y., Lu, B., Steinbeisser, H., Geissert, D., Gont, L.K., and De Robertis, E.M. (1994). Xenopus chordin: a novel dorsalizing factor activated by organizer-specific homeobox genes. Cell *79*, 779-790.

Sasaki, A., Taketomi, T., Kato, R., Saeki, K., Nonami, A., Sasaki, M., Kuriyama, M., Saito, N., Shibuya, M., and Yoshimura, A. (2003). Mammalian Sprouty4 suppresses Ras-independent ERK activation by binding to Raf1. Nat Cell Biol *5*, 427-432.
Sasaki, H., and Hogan, B.L. (1993). Differential expression of multiple fork head related genes during gastrulation and axial pattern formation in the mouse embryo. Development *118*, 47-59.
Sasaki, H., and Hogan, B.L. (1994). HNF-3 beta as a regulator of floor plate development. Cell *76*, 103-115.
Sasaki, H., Hui, C., Nakafuku, M., and Kondoh, H. (1997). A binding site for Gli proteins is essential for HNF-3beta floor plate enhancer activity in transgenics and can respond to Shh in vitro. Development *124*, 1313-1322.
Sato, T., Araki, I., and Nakamura, H. (2001). Inductive signal and tissue responsiveness defining the tectum and the cerebellum. Development *128*, 2461-2469.
Sato, T., and Joyner, A.L. (2009). The duration of Fgf8 isthmic organizer expression is key to patterning different tectal-isthmo-cerebellum structures. Development *136*, 3617-3626.
Sato, T., and Nakamura, H. (2004). The Fgf8 signal causes cerebellar differentiation by activating the Ras-ERK signaling pathway. Development *131*, 4275-4285.
Saucedo-Cardenas, O., Quintana-Hau, J.D., Le, W.D., Smidt, M.P., Cox, J.J., De Mayo, F., Burbach, J.P., and Conneely, O.M. (1998). Nurr1 is essential for the induction of the dopaminergic phenotype and the survival of ventral mesencephalic late dopaminergic precursor neurons. Proc Natl Acad Sci U S A *95*, 4013-4018.
Schlessinger, J. (1994). SH2/SH3 signaling proteins. Curr Opin Genet Dev *4*, 25-30.
Schmidt, R.H., Bjorklund, A., Stenevi, U., Dunnett, S.B., and Gage, F.H. (1983). Intracerebral grafting of neuronal cell suspensions. III. Activity of intrastriatal nigral suspension implants as assessed by measurements of dopamine synthesis and metabolism. Acta Physiol Scand Suppl *522*, 19-28.
Schmidt, R.H., Ingvar, M., Lindvall, O., Stenevi, U., and Bjorklund, A. (1982). Functional activity of substantia nigra grafts reinnervating the striatum: neurotransmitter metabolism and [14C]2-deoxy-D-glucose autoradiography. J Neurochem *38*, 737-748.
Schulte, G., Bryja, V., Rawal, N., Castelo-Branco, G., Sousa, K.M., and Arenas, E. (2005). Purified Wnt-5a increases differentiation of midbrain dopaminergic cells and dishevelled phosphorylation. J Neurochem *92*, 1550-1553.
Schultz, W. (1982). Depletion of dopamine in the striatum as an experimental model of Parkinsonism: direct effects and adaptive mechanisms. Prog Neurobiol *18*, 121-166.
Schultzberg, M., Dunnett, S.B., Bjorklund, A., Stenevi, U., Hokfelt, T., Dockray, G.J., and Goldstein, M. (1984). Dopamine and cholecystokinin immunoreactive neurons in mesencephalic grafts reinnervating the neostriatum: evidence for selective growth regulation. Neuroscience *12*, 17-32.
Schwarz, M., Alvarez-Bolado, G., Urbanek, P., Busslinger, M., and Gruss, P. (1997). Conserved biological function between Pax-2 and Pax-5 in midbrain and cerebellum development: evidence from targeted mutations. Proc Natl Acad Sci U S A *94*, 14518-14523.
Sears, R., Leone, G., DeGregori, J., and Nevins, J.R. (1999). Ras enhances Myc protein stability. Mol Cell *3*, 169-179.

Sgado, P., Alberi, L., Gherbassi, D., Galasso, S.L., Ramakers, G.M., Alavian, K.N., Smidt, M.P., Dyck, R.H., and Simon, H.H. (2006). Slow progressive degeneration of nigral dopaminergic neurons in postnatal Engrailed mutant mice. Proc Natl Acad Sci U S A *103*, 15242-15247.
Shamim, H., Mahmood, R., Logan, C., Doherty, P., Lumsden, A., and Mason, I. (1999). Sequential roles for Fgf4, En1 and Fgf8 in specification and regionalisation of the midbrain. Development *126*, 945-959.
Shih, J., and Fraser, S.E. (1996). Characterizing the zebrafish organizer: microsurgical analysis at the early-shield stage. Development *122*, 1313-1322.
Shimamura, K., and Rubenstein, J.L. (1997). Inductive interactions direct early regionalization of the mouse forebrain. Development *124*, 2709-2718.
Silva, J., Barrandon, O., Nichols, J., Kawaguchi, J., Theunissen, T.W., and Smith, A. (2008a). Promotion of reprogramming to ground state pluripotency by signal inhibition. PLoS Biol *6*, e253.
Silva, S.S., Rowntree, R.K., Mekhoubad, S., and Lee, J.T. (2008b). X-chromosome inactivation and epigenetic fluidity in human embryonic stem cells. Proc Natl Acad Sci U S A *105*, 4820-4825.
Simeone, A., Acampora, D., Gulisano, M., Stornaiuolo, A., and Boncinelli, E. (1992). Nested expression domains of four homeobox genes in developing rostral brain. Nature *358*, 687-690.
Simeone, A., Acampora, D., Mallamaci, A., Stornaiuolo, A., D'Apice, M.R., Nigro, V., and Boncinelli, E. (1993). A vertebrate gene related to orthodenticle contains a homeodomain of the bicoid class and demarcates anterior neuroectoderm in the gastrulating mouse embryo. EMBO J *12*, 2735-2747.
Simeone, A., Avantaggiato, V., Moroni, M.C., Mavilio, F., Arra, C., Cotelli, F., Nigro, V., and Acampora, D. (1995). Retinoic acid induces stage-specific antero-posterior transformation of rostral central nervous system. Mech Dev *51*, 83-98.
Simon, H.H., Saueressig, H., Wurst, W., Goulding, M.D., and O'Leary, D.D. (2001). Fate of midbrain dopaminergic neurons controlled by the engrailed genes. J Neurosci *21*, 3126-3134.
Smidt, M.P., Asbreuk, C.H., Cox, J.J., Chen, H., Johnson, R.L., and Burbach, J.P. (2000). A second independent pathway for development of mesencephalic dopaminergic neurons requires Lmx1b. Nat Neurosci *3*, 337-341.
Smidt, M.P., and Burbach, J.P. (2007). How to make a mesodiencephalic dopaminergic neuron. Nat Rev Neurosci *8*, 21-32.
Smidt, M.P., Smits, S.M., Bouwmeester, H., Hamers, F.P., van der Linden, A.J., Hellemons, A.J., Graw, J., and Burbach, J.P. (2004). Early developmental failure of substantia nigra dopamine neurons in mice lacking the homeodomain gene Pitx3. Development *131*, 1145-1155.
Smidt, M.P., van Schaick, H.S., Lanctot, C., Tremblay, J.J., Cox, J.J., van der Kleij, A.A., Wolterink, G., Drouin, J., and Burbach, J.P. (1997). A homeodomain gene Ptx3 has highly restricted brain expression in mesencephalic dopaminergic neurons. Proc Natl Acad Sci U S A *94*, 13305-13310.
Smith, J.L., and Schoenwolf, G.C. (1989). Notochordal induction of cell wedging in the chick neural plate and its role in neural tube formation. J Exp Zool *250*, 49-62.
Smith, W.C., and Harland, R.M. (1992). Expression cloning of noggin, a new dorsalizing factor localized to the Spemann organizer in Xenopus embryos. Cell *70*, 829-840.

Smith, W.C., Knecht, A.K., Wu, M., and Harland, R.M. (1993). Secreted noggin protein mimics the Spemann organizer in dorsalizing Xenopus mesoderm. Nature *361*, 547-549.
Smith, W.C., McKendry, R., Ribisi, S., Jr., and Harland, R.M. (1995). A nodal-related gene defines a physical and functional domain within the Spemann organizer. Cell *82*, 37-46.
Smits, S.M., Ponnio, T., Conneely, O.M., Burbach, J.P., and Smidt, M.P. (2003). Involvement of Nurr1 in specifying the neurotransmitter identity of ventral midbrain dopaminergic neurons. Eur J Neurosci *18*, 1731-1738.
Soldner, F., Hockemeyer, D., Beard, C., Gao, Q., Bell, G.W., Cook, E.G., Hargus, G., Blak, A., Cooper, O., Mitalipova, M.*, et al.* (2009). Parkinson's disease patient-derived induced pluripotent stem cells free of viral reprogramming factors. Cell *136*, 964-977.
Sommer, L., Ma, Q., and Anderson, D.J. (1996). neurogenins, a novel family of atonal-related bHLH transcription factors, are putative mammalian neuronal determination genes that reveal progenitor cell heterogeneity in the developing CNS and PNS. Mol Cell Neurosci *8*, 221-241.
Sommer, L., Shah, N., Rao, M., and Anderson, D.J. (1995). The cellular function of MASH1 in autonomic neurogenesis. Neuron *15*, 1245-1258.
Spemann, H., and Mangold, H. (1923). Induction of embryonic primordia by implantation of organizers from a different species. 1923. Int J Dev Biol *45*, 13-38.
Stadtfeld, M., Brennand, K., and Hochedlinger, K. (2008). Reprogramming of pancreatic beta cells into induced pluripotent stem cells. Curr Biol *18*, 890-894.
Starr, P.A., Wichmann, T., van Horne, C., and Bakay, R.A. (1999). Intranigral transplantation of fetal substantia nigra allograft in the hemiparkinsonian rhesus monkey. Cell Transplant *8*, 37-45.
Stavridis, M.P., Lunn, J.S., Collins, B.J., and Storey, K.G. (2007). A discrete period of FGF-induced Erk1/2 signalling is required for vertebrate neural specification. Development *134*, 2889-2894.
Stewart, C.L., Kaspar, P., Brunet, L.J., Bhatt, H., Gadi, I., Kontgen, F., and Abbondanzo, S.J. (1992). Blastocyst implantation depends on maternal expression of leukaemia inhibitory factor. Nature *359*, 76-79.
Storey, K.G., Goriely, A., Sargent, C.M., Brown, J.M., Burns, H.D., Abud, H.M., and Heath, J.K. (1998). Early posterior neural tissue is induced by FGF in the chick embryo. Development *125*, 473-484.
Streit, A., Berliner, A.J., Papanayotou, C., Sirulnik, A., and Stern, C.D. (2000). Initiation of neural induction by FGF signalling before gastrulation. Nature *406*, 74-78.
Streit, A., Lee, K.J., Woo, I., Roberts, C., Jessell, T.M., and Stern, C.D. (1998). Chordin regulates primitive streak development and the stability of induced neural cells, but is not sufficient for neural induction in the chick embryo. Development *125*, 507-519.
Streit, A., and Stern, C.D. (1999a). Establishment and maintenance of the border of the neural plate in the chick: involvement of FGF and BMP activity. Mech Dev *82*, 51-66.
Streit, A., and Stern, C.D. (1999b). Mesoderm patterning and somite formation during node regression: differential effects of chordin and noggin. Mech Dev *85*, 85-96.

Stromberg, I., Johnson, S., Hoffer, B., and Olson, L. (1985). Reinnervation of dopamine-denervated striatum by substantia nigra transplants: immunohistochemical and electrophysiological correlates. Neuroscience *14*, 981-990.
Stuhlmiller, T.J., and Garcia-Castro, M.I. (2011). FGF/MAPK signaling is required in the gastrula epiblast for avian neural crest induction. Development.
Su, H.L., Muguruma, K., Matsuo-Takasaki, M., Kengaku, M., Watanabe, K., and Sasai, Y. (2006). Generation of cerebellar neuron precursors from embryonic stem cells. Dev Biol *290*, 287-296.
Sun, X., Meyers, E.N., Lewandoski, M., and Martin, G.R. (1999). Targeted disruption of Fgf8 causes failure of cell migration in the gastrulating mouse embryo. Genes Dev *13*, 1834-1846.
Sunmonu, N.A., Li, K., Guo, Q., and Li, J.Y. (2011). Gbx2 and Fgf8 are sequentially required for formation of the midbrain-hindbrain compartment boundary. Development *138*, 725-734.
Suzuki, A., Ueno, N., and Hemmati-Brivanlou, A. (1997). Xenopus msx1 mediates epidermal induction and neural inhibition by BMP4. Development *124*, 3037-3044.
Tabar, V., Tomishima, M., Panagiotakos, G., Wakayama, S., Menon, J., Chan, B., Mizutani, E., Al-Shamy, G., Ohta, H., Wakayama, T.*, et al.* (2008). Therapeutic cloning in individual parkinsonian mice. Nat Med *14*, 379-381.
Taipale, J., and Beachy, P.A. (2001). The Hedgehog and Wnt signalling pathways in cancer. Nature *411*, 349-354.
Takagi, Y., Takahashi, J., Saiki, H., Morizane, A., Hayashi, T., Kishi, Y., Fukuda, H., Okamoto, Y., Koyanagi, M., Ideguchi, M.*, et al.* (2005). Dopaminergic neurons generated from monkey embryonic stem cells function in a Parkinson primate model. J Clin Invest *115*, 102-109.
Takahashi, K., Tanabe, K., Ohnuki, M., Narita, M., Ichisaka, T., Tomoda, K., and Yamanaka, S. (2007). Induction of pluripotent stem cells from adult human fibroblasts by defined factors. Cell *131*, 861-872.
Takahashi, K., and Yamanaka, S. (2006). Induction of pluripotent stem cells from mouse embryonic and adult fibroblast cultures by defined factors. Cell *126*, 663-676.
Tang, M., Miyamoto, Y., and Huang, E.J. (2009). Multiple roles of beta-catenin in controlling the neurogenic niche for midbrain dopamine neurons. Development *136*, 2027-2038.
Tang, M., Villaescusa, J.C., Luo, S.X., Guitarte, C., Lei, S., Miyamoto, Y., Taketo, M.M., Arenas, E., and Huang, E.J. (2010). Interactions of Wnt/beta-catenin signaling and sonic hedgehog regulate the neurogenesis of ventral midbrain dopamine neurons. J Neurosci *30*, 9280-9291.
Terada, Y., Inoshita, S., Nakashima, O., Kuwahara, M., Sasaki, S., and Marumo, F. (1999). Regulation of cyclin D1 expression and cell cycle progression by mitogen-activated protein kinase cascade. Kidney Int *56*, 1258-1261.
Tesar, P.J., Chenoweth, J.G., Brook, F.A., Davies, T.J., Evans, E.P., Mack, D.L., Gardner, R.L., and McKay, R.D. (2007). New cell lines from mouse epiblast share defining features with human embryonic stem cells. Nature *448*, 196-199.
Thomas, K.R., and Capecchi, M.R. (1990). Targeted disruption of the murine int-1 proto-oncogene resulting in severe abnormalities in midbrain and cerebellar development. Nature *346*, 847-850.
Thomas, P., and Beddington, R. (1996). Anterior primitive endoderm may be responsible for patterning the anterior neural plate in the mouse embryo. Curr Biol *6*, 1487-1496.

Thomas, P.Q., Brown, A., and Beddington, R.S. (1998). Hex: a homeobox gene revealing peri-implantation asymmetry in the mouse embryo and an early transient marker of endothelial cell precursors. Development *125*, 85-94.
Thomson, J.A., Itskovitz-Eldor, J., Shapiro, S.S., Waknitz, M.A., Swiergiel, J.J., Marshall, V.S., and Jones, J.M. (1998). Embryonic stem cell lines derived from human blastocysts. Science *282*, 1145-1147.
Timmer, J.R., Wang, C., and Niswander, L. (2002). BMP signaling patterns the dorsal and intermediate neural tube via regulation of homeobox and helix-loop-helix transcription factors. Development *129*, 2459-2472.
Torres, E.M., Monville, C., Gates, M.A., Bagga, V., and Dunnett, S.B. (2007). Improved survival of young donor age dopamine grafts in a rat model of Parkinson's disease. Neuroscience *146*, 1606-1617.
Toyooka, Y., Shimosato, D., Murakami, K., Takahashi, K., and Niwa, H. (2008). Identification and characterization of subpopulations in undifferentiated ES cell culture. Development *135*, 909-918.
Tsang, M., Friesel, R., Kudoh, T., and Dawid, I.B. (2002). Identification of Sef, a novel modulator of FGF signalling. Nat Cell Biol *4*, 165-169.
Turner, N., and Grose, R. (2010). Fibroblast growth factor signalling: from development to cancer. Nat Rev Cancer *10*, 116-129.
Umbhauer, M., Penzo-Mendez, A., Clavilier, L., Boucaut, J., and Riou, J. (2000). Signaling specificities of fibroblast growth factor receptors in early Xenopus embryo. J Cell Sci *113 (Pt 16)*, 2865-2875.
Ungerstedt, U., and Arbuthnott, G.W. (1970). Quantitative recording of rotational behavior in rats after 6-hydroxy-dopamine lesions of the nigrostriatal dopamine system. Brain Res *24*, 485-493.
Urness, L.D., Li, C., Wang, X., and Mansour, S.L. (2008). Expression of ERK signaling inhibitors Dusp6, Dusp7, and Dusp9 during mouse ear development. Dev Dyn *237*, 163-169.
Vallier, L., Touboul, T., Chng, Z., Brimpari, M., Hannan, N., Millan, E., Smithers, L.E., Trotter, M., Rugg-Gunn, P., Weber, A.*, et al.* (2009). Early cell fate decisions of human embryonic stem cells and mouse epiblast stem cells are controlled by the same signalling pathways. PLoS One *4*, e6082.
Verma-Kurvari, S., Savage, T., Gowan, K., and Johnson, J.E. (1996). Lineage-specific regulation of the neural differentiation gene MASH1. Dev Biol *180*, 605-617.
Vieira, C., Garda, A.L., Shimamura, K., and Martinez, S. (2005). Thalamic development induced by Shh in the chick embryo. Dev Biol *284*, 351-363.
Vieira, C., and Martinez, S. (2005). Experimental study of MAP kinase phosphatase-3 (Mkp3) expression in the chick neural tube in relation to Fgf8 activity. Brain Res Brain Res Rev *49*, 158-166.
Wakioka, T., Sasaki, A., Kato, R., Shouda, T., Matsumoto, A., Miyoshi, K., Tsuneoka, M., Komiya, S., Baron, R., and Yoshimura, A. (2001). Spred is a Sprouty-related suppressor of Ras signalling. Nature *412*, 647-651.
Wallen, A., Zetterstrom, R.H., Solomin, L., Arvidsson, M., Olson, L., and Perlmann, T. (1999). Fate of mesencephalic AHD2-expressing dopamine progenitor cells in NURR1 mutant mice. Exp Cell Res *253*, 737-746.
Wassarman, K.M., Lewandoski, M., Campbell, K., Joyner, A.L., Rubenstein, J.L., Martinez, S., and Martin, G.R. (1997). Specification of the anterior hindbrain and establishment of a normal mid/hindbrain organizer is dependent on Gbx2 gene function. Development *124*, 2923-2934.

Watanabe, K., Kamiya, D., Nishiyama, A., Katayama, T., Nozaki, S., Kawasaki, H., Watanabe, Y., Mizuseki, K., and Sasai, Y. (2005). Directed differentiation of telencephalic precursors from embryonic stem cells. Nat Neurosci *8*, 288-296.
Wataya, T., Ando, S., Muguruma, K., Ikeda, H., Watanabe, K., Eiraku, M., Kawada, M., Takahashi, J., Hashimoto, N., and Sasai, Y. (2008). Minimization of exogenous signals in ES cell culture induces rostral hypothalamic differentiation. Proc Natl Acad Sci U S A *105*, 11796-11801.
Weinstein, D.C., Ruiz i Altaba, A., Chen, W.S., Hoodless, P., Prezioso, V.R., Jessell, T.M., and Darnell, J.E., Jr. (1994). The winged-helix transcription factor HNF-3 beta is required for notochord development in the mouse embryo. Cell *78*, 575-588.
Wernig, M., Meissner, A., Foreman, R., Brambrink, T., Ku, M., Hochedlinger, K., Bernstein, B.E., and Jaenisch, R. (2007). In vitro reprogramming of fibroblasts into a pluripotent ES-cell-like state. Nature *448*, 318-324.
White, N.M. (1989). Reward or reinforcement: what's the difference? Neurosci Biobehav Rev *13*, 181-186.
Whitman, M., Downes, C.P., Keeler, M., Keller, T., and Cantley, L. (1988). Type I phosphatidylinositol kinase makes a novel inositol phospholipid, phosphatidylinositol-3-phosphate. Nature *332*, 644-646.
Whitman, M., Kaplan, D., Roberts, T., and Cantley, L. (1987). Evidence for two distinct phosphatidylinositol kinases in fibroblasts. Implications for cellular regulation. Biochem J *247*, 165-174.
Wichterle, H., Lieberam, I., Porter, J.A., and Jessell, T.M. (2002). Directed differentiation of embryonic stem cells into motor neurons. Cell *110*, 385-397.
Wiedemann, M., and Trueb, B. (2000). Characterization of a novel protein (FGFRL1) from human cartilage related to FGF receptors. Genomics *69*, 275-279.
Wilkinson, D.G., Bailes, J.A., and McMahon, A.P. (1987). Expression of the proto-oncogene int-1 is restricted to specific neural cells in the developing mouse embryo. Cell *50*, 79-88.
Wilkinson, D.G., Peters, G., Dickson, C., and McMahon, A.P. (1988). Expression of the FGF-related proto-oncogene int-2 during gastrulation and neurulation in the mouse. EMBO J *7*, 691-695.
Willert, K., Brown, J.D., Danenberg, E., Duncan, A.W., Weissman, I.L., Reya, T., Yates, J.R., 3rd, and Nusse, R. (2003). Wnt proteins are lipid-modified and can act as stem cell growth factors. Nature *423*, 448-452.
Wills, A.E., Choi, V.M., Bennett, M.J., Khokha, M.K., and Harland, R.M. (2010). BMP antagonists and FGF signaling contribute to different domains of the neural plate in Xenopus. Dev Biol *337*, 335-350.
Wilson, S.I., Rydstrom, A., Trimborn, T., Willert, K., Nusse, R., Jessell, T.M., and Edlund, T. (2001). The status of Wnt signalling regulates neural and epidermal fates in the chick embryo. Nature *411*, 325-330.
Wood, H.B., and Episkopou, V. (1999). Comparative expression of the mouse Sox1, Sox2 and Sox3 genes from pre-gastrulation to early somite stages. Mech Dev *86*, 197-201.
Wuerthele, S.M., Freed, W.J., Olson, L., Morihisa, J., Spoor, L., Wyatt, R.J., and Hoffer, B.J. (1981). Effect of dopamine agonists and antagonists on the electrical activity of substantia nigra neurons transplanted into the lateral ventricle of the rat. Exp Brain Res *44*, 1-10.

Wurst, W., Auerbach, A.B., and Joyner, A.L. (1994). Multiple developmental defects in Engrailed-1 mutant mice: an early mid-hindbrain deletion and patterning defects in forelimbs and sternum. Development *120*, 2065-2075.
Wurst, W., and Bally-Cuif, L. (2001). Neural plate patterning: upstream and downstream of the isthmic organizer. Nat Rev Neurosci *2*, 99-108.
Xu, H., Lee, K.W., and Goldfarb, M. (1998). Novel recognition motif on fibroblast growth factor receptor mediates direct association and activation of SNT adapter proteins. J Biol Chem *273*, 17987-17990.
Xu, J., Liu, Z., and Ornitz, D.M. (2000). Temporal and spatial gradients of Fgf8 and Fgf17 regulate proliferation and differentiation of midline cerebellar structures. Development *127*, 1833-1843.
Xu, N., Papagiannakopoulos, T., Pan, G., Thomson, J.A., and Kosik, K.S. (2009). MicroRNA-145 regulates OCT4, SOX2, and KLF4 and represses pluripotency in human embryonic stem cells. Cell *137*, 647-658.
Xu, R.H., Sampsell-Barron, T.L., Gu, F., Root, S., Peck, R.M., Pan, G., Yu, J., Antosiewicz-Bourget, J., Tian, S., Stewart, R.*, et al.* (2008). NANOG is a direct target of TGFbeta/activin-mediated SMAD signaling in human ESCs. Cell Stem Cell *3*, 196-206.
Yamaguchi, T.P., Bradley, A., McMahon, A.P., and Jones, S. (1999). A Wnt5a pathway underlies outgrowth of multiple structures in the vertebrate embryo. Development *126*, 1211-1223.
Yamaguchi, T.P., Conlon, R.A., and Rossant, J. (1992). Expression of the fibroblast growth factor receptor FGFR-1/flg during gastrulation and segmentation in the mouse embryo. Dev Biol *152*, 75-88.
Yamaguchi, T.P., Harpal, K., Henkemeyer, M., and Rossant, J. (1994). fgfr-1 is required for embryonic growth and mesodermal patterning during mouse gastrulation. Genes Dev *8*, 3032-3044.
Yan, C.H., Levesque, M., Claxton, S., Johnson, R.L., and Ang, S.L. (2011). Lmx1a and lmx1b function cooperatively to regulate proliferation, specification, and differentiation of midbrain dopaminergic progenitors. J Neurosci *31*, 12413-12425.
Ye, W., Bouchard, M., Stone, D., Liu, X., Vella, F., Lee, J., Nakamura, H., Ang, S.L., Busslinger, M., and Rosenthal, A. (2001). Distinct regulators control the expression of the mid-hindbrain organizer signal FGF8. Nat Neurosci *4*, 1175-1181.
Ye, W., Shimamura, K., Rubenstein, J.L., Hynes, M.A., and Rosenthal, A. (1998). FGF and Shh signals control dopaminergic and serotonergic cell fate in the anterior neural plate. Cell *93*, 755-766.
Ying, Q.L., Nichols, J., Chambers, I., and Smith, A. (2003a). BMP induction of Id proteins suppresses differentiation and sustains embryonic stem cell self-renewal in collaboration with STAT3. Cell *115*, 281-292.
Ying, Q.L., and Smith, A.G. (2003). Defined conditions for neural commitment and differentiation. Methods Enzymol *365*, 327-341.
Ying, Q.L., Stavridis, M., Griffiths, D., Li, M., and Smith, A. (2003b). Conversion of embryonic stem cells into neuroectodermal precursors in adherent monoculture. Nat Biotechnol *21*, 183-186.
Ying, Q.L., Wray, J., Nichols, J., Batlle-Morera, L., Doble, B., Woodgett, J., Cohen, P., and Smith, A. (2008). The ground state of embryonic stem cell self-renewal. Nature *453*, 519-523.

Yu, J., Vodyanik, M.A., Smuga-Otto, K., Antosiewicz-Bourget, J., Frane, J.L., Tian, S., Nie, J., Jonsdottir, G.A., Ruotti, V., Stewart, R.*, et al.* (2007). Induced pluripotent stem cell lines derived from human somatic cells. Science *318*, 1917-1920.
Zaehres, H., Lensch, M.W., Daheron, L., Stewart, S.A., Itskovitz-Eldor, J., and Daley, G.Q. (2005). High-efficiency RNA interference in human embryonic stem cells. Stem Cells *23*, 299-305.
Zetterstrom, R.H., Solomin, L., Jansson, L., Hoffer, B.J., Olson, L., and Perlmann, T. (1997). Dopamine neuron agenesis in Nurr1-deficient mice. Science *276*, 248-250.
Zhang, J., and Carthew, R.W. (1998). Interactions between Wingless and DFz2 during Drosophila wing development. Development *125*, 3075-3085.
Zhang, X., Ibrahimi, O.A., Olsen, S.K., Umemori, H., Mohammadi, M., and Ornitz, D.M. (2006). Receptor specificity of the fibroblast growth factor family. The complete mammalian FGF family. J Biol Chem *281*, 15694-15700.
Zhao, S., Maxwell, S., Jimenez-Beristain, A., Vives, J., Kuehner, E., Zhao, J., O'Brien, C., de Felipe, C., Semina, E., and Li, M. (2004). Generation of embryonic stem cells and transgenic mice expressing green fluorescence protein in midbrain dopaminergic neurons. Eur J Neurosci *19*, 1133-1140.
Zimmerman, L.B., De Jesus-Escobar, J.M., and Harland, R.M. (1996). The Spemann organizer signal noggin binds and inactivates bone morphogenetic protein 4. Cell *86*, 599-606.

8 Appendix

Development ePress online publication date 31 August 2011

Development 138, 0000-0000 (2011) doi:10.1242/dev.066746
© 2011. Published by The Company of Biologists Ltd

Temporally controlled modulation of FGF/ERK signaling directs midbrain dopaminergic neural progenitor fate in mouse and human pluripotent stem cells

Ines Jaeger[1], Charles Arber[1,*], Jessica R. Risner-Janiczek[1,*], Judit Kuechler[1], Diana Pritzsche[1], I-Cheng Chen[1], Thulasi Naveenan[1], Mark A. Ungless[2] and Meng Li[1,†]

SUMMARY

Effective induction of midbrain-specific dopamine (mDA) neurons from stem cells is fundamental for realizing their potential in biomedical applications relevant to Parkinson's disease. During early development, the Otx2-positive neural tissues are patterned anterior-posteriorly to form the forebrain and midbrain under the influence of extracellular signaling such as FGF and Wnt. In the mesencephalon, sonic hedgehog (Shh) specifies a ventral progenitor fate in the floor plate region that later gives rise to mDA neurons. In this study, we systematically investigated the temporal actions of FGF signaling in mDA neuron fate specification of mouse and human pluripotent stem cells and mouse induced pluripotent stem cells. We show that a brief blockade of FGF signaling on exit of the lineage-primed epiblast pluripotent state initiates an early induction of *Lmx1a* and *Foxa2* in nascent neural progenitors. In addition to inducing ventral midbrain characteristics, the FGF signaling blockade during neural induction also directs a midbrain fate in the anterior-posterior axis by suppressing caudalization as well as forebrain induction, leading to the maintenance of midbrain Otx2. Following a period of endogenous FGF signaling, subsequent enhancement of FGF signaling by Fgf8, in combination with Shh, promotes mDA neurogenesis and restricts alternative fates. Thus, a stepwise control of FGF signaling during distinct stages of stem cell neural fate conversion is crucial for reliable and highly efficient production of functional, authentic midbrain-specific dopaminergic neurons. Importantly, we provide evidence that this novel, small-molecule-based strategy applies to both mouse and human pluripotent stem cells.

KEY WORDS: Pluripotent stem cell, Dopamine neuron, Cell fate, Mouse, Human

INTRODUCTION

The midbrain dopaminergic (mDA) neuron has been a prime target in stem cell research and developmental neurobiology owing to its association with Parkinson's disease. Recent years have witnessed a rapid advancement in understanding the regulatory cascade that governs ventral midbrain neuroepithelial cell fate specification and the differentiation and maintenance of mDA neurons (Andersson et al., 2006; Ferri et al., 2007; Nakatani et al., 2009). Overexpression of mDA transcription factors offers a valid strategy for generating DA neurons from embryonic stem cells (ESCs) (Andersson et al., 2006; Chung et al., 2005; Kittappa et al., 2007; Konstantoulas et al., 2010; Maxwell et al., 2005). However, mDA specification via genetic manipulation is limited and context dependent (Andersson et al., 2006; Friling et al., 2009; Parmar and Li, 2007; Roybon et al., 2008). This could be attributed to the fact that, during development, the transcription factors employed act only on regionally specified mDA-competent ventral midbrain progenitors, but the extent to which such progenitor populations can be generated from pluripotent stem cells using currently available paradigms remains unclear. Several studies indicate that ESCs give rise to forebrain-like identity under defined conditions or to heterogeneous progenitor phenotypes, which exhibit a broad range of anterior-posterior domain-specific expression profiles, when differentiated under the influence of stromal feeders and/or patterning cues (Bouhon et al., 2005; Gaspard et al., 2008; Kawasaki et al., 2000; Watanabe et al., 2005).

During development, mDA neurons are generated from the ventral midbrain floor plate cells under the cooperative action of the homeobox transcription factor Lmx1a and the forkhead transcription factor Foxa2 (Andersson et al., 2006; Chung et al., 2009; Lin et al., 2009; Nakatani et al., 2009). A recent gain-of-function study in ESCs reported that the early expression of an *Lmx1a* transgene in ESC-derived neural progenitors is crucial for its mDA neuron-inducing activity (Friling et al., 2009), suggesting that temporally restricted characteristics essential for the mDA-competent state become limited in ESC-derived neural cultures soon after neural induction. This change in progenitor competency might explain why sonic hedgehog (Shh), which plays a pivotal role in ventral midbrain patterning and mDA neuron fate specification during development (Ye et al., 1998), is reported to have a widely varying ability to promote mDA neuron production from mouse or human ESCs (Andersson et al., 2006; Friling et al., 2009; Kim et al., 2002; Parmar and Li, 2007; Perrier et al., 2004; Yan et al., 2005). Thus, there is a pressing need to elucidate the essential attributes of mDA-competent neural progenitors and the regulators that are capable of inducing this state.

Molecular signaling is essential for shaping cell fate choice during development. FGF signaling plays multiple roles during the induction and maintenance of the telencephalon (Paek et al., 2009) and, together with Wnt, participates in the formation of the isthmus organizer (IsO) at the midbrain and hindbrain boundary (Olander et al., 2006). However, prior to IsO induction, phosphorylated

[1]Stem Cell Neurogenesis, MRC Clinical Sciences Centre, Faculty of Medicine, Imperial College, London W12 0NN, UK. [2]Neurophysiology, MRC Clinical Sciences Centre, Faculty of Medicine, Imperial College, London W12 0NN, UK.

*These authors contributed equally to this work
†Author for correspondence (meng.li2@imperial.ac.uk)

Accepted 4 August 2011

ERK1/2, which marks regions of FGF signaling, is scarcely detectable in the epiblast of pre-streak vertebrate embryos (Lunn et al., 2007) and in the prospective ventral midbrain of early gastrulating embryos (Corson et al., 2003; Lunn et al., 2007). This temporospatial restriction of FGF/ERK signaling might be necessary for initiating the regulatory cascade that induces competency and cell fate potentials of prospective midbrain neural progenitors.

Using mouse and human pluripotent stem cells and mouse induced pluripotent stem cells (iPSCs), we report here for the first time that a pharmacological blockade of FGF/ERK signaling upon neural induction induces midbrain-specific characteristics, whereas a subsequent activation of FGF signaling consolidates and maintains dopaminergic traits. Combinatorial stimulation with Shh in this experimental paradigm leads to robust production of 'authentic' mDA neurons from mouse and human pluripotent stem cells.

MATERIALS AND METHODS

Cell culture and neural differentiation

Mouse ESCs, mouse iPSCs and mouse epiblast stem cells (EpiSCs) were maintained feeder-free as previously described (Guo et al., 2009; Parmar and Li, 2007; Ying et al., 2003). Mouse EpiSCs were established from E14tg2a, Sox1-GFP (also referred to as 46C), Pitx3-GFP and Lmx1a-GFP mouse ESCs as described (Guo et al., 2009). Human ESCs (hESCs; H1 and H7) were cultured on mitomycin C-inactivated feeder cells in knockout DMEM supplemented with 20% knockout serum replacement (KSR) and 8 ng/ml FGF2. Neural differentiation of hESCs was induced with a 3-day treatment with Smad inhibitor, but otherwise similar to that described by Chambers et al. (Chambers et al., 2009). Monolayer differentiation of EpiSCs was developed based on the method by Ying et al. (Ying et al., 2003). Briefly, EpiSCs were plated on fibronectin-coated plastics and cultured in EpiSC media until 50% confluency. Cells were then rinsed twice with PBS and cultured in retinol-free N2B27. Medium was refreshed every other day, as with ESC differentiation, where the day cells are switched to N2B27 is designated as d0 MD. Where indicated, PD0325901 (1 μM, Axon), PD173074 (50 ng/ml, Sigma), FGF8b (100 ng/ml, Peprotech), Shh (200 ng/ml, C25 II-N, R&D) or cyclopamine (2 μM, Sigma) were added to the cultures.

Immunocytochemistry

Cultures were washed twice in PBS then fixed in 4% paraformaldehyde for 20 minutes. Fixed cultures were washed three times in PBS containing 0.3% Triton X-100 followed by incubation in blocking solution containing the above plus 1% BSA and 10% serum compatible with the secondary antibodies. Cells were then incubated overnight at 4°C with the appropriate primary antibody diluted in blocking solution. Cells were washed three times in PBS followed by incubation for 1-2 hours with fluorescently labeled secondary antibodies and DAPI (Molecular Probes). Primary antibodies used were: TH (rabbit, Pel-Freez), TH (sheep, Pel-Freez), β3-tubulin (mouse, Babco), Pitx3 (rabbit, gift of M. Smidt, University of Amsterdam), Foxa2 (goat, Santa Cruz), Lmx1a (rabbit, gift of M. German, University of California, San Francisco), nestin (DSHB), GFP (mouse, Roche), Otx2 (rabbit, Millipore) and Nurr1 (rabbit, Santa Cruz).

Images were captured using a Leica TCS SP5 confocal microscope. The number of $Otx2^+$ cells was determined using ImageJ macro (NIH), based on the total number of pixels of Otx2-labeled and DAPI-labeled nuclei. Quantification of other markers was carried out manually by examining randomly selected fields from at least three independent experiments and data are presented as mean ± s.e.m. Statistical significance was determined using a two-tailed Student's *t*-test.

Quantitative (q) PCR

Total RNA was extracted using TRI Reagent (Sigma) and processed for RT-PCR on a Chromo4 real-time PCR detection system according to the manufacturer's protocols (Bio-Rad). All PCR data were normalized to the average of two reference genes: *Hmbs* and cyclophilin (peptidylprolyl isomerase A). For PCR primers, see Table S1 in the supplementary material. All qPCR data are presented as mean ± s.e.m. of at least three biological replicates.

Electrophysiology

Day 14-16 MD cultures derived from Pitx3-GFP EpiSCs were placed in a recording chamber and viewed using an Olympus BX51WI microscope with a 40× water-immersion lens and DIC optics. Cells were bathed in 140 mM NaCl, 3.5 mM KCl, 1.25 mM NaH_2PO_4, 2 mM $CaCl_2$, 1 mM $MgCl_2$, 10 mM glucose, 10 mM HEPES pH 7.4. For whole-cell recordings, low-resistance recording pipettes (9-12 MΩ) were pulled from capillary glass (Harvard Apparatus) and coated with ski wax to reduce pipette capacitance. Recording pipettes were filled with 140 mM potassium gluconate, 5 mM NaCl, 2 mM MgATP, 0.5 mM LiGTP, 0.1 mM $CaCl_2$, 1 mM $MgCl_2$, 1 mM EGTA, 10 mM HEPES pH 7.4. The osmolarity and pH of both solutions were adjusted before experiments. Prior to recording, the GFP^+ neurons were identified and targeted for recording using fluorescence via a GFP-selective filter (X-Cite series 120, EXFO). For analysis of action potential frequency and the coefficient of variation of the interspike interval (CV-ISI), the first 30 seconds of recording time were used to avoid potential effects of washout. Data were acquired at room temperature (20-22°C) using an Axon Multiclamp 700B amplifier and a Digidata 1440a acquisition system, with pClamp 10 software (Molecular Devices). Data analysis was carried out using Clampfit 10.2 (Axon), OriginPro 8.1 (OriginLab) and Spike2v5 (Cambridge Electronic Design) software. Data are presented as mean ± s.e.m.

RESULTS

EpiSCs offer an alternative model for efficient neural induction in vitro

In vitro differentiation of ESCs is asynchronous, generating scenarios in which intermediate progenitors of distinct developmental stages and/or positional identity co-exist and elicit heterogeneous responses to a given inductive signal. Mouse ESCs differentiate into somatic cells via the primitive ectoderm/epiblast stage, when lines of EpiSCs can be established (Brons et al., 2007; Guo et al., 2009; Tesar et al., 2007). Thus, EpiSCs are developmentally primed pluripotent stem cells, which might offer a better in vitro differentiation model than mouse ESCs. We therefore subjected EpiSCs to a monolayer differentiation (MD) protocol previously developed in ESCs (Ying et al., 2003). We found that EpiSCs convert to neuroectoderm cells more quickly than ESCs (Fig. 1). At day 4 (d4) MD, when $Oct4^+$ cells were still abundant in ESC MD cultures, few were detected in EpiSC cultures. However, Sox2, which is expressed in both pluripotent stem cells and neuroepithelial stem cells, was detected in the $Oct4^-$ d4 EpiSC derivatives (Fig. 1A). At d6, EpiSC cultures contained numerous $nestin^+$ neural progenitors, whereas significantly fewer were found in ESC progeny.

Consistent with the above observation, qPCR analysis showed a more rapid reduction of *Oct4* (*Pou5f1* – Mouse Genome Informatics) and *Nanog* transcripts in EpiSC than in ESC MD cultures. By contrast, we observed a greater rate of upregulation of the neuroepithelial genes *Sox1* and nestin in EpiSC cultures. This was followed by an earlier upregulation of the pro-neural genes *Ngn2* and *Mash1* (*Neurog2* and *Ascl1* – Mouse Genome Informatics) and, subsequently, of the neuronal marker genes *Ncam1* and β3-tubulin (*Tubb3*) in EpiSC cultures (Fig. 1B).

Taken together, this survey of marker expression indicates that EpiSCs offer a more rapid neural differentiation system than ESCs. Furthermore, the pattern of stage-specific gene expression observed indicates that neural induction occurs during the first 2-3 days of MD using the EpiSC system.

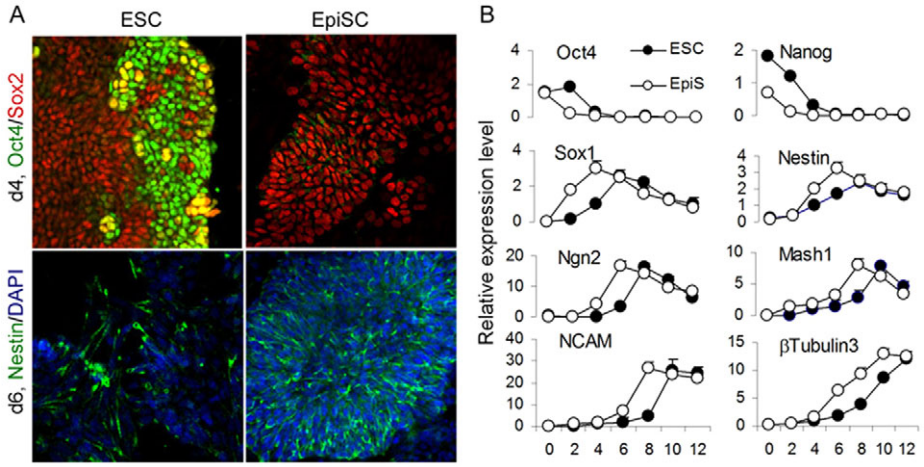


Fig. 1. EpiSCs enter the neuroectoderm lineage faster than ESCs. (**A**) Mouse ESC and EpiSC MD cultures immunostained for Oct4 and Sox2 at day 4 (top) and nestin at day 6 (bottom). DAPI labeling is in blue. (**B**) qPCR analysis for the expression of pluripotency and neural lineage genes over 12-day MD cultures of ESCs and EpiSCs. Data represent mean±s.e.m. from triplicate cultures of a single experiment.

FGF/ERK signaling blockade accelerates the conversion from the epiblast pluripotent state toward neuroectoderm

FGF/ERK signaling promotes the conversion of ESCs toward neural progenitors and this signal may be required at multiple points during neural differentiation (Kunath et al., 2007; Stavridis et al., 2007). Kunath et al. (Kunath et al., 2007) suggest that ERK-dependent FGF signaling is required for the exit from an inner cell mass-like state toward epiblast ectoderm, whereas Stavridis et al. (Stavridis et al., 2007) argue that this signaling acts in the transition of epiblast-like cells to neural progenitors. To distinguish between these possibilities, we performed EpiSC MD in the presence of the specific FGF receptor inhibitor PD173074 or the potent MEK blocker PD0325901 (Stavridis et al., 2007; Ying et al., 2008). Both compounds prevented the phosphorylation of ERK1/2 (Mapk3/1 – Mouse Genome Informatics) (Fig. 2A). Using EpiSCs derived from the 46C ESCs, which harbor a knock-in GFP reporter in the *Sox1* locus (Ying et al., 2003), we observed an early appearance of Sox1-GFP$^+$ neural progenitors (Fig. 2B). This was supported by immunocytochemical analysis for another neuroepithelial marker, PLZF (Zbtb16 – Mouse Genome Informatics) (Fig. 2C). This finding indicates that FGF/ERK signaling blockade accelerates neural induction of EpiSCs.

Blockade of FGF/ERK signaling at the onset of EpiSC differentiation induces mDA neural progenitor characteristics

Isthmus-derived Fgf8 plays an important role in midbrain-rostral hindbrain patterning and mDA development and has been used as a standard inductive cue in all ESC differentiation protocols targeting dopamine neurons (Barberi et al., 2003; Kawasaki et al., 2000; Kim et al., 2002; Lee et al., 2000; Perrier et al., 2004; Ye et al., 1998). Surprisingly, we found that treatment with either PD173074 or PD0325901 at the onset of MD led to early induction of *Lmx1a* and *Foxa2* (Fig. 3A,B, see Fig. S1 in the supplementary material). Moreover, cultures that experienced FGF/ERK blockade for the first 2 days continued to show elevated levels of *Lmx1a* and *Foxa2* between d3 and d5, as compared with no-PD controls. By contrast, MD cultures exposed to PD0325901 continuously for 5 days showed a similar level of *Foxa2* and a reduced level of *Lmx1a* transcript compared with the no-PD culture at d3 and d5 (Fig. 3A,B). Consistent with the RNA analysis, at d5 MD, we observed a pronounced increase of neural progenitors expressing Foxa2 protein or a knock-in Lmx1a-GFP reporter in cultures exposed to 2 days of PD173074 or PD0325901 (Fig. 3C). These results demonstrate that blocking FGF/ERK activity on exit of the epiblast pluripotent state induces appropriate gene markers for the presumptive ventral midbrain in newly converted neural progenitors, which then require FGF/ERK signaling to maintain and consolidate this progenitor trait.

We obtained similar results with PD0325901 and PD173074 for the gene markers described above (Fig. 3) and the additional markers presented in Fig. S1A in the supplementary material. The studies described below were therefore performed with PD0325901 (hereafter referred to as PD) unless stated otherwise.

Temporally controlled modulation of FGF/ERK signaling leads to highly reliable and efficient production of mDA neurons

To investigate whether the observed induction of the mDA progenitor phenotype translates to mDA neuron production either quantitatively [the number of tyrosine hydroxylase-positive (Th$^+$) neurons] or qualitatively (the midbrain-specific identity of Th$^+$ neurons), we assessed a panel of markers by immunocytochemistry at d14 MD. We employed a scheme that is analogous to most DA differentiation protocols in which Shh is applied to nestin$^+$ cells (Fig. 4A, see Fig. S2 in the supplementary material) (Barberi et al., 2003; Kawasaki et al., 2000; Kim et al., 2002; Lee et al., 2000; Parmar and Li, 2007; Perrier et al., 2004). We found that, despite the robust induction of Foxa2$^+$ Lmx1a$^+$ neural progenitors at d5, cultures treated with PD alone did not produce more Th$^+$ neurons than the standard control culture treated with Shh and FGF8 (SF control, see Fig. S2A,B in the supplementary material). This might indicate that the d5 Foxa2$^+$ Lmx1a$^+$ neural progenitors were not sufficiently specified toward an mDA fate. However, when further stimulated with Shh and FGF8 for 4 days, PD-treated cultures had an almost 4-fold increase in Th$^+$ neurons as compared with the SF control (PD, 52.3±8%; control, 13.5±9%) (Fig. 4B,C). Consistent with the increase of Th$^+$ neurons, we detected a near 3-fold increase in extracellular dopamine levels in PD-treated culture supernatant compared with the SF controls (see Fig. S2D in the supplementary material). Using another line of EpiSCs, which carrys a GFP reporter knocked into the *Pitx3* locus and drives mDA-specific GFP expression (Maxwell et al., 2005; Zhao et al., 2004), we found a substantial increase of Pitx3-GFP$^+$ cells in PD-treated cultures as compared with the SF controls (40±6.6% versus

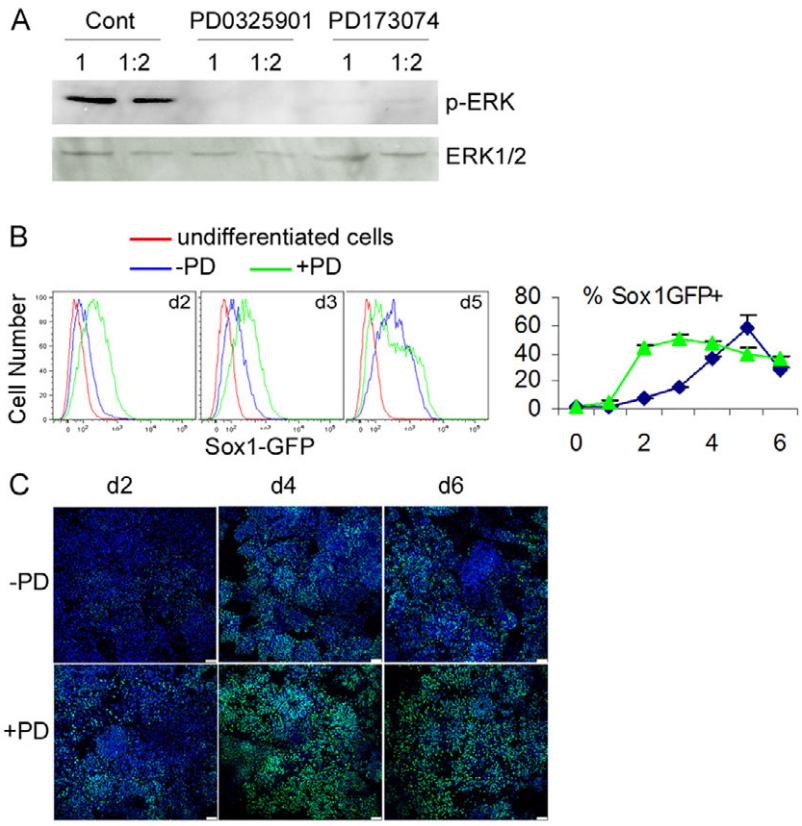


Fig. 2. FGF/ERK inhibition accelerates neural fate conversion of EpiSCs. (**A**) Western blot analysis for phospho-ERK in day-2 mouse EpiSC differentiation cultures treated with PD0325901 (PD) or PD173074. Samples were loaded undiluted (1) or diluted 1:2 in loading buffer. (**B**) MD cultures of Sox1-GFP EpiSCs in the presence or absence of PD. Sox1-GFP reporter expression was analyzed by flow cytometry and the percentage of Sox1-GFP$^+$ cells was determined from three independent cultures. Error bars indicate s.e.m. (**C**) Antibody staining for a neural rosette marker PLZF (green) in d2, d4 and d6 MD cultures with or without PD. DAPI labeling is in blue. Scale bars: 100 μm.

5±3.2%; $P<0.01$) (Fig. 4Be-h). Furthermore, the majority of Th$^+$ neurons in PD-treated cultures were Pitx3-GFP$^+$ (73.8±10.2%). This was also the case for other mDA and pan-DA neuronal markers such as Lmx1a (88.5±3.9%), Foxa2 (99.5±1.2%), Nurr1 (Nr4a2 – Mouse Genome Informatics) (85.4±4%) and VMAT (Slc18a1 – Mouse Genome Informatics) (85.6±12%) (Fig. 4D, see Fig. S2C in the supplementary material).

We next tested the efficacy of this experimental scheme on mouse iPSCs. Consistent with the report that FGF/ERK signaling is required for the progression from the naïve to the primed pluripotent state (Kunath et al., 2007), we found that PD treatment from d0 MD inhibited neural induction (data not shown). However, PD treatment for 2 days either at d1-3 or d2-4 MD significantly enhanced the production of Th$^+$ neurons compared with controls without PD (see Fig. S3 in the supplementary material). Similar to EpiSCs, iPSC-derived Th$^+$ neurons co-expressed Foxa2. Together, these data demonstrate that FGF signaling blockade during neural induction primes a midbrain regional fate in derived neural progenitors that is necessary for their terminal differentiation into DA neurons exhibiting midbrain characteristics.

Blockade of FGF signaling upon exit from the epiblast pluripotent state induces *Shh* and *Wnt1*

We next investigated how FGF inhibition confers mDA competence. Wnt1 and Shh are two essential signaling molecules that govern mDA progenitor fate specification and neurogenesis by forming regulatory loops with Lmx1a and Foxa2 (Andersson et al., 2006; Chung et al., 2009; Echelard et al., 1993). We examined *Wnt1* and *Shh* expression by qPCR in MD cultures treated with PD at d0-2. PD treatment resulted in a sharp increase in *Wnt1* transcript at d1, with a further increase at d2 (Fig. 5A, see Fig. S2B in the supplementary material). This effect was also observed with PD173074 (see Fig. S1A in the supplementary material). Intriguingly, *Wnt1* transcript returned to, or dropped below, control levels at d3-5 irrespective of the continued presence or absence of PD, indicating that early FGF/ERK blockade in EpiSCs initiates downstream molecular events that negatively regulate *Wnt1* expression. For *Shh*, similar (low) levels of transcript were detected at d1 in PD173074- or PD0325901-treated culture and in non-treated cultures. However, 1.5-fold and 4-fold increases of *Shh* transcript were observed at d2 in PD173074 and PD0325901, respectively. The level of *Shh* continued to increase (up to 8-fold) post-PD exposure between d3 and d5 (Fig. 5A, see Fig. S1A in the supplementary material). The kinetics of PD-mediated *Wnt1* induction at d1 and d2 MD is similar to that of *Lmx1a*, whereas the pattern of *Shh* upregulation is similar to that of *Foxa2* (Fig. 3, see Fig. S1B in the supplementary material), indicating a regulatory relationship.

We then investigated the contribution of Shh signaling to the upregulation of *Lmx1a* and *Foxa2*, as these genes are known to be induced by Shh (Andersson et al., 2006; Chung et al., 2009). We performed additional MD in the presence of the Shh inhibitor cyclopamine. This treatment abolished the induction of *Foxa2* by PD, suggesting that PD-mediated *Foxa2* regulation is strictly dependent on Shh signaling (Fig. 5B). Interestingly, cyclopamine did not affect PD-induced *Lmx1a* expression at d1-2, but did exhibit an effect at d3 and d5 (Fig. 5B). Because the *Lmx1a* transcript was already induced at d1 MD after 24 hours of FGF/ERK inhibition, and because *Shh* was not induced until d2 (Fig. 5A,B, see Fig. S1B in the supplementary material), our data suggest that the early induction of *Lmx1a* by PD might be elicited by Wnt1 in an Shh-independent feed-forward fashion. However, sustained expression of *Lmx1a* between d3 and d5 MD requires Shh signaling.

DEVELOPMENT

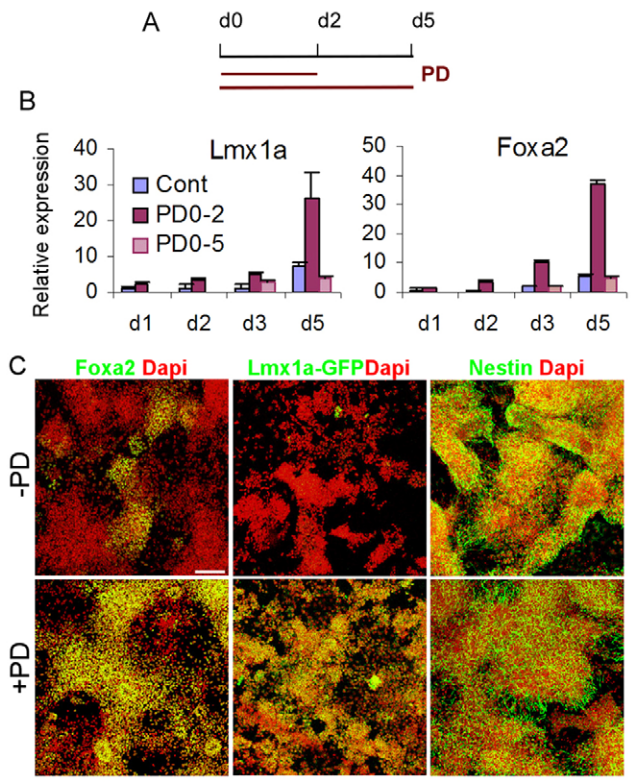


Fig. 3. FGF/ERK blockade at the onset of neural fate conversion induces mDA regulatory genes. (**A**) Experimental schemes. E14tg2a mouse EpiSC monolayer cultures were exposed to PD0325901 (PD) from d0 MD for either 2 days (PD0-2) or 5 days (PD0-5). Cultures were harvested at d1, d2, d3 and d5 MD. (**B**) qPCR analysis of *Lmx1a* and *Foxa2*. The value of the d1 MD control (Cont) was set as 1. Error bars indicate mean±s.e.m. of two sets of experiments performed in duplicate. (**C**) d5 MD of Lmx1a-GFP EpiSCs exposed to PD from d0 MD for 2 days were immunostained for Foxa2 and GFP (both green) and counterstained with DAPI (red). Scale bar: 100 μm.

FGF/ERK inhibition promotes mDA characteristics via modulation of anterior-posteriorization and the maintenance of Otx2

Although PD induces *Shh*, we found that replacing PD with Shh at d0-2 did not recapitulate the highly efficient production of mDA neurons at d14 MD (see Fig. S2A-C in the supplementary material). This could be due to the relatively late and weaker stimulation of Lmx1a and Foxa2 by Shh compared with PD (see Fig. S4A in the supplementary material). However, it is also possible that FGF/ERK inhibition induces other properties that are necessary for mDA fate specification.

An attractive hypothesis is that blocking FGF/ERK maintains anterior neural character, as FGF is known to promote caudal attributes (for a review, see Wilson and Rubenstein, 2000). Consistent with this, we found using qPCR analysis that cultures exposed to PD for 2 days consistently exhibited reduced levels of *Gbx2* (Fig. 5C), which encodes a homeobox protein that is expressed in the anterior hindbrain and prospective spinal cord. By contrast, 2 days of stimulation by Shh had no effect on *Gbx2* expression. Also consistent with this hypothesis, neural progenitors co-expressing Otx2, an anteriorly expressed homeobox protein that forms a mutually repressive circuit with Gbx2, were significantly more abundant in PD-treated cultures than in control cultures (Fig. 5E, see Fig. S4B in the supplementary material) (Millet et al., 1999). Again, Shh in place of PD at d0-2 MD did not increase the number of $Otx2^+$ neural progenitors at d5 MD (Fig. 5E,F). Furthermore, PD-treated and non-treated cultures exposed to Shh and FGF8 for a further 4 days at d5-9 maintained the differential expression of Otx2 at d9 MD (Fig. 5D-F). These findings suggest that FGF/ERK blockade promotes the generation of anterior neural progenitors by suppressing posteriorization.

FGF signaling from the anterior neural ridge plays an important role in the formation of forebrain (Paek et al., 2009). We therefore determined the effect of FGF/ERK inhibition on the expression of the telencephalic gene markers *Six3* and *Foxg1*. As expected, increases of *Six3* and *Foxg1* transcripts were readily detected from d2 and d3 MD, respectively, in the control cultures without PD (Fig. 5G). By contrast, PD-treated cultures did not upregulate either of the telencephalic marker genes. Furthermore, we detected a sharp increase in the mesencephalic transcription factor genes engrailed 1 (*En1*) at d1 and *En2* from d2 MD in PD-treated, but not Shh-treated, cultures (Fig. 5C). Taken together with the finding that PD induces *Wnt1*, these data suggest that FGF/ERK inhibition confers a midbrain bias within the $Otx2^+$ anterior neural progenitor population. Otx2 has been shown to play a regulatory role in *Lmx1a* transcription and in the proliferation and differentiation of mDA progenitors (Brodski et al., 2003; Chung et al., 2009; Omodei et al., 2008; Ono et al., 2007). Thus, the retention of Otx2 in neural progenitors, and the early induction of isthmus-patterning molecules by FGF/ERK inhibition, are likely to serve as additional attributes essential for the observed efficient production of mDA neurons.

It is worth noting that, at d9 MD following 4 days exposure to Shh/FGF8, PD-treated and untreated control cultures had similar proportions of $Foxa2^+/Lmx1a^+$ neural progenitors (Fig. 5E), indicating that either Foxa2/Lmx1a neural progenitor expression at later stage of MD, or Foxa2/Lmx1a expression alone, is not sufficient for mDA commitment, at least in pluripotent stem cell cultures in vitro.

Shh and Fgf8 participate in distinct regulatory pathways governing mDA fate specification and differentiation

Our study shows that both Shh and Fgf8 are necessary during the period d5-9 for achieving the highest number of mDA neurons: those co-expressing Th, Pitx3, Lmx1a and Foxa2. Cultures treated with PD followed by Shh alone contained a large number of faintly stained Th^+ cells with immature neuronal morphology. In addition, few of these Th^+ neurons co-expressed Pitx3-GFP (see Fig. S2 in the supplementary material). By contrast, Th^+ neurons present in cultures treated with PD, followed by FGF8 alone, were mature in appearance and mostly $Pitx3\text{-}GFP^+$. However, the number of Th^+ neurons was similar to that found in the no-PD control cultures. These observations suggest that PD-generated d5 neural progenitors require sustained Shh signaling to specify a dopaminergic phenotype, whereas FGF8 facilitates progenitor differentiation involving Pitx3 expression.

Day 5-9 MD spans the peak of neurogenesis during which the expression of neuronal subtype determination factors rapidly increases (Fig. 1; data not shown). To further elucidate how Shh and FGF affect neural progenitor behavior, we examined their effect on the expression of a number of genes that encode mDA and non-dopaminergic neural progenitor domains by RT-PCR (Fig.

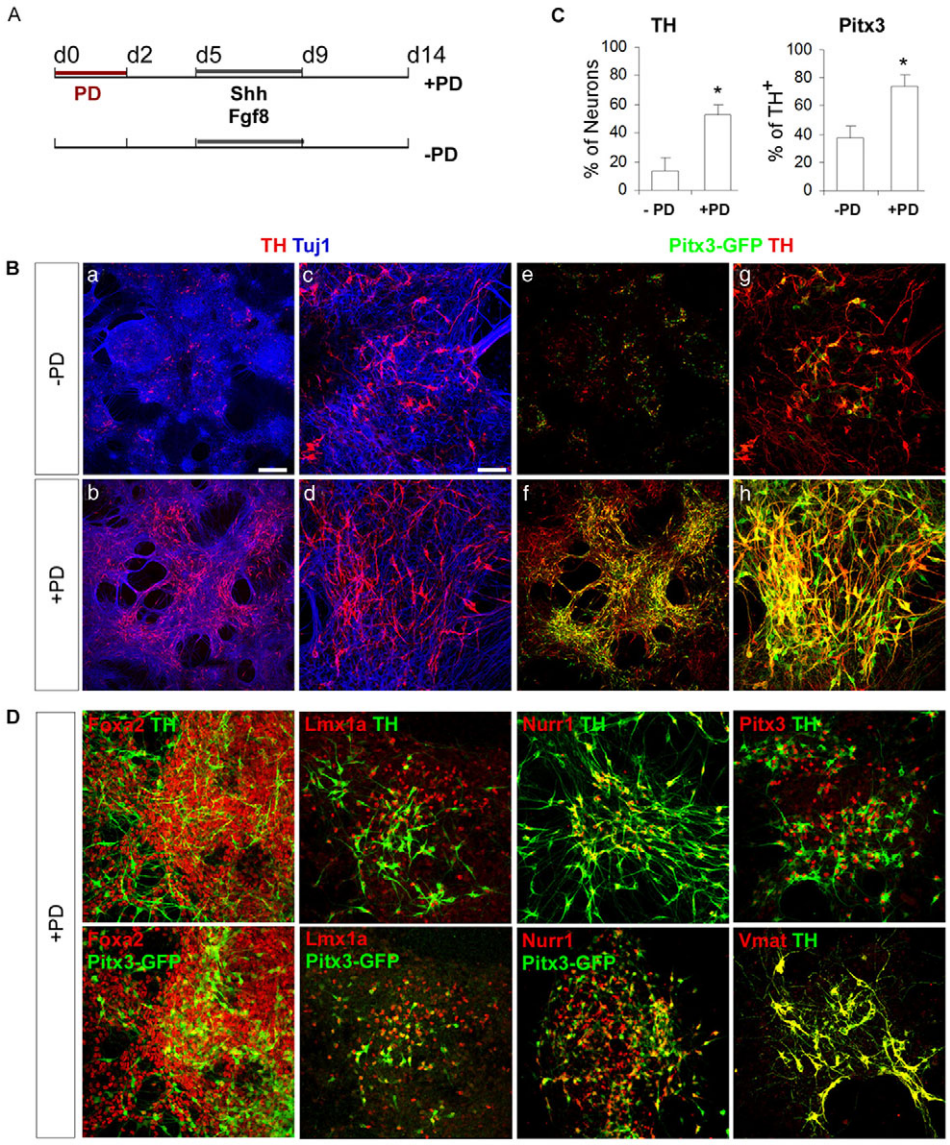


Fig. 4. Stepwise inactivation and activation of FGF/ERK signaling leads to the highly efficient production of dopamine neurons exhibiting mDA components. (**A**) Outline of the experiment using the Pitx3-GFP EpiSCs. (**B**) Immunostaining of mouse d14 MD cultures for (**a-d**) Th (red) and Tuj1 (blue) as well as (**e-h**) Th (red) and Pitx3-GFP (green). (**C**) Quantification of the immunostaining in B, illustrating the percentage of Th^+ neurons and Th^+ neurons co-expressing Pitx3. Mean±s.e.m. *, $P<0.01$ relative to no-PD control (Student's *t*-test). (**D**) Immunostaining of d14 MD cultures for various midbrain and pan-DA markers. Scale bars: 200 μm for Ba,b,e,f; 50 μm for Bc,d,g,h,D.

6). We found that Shh added either at d3-6 MD or d5-9 MD induced a further increase in *Foxa2* and *Msx1* expression, although it had no effect on either *Lmx1a* or *Shh* (Fig. 6B). FGF8 stimulation, by contrast, led to significant upregulation of *Wnt1*, *En1* and *En2*, which are all known to participate in mDA differentiation and survival (Alberi et al., 2004; Joksimovic et al., 2009) (Fig. 6B,C).

We also found that cultures without any exogenous stimuli experienced a sharp increase of gene transcripts controlling GABAergic fate, such as *Gata2* (38-fold), *Helt* (293-fold) and *Gad1* (401-fold) (Fig. 6D), consistent with the suggestion that in vitro-derived neurons are mostly GABAergic (Kala et al., 2009; Nakatani et al., 2007). However, Shh stimulation at d5-9 suppressed the expression of these genes, and progenitors exposed to sequential PD and Shh treatment showed a further reduction in these non-DA markers. Thus, the fold increases in *Helt* and *Gad1* transcripts in the PD-Shh cultures were only 10% of the level of Shh alone cultures and were less than 1% of the level of no factor controls. Together, our data demonstrate that Shh and Fgf8 participate in distinct regulatory pathways that contribute to efficient mDA fate specification and differentiation.

Interestingly, FGF8 treatment, with or without Shh, from d3 MD immediately after PD treatment eliminated the PD-mediated upregulation of *Lmx1a*, *Foxa2*, *Shh* and *Msx1* (Fig. 6B). Consequently, we observed little increase in the number of Th^+ neurons in these cultures at d14 MD compared with the untreated control (data not shown). Together with the finding that persistent FGF/ERK blockade after neural induction abolishes PD-mediated induction of mDA regulators (Fig. 3B, Fig. 5B), our data indicate that a period of autocrine FGF/ERK signaling is crucial for newly converted neural progenitors to process the patterning information that leads to the eventual commitment of the dopaminergic neuron fate.

In vitro-generated mDA neurons exhibit functional neuronal characteristics

We examined whether dopamine neurons generated using these protocols had functional neuron-like properties. We took advantage of the Pitx3-GFP reporter system (Zhao et al., 2004), in which we could target dopamine neurons by their GFP signal (Fig. 7A). We conducted whole-cell recordings at d14-16 MD, from GFP^+ cells differentiated with or without PD. First we examined the passive

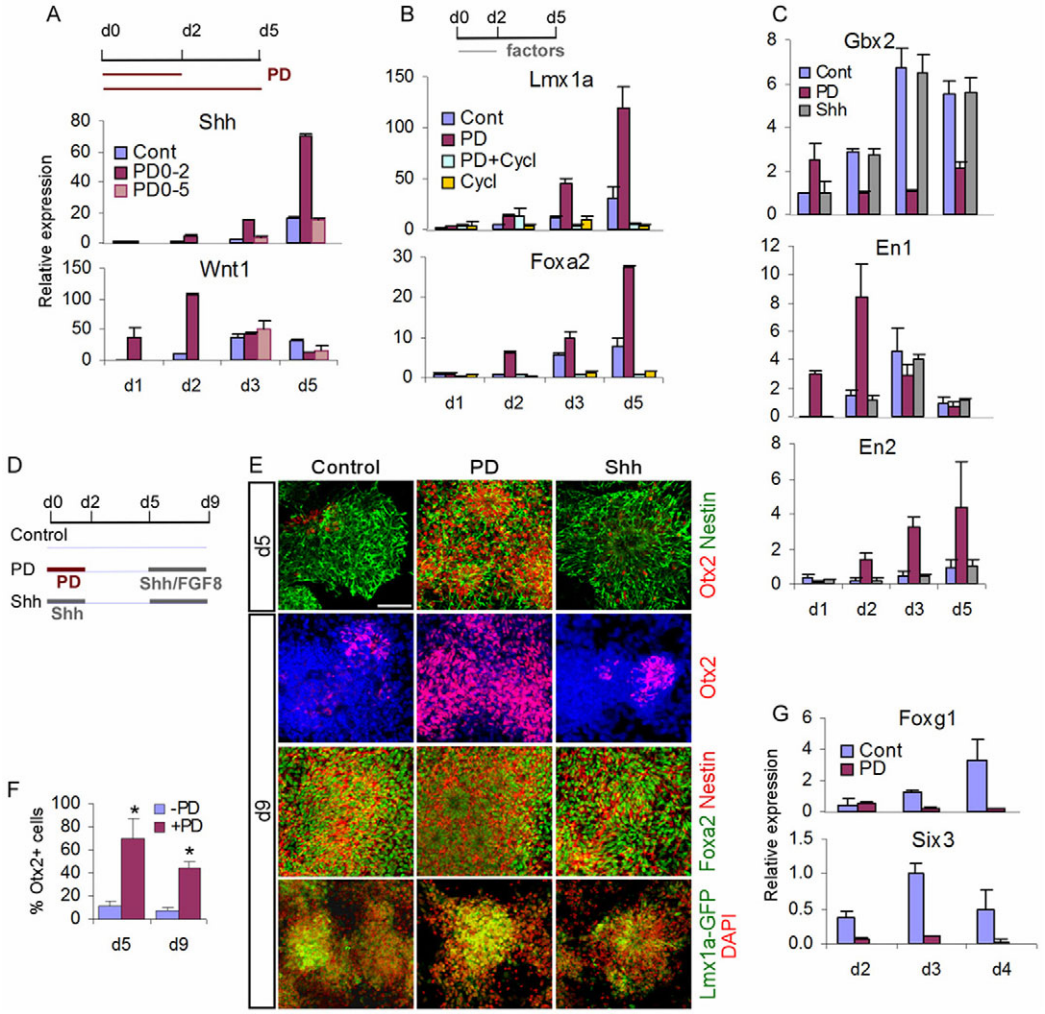


Fig. 5. FGF inhibition directs a midbrain neural progenitor fate. (**A**) Mouse E14tg2a EpiSC monolayer cultures were exposed to PD0325901 (PD) from d0 MD for 2 (PD0-2) or 5 (PD0-5) days. Cultures were harvested at day 1, 2, 3 or 5 for qPCR analysis of *Shh* and *Wnt1*. (**B**) E14tg2a EpiSC MD cultures were treated with PD or cyclopamine (Cycl) or a combination of the two as indicated. Cultures were harvested at day 1, 2, 3 or 5 for qPCR analysis of *Lmx1a* and *Foxa2*. (**C**) EpiSCs were differentiated in the presence of PD or Shh for 2 days from d0 MD, as in B, and analyzed for *Gbx2*, *En1* and *En2* by qPCR at d1-3 and d5 MD. (**D**) Experimental schemes for E-G. (**E**) Immunostaining of d5 and d9 MD E14tg2a (top two rows) and Lmx1a-GFP (bottom two rows) EpiSCs. Antibodies against Otx2 (red) and nestin (green), or Otx2 alone (red), were used in E14tg2a EpiSCs. Foxa2 (green), nestin (red) and GFP (green) were used in the Lmx1a-GFP panels. Scale bar: 100 µm. (**F**) Quantification of immunostaining in E illustrating the percentage of cells expressing Otx2. Mean±s.e.m. of ten fields from two independent experiments. *, $P<0.01$ relative to no-PD control (Student's *t*-test). (**G**) qPCR analysis of the telencephalic markers *Six3* and *Foxg1* in d2-4 MD cultures with or without PD. Data in A-C,G are mean±s.e.m. of three replicate cultures.

membrane properties of the differentiated cells. All cells exhibited a negative resting membrane potential typical of neurons (control, –67±1.3 mV, $n=6$; PD, –37±4.6, $n=13$; $P<0.05$). Interestingly, cells treated with PD had a resting membrane potential that was significantly more depolarized than that of control cells. Both groups had similar input resistance (control, 422±198 MΩ, $n=8$; PD, 558±79 MΩ, $n=15$; $P>0.05$) and whole-cell capacitance (control, 9.6±1 pF, $n=8$; PD, 12±5 pF, $n=15$; $P>0.05$) values, suggesting that PD treatment did not affect cell size.

At d14-16 MD, 14% of these cells (control, 1/7 cells; PD, 2/14 cells) exhibited multiple spontaneous action potentials (Fig. 7B). In all cells, application of a depolarizing current pulse evoked an overshooting action potential ($n=21$), and 19% of cells (control, 1/7 cells; PD, 3/14 cells) fired multiple action potentials in response to the stimulus (Fig. 7C). The cells that were spontaneously active fired at a low frequency (0.95±0.14 Hz; $n=3$) and in an irregular pattern (CV-ISI, 1.19±0.24; $n=3$). However, 67% (6/9) of cells in MD cultures at d40 or later fired spontaneous action potentials. Importantly, these older cells exhibited the pacemaker-like spontaneous activity (Fig. 7E) that is characteristic of mDA neurons (3.54±0.8 Hz; CV-ISI, 0.49±0.08; $n=6$). In voltage-clamp mode, all differentiated cells exhibited a large outward current, typical of a delayed-rectifier K^+ current (control, 2.91±0.39 nA, $n=7$; PD, 2.19±0.28 nA, $n=15$; $P>0.05$) (Fig. 7D, left panel). Fast-activating, fast-inactivating inward currents were also observed that were typical of Na^+ currents (control, 1.38±0.14 nA, $n=7$; PD, 1.69±0.25 nA, $n=15$; $P>0.05$) (Fig. 7D, right panel). Taken together, these recordings show that dopaminergic cells generated using our differentiation protocol exhibit functional, neuron-like properties.

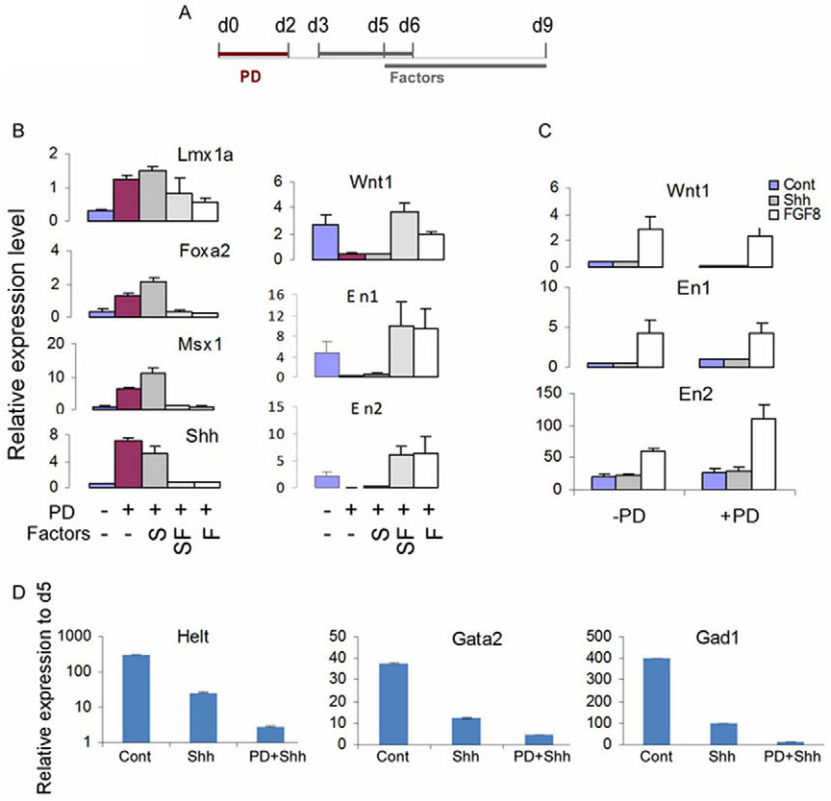


Fig. 6. Shh and FGF8 act on distinct aspects of mDA neuron differentiation. (**A**) Experimental scheme for data in B and C. (**B**) qPCR analysis of mouse d6 MD cultures for the ventral mesencephalic regulator genes *Lmx1a*, *Foxa2*, *Msx1* and *Shh* and the isthmus-expressed midbrain patterning genes *Wnt1*, *En1* and *En2*. (**C**) qPCR analysis at d9 MD for *Wnt1*, *En1* and *En2*. PD0325901 (PD) was added for 2 days from d0-2, whereas Shh and/or FGF8 were added from d5. (**D**) qPCR analysis of *Helt*, *Gata2* and *Gad1* in d5 and d9 MD cultures. Expression levels were examined in control MD cultures with no added factors, control cultures treated with Shh between d5 and d9 alone, as well as in cultures treated with PD at d0-2 followed by Shh between d5 and d9 MD. Data in B and C are mean±s.e.m. of two experiments performed in duplicate, whereas data in D are mean± s.e.m. of triplicate cultures from one representative experiment.

A conserved role for FGF/ERK signaling in mDA fate specification of hESCs

Finally, we asked whether the modulation of FGF/ERK signaling could also promote mDA neuron differentiation of hESCs. H1 and H7 hESCs were induced to differentiate by a 3-day exposure to Smad inhibitors. Under this condition, the primitive ectoderm marker *FGF5* peaked at d3 MD and the majority of the cells became NES$^+$ neural precursors at d11 for H1 and d20 for H7. To mimic the condition experienced by the mouse cells, we applied PD for 4 days from d3 MD (Fig. 8A). Similar to the finding in mouse cells, PD treatment in hESCs also resulted in an increase in *OTX2*, *WNT1*, *EN1/2* and in the suppression of *SIX3*, *FOXG1* and *GBX2* (Fig. 8B), indicating the induction of a midbrain fate and the suppression of caudalization as well as forebrain induction. We also observed similar induction of ventral fate regulators such as *SHH*, *LMX1A*, *FOXA2* and *MSX1*. Interestingly, PD treatment led to robust induction of *DMRT5*, a newly identified midbrain floor plate marker that confers mDA progenitor identity following forced expression in ESC-derived neural progenitors (Fig. 8B) (Gennet et al., 2011).

Consistent with the transcript analysis, the major population of NES$^+$ progenitors in PD-treated cultures co-expressed OTX2, FOXA2 and DMRT5 (Fig. 8C). Of the PD-treated cells, 47.5±7.1% were FOXA2$^+$ OTX2$^+$, a molecular profile characteristic of mDA neural progenitors (see Fig. S5 in the supplementary material). By contrast, this cellular phenotype only constituted 6.8±1.5% of the control population. As cultures progressed toward neuronal differentiation at d35 MD, we detected numerous TH$^+$ neurons co-expressing FOXA2, LMX1A and PITX3 in PD-treated cultures (Fig. 8D,E), which was in dramatic contrast to the no-PD controls, in which LMX1A$^+$ and PITX3$^+$ cells were rarely detected (data not shown). Furthermore, we found that, although FOXA2$^+$ cells were present in the no-PD cultures, they were mostly mutually exclusive with TH$^+$ neurons (Fig. 8D). Thus, PD treatment resulted in a near 7-fold increase of FOXA2$^+$ TH$^+$ neurons when compared with no-PD controls (Fig. 8D-F). Together, the above data demonstrate that FGF/ERK signaling plays a conserved role in mouse and human pluripotent stem cells.

DISCUSSION

Dopamine neurons derived from pluripotent stem cells constitute a powerful resource in neurobiological research. In the context of patient-specific iPS cells, in vitro-derived dopamine neurons also provide a valuable tool for drug discovery, modeling of Parkinson's disease and as a potential alternative cell source for transplantation-based therapy.

Here, we demonstrate a functional impact of the FGF/ERK signaling level on the course of mDA neuron differentiation of mouse and human pluripotent stem cells. Pharmacological inactivation of FGF/ERK activity upon exit of the lineage-primed epiblast pluripotent state initiates transcription activities that govern early mesencephalic patterning of both the anterior-posterior and dorsal-ventral axes, leading to the induction of mDA neural progenitor characteristics and maintenance of dopaminergic competence. The consolidation of these characteristics, however, requires a period of autocrine/paracrine FGF/ERK signaling immediately after neural induction. Either continued FGF/ERK blockade in newly derived neural progenitors, or enhancing FGF signaling activity by exogenous FGF8 in these cells, abolishes the effects of PD. These findings demonstrate a previously unrecognized inhibitory role of FGF/ERK in the induction of ventral midbrain neural progenitors and offer a novel strategy for mDA neuron production from mouse and human pluripotent stem cells and iPSCs. Furthermore, the current method represents a simple, small-molecule-based paradigm for significantly improved efficiency and high

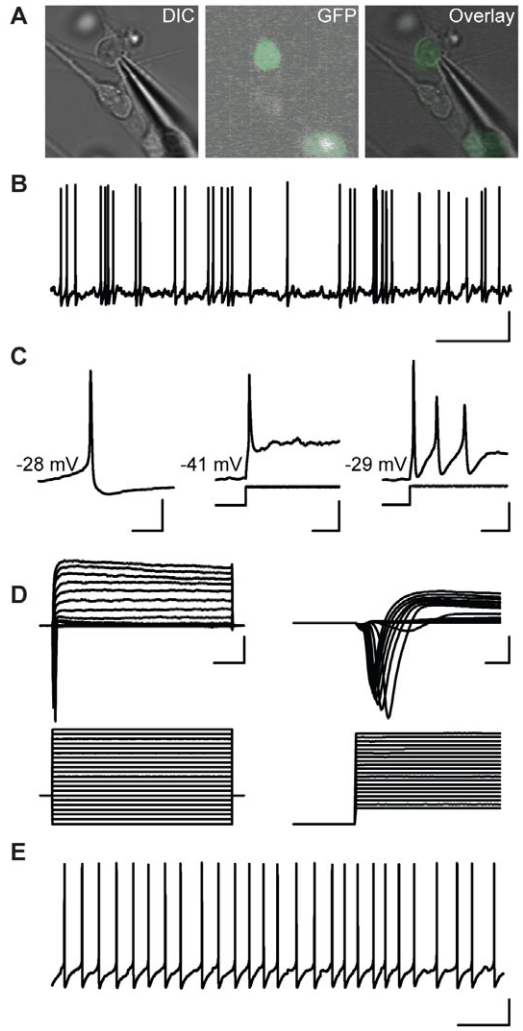


Fig. 7. Pitx3-GFP$^+$ cells exhibit functional neuron-like electrophysiological properties. (**A**) DIC and GFP image showing a recording pipette patched onto a mouse Pitx3-GFP$^+$ cell. (**B**) Spontaneous action potentials fired by a day-14 neuron. Vertical scale bar, 20 mV; horizontal scale bar, 5 mseconds. (**C**) A single spontaneous action potential (left). A single action potential fired in response to a 50 pA depolarizing current pulse (middle). Multiple action potentials fired in response to a 50 pA depolarizing current pulse (right). Vertical bars, 20 mV; horizontal bars, 50, 100 and 100 mseconds, respectively. (**D**) Outward current evoked by a serious of voltage steps (left). Fast inward current evoked by a series of voltage steps (right). Vertical bars, 1 nA; horizontal bars, 50 mseconds. (**E**) Pacemaker-like spontaneous firing a day-41 neuron. Vertical bar, 20 mV; horizontal bar, 1 second.

reproducibility compared with previously reported transgene-free protocols. Importantly, our strategy directs a midbrain regional identity in the derived dopamine neurons, a property that is essential for functional integration of transplanted dopamine neurons in the Parkinsonian brain (Hudson et al., 1994).

Stimulation of ESC-derived neural progenitors with Shh and FGF8 is used by almost all dopamine differentiation protocols (Barberi et al., 2003; Kim et al., 2002; Lee et al., 2000; Perrier et al., 2004; Yan et al., 2005). However, unless combined with genetic manipulation of mDA transcription factors, such as Pitx3 or Lmx1a (Andersson et al., 2006; Chung et al., 2002; Konstantoulas et al., 2010; Maxwell et al., 2005), the midbrain regional identity of the dopamine neurons generated has remained uncertain. Furthermore, the yield of Th$^+$ neurons has often proved unreliable between experiments and even highly variable between different microscopic fields within a single culture. A major limiting factor is the temporal and spatial heterogeneity of ESC-derived neural progenitors. Our findings demonstrate that the above issues can be addressed using EpiSCs. We found that, in the absence of FGF/ERK signaling manipulation, nearly 40% of Th$^+$ neurons generated by EpiSCs already co-expressed Pitx3. This represents a significant improvement over ESC-derived monolayer cultures, where Pitx3$^+$ neurons are rarely observed (Andersson et al., 2006; Friling et al., 2009; Parmar and Li, 2007). This improvement is likely to be due to the more synchronous conversion of EpiSCs to the neuroepithelial fate, which would allow for the effective capture of mDA-competent progenitors.

However, without additional FGF/ERK inhibitor treatment at the neural induction phase, the total numbers of Th$^+$ Pitx3$^+$ cells remained low due to the overall poor efficiency in producing Th$^+$ cells. The early induction of both *Lmx1a* and *Foxa2* by inhibiting FGF receptor or ERK is likely to be a key factor in the observed high efficiency in our experiments. This hypothesis is based on the following observations: (1) d5 PD-treated (EpiSC) MD cultures are highly enriched for Foxa2$^+$ Lmx1a$^+$ neural progenitors compared with untreated controls; (2) although Shh treatment in d5-9 MD results in comparable numbers of Foxa2$^+$ Lmx1a$^+$ cells in PD-primed and no-PD cultures, mDA neuron production was not enhanced in the manner observed with PD treatment; (3) replacing PD with Shh, which turned out to be a slower and less effective inducer of *Lmx1a* and *Foxa2*, also led to poor mDA production; and (4) previous reports have credited the dopaminergic-promoting activity of Lmx1a to its early transgene expression in ESC-derived neural progenitors (Friling et al., 2009) and indicated that Lmx1a functions by cooperating with Foxa2 in specifying mDA fate during midbrain development (Lin et al., 2009; Nakatani et al., 2009).

The robust induction of *Wnt1* and its targets in naïve neural progenitors is likely to be a key downstream mediator that confers the observed early induction of *Lmx1a*, in light of the recent finding that it can be directly regulated by Wnt1/β-catenin signaling (Chung et al., 2009). The same study also showed that, although Otx2 itself had no effect in promoting the expression of terminal mDA neuronal marker genes such as *Th*, *Pitx3* and *Nurr1*, it significantly enhanced the regulatory effect of Lmx1a and Foxa2 on the expression of these genes. Thus, Otx2 plays a permissive role in Lmx1a/Foxa2-mediated mDA neuronal production. It is worth noting that a significant effect of FGF/ERK blockade is the maintenance of Otx2 in derived neural progenitors.

Our study also shows that, in addition to inducing a regulatory cascade for ventralizing nascent neural progenitors, FGF/ERK inhibition suppresses forebrain specification while promoting anterior neural induction, as demonstrated by the strong and consistent repression of the forebrain regulator genes *Six3* and *Foxg1* and the hindbrain marker *Gbx2*. Thus, blocking FGF/ERK at the onset of neural induction leads to a direct and early induction of the midbrain fate at the expense of forebrain and caudal neural fates. Our finding is consistent with the developmental role of FGF signaling in regionalization of the forebrain (Corson et al., 2003; Shimamura and Rubenstein, 1997).

Furthermore, we demonstrate the importance of precise temporal control of cell signaling and its cross-regulation with other signaling pathways in mDA neuronal fate specification. During development,

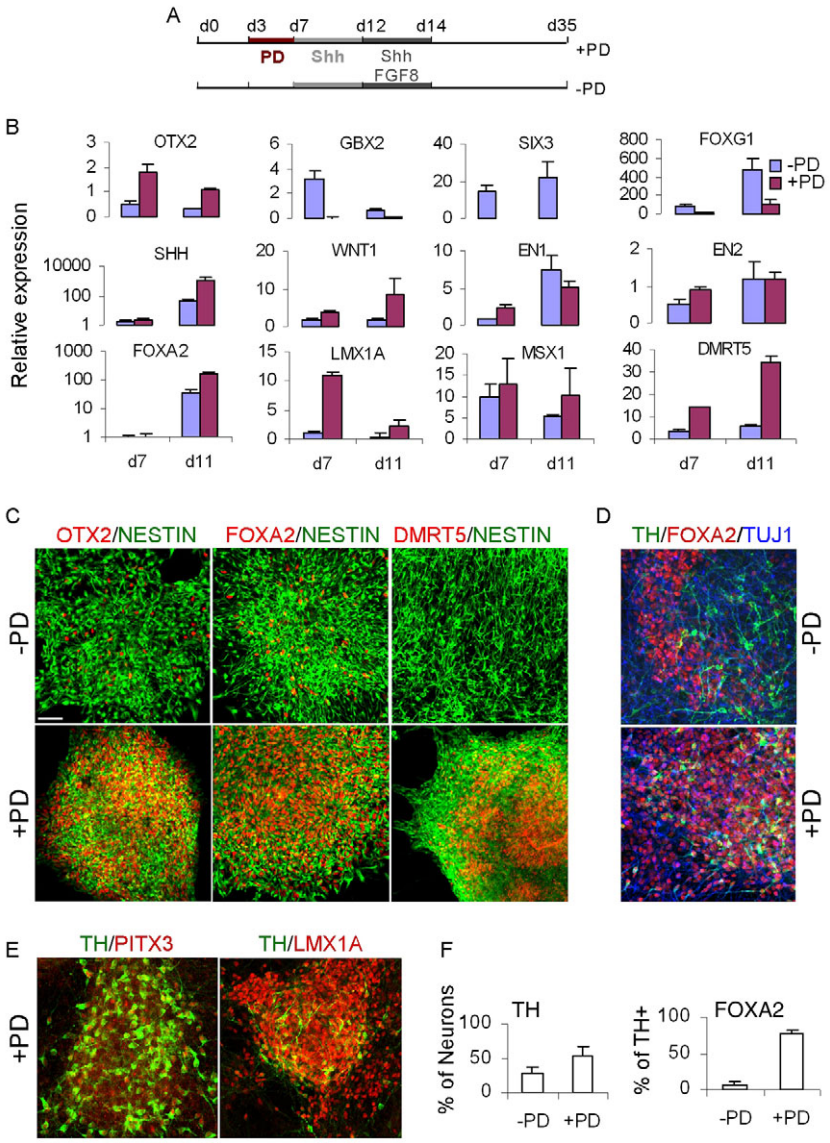


Fig. 8. Generation of mDA neurons from human ESCs. (**A**) Experimental schemes. (**B**) qPCR analysis of regional markers in d7 and d11 H7 MD cultures with or without PD0325901 (PD). Data are mean±s.e.m. of three replicate cultures. (**C**) Double immunostaining of d13 H1 MD cultures for nestin (green) plus OTX2, FOXA2 or DMRT5 (all in red). (**D**) Triple antibody staining of d35 H7 cultures for FOXA2 (red), TH (green) and β3-tubulin (TUJ1, blue). (**E**) Immunostaining of PD-treated d32 H7 MD cultures for PITX3 (red) and TH (green), and for LMX1Aa (red) and TH (green). (**F**) Quantification of the immunostaining in E, illustrating the percentage of TH^+ neurons and TH^+ neurons co-expressing FOXA2. Error bars indicate s.e.m. Scale bars: 75 μm.

Fgf8-mediated signaling can induce the patterned expression of many midbrain/rostral hindbrain genes and is required for normal development of the midbrain and cerebellum (Chi et al., 2003; Liu et al., 1999; Meyers et al., 1998). Fgf8-induced Wnt1 and engrailed are key regulators of midbrain and cerebellum patterning, as well as of the differentiation and survival of dopamine neurons (Prakash et al., 2006; Simon et al., 2001; Tang et al., 2009). In EpiSC-derived neural cultures, after an initial burst of upregulation induced by PD exposure, Wnt1 expression was subsequently reduced to a level below the no-PD control by unknown factors in the newly generated neural progenitors in d3-5 MD. This is the period when Shh, Lmx1a and Foxa2 expression levels continued to rise. Given that Shh and Wnt1 play opposing roles with regard to mDA neurogenesis (Joksimovic et al., 2009), our findings suggest that the delay in FGF reactivation, which suppresses Wnt1 levels, might be crucial for achieving high numbers of Th^+ neurons by consolidating Lmx1a and Foxa2 expression via Shh signaling.

From a technological standpoint, we describe a novel method of mDA neuron differentiation that employs temporally controlled exposure of human and mouse pluripotent stem cells to an FGF/ERK-deficient environment. The highly reliable nature of this method was demonstrated using five independent mouse EpiSC lines, a mouse iPS cell line and two human ESC lines. This protocol offers several advantages over current methods of generating midbrain-specific DA neurons in that it is adherent culture-based and free from genetic manipulation and thus could be readily applied to other cell lines of interest. Furthermore, because it is fully chemically defined, this paradigm could be readily adapted for use in a clinical setting or scaled up for toxicity and drug screening relevant to developing new therapeutics for Parkinson's disease.

Acknowledgements

We thank Dr Michael German for Lmx1a antibody, Dr Marten Smidt for Pitx3 antibody, Drs Johan Ericson and Thomas Perlmann for the Lmx1a-GFP ESCs, Dr Dirk Dormann for expert advice on confocal microscopy and Drs Austin Smith, Tilo Kunath and Tristan Rodriguez for discussion and critical reading of the manuscript.

Funding

This work was supported by the UK Medical Research Council (MRC, G117/560, U120005004) and EU framework program 7 NeuroStemcell, no. 222943 to M.L.; and by the MRC (U120085816) and a Royal Society University Research Fellowship to M.A.U. M.L. was an MRC Senior Non-Clinical Research Fellow. Deposited in PMC for release after 6 months.

Competing interests statement
The authors declare no competing financial interests.

Supplementary material
Supplementary material for this article is available at
http://dev.biologists.org/lookup/suppl/doi:10.1242/dev.066746/-/DC1

References

Alberi, L., Sgado, P. and Simon, H. H. (2004). Engrailed genes are cell-autonomously required to prevent apoptosis in mesencephalic dopaminergic neurons. *Development* **131**, 3229-3236.
Andersson, E., Tryggvason, U., Deng, Q., Friling, S., Alekseenko, Z., Robert, B., Perlmann, T. and Ericson, J. (2006). Identification of intrinsic determinants of midbrain dopamine neurons. *Cell* **124**, 393-405.
Barberi, T., Klivenyi, P., Calingasan, N. Y., Lee, H., Kawamata, H., Loonam, K., Perrier, A. L., Bruses, J., Rubio, M. E., Topf, N. et al. (2003). Neural subtype specification of fertilization and nuclear transfer embryonic stem cells and application in parkinsonian mice. *Nat. Biotechnol.* **21**, 1200-1207.
Bouhon, I. A., Kato, H., Chandran, S. and Allen, N. D. (2005). Neural differentiation of mouse embryonic stem cells in chemically defined medium. *Brain Res. Bull.* **68**, 62-75.
Brodski, C., Weisenhorn, D. M., Signore, M., Sillaber, I., Oesterheld, M., Broccoli, V., Acampora, D., Simeone, A. and Wurst, W. (2003). Location and size of dopaminergic and serotonergic cell populations are controlled by the position of the midbrain-hindbrain organizer. *J. Neurosci.* **23**, 4199-4207.
Brons, I. G., Smithers, L. E., Trotter, M. W., Rugg-Gunn, P., Sun, B., Chuva de Sousa Lopes, S. M., Howlett, S. K., Clarkson, A., Ahrlund-Richter, L., Pedersen, R. A. et al. (2007). Derivation of pluripotent epiblast stem cells from mammalian embryos. *Nature* **448**, 191-195.
Chambers, S. M., Fasano, C. A., Papapetrou, E. P., Tomishima, M., Sadelain, M. and Studer, L. (2009). Highly efficient neural conversion of human ES and iPS cells by dual inhibition of SMAD signaling. *Nat. Biotechnol.* **27**, 275-280.
Chi, C. L., Martinez, S., Wurst, W. and Martin, G. R. (2003). The isthmic organizer signal FGF8 is required for cell survival in the prospective midbrain and cerebellum. *Development* **130**, 2633-2644.
Chung, S., Sonntag, K. C., Andersson, T., Bjorklund, L. M., Park, J. J., Kim, D. W., Kang, U. J., Isacson, O. and Kim, K. S. (2002). Genetic engineering of mouse embryonic stem cells by Nurr1 enhances differentiation and maturation into dopaminergic neurons. *Eur. J. Neurosci.* **16**, 1829-1838.
Chung, S., Hedlund, E., Hwang, M., Kim, D. W., Shin, B. S., Hwang, D. Y., Jung Kang, U., Isacson, O. and Kim, K. S. (2005). The homeodomain transcription factor Pitx3 facilitates differentiation of mouse embryonic stem cells into AHD2-expressing dopaminergic neurons. *Mol. Cell. Neurosci.* **28**, 241-252.
Chung, S., Leung, A., Han, B. S., Chang, M. Y., Moon, J. I., Kim, C. H., Hong, S., Pruszak, J., Isacson, O. and Kim, K. S. (2009). Wnt1-lmx1a forms a novel autoregulatory loop and controls midbrain dopaminergic differentiation synergistically with the SHH-FoxA2 pathway. *Cell Stem Cell* **5**, 646-658.
Corson, L. B., Yamanaka, Y., Lai, K. M. and Rossant, J. (2003). Spatial and temporal patterns of ERK signaling during mouse embryogenesis. *Development* **130**, 4527-4537.
Echelard, Y., Epstein, D. J., St-Jacques, B., Shen, L., Mohler, J., McMahon, J. A. and McMahon, A. P. (1993). Sonic hedgehog, a member of a family of putative signaling molecules, is implicated in the regulation of CNS polarity. *Cell* **75**, 1417-1430.
Ferri, A. L., Lin, W., Mavromatakis, Y. E., Wang, J. C., Sasaki, H., Whitsett, J. A. and Ang, S. L. (2007). Foxa1 and Foxa2 regulate multiple phases of midbrain dopaminergic neuron development in a dosage-dependent manner. *Development* **134**, 2761-2769.
Friling, S., Andersson, E., Thompson, L. H., Jonsson, M. E., Hebsgaard, J. B., Nanou, E., Alekseenko, Z., Marklund, U., Kjellander, S., Volakakis, N. et al. (2009). Efficient production of mesencephalic dopamine neurons by Lmx1a expression in embryonic stem cells. *Proc. Natl. Acad. Sci. USA* **106**, 7613-7618.
Gaspard, N., Bouschet, T., Hourez, R., Dimidschstein, J., Naeije, G., van den Ameele, J., Espuny-Camacho, I., Herpoel, A., Passante, L., Schiffmann, S. N. et al. (2008). An intrinsic mechanism of corticogenesis from embryonic stem cells. *Nature* **455**, 351-357.
Gennet, N., Gale, E., Nan, X., Farley, E., Takacs, K., Oberwallner, B., Chambers, D. and Li, M. (2011). Doublesex and mab-3-related transcription factor 5 promotes midbrain dopaminergic identity in pluripotent stem cells by enforcing a ventral-medial progenitor fate. *Proc. Natl. Acad. Sci. USA* **108**, 9131-9136.
Guo, G., Yang, J., Nichols, J., Hall, J. S., Eyres, I., Mansfield, W. and Smith, A. (2009). Klf4 reverts developmentally programmed restriction of ground state pluripotency. *Development* **136**, 1063-1069.
Hudson, J. L., Bickford, P., Johansson, M., Hoffer, B. J. and Stromberg, I. (1994). Target and neurotransmitter specificity of fetal central nervous system transplants: importance for functional reinnervation. *J. Neurosci.* **14**, 283-290.
Joksimovic, M., Yun, B. A., Kittappa, R., Anderegg, A. M., Chang, W. W., Taketo, M. M., McKay, R. D. and Awatramani, R. B. (2009). Wnt antagonism of Shh facilitates midbrain floor plate neurogenesis. *Nat. Neurosci.* **12**, 125-131.
Kala, K., Haugas, M., Lillevali, K., Guimera, J., Wurst, W., Salminen, M. and Partanen, J. (2009). Gata2 is a tissue-specific post-mitotic selector gene for midbrain GABAergic neurons. *Development* **136**, 253-262.
Kawasaki, H., Mizuseki, K., Nishikawa, S., Kaneko, S., Kuwana, Y., Nakanishi, S., Nishikawa, S. I. and Sasai, Y. (2000). Induction of midbrain dopaminergic neurons from ES cells by stromal cell-derived inducing activity. *Neuron* **28**, 31-40.
Kim, J. H., Auerbach, J. M., Rodriguez-Gomez, J. A., Velasco, I., Gavin, D., Lumelsky, N., Lee, S. H., Nguyen, J., Sanchez-Pernaute, R., Bankiewicz, K. et al. (2002). Dopamine neurons derived from embryonic stem cells function in an animal model of Parkinson's disease. *Nature* **418**, 50-56.
Kittappa, R., Chang, W. W., Awatramani, R. B. and McKay, R. D. (2007). The foxa2 gene controls the birth and spontaneous degeneration of dopamine neurons in old age. *PLoS Biol.* **5**, e325.
Konstantoulas, C. J., Parmar, M. and Li, M. (2010). FoxP1 promotes midbrain identity in embryonic stem cell-derived dopamine neurons by regulating Pitx3. *J. Neurochem.* **113**, 836-847.
Kunath, T., Saba-El-Leil, M. K., Almousailleakh, M., Wray, J., Meloche, S. and Smith, A. (2007). FGF stimulation of the Erk1/2 signalling cascade triggers transition of pluripotent embryonic stem cells from self-renewal to lineage commitment. *Development* **134**, 2895-2902.
Lee, S. H., Lumelsky, N., Studer, L., Auerbach, J. M. and McKay, R. D. (2000). Efficient generation of midbrain and hindbrain neurons from mouse embryonic stem cells. *Nat. Biotechnol.* **18**, 675-679.
Lin, W., Metzakopian, E., Mavromatakis, Y. E., Gao, N., Balaskas, N., Sasaki, H., Briscoe, J., Whitsett, J. A., Goulding, M., Kaestner, K. H. et al. (2009). Foxa1 and Foxa2 function both upstream of and cooperatively with Lmx1a and Lmx1b in a feedforward loop promoting mesodiencephalic dopaminergic neuron development. *Dev. Biol.* **333**, 386-396.
Liu, A., Losos, K. and Joyner, A. L. (1999). FGF8 can activate Gbx2 and transform regions of the rostral mouse brain into a hindbrain fate. *Development* **126**, 4827-4838.
Lunn, J. S., Fishwick, K. J., Halley, P. A. and Storey, K. G. (2007). A spatial and temporal map of FGF/Erk1/2 activity and response repertoires in the early chick embryo. *Dev. Biol.* **302**, 536-552.
Maxwell, S. L., Ho, H. Y., Kuehner, E., Zhao, S. and Li, M. (2005). Pitx3 regulates tyrosine hydroxylase expression in the substantia nigra and identifies a subgroup of mesencephalic dopaminergic progenitor neurons during mouse development. *Dev. Biol.* **282**, 467-479.
Meyers, E. N., Lewandoski, M. and Martin, G. R. (1998). An Fgf8 mutant allelic series generated by Cre- and Flp-mediated recombination. *Nat. Genet.* **18**, 136-141.
Millet, S., Campbell, K., Epstein, D. J., Losos, K., Harris, E. and Joyner, A. L. (1999). A role for Gbx2 in repression of Otx2 and positioning the mid/hindbrain organizer. *Nature* **401**, 161-164.
Nakatani, T., Minaki, Y., Kumai, M. and Ono, Y. (2007). Helt determines GABAergic over glutamatergic neuronal fate by repressing Ngn genes in the developing mesencephalon. *Development* **134**, 2783-2793.
Nakatani, T., Kumai, M., Mizuhara, E., Minaki, Y. and Ono, Y. (2009). Lmx1a and Lmx1b cooperate with Foxa2 to coordinate the specification of dopaminergic neurons and control of floor plate cell differentiation in the developing mesencephalon. *Dev. Biol.* **339**, 101-113.
Olander, S., Nordstrom, U., Patthey, C. and Edlund, T. (2006). Convergent Wnt and FGF signaling at the gastrula stage induce the formation of the isthmic organizer. *Mech. Dev.* **123**, 166-176.
Omodei, D., Acampora, D., Mancuso, P., Prakash, N., Di Giovannantonio, L. G., Wurst, W. and Simeone, A. (2008). Anterior-posterior graded response to Otx2 controls proliferation and differentiation of dopaminergic progenitors in the ventral mesencephalon. *Development* **135**, 3459-3470.
Ono, Y., Nakatani, T., Sakamoto, Y., Mizuhara, E., Minaki, Y., Kumai, M., Hamaguchi, A., Nishimura, M., Inoue, Y., Hayashi, H. et al. (2007). Differences in neurogenic potential in floor plate cells along an anteroposterior location: midbrain dopaminergic neurons originate from mesencephalic floor plate cells. *Development* **134**, 3213-3225.
Paek, H., Gutin, G. and Hebert, J. M. (2009). FGF signaling is strictly required to maintain early telencephalic precursor cell survival. *Development* **136**, 2457-2465.
Parmar, M. and Li, M. (2007). Early specification of dopaminergic phenotype during ES cell differentiation. *BMC Dev. Biol.* **7**, 86.
Perrier, A. L., Tabar, V., Barberi, T., Rubio, M. E., Bruses, J., Topf, N., Harrison, N. L. and Studer, L. (2004). Derivation of midbrain dopamine neurons from human embryonic stem cells. *Proc. Natl. Acad. Sci. USA* **101**, 12543-12548.
Prakash, N., Brodski, C., Naserke, T., Puelles, E., Gogoi, R., Hall, A., Panhuysen, M., Echevarria, D., Sussel, L., Weisenhorn, D. M. et al. (2006). A Wnt1-regulated genetic network controls the identity and fate of midbrain-dopaminergic progenitors in vivo. *Development* **133**, 89-98.

Roybon, L., Hjalt, T., Christophersen, N. S., Li, J. Y. and Brundin, P. (2008). Effects on differentiation of embryonic ventral midbrain progenitors by Lmx1a, MSX1, Ngn2, and Pitx3. *J. Neurosci.* **28**, 3644-3656.

Shimamura, K. and Rubenstein, J. L. (1997). Inductive interactions direct early regionalization of the mouse forebrain. *Development* **124**, 2709-2718.

Simon, H. H., Saueressig, H., Wurst, W., Goulding, M. D. and O'Leary, D. D. (2001). Fate of midbrain dopaminergic neurons controlled by the engrailed genes. *J. Neurosci.* **21**, 3126-3134.

Stavridis, M. P., Lunn, J. S., Collins, B. J. and Storey, K. G. (2007). A discrete period of FGF-induced Erk1/2 signalling is required for vertebrate neural specification. *Development* **134**, 2889-2894.

Tang, M., Villaescusa, J. C., Luo, S. X., Guitarte, C., Lei, S., Miyamoto, Y., Taketo, M. M., Arenas, E. and Huang, E. J. (2009). Interactions of Wnt/beta-catenin signaling and sonic hedgehog regulate the neurogenesis of ventral midbrain dopamine neurons. *J. Neurosci.* **30**, 9280-9291.

Tesar, P. J., Chenoweth, J. G., Brook, F. A., Davies, T. J., Evans, E. P., Mack, D. L., Gardner, R. L. and McKay, R. D. (2007). New cell lines from mouse epiblast share defining features with human embryonic stem cells. *Nature* **448**, 196-199.

Watanabe, K., Kamiya, D., Nishiyama, A., Katayama, T., Nozaki, S., Kawasaki, H., Watanabe, Y., Mizuseki, K. and Sasai, Y. (2005). Directed differentiation of telencephalic precursors from embryonic stem cells. *Nat. Neurosci.* **8**, 288-296.

Wilson, S. W. and Rubenstein, J. L. (2000). Induction and dorsoventral patterning of the telencephalon. *Neuron* **28**, 641-651.

Yan, Y., Yang, D., Zarnowska, E. D., Du, Z., Werbel, B., Valliere, C., Pearce, R. A., Thomson, J. A. and Zhang, S. C. (2005). Directed differentiation of dopaminergic neuronal subtypes from human embryonic stem cells. *Stem Cells* **23**, 781-790.

Ye, W., Shimamura, K., Rubenstein, J. L., Hynes, M. A. and Rosenthal, A. (1998). FGF and Shh signals control dopaminergic and serotonergic cell fate in the anterior neural plate. *Cell* **93**, 755-766.

Ying, Q. L., Stavridis, M., Griffiths, D., Li, M. and Smith, A. (2003). Conversion of embryonic stem cells into neuroectodermal precursors in adherent monoculture. *Nat. Biotechnol.* **21**, 183-186.

Ying, Q. L., Wray, J., Nichols, J., Batlle-Morera, L., Doble, B., Woodgett, J., Cohen, P. and Smith, A. (2008). The ground state of embryonic stem cell self-renewal. *Nature* **453**, 519-523.

Zhao, S., Maxwell, S., Jimenez-Beristain, A., Vives, J., Kuehner, E., Zhao, J., O'Brien, C., de Felipe, C., Semina, E. and Li, M. (2004). Generation of embryonic stem cells and transgenic mice expressing green fluorescence protein in midbrain dopaminergic neurons. *Eur. J. Neurosci.* **19**, 1133-1140.